UNIVERSIDADE FEDERAL DO RIO GRANDE DO SUL
INSTITUTO DE CIÊNCIAS BÁSICAS DA SAÚDE
PROGRAMA DE PÓS-GRADUAÇÃO EM CIÊNCIAS BIOLÓGICAS:
BIOQUÍMICA

Joseane Righes Marafiga

ESTUDO IN VITRO DAS OSCILAÇÕES DA FORMAÇÃO HIPOCAMPAL E O ENVOLVIMENTO DO SISTEMA GABAÉRGICO EM EPILEPSIA

Porto Alegre
2021

Joseane Righes Marafiga

ESTUDO IN VITRO DAS OSCILAÇÕES DA FORMAÇÃO HIPOCAMPAL E O ENVOLVIMENTO DO SISTEMA GABAÉRGICO EM EPILEPSIA

Tese apresentada ao Programa de Pós-Graduação em Ciências Biológicas: Bioquímica do Instituto de Ciências Básicas da Saúde da Universidade Federal do Rio Grande do Sul como requisito parcial para a obtenção do título de doutora em Bioquímica.

Orientador(a): Prof. Dr. Maria Elisa Calcagnotto
Coorientador(a): Prof. Dr. Scott C. Baraban

Porto Alegre

2021

CIP - Catalogação na Publicação

Marafiga, Joseane Righes
ESTUDO IN VITRO DAS OSCILAÇÕES DA FORMAÇÃO HIPOCAMPAL E O ENVOLVIMENTO DO SISTEMA GABAÉRGICO EM EPILEPSIA / Joseane Righes Marafiga. -- 2021.
192 f.
Orientadora: Maria Elisa Calcagnotto.

Coorientador: Scott C. Baraban.

Tese (Doutorado) -- Universidade Federal do Rio Grande do Sul, Instituto de Ciências Básicas da Saúde, Programa de Pós-Graduação em Ciências Biológicas: Bioquímica, Porto Alegre, BR-RS, 2021.

1. Epilepsia. 2. Sistema GABAérgico. 3. Hipocampo. 4. Oscilações Cerebrais. 5. Eletrofisiologia in vitro. I. Calcagnotto, Maria Elisa, orient. II. Baraban, Scott C., coorient. III. Título.

Elaborada pelo Sistema de Geração Automática de Ficha Catalográfica da UFRGS com os dados fornecidos pelo(a) autor(a).

AGRADECIMENTOS

À Deus, ao Universo, e à toda vida que me transmitiu paz, alegria e resiliência durante a elaboração desse trabalho.

À minha família, especialmente minha irmã Carol e minha mãe Maria, as quais sempre apoiaram meus sonhos, celebraram todas as minhas conquistas, me fortaleceram em momentos difíceis, e são “lar” em todos os momentos.

À minha avó, Dinah (in memoriam), por celebrar com alegria as minhas escolhas, por ter sido tão mais sensata do que a sua geração ensinou, e principalmente por me incentivar a seguir os meus sonhos. Ainda sinto teu apoio, esse trabalho é pra ti!

À minha orientadora Maria Elisa, pela confiança, pelo apoio, por ter compartilhado comigo todo conhecimento em Neurociências e Eletrofisiologia, e também por toda troca de ideias, sonhos, princípios e valores.

Ao meu coorientador Scott Baraban, por todo conhecimento e tempo dedicados ao meu aprendizado, e principalmente por me relembrar o quanto a ciência pode ser inspiradora!

À Mayara por todo apoio e amizade, esse trabalho não teria sido realizado sem a tua participação, e eu não teria sanidade mental sem a nossa dose diária de sinceridade e humor, e à Letícia Meier, por ter me apresentado o laboratório, pela amizade e parceria de longa data.

A todos integrantes do laboratório 37, e aos amigos/pesquisadores incríveis que conheci e levarei para a vida toda, Francine, Letícia Bol, Gabriel, Ana Paula Bosquetti, Joelma e Gabriela.

Aos meus amigos de Santa Maria, que me conhecem desde a graduação e sabem o motivo de cada passo meu. Lidiane, Patrícia, Paula, Camila, obrigada pela amizade e pelo apoio incondicional!

A todos amigos que Porto Alegre me apresentou, Cíntia, Lílian, Milene, Adri e Kati, vocês tornaram essa jornada muito mais fácil e leve!

À UFRGS, pelo ensino e pesquisa de excelência.

Ao PPG Bioquímica, pelo suporte; à equipe do biotério, pela dedicação e respeito à pesquisa científica; à secretaria do PPG, pela eficiência e dedicação com todos os alunos.

Ao CNPq e todas agências de fomento, fundamentais para o desenvolvimento desse trabalho. Meus sinceros votos de valorização e respeito pelo investimento na ciência!

Muito obrigada a todos que torceram e contribuíram para essa conquista!

"I want, by understanding myself, to understand others.
I want to be all that I am capable of becoming..."
Katherine Mansfield

RESUMO

As epilepsias afetam aproximadamente 65 milhões de pessoas mundialmente, e representam um grupo de doenças com etiologias, padrões de eletroencefalograma (EEG) e comorbidades heterogêneas. A epilepsia do lobo temporal (ELT) é a forma mais comum de epilepsia focal em adultos, refratária aos tratamentos disponíveis. As características estruturais da ELT envolvem alterações morfofuncionais do hipocampo, como a esclerose hipocampal, reorganização sináptica dos microcircuitos neuronais, prejuízo no funcionamento do sistema GABAérgico, na conectividade neuronal e mudanças nos padrões oscilatórios. A caracterização de padrões oscilatórios, por meio de registros de potencial de campo local *in vitro,* pode contribuir para descobertas que são significativamente úteis para o entendimento da rede hipocampal anormal durante a epileptogênese. A avaliação destes padrões pode ser útil para identificar biomarcadores de processos neuropatológicos em andamento em doenças do sistema nervoso central (SNC), como a epilepsia, e particularmente a ELT com comprometimento da formação hipocampal, que possui uma organização peculiar da rede neuronal. Neste trabalho, caracterizamos a atividade oscilatória *in vitro* e sua sincronia na formação hipocampal de ratos Wistar epilépticos adultos, em dois estágios da epileptogênese, 30 e 60 dias após o *Status Epilepticus* (*SE*) induzido pela pilocarpina. Registros extracelulares foram realizados em pares nas regiões córtex entorrinal (CE)-giro dentado (GD), GD-CA3, CA3-CA1 e CE-CA1 de fatias contendo a formação hipocampal de animais epilépticos (n=19) e de animais controle pareados por idade (n=20). Os registros foram realizados durante hiperexcitabilidade induzida por 4-aminopiridina (4-AP) no líquido de perfusão e durante a atividade espontânea da rede, sem 4-AP. Inicialmente, avaliamos a geração de eventos ictais e interictais induzidos por 4-AP em fatias de animais epilépticos e controle pareados por idade. Em seguida, foram selecionados trechos de 5s no intervalo de eventos epileptiformes interictais nos intervalos dos eventos interictais, e trechos de 5s de atividade espontânea da rede (sem atividade epileptiforme), afim de quantificar a densidade espectral de potência (PSD) (n_{epoch} = 30-50) e coerência de fase (n_{epoch}= 20-25) das oscilações registradas. Foi possível demonstrar que aos 30 dias após *SE*, a região CA1 das fatias de animais epilépticos, perfundidas com 4-AP, obtiveram maior ictogênese e maior potência das oscilações gama em CE, CA1 e CA3 e das oscilações de alta frequência (HFOs) em CA3. A coerência de fase foi maior em gama médio entre CA1-CA3 e CE-CA1 e em HFOs entre CE-CA1 neste período nos animais epilépticos. Aos 60 dias após *SE*, observamos um aumento da ictogênese em CE e GD; maior potência das oscilações gama em CA1, CA3 e GD, e de HFOs em CE, CA3 e GD; e maior coerência de fase em HFOs entre CA1-CA3. Durante a atividade espontânea da rede, sem 4-AP, aos 30 dias após *SE*, as fatias de animais epilépticos também apresentaram maior potência das oscilações gama em todas as regiões registradas, e de HFOs no CE. Aos 60 dias após *SE*, as regiões do CE, CA3 e DG de fatias de animais epilépticos apresentaram maior potência das oscilações gama, maior potência de HFOs no GD; e maior coerência de fase em fast ripples entre GD-CA3, quando comparado ao grupo controle. Os resultados acima mostram alterações específicas nos padrões oscilatórios de acordo com o período da epileptogênese e de acordo com a região da formação hipocampal. Além disso, esses resultados ressaltam o papel crucial das oscilações gama e HFOs em processos patológicos em andamento durante reorganização da rede neuronal, cruciais para o estabelecimento da epilepsia e também para a manutenção recorrente da hiperexcitabilidade da rede. A alteração dos padrões oscilatórios e da sincronia da rede hipocampal podem refletir

o funcionamento dinâmico do sistema GABAérgico inibitório durante o desenvolvimento da ELT. De fato, os interneurônios GABAérgicos coordenam dinamicamente a atividade das redes hipocampais, sendo de fundamental importância para a geração da atividade oscilatória, contribuindo para epileptogênese e ictogênese, demonstrando sua função no controle e na geração das crises epilépticas que vai além da inibição convencional.

Palavras-chave: Epilepsia; Oscilações cerebrais; Formação hipocampal; Registros extracelulares; Sistema GABAérgico.

ABSTRACT

The epilepsies affect approximately 65 million people worldwide, and represent a group of diseases with heterogeneous etiologies, electroencephalogram (EEG) patterns, and comorbidities. Temporal lobe epilepsy (TLE) is the most common form of drug-refractory focal epilepsy in adults. The structural features of TLE involve morphofunctional changes in the hippocampus, such as hippocampal sclerosis, synaptic reorganization of neuronal microcircuits, impairment of the GABAergic system, neuronal connectivity and changes in oscillatory patterns. The characterization of oscillatory patterns, through *in vitro* local field potential recordings, may contribute to findings that are significantly useful for understanding the abnormal hippocampal network during epileptogenesis. The evaluation of these patterns can be useful to identify biomarkers of ongoing neuropathological processes in central nervous system (CNS) diseases, such as epilepsy, and particularly TLE with impairment of the hippocampal formation, which has a peculiar neuronal network organization. Here, we characterized the *in vitro* oscillatory activity and its synchrony within the hippocampal formation of adult epileptic male Wistar rats at two different stages of epileptogenesis, 30 and 60 days after pilocarpine-induced *Status Epilepticus* (*SE*). Extracellular pair recordings were performed in Entorhinal cortex (EC)- Dentate gyrus (DG), DG-CA3, CA3-CA1 and EC-CA1 of hippocampal formation slices of epileptic (n=19) and aged-matched control (n=20) animals under 4-Aminopyridine (4-AP)-induced hyperexcitability or under spontaneous network activity condition, without 4-AP. First, we evaluated the 4-AP-induced ictal and interictal events in hippocampal-EC slices from epileptic and control age-matched rats. Thereafter, we selected 5s-epochs intervals between interictal epileptiform events (IEDs) and 5s-epoch of spontaneous network activity, without 4-AP, to perform the power spectral density (PSD) (n_{epoch}= 30-50) and phase coherence (n_{epoch}= 20-25) analysis. We found that at 30 days post-*SE,* 4-AP bathed slices from epileptic animals had increased ictogenesis in CA1; higher power of gamma bands in EC, CA1 and CA3; and high-frequency oscillations (HFOs) in CA3. Phase coherence was higher in middle gamma between CA1-CA3 and EC-CA1, and in HFOs between EC-CA1. At 60 days post-*SE*, we observed increased ictogenesis in EC and DG; higher power of gamma bands in CA1, CA3 and DG, HFOs in EC, CA3 and DG; and higher phase coherence in HFOs between CA1-CA3. Under spontaneous network activity at 30 days post-*SE,* slices from epileptic animals already presented higher power of gamma bands in all recorded regions, and HFOs in EC. At 60 days post-*SE*, they had higher power of gamma bands in EC, CA3 and DG, higher power of HFOs in DG; and higher phase coherence in fast ripples oscillations between DG-CA3, when compared to controls. We found, in a region- and stage-specific manner, alterations in gamma and HFOs within the hippocampal formation of epileptic animals under a second insult of hyperexcitability and during the spontaneous network activity, without epileptiform activity. Our results suggest the critical role of gamma and HFOs in ongoing pathological processes of network reorganization, crucial to the epilepsy establishment and recurrent feedback of hyperexcitability. The altered oscillatory patterns and network interactions in the hippocampal formation may reflect the functional involvement of inhibitory mechanisms during the development of TLE. In fact, GABAergic interneurons dynamically coordinate the activity of hippocampal networks, being of critical importance for the generation of oscillatory activity, and consequent contributing to epileptogenesis and ictogenesis, demonstrating an unconventional function beyond the control of seizures.

Keywords: Epilepsy; Brain oscillations; Hippocampus; Extracellular recordings; GABAergic system.

LISTA DE ABREVIATURAS

4-AP - 4-aminopiridina

AED – drogas antiepilépticas (do inglês, *antiepileptic drugs*)

BGT-1 - Transportador de betaínas

CA – corno de Amon

CE – córtex entorrinal

CEL – córtex entorrinal lateral

CEM – córtex entorrinal medial

DAG – descarboxilase do ácido glutâmico

ECoG – eletrocorticograma

EEG - eletroencefalograma

EH – esclerose hipocampal

ELT – epilepsia do lobo temporal

ELTm – epilepsia do lobo temporal medial

GABA - ácido gama-aminobutírico

GAT – Transportador de GABA

GD – giro denteado

VACCs – canais de Cálcio dependentes de voltagem (do inglês, *voltage-activated calcium channels*)

HVACCs – canais de Cálcio ativados por alta voltagem (do inglês, *high-voltage-activated calcium channels*)

HFOs – oscilações de alta frequência (do inglês, *high frequency oscillations*)

Hz - Hertz

ILAE – Liga internacional contra epilepsia (do inglês, I*nternational League against Epilepsy*)

LFP – potencial de campo local (do inglês, *local field potential*)

MEG - magnetoencefalograma

PA – potencial de ação

PSD – densidade espectral de potência (do inglês, *power spectral density*)

SE – status epilepticus

SNC – sistema nervoso central

SUDEP- morte súbita e inesperada em epilepsia (do inglês, *sudden unexpected death in epilepsy*)

TEA - transtorno do espectro do autismo

SUMÁRIO

PARTE I- FUNDAMENTAÇÃO TEÓRICA

INTRODUÇÃO

1 EPILEPSIA

A epilepsia é uma doença neurológica crônica com múltiplas causas, caracterizada pela predisposição de gerar crises epilépticas espontâneas e recorrentes (Fisher *et al.*, 2014), associada a comorbidades neurobiológicas, cognitivas, psicológicas e sociais que impactam na qualidade de vida dos pacientes (Fisher *et al.*, 2005). Para a sua definição, é necessária a ocorrência de pelo menos duas crises epilépticas não provocadas (ou reflexas) ocorrendo com um intervalo superior a 24 h; uma crise epiléptica não provocada (ou reflexa) e a probabilidade de ocorrência de outras crises similar ao risco geral de recorrência (de pelo menos 60%) após duas crises epilépticas não provocadas, ocorrendo nos próximos 10 anos; e diagnóstico de uma síndrome epiléptica (Fisher *et al.*, 2014).

A International League Against Epilepsy (ILAE) esclarece que a epilepsia tem sido tradicionalmente mencionada como um distúrbio ou um grupo de distúrbios, afim de enfatizar que é composta de muitas doenças e condições distintas, e que podem ser resultantes de muitas causas diferentes (Fisher *et al.*, 2005, 2014). Em vista disso, a identificação das epilepsias requer informações clínicas específicas, incluindo idade de início, manifestações comportamentais, comorbidades, etiologias, sinais e sintomas associados ao sistema nervoso central (SNC), gravidade e decurso. Outros achados clínicos como de eletroencefalografia (EEG) e imagem também são necessários para maior precisão no diagnóstico (Devinsky *et al.*, 2018).

Para se ter a classificação das epilepsias, é fundamental se conhecer a classificação dos tipos de crises epilépticas (Fisher *et al.*, 2014). De fato, existem muitas razões pelas quais a classificação das crises epilépticas é importante, tanto

para o diagnóstico, prognóstico e escolha do tratamento dos pacientes; quanto para o avanço do conhecimento sobre a epilepsia. Isto permite a popularização do conhecimento e comunicação entre o manejo clínico, ensino e pesquisa.

1.1 Classificação das crises epilépticas

Crises epilépticas são caracterizadas por interrupções recorrentes e imprevisíveis da função normal cerebral, e são interpretadas como um sintoma de epilepsia, definidas como "uma ocorrência transitória de sinais e / ou sintomas devido ao excesso anormal ou excesso de atividade neuronal síncrona no cérebro" (Fisher *et al.*, 2005, 2017). A classificação das crises epilépticas, desenvolvida pela ILAE (Fisher *et al.*, 2017; Falco-Walter, Scheffer e Fisher, 2018) (Figura 1) começa com a determinação das manifestações iniciais das crises, podendo ser divididas como de início focal, generalizado ou desconhecido. O reconhecimento das crises de acordo com sua origem tem uma base anatômica, e é investigada a partir do eletroencefalograma (EEG) e da análise clínica.

O primeiro tipo de crises, as focais, são subclassificadas como perceptivas ou desperceptivas, dependendo se a percepção é mantida ou não. A classificação de acordo com o nível de percepção tem uma base comportamental, justificada pela importância prática do seu comprometimento. Além disso, crises focais também são subagrupadas naquelas com sintomas e sinais motores e não motores no início da crise. Por fim, o tipo de crise "focal evoluindo para tônico-clônica bilateral" é um tipo especial de crise, que reflete um padrão de propagação da crise, mais do que um tipo unitário de crise epiléptica (Fisher *et al.*, 2017).

Crises de início generalizado, a segunda classificação do tipo de crises, são divididas naquelas com sintomas e sinais motores e não motores no início da crise.

Crises de início desconhecido podem ser referidas pela simples palavra “não classificadas” ou com características adicionais, incluindo motoras, não motoras, tônico-clônicas, espasmos epilépticos e parada comportamental (Fisher *et al.*, 2017).

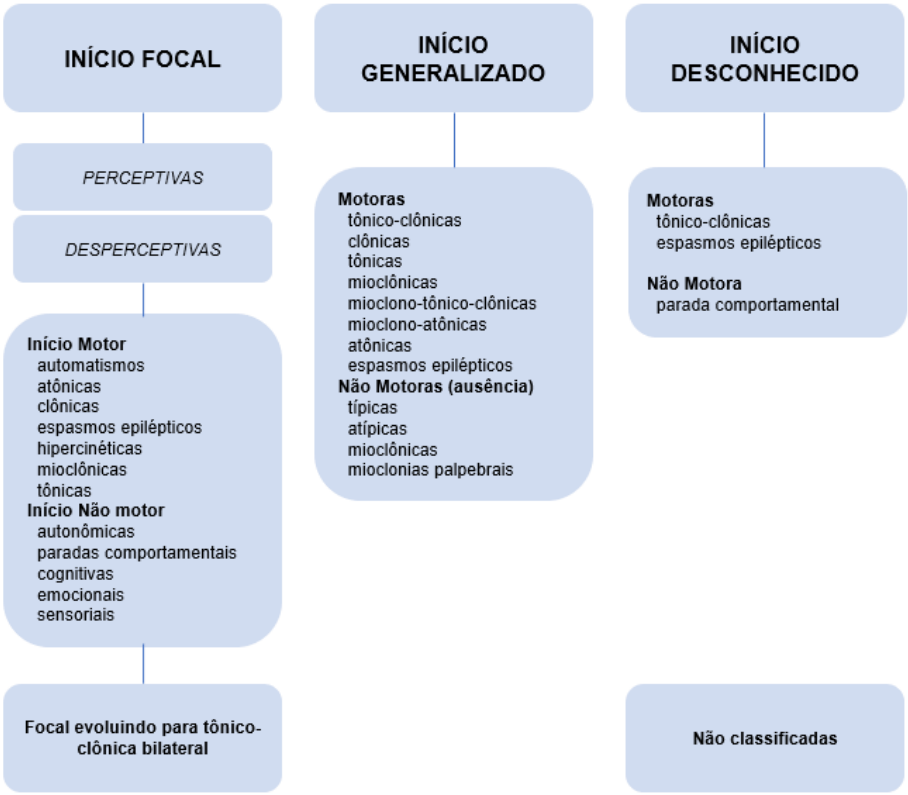

Figura 1 Classificação dos tipos de crises epilépticas. Adaptado de (Fisher et al. 2017).

1.2 Classificação das epilepsias

Após o diagnóstico do tipo de crise epiléptica, o próximo passo é a classificação dos tipos de epilepsias (Scheffer *et al.*, 2017), que incluem as epilepsias focais, epilepsias generalizadas, epilepsias focais e generalizadas combinadas, e também um grupo de epilepsias desconhecidas. A terceira classificação refere-se às síndromes epilépticas no qual um diagnóstico sindrômico específico pode ser feito,

considerando um conjunto de características como tipos de crises, características de EEG e de imagem.

A etiologia responsável pelo desenvolvimento de epilepsia pode ser diagnosticada em muitos casos, no entanto muitos pacientes não possuem a causa definida, e somente o tratamento para controle das crises epilépticas é possível (Pitkänen, 2010; Manford, 2017; Thijs *et al.*, 2019). As etiologias incluem estruturais, genéticas, infecciosas, metabólicas, imune e desconhecidas, e podem ser consideradas determinantes no decurso clínico e prognóstico da doença (Shorvon, 2011). Um esquema da classificação resumida pode ser visualizado na Figura 2.

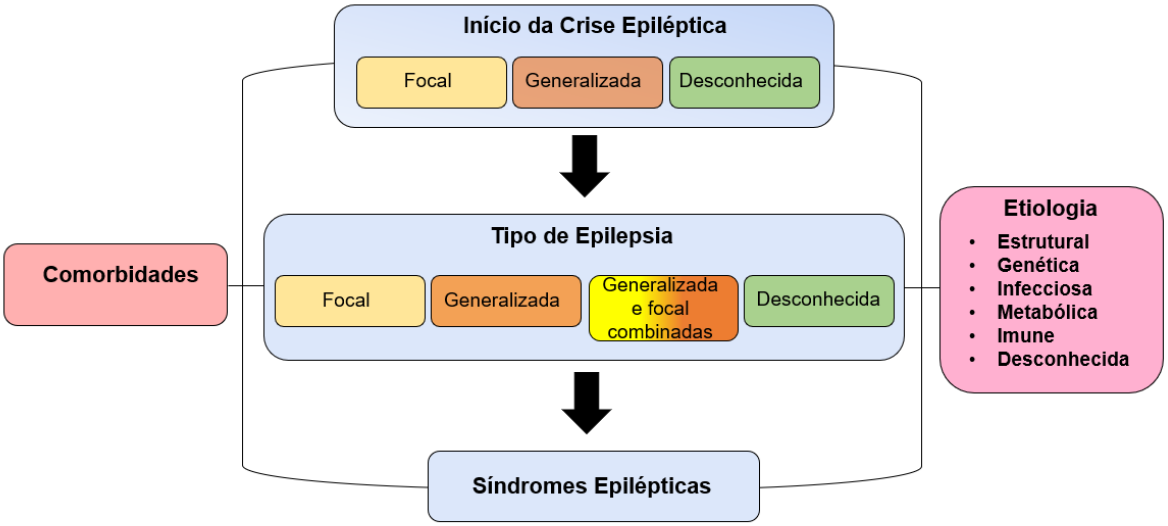

Figura 2 Esquema de classificação dos tipos de epilepsias. Adaptado de (Scheffer et al. 2017).

1.3 Epidemiologia

1.3.1 Incidência e Prevalência

A Epilepsia afeta aproximadamente 70 milhões de pessoas de todas as idades e raças, e é considerada uma das desordens neurológicas crônicas mais comuns de todo o mundo (Ngugi *et al.*, 2010). As epilepsias de início focal são responsáveis por cerca de 60% de todos os casos de epilepsia em adultos, e a epilepsia do lobo temporal (ELT) é o mais comum tipo de epilepsia focal.

Em países desenvolvidos, a prevalência de epilepsia ao longo da vida é de 5,8/1.000 habitantes, enquanto nas áreas rurais de países em desenvolvimento é de 15,4/1.000 habitantes (Ngugi *et al.*, 2010). A incidência de epilepsia é de 45/100.000/ano em países desenvolvidos, em comparação com 81,7/100.000/ano em países em desenvolvimento (Ngugi *et al.*, 2011). A prevalência e incidência são maiores em países de baixa e média renda em decorrência de maiores fatores de risco, como acidentes, risco de traumas e lesões, infecções, intercorrências no pré e pós-natal e erros inatos do metabolismo (Singh e Trevick, 2016; Fiest *et al.*, 2017).

A prevalência de epilepsia tende a ser mais baixa no início da vida, aumenta durante a adolescência e no início da idade adulta, diminuindo após a meia-idade (em torno dos 30 anos), permanecendo razoavelmente constante pelo resto da vida (Fiest *et al.*, 2017). A incidência de epilepsia, por sua vez, tende a ser maior em homens do que em mulheres, e em grupos de idades mais jovens (por exemplo, na infância e no início infância) e grupos de idade mais avançada (por exemplo, acima de 50-60 anos de idade).

1.3.2 Mortalidade

A mortalidade na epilepsia é uma causa de preocupação crescente, considerando que as taxas de mortalidade em pacientes com epilepsia são até três vezes maiores em comparação com a população saudável (Espinosa-Jovel *et al.*, 2018). As causas mais comuns incluem a morte súbita e inesperada em epilepsia (SUDEP- do inglês, *sudden unexpected death in epilepsy*), S*tatus epilepticus (SE)*, afogamento, acidentes, quedas e queimaduras; e também as causas não relacionadas com a epilepsia, como pneumonia por aspiração, suicídio, efeitos

contralaterais de AED (drogas antiepilépticas) e/ou drogas psiquiátricas, como obesidade e efeitos cardiovasculares (Devinsky *et al.*, 2018).

A SUDEP é a principal causa de morte relacionada diretamente à epilepsia (Tomson, Nashef e Ryvlin, 2008). Relata-se que o risco de SUDEP a cada 1000 pessoas com epilepsia por ano varia de 6,3 a 9,3 em candidatos à cirurgia ou em pacientes que continuam com crises epilépticas após cirurgia de epilepsia, principalmente refratária; 1,1 a 5,9 em pacientes com epilepsia com acompanhamento clínico; e 0,35 a 2,3 na população da comunidade (Tomson, Nashef e Ryvlin, 2008; Devinsky *et al.*, 2016).

A taxa de mortalidade prematura relacionada à epilepsia é maior em países em desenvolvimento, de baixa e média renda, quando comparado aos países desenvolvidos, estando diretamente associado à falta de acesso e precarização de assistência médica (Levira *et al.*, 2017).

1.4 Epilepsia do lobo temporal (ELT)

A ELT é um dos tipos mais comuns de epilepsia focal em adultos (Chatzikonstantinou, 2014). É caracterizada principalmente por crises espontâneas recorrentes geralmente refratárias e pela reorganização morfofuncional da formação hipocampal (Curia *et al.*, 2014). A formação hipocampal possui mecanismos anatômicos e fisiológicos bem desenvolvidos que promovem a sincronização neuronal, desempenhando uma função central e possuindo uma relação direta com a fisiopatologia da ELT (Chatzikonstantinou, 2014). Portanto, inicialmente é necessário o entendimento da organização celular e estrutural da formação hipocampal, bem como da conectividade entre as estruturas que compreendem esse circuito.

1.4.1 A formação hipocampal

A formação hipocampal é uma das áreas mais bem descritas do encéfalo, que têm atraído a atenção de neuroanatomistas desde os primeiros estudos de Ramon y Cajal e Lorente de Nó, no início do século 20. A formação hipocampal é uma área pertencente ao sistema límbico, composta pelo giro denteado (GD), hipocampo, o complexo subicular e o córtex entorrinal (CE) (Witter e Amaral, 2004; Schultz e Engelhardt, 2014).

O GD é a região de entrada para o hipocampo, e possui três camadas: a camada molecular; a camada granular; e o hilo, também denominado CA4 (Cappaert, Van Strien e Witter, 2015). A camada molecular, é caracterizada pela ausência de corpos celulares, e é habitada por dendritos das células granulares, *basket cells* e de neurônios polimórficos, assim como ramificações de axônios provenientes do CE e de outras regiões (Insausti e Amaral, 2003; Cappaert, Van Strien e Witter, 2015). A camada granular é uma faixa única compacta de corpos celulares neuronais (células granulares e outros tipos celulares, como *basket cells*), em formato de “U” ou “V” dependendo da posição septotemporal. O hilo, por sua vez, também conhecida como zona polimórfica do GD ou CA4, é composta por variados tipos celulares, com maior presença de células musgosas (Cappaert, Van Strien e Witter, 2015; Hammond, 2015).

O hipocampo é dividido ainda em três regiões do Corno de Amon 1 (CA1), 2 (CA2) e 3 (CA3), e em geral possui uma organização laminar similar para todas as camadas (Insausti e Amaral, 2003; Cappaert, Van Strien e Witter, 2015). A camada principal, é chamada também de camada piramidal ou *stratum piramidale*, caracterizada pelo grande agrupamento de neurônios piramidais; a camada estreita,

relativamente livre de células localizada abaixo da camada piramidal, é chamada de *stratum oriens*, o qual apresenta interneurônios, células trilaminares horizontais e as células oriens-lacunosum-moleculare (células O-LM), assim como dendritos basais de células piramidais. Em CA3, mas não em CA2 e CA1, uma zona acelular estreita, chamada de *stratum lucidum*, está localizada logo acima da camada piramidal, que possui axônios provenientes das células musgosas do GD, e dendritos apicais proximais dos neurônios piramidais de CA3. Superficial ao *stratum lucidum* em CA3, e imediatamente acima da camada piramidal em CA2 e CA1, é o *stratum radiatum*. O *stratum radiatum* pode ser definido como a região suprapiramidal em que conexões associativas CA3-CA3 e CA3-CA1 e conexões da colateral de Schaffer estão localizadas. As células presentes nessa camada são interneurônios, dendritos apicais dos neurônios piramidais, e axônios da colateral de Schaffer e da via comissural. A porção mais superficial do hipocampo é chamada de *stratum lacunosum-moleculare*, que apresenta fibras da via perfurante do CE, fibras oriundas da camada 3 do CE, e interneurônios inibitórios. Aferências de outras regiões, como as do núcleo reuniens do tálamo, também terminam nesta camada, em CA1 (Witter e Amaral, 2004; Cappaert, Van Strien e Witter, 2015; Hammond, 2015).

O complexo subicular é uma estrutura central posicionada entre o hipocampo e o CE, bem como uma série de estruturas corticais e subcorticais (O'Mara, 2005; Lévesque e Avoli, 2021), e representa um importante ponto de retransmissão sináptica da formação hipocampal para estruturas pertencentes do sistema límbico. É composta pelo prosubículo, presubículo, subículo, parasubículo e pós-subículo (Witter e Amaral, 2004; Cappaert, Van Strien e Witter, 2015), e é constituído por três camadas, a camada molecular, a camada piramidal, e a camada polimórfica (O'Mara, 2005). A principal camada de células do subículo apresenta neurônios piramidais

relativamente uniformes em forma e tamanho, e estendem seus dendritos apicais para a camada molecular, e os dendritos basais se estendem em porções mais profundas da camada de células piramidais (Witter e Amaral, 2004).

O córtex entorrinal (CE) trata-se de uma das principais aferências para o hipocampo. Baseado na sua citoarquitetura e padrões de projeção, o CE possui duas subdivisões, as áreas medial e lateral (córtex entorrinal medial e córtex entorrinal lateral, CEM e CEL respectivamente). É subdividido em seis camadas, sendo quatro camadas celulares (camadas II, III, V e VI) e duas camadas acelulares ou plexiformes (camadas I e IV ou lâmina dissecante). O CE é a principal ponto de comunicação entre o hipocampo e estruturas neocorticais, contendo conexões aferentes e eferentes dos córtex de associação, o neocórtex, o bulbo olfatório e o córtex límbico (Schultz e Engelhardt, 2014; Schultz, Sommer e Peters, 2015). A principal via de entrada hipocampal ocorre pela via perfurante, a qual se inicia-se na camada II do CEL e CEM, e perfura o subículo antes de chegar no GD. Além disso, do CE também parte uma outra via originária da camada III, que se conecta diretamente a CA1, chamada de via temporoamônica (Cappaert, Van Strien e Witter, 2015).

A Figura 3 é uma representação da organização do circuito hipocampal-CE. Células das camadas 2 e 3 do córtex entorrinal (CE) se projetam densamente para células granulares individuais do giro dentado (GD) através da via perfurante. As células granulares do GD projetam-se, através das fibras musgosas, para a área CA3. A região CA3 é caracterizada por conexões recorrentes auto associativas entre seus neurônios piramidais e também projeções para os neurônios piramidais de CA1 (e para outras estruturas subcorticais), através das colaterais de Schaffer. A área CA1 do hipocampo recebe duas entradas excitatórias principais, uma da área CA3 (via colaterais de Schaffer) e a outra da CE (via perfurante). Finalmente, neurônios da

região CA1 têm aferências principalmente para o subículo, a região terminal do hipocampo, que está conectado à camada profunda do CE. Fisiologicamente, o CE fornece a principal entrada para o hipocampo alcançando o GD através da via perfurante, e também recebe saída de CA1 através do subículo, completando assim o circuito hipocampal-CE (Witter *et al.*, 2000).

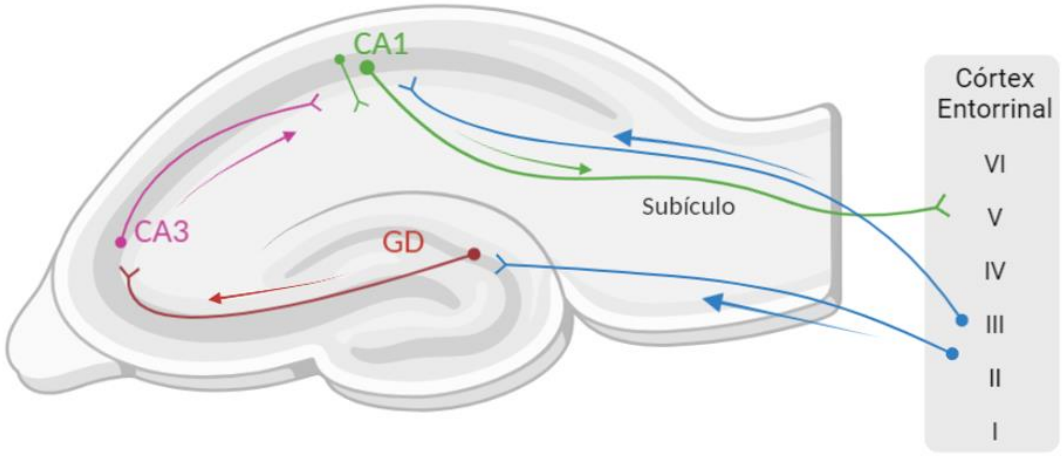

Figura 3 Circuito hipocampal-CE. A principal via aferente do hipocampo origina-se no CE, que forma conexões com o GD. As células granulares do GD projetam, através das fibras musgosas, para a área CA3 hipocampal. Os neurônios piramidais de CA3 enviam axônios para os neurônios piramidais de CA1, através das colaterais de Schaffer (via trissináptica).Os axônios das células piramidais de CA1, projetam-se o CE, formando o loop hipocampo-CE. O hipocampo também recebe aferência da camada 3 do CE, diretamente para os neurônios piramidais de CA1, denominada via temporoamônica (Witter *et al.*, 2000; Cappaert, Van Strien e Witter, 2015). Criado em BioRender.com.

As conexões CE-DG, GD-CA3 e CA3-CA1, são conhecidas como a via trissináptica do hipocampo, enquanto a sinapse entre CE-CA1 é denominada via temporoamônica (Insausti e Amaral, 2003; Witter e Amaral, 2004).

1.4.2 Fisiopatologia da ELT

A ELT abrange uma variedade de distúrbios que apresentam a característica comum de crises epilépticas que surgem no lobo temporal (Bertram, 2009). Em geral, as características fisiopatológicas da ELT incluem um GD reorganizado, uma depleção neuronal e aumento da gliose na região do Corno de Amon (CA), e a perda

neuronal da camada 2 e 3 do CE (Cross e Cavazos, 2007; Sloviter, 2008; Danzer *et al.*, 2010; Noebels *et al.*, 2012; Ren *et al.*, 2014). No entanto, é importante ressaltar que as alterações decorrentes da ELT são geralmente associadas a uma patologia subjacente, incluindo tumores, malformações vasculares, displasias corticais, trauma, e esclerose hipocampal (Mcintyre e Gilby, 2010), fornecendo também características específicas de geração e propagação das crises epilépticas.

A epilepsia límbica é uma das formas mais comuns de epilepsia focal e também é uma das epilepsias mais submetidas a intervenção cirúrgica (Janszky *et al.*, 2005; Chatzikonstantinou, 2014). Estruturas temporais mediais como o hipocampo, CE, córtex piriforme e olfatório, e amígdala, são fortemente associadas ao início das crises epilépticas (Bertram, 2009; Noebels *et al.*, 2012; Goldberg e Coulter, 2013), uma vez que quando identificadas como foco epiléptico e ressecadas, é possível obter o controle das crises epilépticas nos pacientes com epilepsia do lobo temporal mesial (ELTm) (Ahmad, Khanna e Sani, 2020). As perturbações do sistema límbico frequentemente resultam em comorbidades debilitantes e deficiências funcionais, além das consequências diretas das crises epilépticas (Mcintyre e Gilby, 2010).

O hipocampo, em particular, exerce um papel fundamental no desenvolvimento da ELTm, uma vez que processos fisiopatológicos hipocampais são fortemente associados à origem e manutenção das crises epilépticas (Chatzikonstantinou, 2014). A esclerose hipocampal (EH) por exemplo, é o achado patológico mais comum na ELTm (Cendes *et al.*, 2014; Thom, 2014; Walker, 2015). No entanto, ainda permanece inconclusivo se a EH é consequência das crises epilépticas recorrentes, ou trata-se de uma alteração patológica desencadeante da geração das crises.

A região do CA de pacientes com ELTm pode ser considerada a área mais vulnerável à perda neuronal (Blümcke, Mrcpath e Wiestler, 2002; Sloviter, 2008; Walker, 2015), que pode variar ao longo das regiões do CA e estruturas adjacentes, podendo ser superior a 50% até a perda neuronal quase completa em pacientes com ELTm comparados com pacientes neurologicamente normais. A ILAE (International League Against Epilepsy) classifica a EH em quatro tipos (Blümcke *et al.*, 2013). A EH do tipo 1 é a mais comum, correspondendo a 60-80% dos casos. A área de CA1 apresenta em torno de 80% de morte de neurônios piramidais, CA2 possui morte neuronal de 30-50%, CA3 apresenta entre 30 a 90% de perda neuronal, enquanto CA4 possui 40-90% de morte neuronal, assim como o GD possui 50-60% de perda de células granulares. A EH do tipo 2 é uma forma mais rara de EH, onde somente 5-10% dos pacientes com ELTm apresentam esse padrão histopatológico. A HS do tipo 2 é caracterizada pela perda de 80% dos neurônios piramidais, predominantemente na região de CA1. A EH do tipo 3 ocorre principalmente na região de CA4 e GD, com morte neuronal de 50% e 30%, respectivamente; enquanto CA3, CA2 e CA1 são moderadamente afetadas (< 30%). Possui incidência de 4-7% entre os pacientes com ELTm. O tipo 4, é caracterizado pela presença de gliose e ausência de EH, ou seja, quando não há morte neuronal significativa, apenas gliose; e ocorre em 20% dos pacientes com ELTm (Blümcke *et al.*, 2013; Cendes *et al.*, 2014; Walker, 2015).

Na ELT com EH, também é possível observar a desorganização das células granulares e sua dispersão ao longo do GD (Sparks *et al.*, 2020). Na dispersão das células granulares, a laminação compacta dos corpos celulares é perdida, e tem sido associada com a redução da proteína da matriz extracelular Relina (Haas *et al.*, 2002). Dessa forma, a conectividade entre células granulares é facilitada, promovendo hiperexcitabilidade.

O brotamento de fibras musgosas também já foi descrito na ELT (Sutula *et al.*, 1989; Noebels *et al.*, 2012). Nessa forma de sinaptogênese, os axônios das células granulares formam novas sinapses excitatórias anormais com os dendritos de células granulares, resultando em uma rede excitatória recorrente (Zhang *et al.*, 2009). Alternativamente, o brotamento das fibras musgosas também pode desencadear uma inibição aumentada no GD ao invés de hiperexcitabilidade, ao promover a excitação das células em cesto (*basket cells*), que em seguida promovem a inibição das células granulares (Boyett e Buckmaster, 2001; Noebels *et al.*, 2012).

O CE, a principal via eferente para o hipocampo, e com grande projeção para o GD e CA1, apresenta perda neuronal e gliose na camada III e, em menor grau, na camada II do CE em modelos animais e pacientes com ELTm (Du *et al.*, 1993, 1995). No entanto, apesar da perda neuronal, ocorre o aumento da excitabilidade dos neurônios do CE (Kobayashi e Buckmaster, 2003; Tolner *et al.*, 2007), o que pode facilitar a geração de crises epilépticas em CE, e a propagação dessa atividade ao longo do hipocampo (Ren *et al.*, 2014).

Interessantemente, as alterações morfofuncionais encontradas ao longo da formação hipocampal de pacientes com ELTm, podem tanto facilitar ou promover a hiperexcitabilidade; quanto prejudicar a inibição GABAérgica, ou também restabelecê-la, embora talvez de forma inadequada (Noebels *et al.*, 2012). Alterações da interação entre áreas límbicas já foram evidenciadas em fatias cerebrais de animais epilépticos (Barbarosie e Avoli, 1997; Calcagnotto, Barbarosie e Avoli, 2000; D'Antuono *et al.*, 2002). Porém, em adição às mudanças de conectividade do sistema límbico decorrentes da perda neuronal, a integridade funcional dos neurônios do hipocampo representa um ponto de controle crítico para a geração e recorrência de crises límbicas e a possibilidade de interações reverberantes entre regiões menos

afetadas. Na epilepsia, a maioria dos estudos concentra-se na investigação das alterações celulares e moleculares causadas por insultos patológicos, que resultam em uma condição epiléptica ativa; e também as alterações decorrentes da geração e recorrência de crises epilépticas. No entanto, o papel específico de cada estrutura pertencente a formação hipocampal e sua relação com a epileptogênese e ictogênese ainda precisam ser elucidados.

1.4.3 Sistema GABAérgico

Evidências clínicas e experimentais demonstram o importante papel do sistema GABAérgico em inúmeros processos neuronais, incluindo na neurogênese, maturação neuronal, apoptose neuronal, no controle da excitabilidade e nas oscilações da rede (Ben-Ari *et al.*, 2007, 2012; Kilb, 2012; Luhmann, Fukuda e Kilb, 2015). Diante disso, as alterações no sistema GABAérgico são associadas a inúmeros processos patológicos e doenças do sistema nervoso central (SNC) (Zhang *et al.*, 2021), incluindo epilepsia, esquizofrenia, transtorno do espectro autista (TEA), doença de Alzheimer, e doença de Parkinson (Wu e Sun, 2015; Zandt e Naegele, 2017; Jahangir *et al.*, 2021; Jiménez-Balado e Eich, 2021; Tang, Jaenisch e Sur, 2021; Zhang *et al.*, 2021).

O ácido gama-aminobutírico (GABA) é o principal neurotransmissor inibitório no SNC de mamíferos, o qual é sintetizado pela enzima descarboxilase do ácido glutâmico (DAG) e estocado em vesículas sinápticas em neurônios GABAérgicos (Purves *et al.*, 2010; Kandel *et al.*, 2014). O sistema GABAérgico também inclui transportadores de GABA, como GAT1-3 e BGT-1, que estão envolvidos na captação ou liberação de GABA (Kilb, 2012; Merino, 2019). Dentre os receptores componentes desse sistema, estão os receptores ionotrópicos $GABA_A$ e $GABA_C$, e receptores

metabotrópicos $GABA_B$ (Purves *et al.*, 2010). Após ativação neuronal, as moléculas de GABA são liberadas, através da fusão das vesículas na fenda sináptica, atingindo uma concentração na faixa milimolar (Purves *et al.*, 2010). Por conseguinte, o GABA pode agir tanto em receptores pós-sinápticos quanto extra sinápticos, de modo geral, fornecendo controle inibitório sobre o fluxo excitatório da rede neuronal (Purves *et al.*, 2010; Merino, 2019).

A inibição sináptica no SNC é mediada por grupos distintos de interneurônios, os quais desempenham papéis funcionais únicos no microcircuito (Kepecs e Fishell, 2014). Interneurônios podem ser classificados em mais de 20 subtipos com base em critérios específicos, incluindo morfologia, padrão de conectividade, perfil molecular e fisiologia (Figura 4) (Ascoli *et al.*, 2008; Kepecs e Fishell, 2014). Com relação a morfologia, leva-se em consideração os principais componentes estruturais dos interneurônios incluindo o soma, os dendritos, o axônio, além dos seus componentes elétricos e químicos, e também suas conexões sinápticas. Quanto às características moleculares, a classificação é especialmente de acordo com a expressão de moléculas como proteínas de ligação de Ca^{2+}, como por exemplo os interneurônios que expressam PV (parvalbumina), e os neuropeptídeos SOM (somatostatina), VIP (peptídeo intestinal vasoativo), CR (calretinina), CB (calbindina) e NPY (neuropeptídeo Y). Além disso, existem outras categorias de moléculas como fatores de transcrição, neurotransmissores ou suas enzimas de síntese, receptores, proteínas estruturais, canais iônicos, conexinas, panexinas e transportadores de membrana. Por fim, a classificação referente às características eletrofisiológicas inclui as características ativas e passivas da membrana celular, padrões de disparo de potenciais de ação e formas de propagação, sendo fundamental para determinar que

papel essas células desempenham na atividade do circuito (Ascoli *et al.*, 2008; Kepecs e Fishell, 2014).

A nível celular, a transmissão sináptica GABAérgica é importante na regulação da sensibilidade do circuito neuronal e na sincronização das oscilações da rede (Avoli e de Curtis, 2011). As propriedades fisiológicas e de conectividade dos interneurônios permitem controlar a produção rítmica de grandes populações de células piramidais excitatórias, bem como outras populações interneuronais (Zaitsev, 2017).

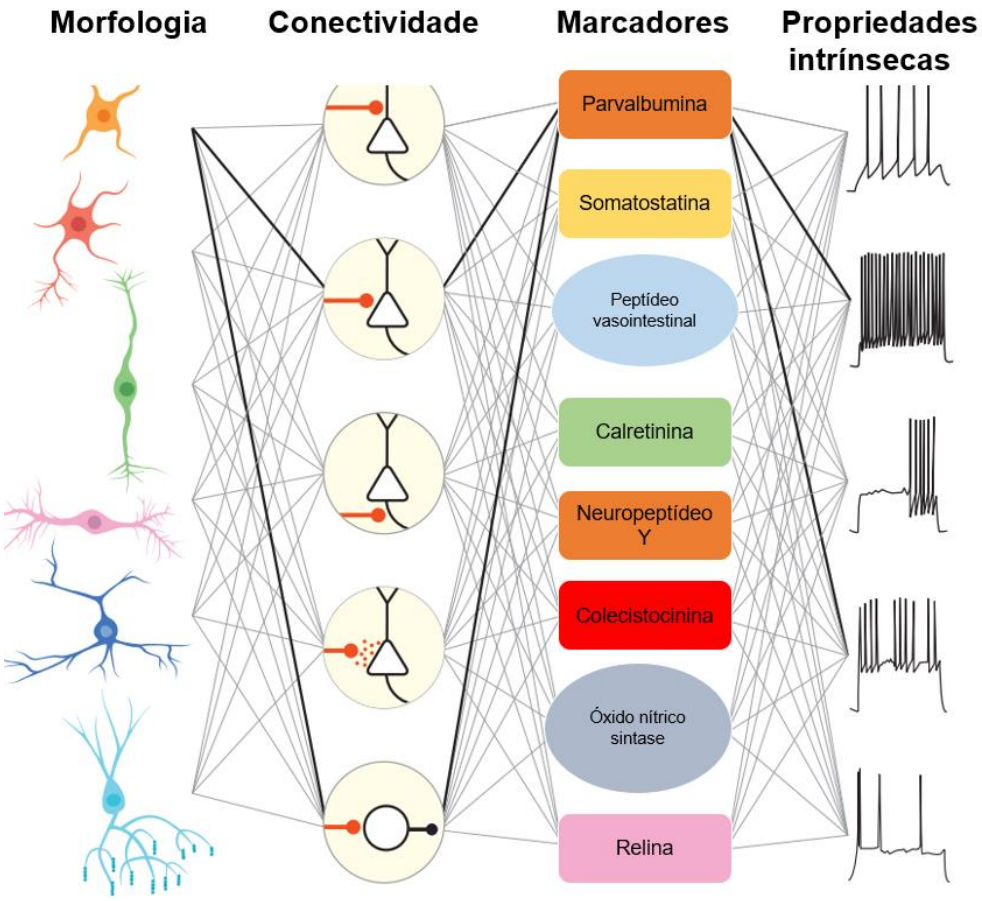

Figura 4 Classificação dos interneurônios de acordo com as propriedades morfológicas, de conectividade, marcadores moleculares e propriedades intrínsecas. Adaptado de (Kepecs e Fishell, 2014).

A inibição no SNC é exercida por interneurônios perissomáticos e dendríticos que podem realizar diferentes tarefas inibitórias (Miles *et al.*, 1996; Royer *et al.*, 2012). Em geral, interneurônios GABAérgicos com contato pós-sináptico perissomático,

como os interneurônios PV, são bem compreendidos em termos de sua capacidade de controlar os disparos de potencial de ação, sincronia e as oscilações da rede (Cobb *et al.*, 1995). As sinapses dendríticas, promovidas por interneurônios SOM, promovem o controle da eletrogênese, a plasticidade sináptica, e estados de atividade em seus alvos (Savanthrapadian *et al.*, 2014). Além disso, interneurônios que expressam VIP, têm sido propostos por mediarem a desinibição, por meio da inibição de interneurônios SST e uma fração menor de interneurônios PV. A inibição desses interneurônios, por sua vez, desinibe as células principais. Dessa forma, considerando que os diferentes subtipos de interneurônios possuem diferentes padrões de controle da atividade neuronal, cada subtipo interneuronal possui funções especializadas em gerar ou modular diferentes ritmos cerebrais (Dupret, Pleydell-Bouverie e Csicsvari, 2008; Klausberger e Somogyi, 2008).

A relação entre o sistema GABAérgico e as crises epilépticas foi inicialmente sugerida quando crianças, no seu primeiro ano de vida, alimentadas com uma fórmula acidentalmente deficiente em piridoxina, apresentaram convulsões (Molony e Parmelee, 1954). A piridoxina (também conhecida como vitamina B6) é essencial para o equilíbrio excitação/inibição neuronal, pois trata-se de uma coenzima para a síntese de GABA a partir do ácido glutâmico por meio da enzima DAG (Purves *et al.*, 2010). Dessa forma, a restrição de piridoxina no organismo das crianças foi relacionada ao desenvolvimento de alterações comportamentais e crises epilépticas duradouras (Nelson, 1956; Purves *et al.*, 2010). Desde então, a relação entre sistema GABAérgico e epilepsia tem sido investigada (Treiman, 2001; Trevelyan e Schevon, 2013).

Estudos mostram que alterações na neurotransmissão GABAérgica estão envolvidas na geração de atividade epileptiforme *in vitro* (Avoli *et al.*, 1996; Köhling *et al.*, 2000; Khazipov *et al.*, 2004; Uva *et al.*, 2005, 2017; Avoli e de Curtis, 2011;

Gafurov e Bausch, 2013; Boido *et al.*, 2014) e crises epilépticas *in vivo* (Khazipov e Holmes, 2003; Hansen, Sperling e Sánchez, 2004; Vendramin Pasquetti *et al.*, 2017; Di Cristo *et al.*, 2018), e no aumento de padrões oscilatórios patológicos, como as HFOs (Wendling *et al.*, 2002; Khazipov, 2016; Uva *et al.*, 2017). Além disso, o bloqueio da transmissão GABAérgica é uma abordagem experimental amplamente utilizada para a indução de crises epilépticas e epilepsia (Hansen, Sperling e Sánchez, 2004; Cymerblit-Sabba e Schiller, 2010; Salami *et al.*, 2015; Reschke *et al.*, 2018; Lazzarotto *et al.*, 2021). Portanto, esses estudos confirmam que a disfunção GABAérgica, por meio da alteração da transmissão sináptica inibitória ou pela alteração dos circuitos neuronais, contribuem para o desenvolvimento de crises epilépticas.

A partir dessa perspectiva, deve-se considerar que os subtipos de neurônios GABAérgicos podem desempenhar papéis distintos na geração de crises epilépticas, e irão contribuir para propriedades fisiopatológicas específicas das redes neuronais onde estão envolvidos (Ledri *et al.*, 2014; Zaitsev, 2017). Portanto, a inibição mediada por GABA pode restringir a atividade neuronal, mas também pode promover a sincronização neuronal (Avoli e de Curtis, 2011; Khazipov, 2016) e consequentemente facilitar a geração de eventos semelhantes a crises epilépticas (Köhling *et al.*, 2000; Barbarosie *et al.*, 2002; Khazipov e Holmes, 2003).

No entanto, evidências experimentais ainda sugerem que o tratamento celular baseado em precursores de interneurônios são um tratamento promissor para crises epilépticas (Richardson *et al.*, 2008; Hunt e Baraban, 2015; Spatazza, Mancia Leon e Alvarez-Buylla, 2017). Além disso, evidências experimentais e clínicas demonstram que a restauração da inibição interrompe ou previne significativamente a geração de crises epilépticas (Greenfield, 2013; Liu *et al.*, 2013; Paschen *et al.*, 2020). De fato, drogas que possuem como alvo o sistema GABAérgico, principalmente o receptor

$GABA_A$, são amplamente utilizadas para o tratamento das epilepsias (Mula, 2011; Greenfield, 2013).

2 RITMOS CEREBRAIS

Os ritmos, ou oscilações cerebrais, refletem as flutuações de voltagem extracelular, decorrentes da somação da atividade elétrica e sináptica de conjuntos neuronais (Buzsáki, 2006). O estudo das oscilações cerebrais fornece a oportunidade de investigar, em diferentes regiões do encéfalo, o padrão oscilatório neuronal e suas funções, os mecanismos celulares e sinápticos subjacentes à rede neuronal, e a sua correlação com funções cerebrais superiores; tanto em estados fisiológicos quanto em estados patológicos.

As características do potencial de campo local (LFP, do inglês *local field potential*) dependem das propriedades estruturais e funcionais do tecido cerebral, associada à contribuição conjunta de fontes geradoras das correntes elétricas e sinápticas (Buzsáki, Anastassiou e Koch, 2012). O LFP é gerado pela soma de correntes de entrada e saída (*sink* e *source*) em redes neuronais que circundam o eletrodo de registro extracelular (Buzsáki, 2006), e também possui a contribuição de potenciais de ação mediados por Ca^{2+}, respostas intrínsecas dependentes de voltagem, bem como de potenciais de ação, e potenciais de ação rebote após a hiperpolarização (Buzsáki, 2006; Buzsáki, Anastassiou e Koch, 2012).

Além disso, dois fatores que influenciam a geração do LFP incluem a organização celular e sináptica da rede e a sincronia das fontes geradoras de corrente, sendo estas fundamentais para o processamento e comunicação neural (Buzsaki e Draguhn, 2004; Fries, 2005; Uhlhaas *et al.*, 2010). A atividade sincronizada de diferentes áreas cerebrais determina o nível de interação entre as mesmas e

fornece um mecanismo de coordenação de grupos neuronais (Buzsáki e Watson, 2012; Igarashi *et al.*, 2014). Dessa forma, as oscilações cerebrais são altamente associadas a processos cognitivos de alto nível, bem como tarefas de menor complexidade (Ward, 2003; Fries, 2005, 2015; Dipoppa, Szwed e Gutkin, 2016).

As oscilações cerebrais registradas no eletroencefalograma (EEG) são categorizadas dependendo da sua faixa de frequência (número de ciclos por segundo- Hz). Os diferentes tipos de oscilações incluem: delta (1-4 Hz), teta (4-12 Hz), alfa (8-12 Hz), beta (12-30 Hz), high-frequency oscillations (HFOs) (gama, ripples e fast ripples: 30-500 Hz) (Buzsáki, 2006; Belluscio *et al.*, 2012; Tort *et al.*, 2013; Pasquetti *et al.*, 2019) (Figura 5). A atividade neural oscilatória também pode ser registrada utilizando outras metodologias, incluindo a magnetoencefalografia (MEG) e o eletrocorticograma (ECoG). Além disso, as oscilações cerebrais também podem ser detectadas *in vitro* por meio do registro extracelular (Buzsáki, 2006). Em geral, o traçado bruto registrado no EEG é composto por ondas senoidais de diferentes frequências, amplitude e fase. Dessa forma, a análise da atividade oscilatória se baseia na decomposição desse traçado bruto em suas ondas componentes (Mathalon e Sohal, 2015). A contribuição de cada frequência que compõe o sinal é mensurada pela sua potência relativa, em uma análise denominada densidade espectral de potência (PSD, do inglês *power spectral density*). A potência de uma frequência específica pode revelar a funcionalidade de um conjunto de neurônios de uma determinada região, e refletir as alterações rítmicas na excitabilidade neuronal (Fries, 2005). A conectividade entre regiões distintas, por sua vez, pode ser analisada através da magnitude quadrática da coerência. (do inglês, *magnitude-squared coherence*) (Roach e Mathalon, 2008; Mathalon e Sohal, 2015), a qual reflete a sincronização de dois sinais em uma frequência específica, sendo assim

demonstrando o padrão oscilatório e a atividade síncrona de diferentes grupos neuronais e regiões cerebrais. Portanto, essas ferramentas podem fornecer informações relevantes sobre os processos cerebrais fisiológicos dinâmicos, e também sobre a fisiopatologia de doenças neurológicas, psiquiátricas e neurodegenerativas (Roach e Mathalon, 2008; Yener e Basar, 2013; Mathalon e Sohal, 2015).

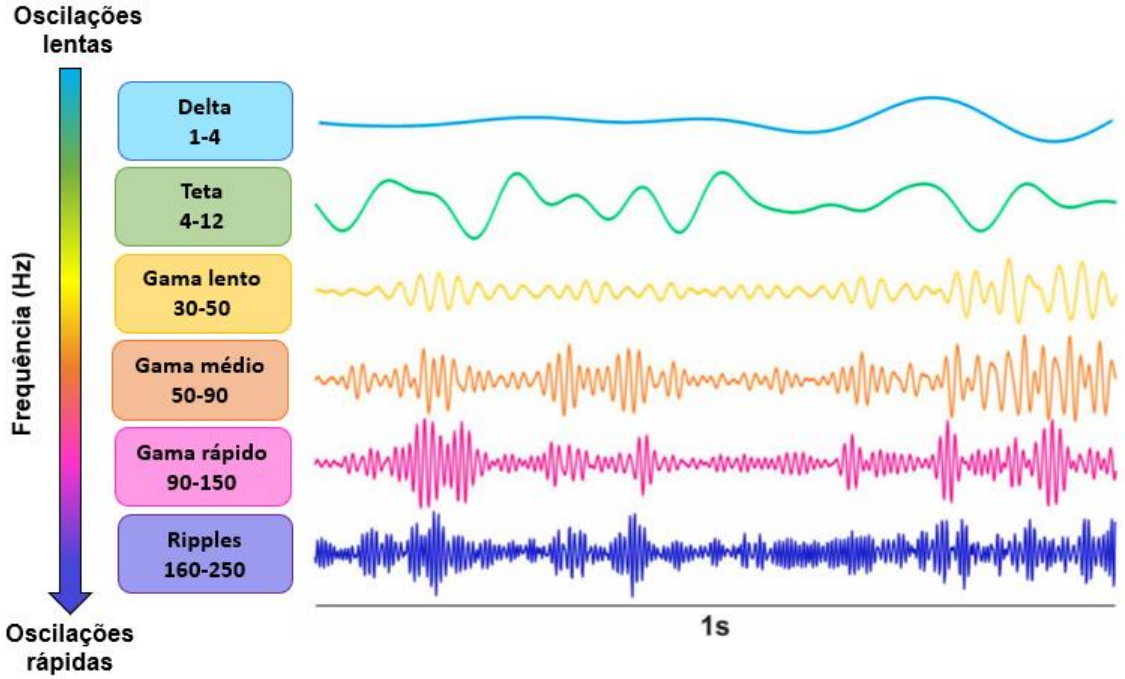

Figura 5. Exemplo de faixas de frequência registradas no EEG. Adaptado de Vendramin Pasquetti, 2019.

2.1 Ritmos Cerebrais, como biomarcadores fisiológicos e patológicos

Diferentes bandas de frequência refletem diferentes processos fisiológicos em indivíduos saudáveis. A oscilação delta está associada ao sono e estados de consciência reduzida, além de estar associada com a motivação e sistemas de recompensa (Dang-Vu *et al.*, 2008; Knyazev, 2012). Teta está associado ao comportamento exploratório, aprendizado e na memória episódica (Herweg, Solomon e Kahana, 2020). Alfa está associada à ociosidade, e também atribuída à inibição de processos neurais associados ao processamento cognitivo (Klimesch, Sauseng e

Hanslmayr, 2007). A oscilação beta reflete um estado cerebral de equilíbrio da atividade neuronal, e estão associadas à integração sensório-motora, e processos perceptuais, cognitivos e motores (Schmidt *et al.*, 2019). As oscilações gama estão associada à percepção, atenção e memória (Fries, Nikolić e Singer, 2007; Colgin *et al.*, 2009). Enquanto as HFOs, podem ser registradas durante processos sensoriais e processamento de informações, aprendizado e memória (Kucewicz *et al.*, 2014).

No entanto, além do seu envolvimento em processos neurofisiológicos e cognitivos, as alterações nos padrões oscilatórios têm sido associadas a várias neuropatologias, incluindo doença de Alzheimer, doença de Parkinson, transtorno do espectro do autismo (TEA), esquizofrenia e epilepsia (Uhlhaas e Singer, 2010; Goutagny *et al.*, 2013; Wang *et al.*, 2013; Nina *et al.*, 2014; Staba, Stead e Worrell, 2014; Kessler, Seymour e Rippon, 2016; Takeuchi e Berényi, 2020). Por isso, a análise das alterações dos padrões oscilatórios tem cada vez mais se tornado útil para o diagnóstico de doenças neurológicas já estabelecidas e processos patológicos em andamento, assim como prognóstico terapêutico (Yener e Basar, 2013; Takeuchi e Berényi, 2020).

Na epilepsia, as alterações nos padrões oscilatórios são indicados como preditivos de crises epilépticas, uma vez que refletem processos patológicos dos circuitos neuronais (Zijlmans *et al.*, 2012; Staba, Stead e Worrell, 2014; Pitkänen *et al.*, 2016). Estudos já demonstraram a alteração das oscilações delta (1-4Hz) (Pasquetti *et al.*, 2019), teta (4-8 Hz) (Arabadzisz *et al.*, 2005; Dugladze *et al.*, 2007; Chauvière *et al.*, 2009; Kitchigina e Butuzova, 2009; Grasse, Karunakaran e Moxon, 2013; Broggini *et al.*, 2016) e também das HFOs (80-500 Hz) (Bragin, Engel, Wilson, Fried e Buzsáki, 1999; Worrell *et al.*, 2008; Zijlmans *et al.*, 2012; Matsumoto *et al.*, 2013; Pearce *et al.*, 2013; Hamidi, Lévesque e Avoli, 2014; Uva *et al.*, 2017) em

estágios precoces da epileptogênese e durante crises epilépticas, sendo indicadores da zona de início da crise e também estimulando a formação de redes neuronais geradoras de crises (Bragin, Engel, Wilson, Fried e Mathern, 1999; Jirsch *et al.*, 2006; Lévesque *et al.*, 2012, 2017; Weiss *et al.*, 2016).

As análises de padrões oscilatórios de áreas isoladas do cérebro são importantes, mas não o suficiente para explicar todos os aspectos de processamento de informações dentro do cérebro. Portanto, além das mudanças locais na dinâmica das oscilações cerebrais, a dinâmica de conectividade entre diferentes áreas do cérebro devem ser investigadas para uma descrição mais precisa dos mecanismos neurofisiológicos subjacentes às doenças neurológicas (Mathalon e Sohal, 2015).

O sistema límbico gera ritmos fisiológicos sincronizados no cérebro normal, no entanto no cérebro de pacientes e animais com epilepsia, a sincronização se torna patológica (Avoli, 2014). O aumento da sincronia já foi demonstrado em modelos experimentais de ELT, onde há o aumento de sincronização entre diferentes regiões límbicas (Avoli *et al.*, 1996; Barbarosie e Avoli, 1997; Gafurov e Bausch, 2013; Grasse, Karunakaran e Moxon, 2013; Broggini *et al.*, 2016). Além disso, alterações de sincronia em bandas de frequência específicas também foram evidenciadas em modelos experimentais (Grasse, Karunakaran e Moxon, 2013; Broggini *et al.*, 2016; Pasquetti *et al.*, 2019) e pacientes com epilepsia (Warren *et al.*, 2010; Cotic *et al.*, 2013, 2015). Portanto, a sincronização neuronal excessiva é um fenômeno que ocorre entre as células, dentro de redes locais e entre estruturas límbicas, sendo considerado um biomarcador das epilepsias, principalmente por ser determinante na geração de crises espontâneas recorrentes (Grasse, Karunakaran e Moxon, 2013; Jiruska *et al.*, 2013; Avoli, 2014).

3 MODELOS ANIMAIS DE EPILEPSIAS

O entendimento sobre os mecanismos subjacentes à epileptogênese e geração de crises na ELT e outras formas de epilepsia não pode ser totalmente adquirido em estudos clínicos com humanos. Como resultado, o uso de modelos animais adequados é essencial. Os modelos animais *in vivo* de epilepsia incluem várias ferramentas, incluindo agentes neuroquímicos, protocolos de estimulação elétrica, insultos térmicos ou hipóxicos, lesões traumáticas, optogenética, e linhagens de roedores com indução idiopática ou crises audiogênicas. Dessa forma, torna-se viável a investigação e manipulação dos mecanismos subjacentes às epilepsias, sendo assim uma área importante da pesquisa em epilepsia (Kandratavicius *et al.*, 2014).

Modelos *in vitro* compostos por sistemas biológicos mais simples também podem ser particularmente úteis para o estudo de mecanismos celulares e moleculares envolvidos na progressão da epileptogênese. As preparações de tecido cerebral *in vitro* permitem o estudo acessível das redes cerebrais e a identificação de características moleculares, celulares e eletrofisiológicas sobre a função cerebral muitas vezes não disponível nos modelos *in vivo*. Nesses modelos, preparações cerebrais de roedores e de tecido humano pós-cirúrgico podem ser usadas de forma aguda ou através de uma preparação organotípica, e podem gerar uma atividade elétrica *in vitro* semelhante à atividade eletrográfica observada em pacientes com epilepsia. Além disso, os modelos *in vitro* podem consumir menos tempo e recursos em comparação aos modelos *in vivo*, principalmente considerando os modelos crônicos de epilepsia (Dulla *et al.*, 2018).

3.1 Modelos *in vivo* de ELT

A maior parte do conhecimento atual sobre a fisiopatologia da ELT é baseado em modelos animais que reproduzem uma sequência de eventos semelhantes aos observados em pacientes com ELT. Os três modelos mais comumente utilizados de ELT são o modelo de abrasamento ou kindling (Goddard, 1967), modelo de ácido caínico (Nadler, Perry e Cotman, 1978; Lévesque; e Avoli, 2013) e o modelo de pilocarpina (Turski *et al.*, 1983; Curia *et al.*, 2008). Cada modelo compartilha similaridades com a epilepsia humana, no entanto, nenhum modelo é uma representação perfeita (homóloga). Fazendo uso do modelo adequado, os pesquisadores podem investigar as mudanças que ocorrem durante a epileptogênese e a ictogênese.

3.1.1 Modelo de epilepsia induzida por pilocarpina

Descrito pela primeira vez no início da década de 1980, o modelo de pilocarpina é o terceiro modelo de epilepsia mais comumente utilizado e acredita-se que esse é o modelo que mais se assemelha ao decurso da ELT adquirida (Turski *et al.*, 1983; Cavalheiro *et al.*, 2006; Curia *et al.*, 2008; Scorza *et al.*, 2009).

A Pilocarpina é um agonista não específico de receptores colinérgicos do tipo muscarínico, que induz *Status Epilepticus (SE)* por meio da ativação do receptor muscarínico M1. A ativação do receptor M1 regula positivamente a fosfolipase C, o trifosfato de inositol e o Ca^{+2} intracelular, alterando correntes de K^{+} e Ca^{+2}. O aumento da excitabilidade ocorre provavelmente devido à diminuição da atividade das ATPases no hipocampo, que não repolarizam a membrana. O aumento do Ca^{+2} promove a liberação de glutamato, que age nos receptores AMPA, permitindo a entrada de Na^{+} e de mais Ca^{+2}. A despolarização permite a ativação dos receptores

NMDA, que novamente permitem a entrada de Ca^{+2} na célula pós-sináptica, o que, de maneira prolongada, induz excitotoxicidade e morte celular. A massiva ativação de receptores de glutamato, com retroalimentação positiva pela entrada constante de Ca^{+2} acaba por gerar um prolongado *SE*, capaz de danificar permanentemente a rede neuronal do animal, o que desencadeará a epileptogênese (Cavalheiro *et al.*, 2006).

Em camundongos nocaute para o receptor muscarínico M1, a pilocarpina não induz crises epilépticas (Hamilton *et al.*, 1997). Além disso, o *SE* induzido por pilocarpina pode ser bloqueado pela administração do antagonista muscarínico atropina (Maslanski *et al.*, 1994).

O modelo de pilocarpina é caracterizado pela administração de uma única dose de pilocarpina pela via sistêmica (ou intraperitoneal, i.p.) ou via intrahipocampal (De Furtado *et al.*, 2002; Lévesque, Avoli e Bernard, 2016). Ambos os métodos de administração induzem similares características eletrofisiológicas, comportamentais, bem como alterações histopatológicas, às observadas em pacientes com ELT (Curia *et al.*, 2008). No entanto, este conceito ainda precisa ser revisto pois a quantidade de áreas lesadas e redes associadas no método de administração sistêmico (Leite, Garcia-Cairasco e Cavalheiro, 2002; Castro *et al.*, 2011), indicam que estruturas extratemporais e subcorticais estão envolvidas na expressão de alterações comportamentais, EEG, celulares e moleculares, muito além das classicamente associadas à ELT.

Os eventos induzidos pela administração de pilocarpina incluem o *SE* seguido por um período latente com a ausência de crises epilépticas (Turski *et al.*, 1983), que está associado à reorganização das redes neurais e mudanças na excitabilidade celular (Pitkänen e Sutula, 2002; Cavalheiro *et al.*, 2006). A duração do período latente depende de inúmeros fatores, incluindo dose e suscetibilidade à pilocarpina,

tempo do *SE*, idade e peso (Curia *et al.*, 2008). Após o período latente, entre 1−4 semanas, se inicia uma condição crônica de crises espontâneas recorrentes (Cavalheiro *et al.*, 2006; Curia *et al.*, 2008; Lévesque, Avoli e Bernard, 2016).

A manifestação motora das crises epilépticas é classificada em cinco estágios de acordo com a escala de Racine, iniciando com um leve comportamento anormal (estágio um) até as crises tônico-clônicas (estágio cinco) (Racine, 1972). As taxas de mortalidade neste modelo são muito altas, com alguns estudos relatando entre 20% - 40% de mortalidade (Curia *et al.*, 2008; Lévesque, Avoli e Bernard, 2016). Como uma abordagem alternativa para reduzir a mortalidade dos animais, pode-se reduzir a duração do *SE*, utilizando diazepam (5 – 10 mg/ kg) (Pitkänen *et al.*, 2005). No entanto, deve-se notar que a duração do *SE* é crucial para o desenvolvimento da epilepsia (Curia *et al.*, 2008; Chen *et al.*, 2013).

O dano neuronal excitotóxico associado a alterações moleculares levam à morte neuronal, reorganização sináptica, sinaptogênese e neurogênese no GD, bem como mudanças nas propriedades eletrofisiológicas neuronais e nos circuitos inibitórios, perda de interneurônios GABAérgicos no hipocampo, brotamento de fibras musgosas, proliferação de astrócitos e outras características muito similares às observadas em pacientes com ELT (Pitkänen e Sutula, 2002; Cavalheiro *et al.*, 2006; Nirwan, Vyas e Vohora, 2018). As regiões hipocampais CA1 e CA3, amígdala, tálamo, neocórtex e córtex piriforme são altamente suscetíveis ao danos neuronais induzidos pela pilocarpina (Kandratavicius *et al.*, 2014; Nirwan, Vyas e Vohora, 2018). No entanto, independentemente da lesão encontrada em pacientes ou modelos animais de ELT, o principal questionamento são os mecanismos envolvidos na geração das crises espontâneas na ELT.

3.2 Modelos *in vitro* de epilepsia

As preparações *in vitro* de fatias cerebrais são um meio extremamente útil para o estudo de crises epilépticas e epilepsia. Alguns dos modelos de atividade epileptiforme induzida em tecido cerebral *in vitro* mimetizam a atividade gerada no tecido epiléptico durante o período crônico, além de serem semelhantes à epilepsia humana fármaco-resistente (Dulla *et al.*, 2018). Há uma série de modelos utilizando fatias cerebrais e a indução de atividade epileptiforme *in vitro*, os quais são utilizados para investigar os mecanismos da gênese e propagação de atividade epiléptica, atividades celulares e de rede, e também o estudo da eficácia de tratamentos farmacológicos (Heinemann, Kann e Schuchmann, 2006; Avoli e Jefferys, 2015; Heuzeroth *et al.*, 2019).

A utilização *in vitro* de preparações de fatias cerebrais foi sugerida pela primeira vez por um estudo no qual eventos semelhantes a crises epilépticas foram induzidos pela redução da concentração extracelular de Cl^- no meio de perfusão de fatias agudas de hipocampo (Yamamoto, 1972). Eventos semelhantes a crises epilépticas podem ser induzidos pela redução do Ca^{2+} ou Mg^{2+} ou aumento da concentração de K^+ no meio extracelular (Subramanian *et al.*, 2018; Codadu, Parrish e Trevelyan, 2019). Esses estudos reforçaram que além do hipocampo outras estruturas corticais são suscetíveis ao desenvolvimento de eventos semelhantes a crises epilépticas, fornecendo também ferramentas para o estudo de propagação desse tipo de eventos entre regiões distintas das fatias cerebrais (Avoli e Jefferys, 2015; Dulla *et al.*, 2018). Alternativamente, a aplicação farmacológica de drogas com potencial ictogênico, como 4-aminopiridina (4-AP), ácido caínico ou pilocarpina podem ser utilizados (Lévesque; e Avoli, 2013; Avoli e Jefferys, 2015; Nirwan, Vyas e Vohora, 2018).

No entanto, ao utilizar esses modelos deve-se ter em mente as desvantagens de tais preparações, uma vez que não possuem elementos importantes de modelos *in vivo*, como conectividade de longo alcance no cérebro, diferenças na fisiologia e anatomia cerebral entre as espécies e também características comportamentais, dessa maneira refletindo aspectos limitados da epilepsia (Dulla *et al.*, 2018).

3.2.1 4-aminopiridina

O modelo de epilepsia *in vitro* induzido por 4-aminopiridina (4-AP) tem sido amplamente utilizado nas últimas três décadas, com o objetivo de identificar os mecanismos subjacentes à sincronização do hipocampo e redes neuronais parahipocampais (Perreault e Avoli, 1991; Avoli *et al.*, 1996; Barbarosie e Avoli, 1997; Calcagnotto, Barbarosie e Avoli, 2000; D'Antuono *et al.*, 2002; Avoli e de Curtis, 2011; Lisgaras, Mikroulis e Psarropoulou, 2021).

A 4-AP é um composto bloqueador de canais de K^+ dependentes de voltagem (Figura 6), bem conhecido pela preservação da transmissão GABAérgica e glutamatérgica (Buckle e Haas, 1982; Perreault e Avoli, 1991; Traub, Colling e Jefferys, 1995). Com o bloqueio dos canais de K^+ dependentes de voltagem há uma despolarização da membrana plasmática e um aumento da duração do potencial de ação. Além disso, a 4-AP também atua na ativação de canais de Ca^{2+} dependentes de voltagem (VACCs), especificamente canais de Ca^{2+} ativados por alta voltagem (HVACCs) (Wu *et al.*, 2009). Dessa forma, a 4-AP aumenta a concentração de Ca^{2+} intracelular e liberação de neurotransmissores. Essa ação juntamente com o aumento da duração do potencial de ação contribui para a excitabilidade neuronal; e consequente indução de atividade epileptiforme em fatias cerebrais (Voskuyl e Albus, 1985; Rutecki, Lebeda e Johnston, 1987; Avoli *et al.*, 1996; Avoli e Jefferys, 2015).

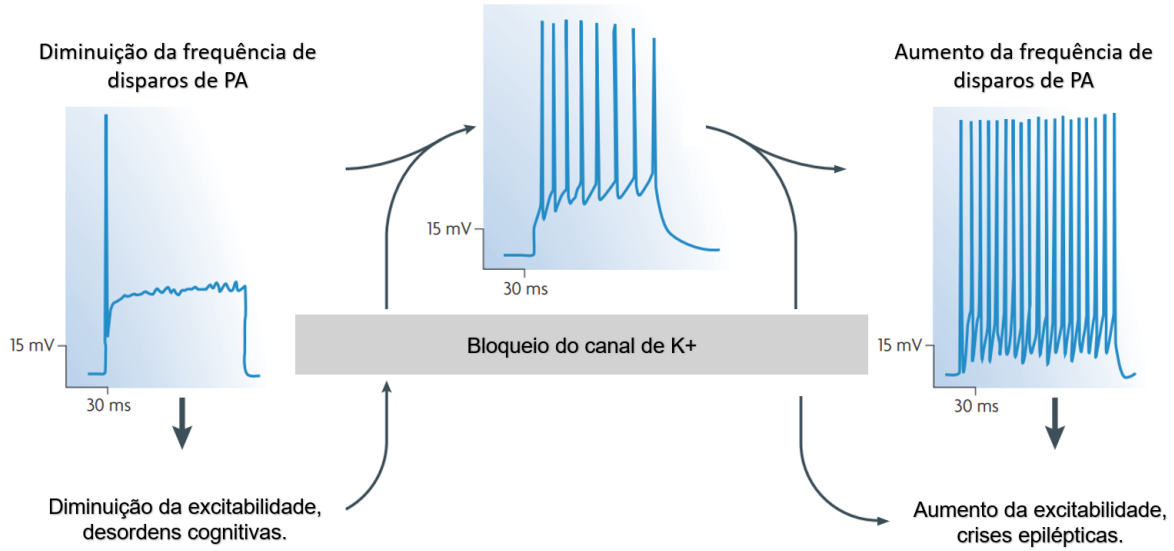

Figura 6 Células excitáveis que geram potenciais de ação (PAs) com uma frequência reduzida, podem ter essa frequência aumentada a níveis normais, através do bloqueio dos canais de K+. O bloqueio dos canais de K+ leva à despolarização da membrana celular tornando seu potencial mais próximo do limiar de disparo de PAs, facilitando a geração, e também aumentando a duração dos PAs e a hiperexcitabilidade. Figura modificada de (Wulff, Castle e Pardo, 2009).

A sua utilização *in vitro* foi primeiramente demonstrada por Galvan e colaboradores (Galvan, Grafe e Bruggencate, 1982), onde a 4-AP foi capaz de induzir eventos ictais espontâneos ou evocados por estímulo em fatias corticais de porquinho-da-índia. Em fatias hipocampais, Voskuyl & Albus (1985) identificaram dois tipos de eventos, denominados interictais; o primeiro tipo de evento interictal se assemelhava a atividade epileptiforme espontânea induzida por antagonistas de receptor $GABA_A$, e se originava na região CA3, enquanto o segundo tipo de evento interictal teve maior duração, e propagou-se de forma mais lenta, e não teve alteração na presença de antagonistas glutamatérgicos (Voskuyl e Albus, 1985). Esses resultados foram confirmados posteriormente por outros estudos (Rutecki, Lebeda e Johnston, 1987; Perreault e Avoli, 1991; Avoli *et al.*, 1996).

Os eventos epileptiformes registrados em preparações de fatias cerebrais *in vitro* consistem em despolarizações neuronais, levando ao disparo do potencial de ação síncrono e sustentado neuronal (Avoli *et al.*, 2002). Como mencionado

anteriormente, ambas as transmissões excitatórias e inibitórias são preservadas no modelo *in vitro* de 4-AP (Rutecki, Lebeda e Johnston, 1987), e dessa forma modulam as frequências e durações dos eventos epileptiformes (Avoli *et al.*, 2002), gerando um potencial de campo local específico, o qual possui similaridade com a atividade de potencial de campo observada em pacientes com epilepsia focal (Avoli *et al.*, 2002; Gonzalez-Sulser *et al.*, 2011; Dulla *et al.*, 2018). Dessa forma, os eventos gerados pela aplicação de 4-AP no meio de perfusão de fatias cerebrais consistem em três tipos de atividade no potencial de campo: i) eventos interictais rápidos mediados principalmente por receptores de glutamato, ii) eventos interictais lentos mediados por GABA e iii) eventos ictais de longa duração, mediados por ambas transmissões excitatórias e inibitórias (Barbarosie e Avoli, 1997; Avoli *et al.*, 2002; Gonzalez-Sulser *et al.*, 2011).

A atividade interictal, que é mediada por receptores de glutamato, origina-se em CA3, se espalha através de CA1 e do subículo para a CE, e retorna para CA3 através do GD (via perfurante). Em contraste, os eventos ictais, dependentes da ativação dos receptores glutamatérgicos e $GABA_A$, são iniciados no CE de onde se propagam sucessivamente para o GD, áreas CA3 e CA1 hipocampais, e o subículo (Gonzalez-Sulser *et al.*, 2011). Além disso, para que eventos ictais estejam presentes no hipocampo é necessária uma conexão preservada entre o CE e o hipocampo (Barbarosie e Avoli, 1997; Barbarosie *et al.*, 2000).

A utilização de 4-AP em preparações cerebrais *in vitro* é uma ferramenta útil para o estudo dos mecanismos subjacentes à epilepsia. Além disso, o modelo de epilepsia *in vitro* induzido por 4-AP tem sido utilizado para a avaliação de AEDs, e apresenta resultados coerentes em relação à eficácia clínica das mesmas (D'Antuono *et al.*, 2010; Heuzeroth *et al.*, 2019).

Os eventos interictais, em particular, desempenham um papel extremamente relevante na epileptogênese, sendo considerados um biomarcador eletroencefalográfico de processos neuropatológicos em andamento no tecido epiléptico (de Curtis e Avanzini, 2001; Rosati *et al.*, 2003; de Curtis, Jefferys e Avoli, 2013). As descargas epileptiformes interictais são um fenômeno complexo que envolve vários processos celulares e da rede neuronal (de Curtis e Avanzini, 2001; Huberfeld *et al.*, 2011; Chvojka *et al.*, 2019), e a sua detecção no EEG possui alto valor diagnóstico e também preditivo para a ocorrência de crises epilépticas (Rosati *et al.*, 2003; Jacobs *et al.*, 2008; Bortel *et al.*, 2010; Chauvière *et al.*, 2012; Chvojka *et al.*, 2019; Glaba *et al.*, 2020). O entendimento dos mecanismos neurofisiológicos, dinâmica temporal, e a organização da rede neuronal durante o período interictal e/ou entre eventos interictais pode fornecer um redirecionamento significativo e altamente informativo sobre a epileptogênese (Salami, Lévesque, *et al.*, 2014; Lévesque, Salami, *et al.*, 2018).

4 HIPÓTESE E JUSTIFICATIVA

A formação hipocampal apresenta uma rede sináptica extremamente organizada entre aferências, interações locais e eferências para as demais regiões corticais/subcorticais. Sabemos que existem alterações estruturais e sinápticas na rede neuronal da formação hipocampal na ELT (Curia *et al.*, 2014; Navidhamidi, Ghasemi e Mehranfard, 2017) e que o sistema GABAérgico tem um papel muito importante na epileptogênese (Treiman, 2001; Khazipov, 2016; Zandt e Naegele, 2017; Dudek, 2020). Estas alterações podem induzir mudanças nos padrões de oscilações e na sincronia entre diferentes áreas envolvidas no processo de hiperexcitabilidade, epileptogênese e ictogênese.

Portanto, nossa hipótese é que as áreas que compreendem a formação hipocampal apresentam um aumento da susceptibilidade à ictogênese e mudanças nos padrões oscilatórios associados a descargas epileptiformes, e que tais alterações são específicas de cada fase de desenvolvimento da epileptogênese.

Além disso, como o envolvimento do sistema GABAérgico é crucial na epileptogênese, e a função específica dos vários subtipos de interneurônios inibitórios está comprometida durante o processo epileptogênico, buscamos fazer uma revisão crítica sobre o conceito pré-estabelecido de que a característica chave no desenvolvimento da epilepsia é apenas o aumento da excitação e a diminuição da inibição.

5 OBJETIVOS

5.1 Objetivos gerais

Investigar os padrões de geração de atividade epileptiforme, potência e sincronia nas vias trissináptica hipocampal e temporoamônica, em diferentes períodos da epileptogênese, em modelo de epilepsia induzida por pilocarpina em ratos. Além disso, revisar o papel do sistema GABAérgico na fisiopatologia da epilepsia, e revisitar os mecanismos inibitórios envolvidos no balanço entre excitação e inibição no cérebro.

5.2 Objetivos específicos

5.2.1. Caracterizar a geração de atividade epileptiforme no CE, GD, CA3 e CA1 em fatias de hipocampo-CE de animais epilépticos e controle, 30 e 60 dias após o *SE*, durante a hiperexcitabilidade induzida por 4-AP.

5.2.2. Investigar as alterações dos padrões oscilatórios em CE, GD, CA3 e CA1 em fatias de hipocampo-CE de animais epilépticos e controle, 30 e 60 dias após o *SE*, durante a hiperexcitabilidade induzida por 4-AP.

5.2.3. Examinar a sincronia das oscilações entre CE, GD, CA3 e CA1 em fatias de hipocampo-CE de animais epilépticos e controle, 30 dias e 60 após o *SE*, durante a hiperexcitabilidade induzida por 4-AP.

5.2.4. Investigar as alterações nos padrões oscilatórios em CE, GD, CA3 e CA1 em fatias de hipocampo-CE de animais epilépticos e controle, 30 e 60 dias após o *SE*, durante a atividade de rede basal e espontânea.

5.2.5. Detectar alterações na sincronia de oscilações entre CE, GD, CA3 e CA1 em fatias de hipocampo-CE de animais epilépticos e controle, 30 e 60 dias após o *SE*, durante a atividade de rede basal e espontânea.

5.2.6. Revisar a fisiopatologia da epilepsia e o envolvimento do sistema GABAérgico no desbalanço entre excitação e inibição no cérebro, revisitando a função dos interneurônios além da inibição no circuito.

PARTE II- METODOLOGIA E RESULTADOS

A parte II do presente trabalho está dividida em dois capítulos.

O capítulo I contém a versão aceita permitida para divulgação pela revista do artigo científico *"In vitro oscillation patterns throughout the hippocampal formation in a rodent model of epilepsy"*, publicado na revista científica ***Neuroscience*** (DOI:10.1016/j.neuroscience.2021.10.020). Neste capítulo descrevemos as alterações encontradas na geração de atividade epileptiforme, nos padrões oscilatórios e na sincronia entre regiões da formação hipocampal *in vitro* de animais epilépticos, durante dois períodos da epileptogênese.

O capítulo II contém a versão aceita permitida para divulgação pela revista do artigo de revisão *"GABAergic interneurons in epilepsy: More than a simple change in inhibition"*, publicado na revista científica ***Epilepsy & Behavior*** (DOI: 10.1016/j.yebeh.2020.106935). Este artigo ressalta o envolvimento do sistema GABAérgico na fisiopatologia da epilepsia, e em particular, debate a função dos interneurônios na regulação da excitação e inibição no cérebro.

Capítulo I

In vitro oscillation patterns throughout the hippocampal formation in a rodent model of epilepsy

***In vitro* oscillation patterns throughout the hippocampal formation in a rodent model of epilepsy**

Joseane Righes Marafiga[a,b], Mayara Vendramin Pasquetti[a,b], Maria Elisa Calcagnotto[a,b*].

[a] Neurophysiology and Neurochemistry of Neuronal Excitability and Synaptic Plasticity Laboratory (NNNESP Lab.), Department of Biochemistry, ICBS, Universidade Federal do Rio Grande do Sul, Porto Alegre 90035-003, RS, Brazil

[b] Graduate Program in Biological Science: Biochemistry, Universidade Federal do Rio Grande do Sul, Porto Alegre 90035-003, RS, Brazil

*** Corresponding author:**

Maria Elisa Calcagnotto, MD, PhD

Address: NNNESP Lab., Department of Biochemistry, ICBS, Universidade Federal do Rio Grande do Sul (UFRGS), R. Ramiro Barcelos 2600, Anexo 21111, Porto Alegre, RS, 90035-003, Brazil.

Phone: +55 51 33085570

E-mail: elisa.calcagnotto@ufrgs.br

ABSTRACT

Specific oscillatory patterns are considered biomarkers of pathological neuronal network in brain diseases, such as epilepsy. However, the dynamics of underlying oscillations during the epileptogenesis throughout the hippocampal formation in the temporal lobe epilepsy is not clear. Here, we characterized *in vitro* oscillatory patterns within the hippocampal formation of epileptic rats, under 4-aminopyridine (4-AP)-induced hyperexcitability and during the spontaneous network activity, at two periods of epileptogenesis. First, at the beginning of epileptic chronic phase, 30 days post-pilocarpine-induced *Status Epilepticus (SE*). Second, at the established epilepsy, 60 days post-*SE.* The 4-AP-bathed slices from epileptic rats had increased susceptibility to ictogenesis in CA1 at 30 days post-*SE,* and in entorhinal cortex and dentate gyrus at 60 days post-*SE.* Higher power and phase coherence were detected mainly for gamma and/or high frequency oscillations (HFOs), in a region- and stage-specific manner. Interestingly, under spontaneous network activity, even without 4-AP-induced hyperexcitability, slices from epileptic animals already exhibited higher power of gamma and HFOs in different areas of hippocampal formation at both periods of epileptogenesis, and higher phase coherence in fast ripples at 60 days post-*SE.* These findings reinforce the critical role of gamma and HFOs in each one of the hippocampal formation areas during ongoing neuropathological processes, tuning the neuronal network to epilepsy.

Key words: gamma rhythm, high-frequency oscillations, *in vitro* electrophysiology, hippocampus, coherence, synchrony

INTRODUCTION

Epilepsy is one of the most common neurological disorders. About 65 million people worldwide are diagnosed with epilepsy (Thurman *et al.*, 2011; Sirven, 2015). In particular, the temporal lobe epilepsy (TLE), a common form of refractory epilepsy in adulthood (Berg *et al.*, 2010), is characterized by seizures generated in the temporal cortex and limbic structures, including hippocampus, entorhinal cortex (EC) and amygdala (Bertram, 2009; Goldberg e Coulter, 2013; Toyoda *et al.*, 2013; Boido *et al.*, 2014). TLE can be also associated with hippocampal sclerosis characterized by cell loss in the hippocampal CA3 and CA1 areas and in the dentate gyrus (DG) (Sloviter, 2008; Bertram, 2009; Thom, 2014; Walker, 2015), synaptic reorganization (Sutula *et al.*, 1989; Cross e Cavazos, 2007; Danzer *et al.*, 2010; Zhang *et al.*, 2014) and altered GABAergic inhibition (Zandt e Naegele, 2017; Righes Marafiga, Vendramin Pasquetti e Calcagnotto, 2020).

Neural network oscillations are considered as indicator of the rhythmic neuronal excitability and synaptic function and are fundamental in coordinating neural activity throughout the brain (Fries, 2005). An important hallmark of dysfunctional neural networks is the excessive or abnormal neuronal activity (Fisher *et al.*, 2005; Grasse, Karunakaran e Moxon, 2013; Jiruska *et al.*, 2013) that can be recorded on the electroencephalogram (EEG) (Fisher, Scharfman e deCurtis, 2014). The altered brain oscillation patterns seen in epilepsy patients (Bartolomei *et al.*, 2001; Kramer e Cash, 2012), have also been identified in neurological and psychiatric disorders, such as schizophrenia (Uhlhaas e Singer, 2010), Alzheimer's disease (Goutagny *et al.*, 2013), and autism spectrum disorder (ASD) (Kessler, Seymour e Rippon, 2016).

Changes in brain oscillation patterns are becoming useful biomarkers to identify the epileptic foci and to predict the development of pathological neural networks

(Zijlmans *et al.*, 2012; Staba, Stead e Worrell, 2014; Pitkänen *et al.*, 2016). Studies have demonstrated an altered power spectral density (PSD) of delta (1−4 Hz) (Pasquetti *et al.*, 2019), theta (4−12 Hz) (Arabadzisz *et al.*, 2005; Dugladze *et al.*, 2007; Chauvière *et al.*, 2009; Kitchigina e Butuzova, 2009), and high-frequency oscillations (HFOs) (80−500 Hz) (Worrell *et al.*, 2008; Zijlmans *et al.*, 2012; Matsumoto *et al.*, 2013; Pearce *et al.*, 2013; Hamidi, Lévesque e Avoli, 2014; Uva *et al.*, 2017) at early stages of epileptogenesis and during the chronic spontaneous recurrent seizures (SRS). Interictal oscillations in particular, which include interictal epileptiform discharges (IEDs) and the occurrence of pathological HFOs (termed fast ripples) are considered markers of abnormal neural network activity (Jefferys *et al.*, 2012; Salami, Lévesque, *et al.*, 2014; Staba *et al.*, 2017), reflecting the dynamic processes occurring at the seizure onset zone and pathological mechanisms underlying the establishment of focal epileptic disorders (Lévesque *et al.*, 2011; Jefferys *et al.*, 2012; Salami, Lévesque, *et al.*, 2014; Lévesque, Salami, *et al.*, 2018; Ewell *et al.*, 2019)**.**

In addition to changes in oscillatory patterns, synchronization between distinct network activities also could be predictive of seizure development (Grasse, Karunakaran e Moxon, 2013; Jiruska *et al.*, 2013; Broggini *et al.*, 2016; Kitchigina, 2018). Synchronized activities between different areas of the brain provide dynamic changes in neuronal ensembles coordination, which is crucial to the control of network excitability, and consequently the ictogenesis and epileptogenesis processes (Uhlhaas e Singer, 2006; Buzsáki e Watson, 2012). In limbic regions, changes in neuronal synchronization can precede and facilitate development of SRS (Traub *et al.*, 2004; Grasse, Karunakaran e Moxon, 2013; Jiruska *et al.*, 2013). Therefore, it is crucial to investigate the network oscillatory changes underlying epileptiform activity initiation and propagation in the hippocampal formation.

Considering that seizures are difficult to predict and can be quite disruptive to the patient's life (Jacoby, 2008), it is relevant to advance our understanding about the pathogenesis of TLE, and the dynamics of underlying oscillations and synchrony during the epileptogenic process. Here, we studied the *in vitro* oscillation patterns and synchrony in hippocampal-entorhinal cortex slices from epileptic rats under 4-aminopyridine (4-AP)-induced hyperexcitability and during the spontaneous network activity, at two periods of epileptogenesis. At the beginning of epileptic chronic phase, 30 days post-*Status Epilepticus (SE*) induced by pilocarpine, and at the established epilepsy, 60 days post-*SE.*

EXPERIMENTAL PROCEDURES

Animals

All procedures in this study were performed according to the Brazilian Society for Neurosciences (SBNeC) and the Brazilian Law on the Use of Animals (Federal Law 11.794/2008), and approved by the Institutional Ethical Committee (CEUA UFRGS protocol no. 33274). We used adult male Wistar rats (30-40 days old; 100-200 g) obtained from the institutional animal facility (Department of Biochemistry, UFRGS). We focus on adult male Wistar rats in order to reduce the number of animals needed, once the female rats need to be differentiated according to the estrous cycle, and 6 more groups *per* age (30 and 60-days post-*SE* induction) will be necessary to perform such study. Animals were housed in 65x25x15 cm Plexyglass cages (2-3 animals *per* cage) and maintained under a standard 12/12-h light/dark cycle (light cycle starting at 7 am and ending at 7 pm) at an acclimatized room (22–26°C). The animals had access to water and food *ad libitum*. The study design and procedures

were reported according to the Animals in Research: Reporting in Vivo Experiments (ARRIVE) guidelines (Percie Du Sert *et al.*, 2020).

Drugs

For the *Status Epilepticus* (*SE*) induction, we used pilocarpine hydrochloride (360 mg/kg, i.p.; Sigma-Aldrich); methyl scopolamine (1 mg/kg i.p.; Sigma-Aldrich) and diazepam (10 mg/kg, i.p.; Teuto). During the *in vitro* electrophysiology, in order to induce epileptiform activity, we used 4-Aminopyridine (4-AP - 50-100 µM; Sigma-Aldrich) added to the normal artificial cerebrospinal fluid (nACSF) perfusion system (2 mL/min).

Status epilepticus induction

Aged-matched rats (*n*=45) were randomly divided in two groups: (1) injected with pilocarpine (*n*=25), and (2) injected with saline instead of pilocarpine (control group; N=20). The pilocarpine hydrochloride (360 mg/kg, i.p.; Sigma-Aldrich) was administrated intraperitoneally 20 min after methyl scopolamine administration (1 mg/kg i.p.; Sigma-Aldrich) and then each animal was observed for 90 minutes, while their seizure behavior was scored according to the Racine scale (Racine, Gartner e McIntyre Burnham, 1972). For all procedures mentioned above the final volume of injection was calculated based on 1mL/Kg of body weight. Status epilepticus (*SE*) was defined as continuous seizures with Racine score III to V, with no return to lower scores for at least 5 min. The *SE* was ended after 90 min using diazepam (10 mg/Kg, i.p.; Teuto). Four animals did not developed *SE* and were excluded of the study, and two animals died during the *SE* induction. Thereafter, the animals were subdivided in two groups: 30 days post-*SE* (*n*=9); 60 days post-*SE* (*n*=10). Studies already showed

that 30 days after pilocarpine administration animals that had *SE* can present SRS, with a mean latent period of 14.8 days (range of 4-44 days) (Curia *et al.*, 2008; Scorza *et al.*, 2009). Our group previously observed occurrence of SRS at the period after 30 days post-*SE* (Pasquetti *et al.*, 2019). Therefore, the *in vitro* electrophysiology was started at this point. SRS occurred in all animals that had *SE* and survived until 30 days after pilocarpine administration. We detected the later presence of SRS in the *SE* animals by behavioral manifestation and random observation. Animals were considered epileptic when at least two SRS were visually observed during a period of 30 to 60 days post-*SE* induction. Food and water consumption were monitored weekly after *SE* induction to guarantee the animals health. No animals needed to be euthanized.

Slice preparation

Horizontal hippocampal-EC slices (Barbarosie e Avoli, 1997; Calcagnotto, Barbarosie e Avoli, 2000) were prepared from epileptic rats at 30 and 60 days after *SE* induction, and age-matched controls. Following anesthesia with isoflurane, rats were euthanized by decapitation. The brain was rapidly removed in ice-cold oxygenated (95% O_2/5% CO_2) high-sucrose artificial cerebrospinal fluid (sACSF) containing (in mM) 150 sucrose, 50 NaCl, 25 $NaHCO_3$, 10 dextrose, 7 $MgSO_4$, 2.5 KCl, 1 NaH2PO_4 and 0.5 $CaCl_2$. The 400 µm thickness slices were cut in 4°C oxygenated sACSF using a VT 1000S microtome (Leica), incubated at 35°C for 45 min, and thereafter maintained at room temperature in normal artificial cerebrospinal fluid (nACSF) containing (in mM) 124 NaCl, 26 $NaHCO_3$, 10 dextrose, 3 KCl, 2 $CaCl_2$, 2 $MgSO_4$, and 1.25 NaH_2PO_4. Dual extracellular recordings were performed

simultaneously in the entorhinal cortex (EC) (upper layers), CA1 (*stratum radiatum*), CA3 (*stratum radiatum*) and/or dentate gyrus (DG) (granule cell layer).

In vitro electrophysiology

Each slice was individually transferred to the recording chamber, which was continuously perfused with oxygenated nACSF (2-3 mL/min at room temperature). Dual extracellular recordings were performed simultaneously within the hippocampal formation (CA1, CA3, DG and EC) of individual slice, visualized using an infrared differential interference contrast (IR-DIC) video-microscopy system (BX51WI, Olympus), and 4x objective. Patch micropipettes (4–7 MΩ) were pulled from borosilicate glass using a computer-controlled micropipette puller (P-1000, Sutter Instrument) and filled with nACSF.

The spontaneous local field potentials (LFP) of hippocampus and EC were recorded during 5 min of nACSF slice perfusion. Thereafter, field potential profiles were recorded during nACSF slice perfusion with 4-AP (50-100µM) for at least 2 hours, to the development of epileptiform activity. As previously described (Avoli *et al.*, 1996; Calcagnotto, Barbarosie e Avoli, 2000; D'Antuono *et al.*, 2002), hippocampal–EC slices from pilocarpine-treated and control rats responded to 4-AP by generating interictal and ictal discharges. *In vitro* dual extracellular recordings were made in a total of four locations, always in one of hippocampal recording sites: CA1 (stratum radiatum), CA3 (stratum radiatum), granule cell layer of DG; and also, in the layer 2/3 of EC. The pair of electrodes were placed as follows: EC-DG, EC-CA1, CA1-CA3, and DG-CA3. Data were monitored and recorded using the Multiclamp 700B amplifier (Molecular Devices), coupled oscilloscope and acquired by pClamp 10.3 software

(Molecular Devices). Recordings were sampled at 10 kHz, and low pass filtered at 2 kHz.

Data analysis

Subsequent data analyses were performed with CLAMPFIT 10.3 (Molecular Devices). The latency, rate of occurrence and duration of interictal and ictal discharges were analyzed offline (Calcagnotto, Barbarosie e Avoli, 2000; D'Antuono *et al.*, 2002; Codadu *et al.*, 2019). Comparisons were made between control and epileptic aged-matched animals, and between aged-matched animals with the same treatment (saline or pilocarpine).

We performed the power spectral densities (PSD) and phase coherence analysis using MATLAB (Pasquetti *et al.*, 2019). In slices perfused with nACSF without developing epileptiform activity, we selected 5s-epochs of the spontaneous LFP activity, recorded from slices of both groups 30- and 60-days post-SE. For recordings under 4-AP-bath application, we selected 5s-epochs of LFP of interictal periods, corresponding to the intervals between interictal events discharges (IEDs), to make sure that no interictal spike was present**.** We computed the PSD using the *pwelch* function from the Signal Processing Toolbox. Phase coherence was computed using *mscohere function* (Signal Processing Toolbox). Both calculations were carried out using 4-s Hamming windows with 50% overlap. The frequency bands were separated in delta (1-4 Hz), theta (4-12 Hz), beta (12- 30 Hz), slow gamma (30-50 Hz), middle gamma (50-90 Hz) and HFOs (fast gamma (90-150 Hz), ripples (150-250 Hz) and fast ripples (250-400 Hz) (Buzsáki, 2006; Belluscio *et al.*, 2012; Tort *et al.*, 2013; Pasquetti *et al.*, 2019). In order to verify the presence of oscillations, we estimate the peak frequency according to (Scheffzük *et al.*, 2013). To estimate the peak of frequency,

we fitted a 1/f curve using power values around each frequency band of interest and then we obtained a normalized peak power value by subtracting the 1/f fit from the real peak power value (Scheffzük *et al.*, 2013; Scheffer-Teixeira e Tort, 2017). To ensure that changes in power can be observed besides aperiodic activity in the signal, we analyzed the PSD of two control conditions (4-AP perfusion and basal activity in control slices) removing the 1/f-like aperiodic activity from the PSD.

We presented the PSD values for each experimental conditions with the periodic and aperiodic frequency components. However, taking into account the presence of oscillations in the LFP signals identified by the PSD analysis and 1/f fitting, we observed that the 1/f background induce a modest increase of PSD values (Fig. S3 and S6), and at least in this study, the oscillatory components seem not to be either confounded with or masked by the predominant activity of 1/f noise, since the peak of frequencies are visible in the original PSD even with the 1/f background, and are still very evident after filtering (Fig. S3 and S6).

Statistical Analysis

The sample size was calculated using the Minitab 17®, based on the standard deviation, significance level and estimated statistical power of our previous work (Pasquetti *et al.*, 2019). To test the normality of the data we used the Kolmogorov-Smirnov test. Parametric data were analyzed using the Student's *t*-test. For non-parametric data, we used Mann-Whitney U test. In order to identify outliers, we used ROUT method in the GraphPad Prism. No blinding was performed in our analysis. Results were considered significant if the *p*-value was less than 0.05. Statistical analysis was performed with either GraphPad Prism version 6.01 or SPSS.

RESULTS

Characteristics of 4-AP-induced epileptiform activity in hippocampal-EC slices at 30 days post-SE induction

The 4-AP-induced epileptiform events in EC and in CA1 showed no differences either in frequency and latency of IEDs ($P > 0.05$; Fig. 1Ab, c; and $P > 0.05$, Fig. 1Ae, f, respectively; Table S1), or in frequency and duration of ictal events ($P > 0.05$; Fig. 1Ab, d and $P > 0.05$; Fig. 1Ae, g, respectively; Table S1) between epileptic and control groups. However, in CA1, the latency for the first ictal event was shorter in slices from epileptic animals, when compared to the control group ($P = 0.04$, Fig. S1B; Table S1).

In CA3, slices from epileptic animals also did not present differences either in frequency and latency of IEDs ($P > 0.05$; Fig. 1Bb, c; Table S1), or in frequency of ictal events ($P > 0.05$; Fig. 1Bb, d; Table S1). However, ictal events in CA3 of slices from epileptic animals had longer duration when compared to controls ($P = 0.03$, Fig. 1Bb, d; Table S1). In DG, IEDs in slices from epileptic animals presented lower frequency ($P = 0.02$, Fig. 1Be, f; Table S1) but with no significant difference in latency ($P > 0.05$, Fig. 1Be, f; Table S1) when compared to controls. Ictal events had lower frequency ($P < 0.0001$, Fig. 1Be, g; Table S1) and shorter duration ($P < 0.0001$, Fig. 1Be, g; Table S1) in DG, when compared to the control group. In addition, similar to CA1, the latency for the first ictal event was higher in DG in slices from epileptic animals when compared to the control group (DG: $P = 0.03$, Fig. S1D; Table S1).

We also quantified the percentage of slices able to generate ictal events recorded at 30 days post-*SE*, in epileptic and aged-matched control rats (Fig. S2; Table S1). In control slices, ictal events were observed in 90% of EC (n= 9/10 slices), 90.9% of CA1 (n= 10/11 slices), 100% of CA3 (n= 9/9 slices) and 75% of DG (n= 6/8 slices). In slices from epileptic animals, ictal events were observed in 87.5% of EC (n=

7/8 slices), 100% of CA1 (*n*= 7/7 slices), 83.3% of CA3 (*n*= 5/6 slices) and 85.7% of DG (*n*= 6/7 slices) (Fig. S2). The CA1 of slices from epileptic group had a higher percentage to generated ictal events than the control group (P =0.0032, Fig. S2B). In CA3 instead, we found a lower percentage of slices generating ictal events in the epileptic group, when compared to the control group (P < 0.001, Fig. S2C). In other hand, in EC and DG there were no significant difference between epileptic and control groups (*P* > 0.05, Fig. S2A, D).

Power spectral density in hippocampal-EC slices at periods between 4-AP-induced IEDs at 30 days post-SE induction

We next performed the PSD analysis at periods of 5s-epochs between IEDs, induced by 4-AP perfusion of hippocampal-EC slices from epileptic and control animals (Table S2). We observed that slices from epileptic animals, at 30 days post-*SE*, exhibited significantly higher power of slow gamma in EC (*P* = 0.018; Fig. 2Ab) than control slices. No significant differences were found for the other frequencies (*P* > 0.05; Fig. 2Aa, b, c, d). In CA1, there was higher power of middle gamma (*P* = 0.008) in slices from epileptic animals (Fig. 2Bb), but no significant differences for the other frequencies when compared to the control animals (*P* > 0.05 for all cases; Fig. 2Ba, b, c, d). In CA3, slices from epileptic animals presented lower power of delta (*P* < 0.0001) and theta (*P* = 0.011, Fig. 2Ca), and higher power of slow gamma (*P* = 0.008), middle gamma (*P* < 0.0001) and fast gamma (*P* < 0.0001) (Fig. 2Cb) than controls. We also found higher power of ripples (150-250 Hz) (*P* < 0.0001) and fast ripples (250-400 Hz) in CA3 (*P* = 0.002) (Fig. 2Cc, d) in slices from epileptic animals, when compared to the control. The DG of slices from epileptic animals had higher theta power (*P* = 0.012;

Fig. 2Da), with no differences in the other frequencies when compared to the control group (Fig. 2Da, b, c, d).

To confirm that changes of oscillatory activity are present although the aperiodic activity contribution, we analyzed peak frequencies of PSD separating periodic signal of aperiodic activity in 5s-epochs of in vitro recordings from 4-AP-bathed slices (Fig. S3). Peak frequency of oscillations was found in EC (Fig. S3A-F), as follows: 2.3 Hz for delta, 5.9 Hz for theta, 18.8 Hz for beta, 47.2 Hz for slow gamma, 54.9 Hz for middle gamma, 91.4 Hz for fast gamma, 156 Hz ripples and 258 Hz for fast ripples. Similar to EC, in CA1 the peak frequency of oscillations was found (Fig. S3G-L), as follows: 1.03 Hz for delta, 6.34 Hz for theta, 17.6 Hz for beta, 36.7 Hz for slow gamma, 85.1 Hz for middle gamma, 99 Hz for fast gamma, 229 Hz ripples and 261 Hz for fast ripples. In CA3 (Fig. S3M-R), the peak frequency of oscillations was 3.1 Hz for delta, 5 Hz for theta, 14.6 Hz for beta, 31.8 Hz for slow gamma, 63.1 Hz for middle gamma, 90.9 Hz for fast gamma, 165 Hz ripples and 293 Hz for fast ripples. Finally, in DG (Fig. S3S-Z), the peak frequency of oscillations was 1.95 Hz for delta, 11.9 Hz for theta, 16.5 Hz for beta, 41.5 Hz for slow gamma, 89.1 Hz for middle gamma, 101 Hz for fast gamma, 169 Hz ripples and 251 Hz for fast ripples.

Characteristics of 4-AP-induced epileptiform activity in hippocampal-EC slices at 60 days post-SE induction

In EC, we found significantly lower frequency of IEDs in slices from epileptic animals when compared to slices from control animals (P = 0.009, Fig. 3Ab, c; Table S1). However, the latency for the first interictal event was shorter in EC of slices from epileptic animals (P = 0.022, Fig.3Ab, c; Table S1). In addition, EC of slices from epileptic animals at 60 days post-*SE* had higher duration of ictal events when compared to EC of slices from epileptic animals at 30 days post-*SE* (P = 0.04; Table

S1). In CA1, there were no significant differences either in frequency and latency of IEDs (*P* > 0.05; Fig. 3Ae, f; Table S1), or in frequency and duration of ictal events (*P* > 0.05; Fig.3Ae, g; Table S1) between groups. However, ictal events in CA1 slices from epileptic animals at 60 days post-*SE* presented a higher latency to the first event than the same region at 30 days post-*SE* (*P* = 0.005; Table S1). In CA3, there were no significant differences either in frequency or latency for IEDs between epileptic and control groups (*P* > 0.05; Fig. 3Bb, c; Table S1). In addition, there was no significant difference in frequency of ictal events in CA3 of slices from epileptic animals when compared to the control group (*P* > 0.05; Fig. 3Bb, d; Table S1), but the duration of ictal events was smaller in slices from epileptic animals when compared to controls (*P* = 0.02; Fig. 3Bb, d; Table S1). Besides, the CA3 from epileptic animals at 60 days post-*SE* had a lower duration of ictal events than slices from epileptic animals at 30 days post-*SE* (*P* = 0.03; Table S1).

In DG, we did not find significant differences either in frequency or latency for IEDs in slices from epileptic animals when compared to the control group (P > 0.05; Fig. 3Be, f; Table S1). Frequency of ictal events in DG also was not different between groups (P > 0.05; Fig. 3Be, g; Table S1), but the duration of ictal events was smaller in slices from epileptic animals when compared to controls (*P* = 0.02; Fig. 3Be, g; Table S1). There was no difference in the latency for the first ictal event in all recorded regions between groups (*P* > 0.05, Fig. S4). However, the DG of slices from epileptic animals at 60 days post-*SE* still had a higher frequency of IEDs, and higher duration of ictal event, when compared to DG of slices at 30 days post-*SE* (*P* = 0.008; *P* = 0.001; Table S1).

We also evaluated the percentage of slices able to generate ictal events induced by 4-AP in epileptic rats and aged-matched control rats, at 60 days post-*SE*

induction (Fig. S5; Table S1). We are able to demonstrate that control slices presented ictal events in 66.6% of EC (*n*= 6/9 slices), 80% of CA1 (*n* = 8/10 slices), 80% of CA3 (*n*= 8/10 slices) and 44.4% of DG (*n*= 4/9 slices). In slices from epileptic animals, the ictal events were observed in 70% of EC (*n*= 7/10 slices), 80% of CA1 (*n*= 8/10 slices), 80 % of CA3 (*n*= 8/10 slices) and 75% of DG (*n*= 6/8 slices). There were no significant differences in the percentage of EC (Fig. S5A), CA1 (Fig. S5B) and CA3 (Fig. S5C) with ictal events, when compared epileptic to the control groups. However, in DG, the percentage of slices able to generate ictal events in the epileptic group was significantly higher than the control group ($P < 0.0001$, Fig. S5D).

Power spectral density in hippocampal-EC slices at periods between 4-AP-induced IEDs at 60 days post-SE induction

At 60 days post-*SE*, the hippocampal-EC slices from epileptic animals exhibited significantly differences in PSD values of different frequencies when compared to slices from the control group (Table S2). The EC had higher power of theta ($P = 0.044$) and beta ($P = 0.020$) (Fig. 4Aa). The CA1 had higher power of beta ($P = 0.013$) and slow gamma ($P = 0.020$) (Fig. 4Ba, b). The CA3 had higher power of theta ($P = 0.004$), beta ($P = 0.0002$), slow- ($P = 0.005$), middle- ($P < 0.0001$) and fast- gamma ($P = 0.021$) (Fig. 4Ca, b). Finally, the DG presented higher power of slow- ($P = 0.018$), middle- ($P < 0.0001$), and fast- gamma ($P = 0.0001$) (Fig. 4Db).

The EC of slices from the epileptic animals also had higher fast ripples power ($P < 0.0001$) (Fig. 4Ad) than the control group. In CA1, the epileptic group presented lower power of ripples ($P < 0.001$), and fast ripples ($P = 0.010$) when compared to the control group (Fig. 4Bc, d). There were no differences in power of ripples and fast ripples in CA3 between groups ($P > 0.05$; Fig. 4Cc, d). However, DG of epileptic

animals had a higher power of ripples (P = 0.012) and fast ripples (P < 0.001) (Fig. 4Dc, d), when compared to the control group.

Phase coherence analysis within hippocampal formation regions at periods between 4-AP-induced IEDs at 30- and 60-days post-SE induction

Figure 5 shows the phase coherence analysis, with corresponding matrices for control and SE groups, where x-axis represents the respective pair of electrodes recorded, while y-axis shows the mean coherence for the frequency bands (0 to 400 Hz).

At 30 days post-*SE* (Fig. 5A; Table S3), slices from epileptic animals had a lower phase coherence in middle gamma (U=188; P = 0.015) and fast ripples (U=53; P < 0.0001) between EC-DG, when compared to the control group. Also, the epileptic group had higher phase coherence in middle gamma (U=143; P = 0.01), fast gamma (t=5.33; P < 0.0001) and ripples (t=5.12; P < 0.0001) between EC-CA1. Between CA1-CA3, there were significant lower phase coherence in theta (t=2.97; P = 0.004), and fast ripples (U=202; P = 0.031); and higher in middle gamma (t=3.54; P = 0.001). Finally, between DG-CA3, slices from epileptic animals had lower phase coherence in fast ripples (P < 0.0001).

At 60 days post-*SE* (Fig. 5B; Table S3), slices from epileptic animals had lower phase coherence in middle gamma (t=2.15; P = 0.036) and ripples (t=2.52; P = 0.016) between EC-DG, both when compared to the control group. The epileptic group had lower phase coherence in delta (t=2.08; P = 0.043), beta (t=3.88; P = 0.0003), middle gamma (U=155; P = 0.009), fast gamma (U=114; P = 0.001) and ripples (U=120; P = 0.006) between EC-CA1. Higher phase coherence in fast gamma (t=3.97; P = 0.0003) was found between CA1-CA3 in slices from epileptic animals. Slices from epileptic

animals had lower phase coherence in delta (t= 3.99; *P* = 0.0003), theta (*U*=178; *P* = 0.0085), middle gamma (*t*=3.97; *P* = 0.0003), fast gamma (*t*=4.58; *P* < 0.0001) and ripples (*t*=4.42; *P* < 0.0001) between DG-CA3.

Changes in power spectral density in hippocampal-EC slices, during the spontaneous network activity, at 30 days post-SE induction

The structural, morphological and functional changes reported in the brain tissue from epileptic animals generate aberrant and pathological neuronal network and recruit different microcircuits (Riban *et al.*, 2002; Arabadzisz *et al.*, 2005; Sharma *et al.*, 2007; Curia *et al.*, 2008) that modify oscillation patterns. Would be of a great significance to detect different oscillation patterns in slices from epileptic animals even in absence of epileptiform activity induced by 4-AP.

To ensure the presence of oscillatory activity during the spontaneous network activity, through *in vitro* extracellular recordings, first we measured the PSD removing the contribution of aperiodic 1/f-like signal. Peak frequency of oscillations was found in EC (Fig. S6A-F), as follows: 3.2 Hz for delta, 5.8 Hz for theta, 17.9 Hz for beta, 41.8 Hz for slow gamma, 77.7 Hz for middle gamma, 95.2 Hz for fast gamma, 160 Hz ripples and 376 Hz for fast ripples. Similar to EC, in CA1 the peak frequency of oscillations was found (Fig. S6G-L), as follows: 3.3 Hz for delta, 5.7 Hz for theta, 27.1 Hz for beta, 44.7 Hz for slow gamma, 60 Hz for middle gamma, 109 Hz for fast gamma, 157 Hz ripples and 258 Hz for fast ripples. In CA3 (Fig. S6M-R), the peak frequency of oscillations was 2.8 Hz for delta, 6.1 Hz for theta, 18.4 Hz for beta, 42 Hz for slow gamma, 84 Hz for middle gamma, 108 Hz for fast gamma, 156 Hz ripples and 254 Hz for fast ripples. Finally, in DG (Fig. S6S-Z), the peak frequency of oscillations was 3.54 Hz for delta, 6.8 Hz for theta, 17.7 Hz for beta, 46.2 Hz for slow gamma, 57.5 Hz for middle gamma, 98 Hz for fast gamma, 154 Hz ripples and 262 Hz for fast ripples.

Although no ictal or interictal epileptiform discharges were detected, at 30 days post-*SE*, the EC of slices from epileptic animals had higher power of middle gamma (*P* =0.0008) and fast gamma (*P* = 0.010) (Fig. 6Ab; Table S4) than controls. The CA1 of slices from epileptic animals had higher power of slow gamma (*P* = 0.001) and middle gamma (*P* = 0.002), when compared to the control group (Fig. 6Bb; Table S4). In CA3, the epileptic group presented higher power of beta (*P* = 0.008) and slow gamma (*P* = 0.018) when compared to the control group (Fig. 6Ca, b; Table S4). The DG of slices from epileptic animals had higher power of delta (*P* = 0.0006) and slow gamma (*P* = 0.0002), and lower power of fast gamma (*P* = 0.040) than controls (Fig. 6Da, b; Table S4).

We did not find significant differences in power of oscillations in the range of 150 to 400 Hz between groups in EC (Fig. 6Ac, d; Table S4), CA1 (Fig. 6Bc, d; Table S4) or CA3 (Fig. 6Cc, d; Table S4). On the other hand, the DG of slices from epileptic animals had lower power of ripples than controls (*P* = 0.040) (Fig. 6Dc; Table S4).

Changes in power spectral density in hippocampal-EC slices, during the spontaneous network activity, at 60 days post-SE induction

At 60 days post-*SE*, no ictal or interictal epileptiform activity were recorded but we were able to find that the EC had higher power of delta (*P* = 0.009), beta (*P* = 0.009), slow gamma (*P* = 0.003), and lower power of fast gamma (*P* = 0.002), when compared to controls (Fig. 7Aa, b; Table S4). The CA1 of slices from epileptic animals had lower power of fast gamma (*P* = 0.001) (Fig. 7Bb; Table S4). The CA3 had higher power of delta (*P* = 0.014), theta (*P* = 0.003), beta (*P* = 0.0002), slow- (*P* = 0.002) and middle gamma (*P* = 0.040) (Fig. 7Ca, b; Table S4) than controls. Finally, the DG from epileptic animals presented higher power of beta (*P* = 0.009), slow gamma (*P* = 0.009),

middle gamma ($P < 0.0001$), and fast gamma than controls ($P < 0.0001$) (Fig. 7Da, b; Table S4).

Regarding the PSD of oscillations in the range of 150 to 400 Hz (Table S4), we found significant differences between groups in EC, CA1 and DG (Fig. 7). The EC and CA1 of slices from epileptic animals had lower power of ripples ($P < 0.0001$; $P < 0.0001$) and fast ripples ($P = 0.002$; $P < 0.0001$) (Fig. 7Ac, d; 7Bc, d) when compared to the same region in controls. There were no differences between groups in CA3 ($P > 0.05$) (Fig. 7Cc, d), while in DG, the epileptic group had higher power of ripples ($P = 0.006$) and fast ripples ($P = 0.0004$), when compared to controls (Fig. 7Dc, d).

Phase coherence analysis within hippocampal formation regions at 30- and 60-days post-SE induction during the spontaneous network activity

At 30 days post-*SE*, there were no differences in phase coherence in all oscillations between EC-DG, EC-CA1, CA1-CA3 and DG-CA3 of slices from epileptic and control animals, perfused with ACSF ($P > 0.05$) (Fig. 8A; Table S5). At 60 days post-*SE* (Fig. 8B; Table S5), the phase coherence between EC-DG also did not present significant differences in all frequencies analyzed ($P > 0.05$). However, phase coherence was lower not only in theta ($t=2.16$; $P = 0.035$), slow gamma ($t=2.37$; $P = 0.022$), middle gamma ($t=3.05$; $P = 0.004$) and ripples ($t=5.46$; $P < 0.0001$) between EC-CA1, but also in slow gamma ($t=2.39$; $P = 0.020$) and fast ripples ($U=189$; $P = 0.016$) between CA1-CA3 when compared to control slices. Finally, slices from epileptic animals presented higher phase coherence in fast ripples between DG-CA3 ($U=50$; $P < 0.0001$).

DISCUSSION

Characterization of the oscillation patterns underlying pathological neuronal network, at specific areas of hippocampal formation, during the epileptogenesis is important to understand the dynamics of epileptiform activity in TLE. Our main findings include that the 4-AP-induced higher susceptibility to ictogenesis in CA1 at 30 days post-*SE,* and in EC and DG at 60 days post-*SE;* lower power of theta oscillations in CA3 at 30 days post-*SE* and higher power of gamma and HFOs in different areas of hippocampal formation at both stages of epileptogenesis. In addition, the spontaneous network activity of hippocampal-EC slices from epileptic animals already revealed a higher power of gamma and HFOs in EC at both stages of epileptogenesis, and higher phase coherence in HFO at 60 days post-*SE* even without epileptiform discharges, reflecting the aberrant reorganization of the hippocampal formation network.

In vitro epileptiform activity induced by 4-AP

As expected, bath application of 4-AP induced epileptiform activity in hippocampal-EC slice preparations (Avoli *et al.*, 1996; Avoli e Jefferys, 2015). Also, our data reinforces that slices from pilocarpine-treated rats are susceptible to generate epileptiform activity induced by an insult of hyperexcitability as 4-AP bath application (D'Antuono *et al.*, 2002; Panuccio *et al.*, 2010).

CA1 area of slices from epileptic rats, at 30 days post-*SE,* had increased susceptibility to ictogenesis induced by 4-AP, identified by lower latency to generate ictal events, and the higher percentage of slices generating those events, when compared with control slices**.** This latency increased at 60 days post-*SE* when compared to 30 days post-*SE*, but it was similar to aged-matched controls. The hippocampal CA1 area is one of the most vulnerable regions in epilepsy in both, human and animal models of epilepsy (Lehmann *et al.*, 2000; Scharfman, 2007;

Navidhamidi, Ghasemi e Mehranfard, 2017). Several adaptive changes in the CA1 area of epileptic animals may contribute to hyperexcitability. For example, cell damage and synaptic loss (Turski *et al.*, 1983), axonal sprouting (Esclapez *et al.*, 1999; Lehmann *et al.*, 2000), altered intrinsic properties, and decreased dendritic inhibition (Cossart *et al.*, 2001) of CA1 pyramidal cells.

On the contrary, CA3 area of slices from epileptic animals at 30 days post-*SE* were less susceptible to generate ictal events induced by 4-AP than controls. In hippocampal slice preparation from patients with TLE, the CA3 area also showed to be less susceptible to generate epileptiform activity (Reyes-Garcia *et al.*, 2018). Similarly, experiments using intrinsic optical signal (IOS) showed low activity in CA3 area of slices from epileptic animals, with lower IOS at 3 weeks post-*SE*, when compared to other limbic areas, regardless of the presence of 4-AP (Biagini *et al.*, 2005). In our study, the ictal events in CA3 were longer in slices from epileptic animals than controls. This duration decreased at 60 days post-*SE* when compared to the 30 days post-*SE*, but did not show difference from the aged-matched control. Despite relatively resistant to generate prolonged discharges, long-lasting epileptiform activity had been recorded in CA3 of slices containing EC, that were in fact driven by the EC (Walther *et al.*, 1986; Jones e Lambert, 1990; Avoli *et al.*, 1996; Barbarosie e Avoli, 1997).

The DG of slices from epileptic animals at 30 days post-*SE* had longer latency to ictal events with shorter duration, and less frequent IEDs, than controls. At 60 days post-*SE*, although the duration of ictal events was shorter in DG from epileptic animals, the susceptibility to generate ictal events was higher, when compared to control group; and the duration of ictal events increased when compared to the 30 days post-*SE* group, demonstrating a higher ictogenesis in the DG at established epilepsy. DG plays

an important role in battling the epileptiform discharges propagation from EC to hippocampus (Barbarosie *et al.*, 2000; Hsu, 2007). As observed in animal models and patients with TLE, the DG undergoes a variety of pathological changes that may disrupt the gating function, contributing to the development of epilepsy (Scharfman, 2019). In slices from epileptic animals, this effect could be attributed to the altered intrinsic and network properties of granule cells (Kelly e Beck, 2017) and reduced granule cell inhibition in DG (Kobayashi e Buckmaster, 2003). Moreover, a transient loss of feedback inhibition in the DG, could facilitate, but not sustain the ictogenesis in hippocampal circuitry as much as the control slices, probably by functional disconnection of hilar border interneurons (Jarero-Basulto *et al.*, 2018).

The 4-AP induced-epileptiform activity in EC at 30 days post-*SE* was similar in both groups, but at 60 days post-*SE*, despite the lower frequency of IEDs, those events had a shorter latency to the first occurrence, while ictal events had higher frequency than control slices, indicating a higher propensity to ictogenesis at established epilepsy. Several studies using hippocampal-EC slice preparations have shown that the EC is able to generate epileptiform events, and may have lower seizure threshold than the hippocampus *per se* (Panuccio *et al.*, 2010; Ren *et al.*, 2014). The lower frequency of IEDs in slices from epileptic animals may be attributed to either the loss of EC cells, preferentially in layer III, observed in human and animal models of TLE (Du *et al.*, 1993, 1995), or to the impaired propagation of IEDs from CA3, via hippocampal CA1 and subiculum, back to the EC, caused by the hippocampal–entorhinal loop rupture (Avoli et al., 1996, Barbarosie and Avoli, 1997). Interestingly, despite the EC cell loss, the remaining cells have increased excitability in TLE (Kobayashi e Buckmaster, 2003; Tolner *et al.*, 2007) and could contribute to the increased ictogenesis.

The *in vitro* characterization of epileptiform activity at different areas of hippocampal formation reinforces the critical role of each one of them in the pathological circuit. The EC being crucial for ictal and interictal discharges generation and modulation; DG controlling the hyperexcitability during the ongoing epileptogenesis; CA1 exhibiting the increment of vulnerability and susceptibility to ictogenesis; and CA3 driving the activity in the hippocampal-EC circuit.

Oscillation patterns during 4-AP-induced hyperexcitability

Modified hippocampal oscillatory patterns constitutes an important key in brain diseases, mainly by controlling other connected neuronal networks (Scharfman, 2007; Colgin, 2011). We demonstrated that CA3 area of 4-AP-bathed hippocampal-EC slices from epileptic animals at 30 days post-*SE* had lower power of delta and theta oscillations during the IED intervals than controls. Decreased hippocampal theta rhythm is also observed after IEDs in patients (Fu *et al.*, 2018), and in animal model of TLE during the latent and chronic stages (Ge *et al.*, 2013; Pasquetti *et al.*, 2019), suggesting that IEDs have a significant impact on theta rhythm in epilepsy. On the other hand, higher power of theta was detected in DG at 30 days post-*SE,* and in EC and in CA3 at 60 days post-*SE* in slices from epileptic animals. The higher power of theta in these hippocampal formation areas had been suggested as a compensatory mechanism to the high-frequency excitatory activity generation triggered by GABAergic dysfunction (Genovesi *et al.*, 2011). Therefore, the heterogeneity in power of theta rhythm in the hippocampal-EC slices at the two periods of epileptogenesis may reflect the ongoing neural reorganization (Curia *et al.*, 2008).

Beta oscillations are important for long-range synchronization (Traub *et al.*, 1996; Whittington *et al.*, 1997), contributing to epileptiform discharges generation

during the epileptogenic process. Here, we observed higher power of beta in EC, CA1 and CA3, at 60 days post-*SE* but not at 30 days post-*SE* when compared to controls. This late increased in power of beta may reflect mechanisms of ictogenesis during chronic stages of epilepsy. Interestingly, increased power of pre-ictal beta oscillation (Sorokin, Paz e Huguenard, 2016) in patients and rat model of absence seizures had been related with seizure susceptibility (Glaba *et al.*, 2020).

Gamma oscillations have a close relation with epileptiform activity generation recorded *in vitro* (Quilichini *et al.*, 2012). At 30 days post-*SE*, we found higher power of slow gamma in EC, middle gamma in CA1, and all gamma bands in CA3 areas of slices from epileptic animals than control slices. At 60 days post-*SE*, we found higher power of all gamma bands in CA3 and DG, and slow gamma in CA1 area of slices from epileptic animals, than control slices. At different stages of epileptogenesis, after a 4-AP-induced hyperexcitability, the ongoing pathological neuronal network induced the increment of gamma oscillations within the hippocampal formation, mainly in CA3 and CA1 hippocampal areas. This may reflect the role of gamma oscillations as a potential biomarker to localize pathological neuronal network with IEDs generation in the brain (Ren *et al.*, 2015).

Not only gamma, but also faster oscillations are implicated in the epileptiform activity generation (Hamidi, Lévesque e Avoli, 2014; Salami, Lévesque, *et al.*, 2014), and both HFOs, ripples and fast ripples bands have been identified in EEG of patients and animal models of TLE (Bragin *et al.*, 2004; Pearce *et al.*, 2013; Ewell *et al.*, 2019; Jacobs e Zijlmans, 2020). Here, we demonstrated that HFOs could be detected at inter-IEDs in hippocampal-EC slices under 4-AP application. There are evidences supporting that HFOs at ripples (150–250 Hz) and fast ripples (250–500 Hz) bands associated with IEDs are good biomarkers of the epileptogenic processes (Salami,

Levesque, *et al.*, 2014; Jacobs *et al.*, 2016; Thomschewski, Hincapié e Frauscher, 2019). At 30 days post-*SE*, the hippocampal CA3 area presented higher power of ripples and fast ripples. Functional changes of CA3 oscillatory network at earlier stages of epileptogenesis, during 4-AP-induced hyperexcitability, may be relevant to establish the chronic process. At 60 days post-*SE*, EC had higher power of fast ripples, and the DG, higher power of ripples and fast ripples. Accordingly HFOs increased during neuronal networks hyperexcitability, reflecting abnormal and enhanced forms of neuronal synchronization (Jefferys *et al.*, 2012). Studies have shown that oscillations within the range of 80 to 250 Hz (named ripples) and 250 to 400 Hz (termed fast ripples) can be observed in the local field potential recorded from the hippocampus and the temporal cortex of rodent models and patients with epilepsy (Bragin, Engel, Wilson, Fried e Buzsáki, 1999; Bragin, Engel, Wilson, Fried e Mathern, 1999; Bragin *et al.*, 2002, 2004; Staba *et al.*, 2002; Schevon *et al.*, 2009; Weiss *et al.*, 2016)**.** Our results confirm that the CA3 region appears to have an important role in TLE, becoming a generator of pathological HFOs, and the source of pathological processes to other hippocampal regions (Barbarosie e Avoli, 1997; D'Antuono *et al.*, 2002; Lévesque, Behr e Avoli, 2015). In fact, studies have already shown that the occurrence of interictal spikes with fast ripples is increased in CA3, and are associated with an increased seizure frequency (Lévesque *et al.*, 2011; Salami, Lévesque, *et al.*, 2014). This suggests that CA3 interictal oscillations (interictal spikes associated with pathological HFOs) reflect the ongoing pathological processes in the CA3, crucial to the establishment of epilepsy. Accordingly, in our study the CA3 area was less affected and therefore, less susceptible to generate ictal events in the hippocampal-EC slices from epileptic animals during the 4-AP-induced epileptiform activity. This suggests that the circuit reorganization of CA3 facilitates the generation of pathological processes

and ictogenesis in other regions of hippocampal formation. Besides, as other hippocampal areas presented important damage and changes in epileptiform activity, we particularly suggest that structural and functional impairment in the pilocarpine model of epilepsy affected the hippocampal output, facilitating the ictogenesis in these regions (Panuccio *et al.*, 2010).

Altogether, the higher power of HFOs may be predictive of epileptogenic networks formation, as in the CA3 hippocampal area at 30 days post-*SE*; and of specific targets of epileptogenesis, as in the EC and DG at 60 days post-*SE* (Fedele *et al.*, 2017; Jacobs e Zijlmans, 2020).

Phase coherence of gamma and HFOs during 4-AP-induced hyperexcitability

In this study, the phase coherence analysis can reveal the synchronized activity between distinct regions of hippocampal-EC circuit at specific frequency bands (Horwitz, 2003), and may emphasize pivotal clues of epileptogenesis and ictogenesis. We show higher phase coherence of gamma oscillations between CA1-CA3 in slices from epileptic animals, at 30 days post-*SE* when compared to aged-matched controls. Therefore, gamma oscillations are synchronized at the beginning of the chronic phase of epileptogenesis throughout the hippocampal-EC slices from epileptic animals, contributing to ictogenesis. However, at 60 days post-*SE*, we observed lower phase coherence in slow and/or middle gamma between EC-DG, EC-CA1 and DG-CA3 of slices from epileptic animals compared to controls. These findings suggested that, at the established epilepsy, the synchronization of gamma oscillations may be impaired by induced interneuron cell loss, abnormal maturation of granule cells and mossy fiber sprouting (Scharfman, 2019; Lybrand *et al.*, 2021) during the earlier epileptogenesis.

Higher phase coherence in HFOs was found between EC-CA1, at 30 days post-*SE*. As reported by several studies of surgical treatment for epilepsy, the brain tissue resection-based on HFO rates and spectral power changes are correlated with the good seizure-free outcomes (Jacobs *et al.*, 2008; Fujiwara *et al.*, 2012; Fedele *et al.*, 2017). The occurrence of HFOs during epileptogenesis indicates a pathological network reorganization evolving to epilepsy (Bragin *et al.*, 2004). At 60 days post-*SE*, we also found higher phase coherence in HFOs, in CA3-CA1 areas of 4-AP bathed slices from epileptic animals. Overall, the two periods of epileptogenesis in the pilocarpine model of epilepsy were characterized by dynamic changes in oscillation patterns and phase coherence, mainly at HFOs range.

Oscillation patterns during the spontaneous network activity

Spontaneous network activity propagates through developing neuronal circuits in specific patterns (Kerschensteiner, 2014). Although neither ictal nor IEDs were detected in the hippocampal-EC slices in absence of 4-AP, the power of gamma oscillations in the EC, CA1, CA3 and DG areas was higher in slices from epileptic animals than controls at 30- and 60-days post-*SE*. These gamma oscillations in the hippocampus were similar to what we observed in slices from epileptic animals under 4-AP-induced hyperexcitability and may reflect an ongoing epileptogenic process in epileptic animals (Goldberg e Coulter, 2013). In fact, increased gamma oscillations has been observed in brain areas associated with seizures in patients and animal models of epilepsy (Hughes, 2008; de Curtis e Gnatkovsky, 2009). These results confirm again that gamma oscillations are valuable biomarkers for the epileptogenesis and ictogenesis. Despite of HFOs at the range of ripples and fast ripples been reported as strong indicators of epileptogenic processes, during the spontaneous LFP recorded

in slices from epileptic animals, we observed higher power of ripples and fast ripples only in the DG at 60 days post-*SE*, when compared to controls. It may reinforce that the DG represents a key area to the epileptogenic process, by losing its gating function.

Phase coherence during the spontaneous network activity

At 30 days post-*SE*, under spontaneous network activity, no differences were found in phase coherence on different oscillations between slices from epileptic and control animals. However, at 60 days post-*SE* phase coherence was higher in fast ripples between DG-CA3 regions of slices from epileptic animals. Indeed, DG was the area with higher power of fast ripples oscillations in these slices in absence of 4-AP. Therefore, the local network dynamics are affected by the pathological reorganization subsequent to pilocarpine-induced *SE* (Garrido Sanabria *et al.*, 2002). This ongoing pathological process may affect the long-range aberrant connectivity throughout the hippocampal-EC slices from epileptic animals, including the neuronal network of DG-CA3 circuitry that undergo to important morphological and functional changes that contribute to the epileptogenesis (Zhang, Fan e Wang, 2017).

Major findings and significance

Specific neural networks oscillatory patterns associated with epileptiform discharges are hallmarks of pathological excessive or abnormal ongoing neuronal activity in epilepsy. In a region-specific manner, we demonstrated the 4-AP-induced increased ictogenesis and distinct oscillations dynamics in the hippocampal formation of epileptic animals at two period of epileptogenesis. Gamma and high frequency oscillations are key features during ongoing neuropathological processes of neuronal

networks activity and hyperexcitability in the hippocampal formation *in vitro*. We emphasize that the spontaneous neuronal network of slices from epileptic animals, even before an insult of excitability, present dysfunctional oscillation patterns and synchronicity, reinforcing the development of aberrant neuronal circuitry throughout the hippocampal formation induced by the already established aberrant network and epileptogenesis.

ACKNOWLEDGEMENTS

This work was supported by Conselho Nacional de Desenvolvimento Científico e Tecnológico (CNPq), Brazil, no. 141124/2017-2 and 465671/2014-4 and Coordenação de Aperfeiçoamento de Pessoal de Nível Superior (CAPES), Brazil. We thank the members of the NNNESP Lab. for their support with the animal care, and Prof. Scott C. Baraban from University of California, San Francisco (UCSF) for his thoughtful comments on the draft, and Prof. Robson Scheffer Teixeira from University of Cologne, Germany who provided important assistance in the signal analysis.

DECLARATION OF COMPETING INTEREST

All authors declare no competing financial interests.

AUTHORS' CONTRIBUTION

JRM designed and performed the experiments, formal analysis, contributed to project administration, and wrote the manuscript. MVP participated in the methodological design, formal analysis and reviewed the manuscript. MEC contributed to project design, methodology and administration, and wrote and review the manuscript.

REFERENCES

Arabadzisz D, Antal K, Parpan F, Emri Z, Fritschy JM (2005) Epileptogenesis and chronic seizures in a mouse model of temporal lobe epilepsy are associated with distinct EEG patterns and selective neurochemical alterations in the contralateral hippocampus. Exp Neurol 194:76–90.

Avoli M, Barbarosle M, Lücke A, Nagao T, Lopantsev V, Köhling R (1996) Synchronous GABA-mediated potentials and epileptiform discharges in the rat limbic system in vitro. J Neurosci 16:3912–3924.

Avoli M, Jefferys JGR (2015) Models of drug-induced epileptiform synchronization in vitro. J Neurosci Methods 260:26–32 Available at: http://dx.doi.org/10.1016/j.jneumeth.2015.10.006.

Barbarosie M, Avoli M (1997) CA3-driven hippocampal-entorhinal loop controls rather than sustains in vitro limbic seizures. J Neurosci 17:9308–9314.

Barbarosie M, Louvel J, Kurcewicz I, Avoli M (2000) CA3-released entorhinal seizures disclose dentate gyrus epileptogenicity and unmask a temporoammonic pathway. J Neurophysiol 83:1115–1124.

Bartolomei F, Wendling F, Bellanger JJ, Régis J, Chauvel P (2001) Neural networks involving the medial temporal structures in temporal lobe epilepsy. Clin Neurophysiol 112:1746–1760.

Belluscio MA, Mizuseki K, Schmidt R, Kempter R, Buzsáki G (2012) Cross-frequency phase-phase coupling between theta and gamma oscillations in the hippocampus. J Neurosci 32:423–435.

Berg AT, Berkovic SF, Brodie MJ, Buchhalter J, Cross JH, Van Emde Boas W, Engel J, French J, Glauser TA, Mathern GW, Moshé SL, Nordli D, Plouin P, Scheffer IE (2010) Revised terminology and concepts for organization of seizures and epilepsies: Report of the ILAE Commission on Classification and Terminology, 2005-2009. Epilepsia 51:676–685.

Bertram EH (2009) Temporal lobe epilepsy: Where do the seizures really begin? Epilepsy Behav 14:32–37 Available at: https://linkinghub.elsevier.com/retrieve/pii/S1525505008002941.

Biagini G, D'Arcangelo G, Baldelli E, D'Antuono M, Tancredi V, Avoli M (2005) Impaired activation of CA3 pyramidal neurons in the epileptic hippocampus. NeuroMolecular Med 7:325–342.

Boido D, Jesuthasan N, De Curtis M, Uva L (2014) Network dynamics during the progression of seizure-like events in the hippocampal-parahippocampal regions. Cereb Cortex 24:163–173.

Bragin A, Engel J, Wilson CL, Fried I, Buzsáki G (1999a) High-frequency oscillations in human brain. Hippocampus 9:137–142.

Bragin A, Engel J, Wilson CL, Fried I, Mathern GW (1999b) Hippocampal and entorhinal cortex high-frequency oscillations (100-500 Hz) in human epileptic brain and in kainic acid-treated rats with chronic seizures. Epilepsia 40:127–137.

Bragin A, Mody I, Wilson CL, Engel J (2002) Local generation of fast ripples in epileptic brain. J Neurosci 22:2012–2021.

Bragin A, Wilson CL, Almajano J, Mody I, Engel J (2004) High-frequency oscillations after status epilepticus: Epileptogenesis and seizure genesis. Epilepsia 45:1017–1023.

Broggini ACS, Esteves IM, Romcy-Pereira RN, Leite JP, Leão RN (2016) Pre-ictal increase in theta synchrony between the hippocampus and prefrontal cortex in a rat

model of temporal lobe epilepsy. Exp Neurol 279:232–242 Available at: http://dx.doi.org/10.1016/j.expneurol.2016.03.007.
Buzsáki G (2006) Rhythms of the Brain. Oxford University Press, Inc.
Buzsáki G, Watson BO (2012) Brain rhythms and neural syntax: Implications for efficient coding of cognitive content and neuropsychiatric disease. Dialogues Clin Neurosci 14:345–367.
Calcagnotto ME, Barbarosie M, Avoli M (2000) Hippocampus-entorhinal cortex loop and seizure generation in the young rodent limbic system. J Neurophysiol 83:3183–3187.
Chauvière L, Rafrafi N, Thinus-Blanc C, Bartolomei F, Esclapez M, Bernard C (2009) Early deficits in spatial memory and theta rhythm in experimental temporal lobe epilepsy. J Neurosci 29:5402–5410.
Codadu NK, Graham RT, Burman RJ, Jackson-Taylor RT, Raimondo J V., Trevelyan AJ, Parrish RR (2019) Divergent paths to seizure-like events. Physiol Rep 7:1–15.
Colgin LL (2011) Oscillations and hippocampal-prefrontal synchrony. Curr Opin Neurobiol 21:467–474.
Cossart R, Dinocourt C, Nirsch JC, Merchan-Perez A, De Felipe J, Ben-Ari Y, Esclapez M, Bernard C (2001) GABAergic inhibition is decreased in experimental epilepsy. Nat Neurosci 4:52–62.
Cross DJ, Cavazos JE (2007) Synaptic reorganization in subiculum and CA3 after early-life status epilepticus in the kainic acid rat model. Epilepsy Res 73:156–165.
Curia G, Longo D, Biagini G, Jones RSG, Avoli M (2008) The pilocarpine model of temporal lobe epilepsy. J Neurosci Methods 172:143–157 Available at: http://dx.doi.org/10.1016/j.jneumeth.2008.04.019.
D'Antuono M, Benini R, Biagini G, D'Arcangelo G, Barbarosie M, Tancredi V, Massimo Avoli AND (2002) Limbic network interactions leading to hyperexcitability in a model of temporal lobe epilepsy. J Neurophysiol 87:634–639.
Danzer SC, He X, Loepke AW, McNamara JO (2010) Structural plasticity of dentate granule cell mossy fibers during the development of limbic epilepsy. Hippocampus 20:113–124.
de Curtis M, Gnatkovsky V (2009) Reevaluating the mechanisms of focal ictogenesis: The role of low-voltage fast activity. Epilepsia 50:2514–2525.
Du F, Eid T, Lothman EW, Köhler C, Schwarcz R (1995) Preferential neuronal loss in layer III of the medial entorhinal cortex in rat models of temporal lobe epilepsy. J Neurosci 15:6301–6313.
Du F, Whetsell WO, Abou-Khalil B, Blumenkopf B, Lothman EW, Schwarcz R (1993) Preferential neuronal loss in layer III of the entorhinal cortex in patients with temporal lobe epilepsy. Epilepsy Res 16:223–233.
Dugladze T, Vida I, Tort AB, Gross A, Otahal J, Heinemann U, Kopell NJ, Gloveli T (2007) Impaired hippocampal rhythmogenesis in a mouse model of mesial temporal lobe epilepsy. Proc Natl Acad Sci U S A 104:17530–17535.
Esclapez M, Hirsch JC, Ben-Ari Y, Bernard C (1999) Newly formed excitatory pathways provide a substrate for hyperexcitability in experimental temporal lobe epilepsy. J Comp Neurol 408:449–460.
Ewell LA, Fischer KB, Leibold C, Leutgeb S, Leutgeb JK (2019) The impact of pathological high-frequency oscillations on hippocampal network activity in rats with chronic epilepsy. Elife 8:1–24.
Fedele T, Burnos S, Boran E, Krayenbühl N, Hilfiker P, Grunwald T, Sarnthein J (2017) Resection of high frequency oscillations predicts seizure outcome in the individual patient. Sci Rep 7:1–10.

Fisher RS, Scharfman HE, deCurtis M (2014) How Can We Identify Ictal and Interictal Abnormal Activity? :3–23.
Fisher RS, Van Emde Boas W, Blume W, Elger C, Genton P, Lee P, Engel J (2005) Epileptic Seizures and Epilepsy: Definitions Proposed by the International League Against Epilepsy (ILAE) and the International Bureau for Epilepsy (IBE). Epilepsia 46:1701–1702.
Fries P (2005) A mechanism for cognitive dynamics: Neuronal communication through neuronal coherence. Trends Cogn Sci 9:474–480.
Fu X, Wang Y, Ge M, Wang D, Gao R, Wang L, Guo J, Liu H (2018) Negative effects of interictal spikes on theta rhythm in human temporal lobe epilepsy. Epilepsy Behav 87:207–211.
Fujiwara H, Greiner HM, Lee KH, Holland-Bouley KD, Seo JH, Arthur T, Mangano FT, Leach JL, Rose DF (2012) Resection of ictal high-frequency oscillations leads to favorable surgical outcome in pediatric epilepsy. Epilepsia 53:1607–1617.
Garrido Sanabria ER, Da Silva A V., Spreafico R, Cavalheiro EA (2002) Damage, reorganization, and abnormal neocortical hyperexcitability in the pilocarpine model of temporal lobe epilepsy. Epilepsia 43:96–106.
Ge M, Wang D, Dong G, Guo B, Gao R, Sun W, Zhang J, Liu H (2013) Transient impact of spike on theta rhythm in temporal lobe epilepsy. Exp Neurol 250:136–142 Available at: http://dx.doi.org/10.1016/j.expneurol.2013.09.023.
Genovesi S, Provenzano G, Dunleavy M, Sgado P, Bozzi Y (2011) GABAergic Dysfunction in Autism and Epilepsy. In: Autism - A Neurodevelopmental Journey from Genes to Behaviour.
Glaba P, Latka M, Krause MJ, Kuryło M, Jernajczyk W, Walas W, West BJ (2020) Changes in Interictal Pretreatment and Posttreatment EEG in Childhood Absence Epilepsy. Front Neurosci 14:1–9.
Goldberg EM, Coulter DA (2013) Mechanisms of epileptogenesis: A convergence on neural circuit dysfunction. Nat Rev Neurosci 14:337–349 Available at: http://dx.doi.org/10.1038/nrn3482.
Goutagny R, Gu N, Cavanagh C, Jackson J, Chabot JG, Quirion R, Krantic S, Williams S (2013) Alterations in hippocampal network oscillations and theta-gamma coupling arise before Aβ overproduction in a mouse model of Alzheimer's disease. Eur J Neurosci 37:1896–1902.
Grasse DW, Karunakaran S, Moxon KA (2013) Neuronal synchrony and the transition to spontaneous seizures. Exp Neurol 248:72–84 Available at: http://dx.doi.org/10.1016/j.expneurol.2013.05.004.
Hamidi S., Lévesque M., Avoli M (2014) Epileptiform synchronization and high-frequency oscillations in brain slices comprising piriform and entorhinal cortices. Neuroscience 281:258–268.
Horwitz B (2003) The elusive concept of brain connectivity. Neuroimage 19:466–470.
Hsu D (2007) The dentate gyrus as a filter or gate: a look back and a look ahead. Prog Brain Res 163:601–613.
Hughes JR (2008) Gamma, fast, and ultrafast waves of the brain: Their relationships with epilepsy and behavior. Epilepsy Behav 13:25–31.
Jacobs J, LeVan P, Chander R, Hall J, Dubeau F, Gotman J (2008) Interictal high-frequency oscillations (80-500 Hz) are an indicator of seizure onset areas independent of spikes in the human epileptic brain. Epilepsia 49:1893–1907.
Jacobs J, Vogt C, LeVan P, Zelmann R, Gotman J, Kobayashi K (2016) The identification of distinct high-frequency oscillations during spikes delineates the seizure onset zone better than high-frequency spectral power changes. Clin

Neurophysiol 127:129–142 Available at: http://dx.doi.org/10.1016/j.clinph.2015.04.053.
Jacobs J, Zijlmans M (2020) HFO to Measure Seizure Propensity and Improve Prognostication in Patients With Epilepsy. Epilepsy Curr 20:338–347.
Jacoby A (2008) Epilepsy and stigma: An update and critical review. Curr Neurol Neurosci Rep 8:339–344.
Jarero-Basulto JJ, Gasca-Martínez Y, Rivera-Cervantes MC, Ureña-Guerrero ME, Feria-Velasco AI, Beas-Zarate C (2018) Interactions between epilepsy and plasticity. Pharmaceuticals 11:1–18.
Jefferys JGR, Menendez de la Prida L, Wendling F, Bragin A, Avoli M, Timofeev I, Lopes da Silva FH (2012) Mechanisms of physiological and epileptic HFO generation. Prog Neurobiol 98:250–264.
Jiruska P, de Curtis M, Jefferys JGR, Schevon CA, Schiff SJ, Schindler K (2013) Synchronization and desynchronization in epilepsy: Controversies and hypotheses. J Physiol 591:787–797.
Jones RSG, Lambert JDC (1990) The role of excitatory amino acid receptors in the propagation of epileptiform discharges from the entorhinal cortex to the dentate gyrus in vitro. Exp Brain Res 80:310–322.
Kelly T, Beck H (2017) Functional properties of granule cells with hilar basal dendrites in the epileptic dentate gyrus. Epilepsia 58:160–171.
Kerschensteiner D (2014) Spontaneous network activity and synaptic development. Neuroscientist 20:272–290.
Kessler K, Seymour RA, Rippon G (2016) Brain oscillations and connectivity in autism spectrum disorders (ASD): new approaches to methodology, measurement and modelling. Neurosci Biobehav Rev 71:601–620 Available at: http://dx.doi.org/10.1016/j.neubiorev.2016.10.002.
Kitchigina VF (2018) Alterations of Coherent Theta and Gamma Network Oscillations as an Early Biomarker of Temporal Lobe Epilepsy and Alzheimer's Disease. Front Integr Neurosci 12:1–15.
Kitchigina VF, Butuzova M V. (2009) Theta activity of septal neurons during different epileptic phases: The same frequency but different significance? Exp Neurol 216:449–458 Available at: http://dx.doi.org/10.1016/j.expneurol.2009.01.001.
Kobayashi M, Buckmaster PS (2003) Reduced inhibition of dentate granule cells in a model of temporal lobe epilepsy. J Neurosci 23:2440–2452.
Kramer MA, Cash SS (2012) Epilepsy as a disorder of cortical network organization. Neuroscientist 18:360–372.
Lehmann TN, Gabriel S, Kovacs R, Eilers A, Kivi A, Schulze K, Lanksch WR, Meencke HJ, Heinemann U (2000) Alterations of neuronal connectivity in area CA1 of hippocampal slices from temporal lobe epilepsy patients and from pilocarpine-treated epileptic rats. Epilepsia 41:190–194.
Lévesque M, Behr C, Avoli M (2015) The anti-ictogenic effects of levetiracetam are mirrored by interictal spiking and high-frequency oscillation changes in a model of temporal lobe epilepsy. Seizure 25:18–25.
Lévesque M, Bortel A, Gotman J, Avoli M (2011) High-frequency (80-500Hz) oscillations and epileptogenesis in temporal lobe epilepsy. Neurobiol Dis 42:231–241.
Lévesque M, Salami P, Shiri Z, Avoli M (2018) Interictal oscillations and focal epileptic disorders. Eur J Neurosci 48:2915–2927.
Lybrand ZR, Goswami S, Zhu J, Jarzabek V, Merlock N, Aktar M, Smith C, Zhang L, Varma P, Cho K, Ge S, Hsieh J (2021) A critical period of neuronal activity results

in aberrant neurogenesis rewiring hippocampal circuitry in a mouse model of epilepsy. Nat Commun:1–14 Available at: http://dx.doi.org/10.1038/s41467-021-21649-8.
Matsumoto A, Brinkmann BH, Stead SM, Matsumoto J, Kucewicz MT, Marsh WR, Meyer F, Worrell G (2013) Pathological and physiological high-frequency oscillations in focal human epilepsy. J Neurophysiol 110:1958–1964.
Navidhamidi M, Ghasemi M, Mehranfard N (2017) Epilepsy-associated alterations in hippocampal excitability. Rev Neurosci 28:307–334.
Panuccio G, D'Antuono M, de Guzman P, De Lannoy L, Biagini G, Avoli M (2010) In vitro ictogenesis and parahippocampal networks in a rodent model of temporal lobe epilepsy. Neurobiol Dis 39:372–380 Available at: http://dx.doi.org/10.1016/j.nbd.2010.05.003.
Pasquetti MV, Meier L, Marafiga JR, Barbieri Caus L, Tort ABL, Calcagnotto ME (2019) Hippocampal CA1 and cortical interictal oscillations in the pilocarpine model of epilepsy. Brain Res 1722.
Pearce A, Wulsin D, Blanco JA, Krieger A, Litt B, Stacey WC (2013) Temporal changes of neocortical high-frequency oscillations in epilepsy. J Neurophysiol 110:1167–1179.
Percie Du Sert N et al. (2020) The ARRIVE guidelines 2.0: Updated guidelines for reporting animal research. BMC Vet Res 16:1–7.
Pitkänen A, Löscher W, Vezzani A, Becker AJ, Simonato M, Lukasiuk K, Gröhn O, Bankstahl JP, Friedman A, Aronica E, Gorter JA, Ravizza T, Sisodiya SM, Kokaia M, Beck H (2016) Advances in the development of biomarkers for epilepsy. Lancet Neurol 15:843–856 Available at: http://dx.doi.org/10.1016/S1474-4422(16)00112-5.
Quilichini PP, Quyen ML Van, Ivanov A, Turner DA, Carabalona A, Gozlan H, Esclapez M, Bernard C (2012) Hub GABA neurons mediate gamma-frequency oscillations at ictal-like event onset in the immature hippocampus. Bone 74:57–64 Available at: https://www.ncbi.nlm.nih.gov/pmc/articles/PMC3624763/pdf/nihms412728.pdf.
Racine RJ, Gartner JG, McIntyre Burnham W (1972) Epileptiform activity and neural plasticity in limbic structures. Brain Res 47:262–268.
Ren H, Shi YJ, Lu QC, Liang PJ, Zhang PM (2014) The role of the entorhinal cortex in epileptiform activities of the hippocampus. Theor Biol Med Model 11:1–22.
Ren L, Kucewicz MT, Cimbalnik J, Matsumoto JY, Brinkmann BH, Hu W, Marsh WR, Meyer FB, Stead SM, Worrell GA (2015) Gamma oscillations precede interictal epileptiform spikes in the seizure onset zone. Neurology 84:602–608.
Reyes-Garcia SZ, Scorza CA, Araújo NS, Ortiz-Villatoro NN, Jardim AP, Centeno R, Yacubian EMT, Faber J, Cavalheiro EA (2018) Different patterns of epileptiform-like activity are generated in the sclerotic hippocampus from patients with drug-resistant temporal lobe epilepsy. Sci Rep 8:1–15.
Riban V, Bouilleret V, Pham-Lê BT, Fritschy JM, Marescaux C, Depaulis A (2002) Evolution of hippocampal epileptic activity during the development of hippocampal sclerosis in a mouse model of temporal lobe epilepsy. Neuroscience 112:101–111.
Righes Marafiga J, Vendramin Pasquetti M, Calcagnotto ME (2020) GABAergic interneurons in epilepsy: More than a simple change in inhibition. Epilepsy Behav.
Salami P, Levesque M, Benini R, Behr C, Gotman J, Avoli M (2014a) Dynamics of interictal spikes and high-frequency oscillations during epileptogenesis in temporal lobe epilepsy. Epilepsia 54:52 Available at: http://www.embase.com/search/results?subaction=viewrecord&from=export&id=L

71137106%0Ahttp://dx.doi.org/10.1111/epi.12229%0Ahttp://sfx.library.uu.nl/utrecht?sid=EMBASE&issn=00139580&id=doi:10.1111%2Fepi.12229&atitle=Interictal+spikes+and+high-frequency+osc.
Salami P, Lévesque M, Benini R, Behr C, Gotman J, Avoli M (2014b) Dynamics of interictal spikes and high-frequency oscillations during epileptogenesis in temporal lobe epilepsy. Neurobiol Dis 67:97–106 Available at: http://dx.doi.org/10.1016/j.nbd.2014.03.012.
Scharfman HE (2007) The neurobiology of epilepsy. Curr Neurol Neurosci Rep 7:348–354.
Scharfman HE (2019) The Dentate Gyrus and Temporal Lobe Epilepsy: An “Exciting” Era. Epilepsy Curr 19:249–255.
Scheffer-Teixeira R, Tort ABL (2017) Unveiling fast field oscillations through comodulation. eNeuro 4.
Scheffzük C, Kukushka VI, Vyssotski AL, Draguhn A, Tort ABL, Brankačk J (2013) Global slowing of network oscillations in mouse neocortex by diazepam. Neuropharmacology 65:123–133.
Schevon CA, Trevelyan AJ, Schroeder CE, Goodman RR, McKhann G, Emerson RG (2009) Spatial characterization of interictal high frequency oscillations in epileptic neocortex. Brain 132:3047–3059.
Scorza FA, Arida RM, Naffah-Mazzacoratti M da G, Scerni DA, Calderazzo L, Cavalheiro EA (2009) The pilocarpine model of epilepsy: What have we learned? An Acad Bras Cienc 81:345–365.
Sharma AK, Reams RY, Jordan WH, Miller MA, Thacker HL, Snyder PW (2007) Mesial temporal lobe epilepsy: Pathogenesis, induced rodent models and lesions. Toxicol Pathol 35:984–999.
Sirven JI (2015) Epilepsy: A Spectrum Disorder. Cold Spring Harb Perspect Med 5:a022848.
Sloviter RS (2008) Hippocampal epileptogenesis in animal models of mesial temporal lobe epilepsy with hippocampal sclerosis: The importance of the “latent period” and other concepts. Epilepsia 49:85–92.
Sorokin JM, Paz JT, Huguenard JR (2016) Absence seizure susceptibility correlates with pre-ictal β oscillations. 110:372–381.
Staba RJ, Bragin A, Aibel-Weiss S, Van’t Klooster MA, Engel J (2017) Oscillatory activity: Neuronal networks generating pathological high frequency oscillations. Elsevier. Available at: http://dx.doi.org/10.1016/B978-0-12-809324-5.00171-1.
Staba RJ, Stead M, Worrell GA (2014) Electrophysiological Biomarkers of Epilepsy. Neurotherapeutics 11:334–346.
Staba RJ, Wilson CL, Bragin A, Fried I (2002) Quantitative analysis of high-frequency oscillations (80-500 Hz) recorded in human epileptic hippocampus and entorhinal cortex. J Neurophysiol 88:1743–1752.
Sutula T, Cascino G, Cavazos J, Parada I, Ramirez L (1989) Mossy fiber synaptic reorganization in the epileptic human temporal lobe. Ann Neurol 26:321–330.
Thom M (2014) Review: Hippocampal sclerosis in epilepsy: A neuropathology review. Neuropathol Appl Neurobiol 40:520–543.
Thomschewski A, Hincapié AS, Frauscher B (2019) Localization of the epileptogenic zone using high frequency oscillations. Front Neurol 10.
Thurman DJ et al. (2011) Standards for epidemiologic studies and surveillance of epilepsy. Epilepsia 52:2–26.

Tolner EA, Frahm C, Metzger R, Gorter JA, Witte OW, Lopes da Silva FH, Heinemann U (2007) Synaptic responses in superficial layers of medial entorhinal cortex from rats with kainate-induced epilepsy. Neurobiol Dis 26:419–438.
Tort ABL, Scheffer-Teixeira R, Souza BC, Draguhn A, Brankačk J (2013) Theta-associated high-frequency oscillations (110-160Hz) in the hippocampus and neocortex. Prog Neurobiol 100:1–14.
Toyoda I, Bower MR, Leyva F, Buckmaster PS (2013) Early activation of ventral hippocampus and subiculum during spontaneous seizures in a rat model of temporal lobe epilepsy. J Neurosci 33:11100–11115.
Traub RD, Bibbig A, LeBeau FEN, Buhl EH, Whittington MA (2004) Cellular mechanisms of neuronal population oscillations in the hippocampus in vitro. Annu Rev Neurosci 27:247–278.
Traub RD, Whittington MA, Colling SB, Buzsáki G, Jefferys JGR (1996) Analysis of gamma rhythms in the rat hippocampus in vitro and in vivo. J Physiol 493:471–484.
Turski WA, Cavalheiro EA, Schwarz M, Czuczwar SJ, Kleinrok Z, Turski L (1983) Limbic seizures produced by pilocarpine in rats: Behavioural, electroencephalographic and neuropathological study. Behav Brain Res 9:315–335.
Uhlhaas PJ, Singer W (2006) Neural Synchrony in Brain Disorders: Relevance for Cognitive Dysfunctions and Pathophysiology. Neuron 52:155–168.
Uhlhaas PJ, Singer W (2010) Abnormal neural oscillations and synchrony in schizophrenia. Nat Rev Neurosci 11:100–113 Available at: http://dx.doi.org/10.1038/nrn2774.
Uva L, Boido D, Avoli M, de Curtis M, Lévesque M (2017) High-frequency oscillations and seizure-like discharges in the entorhinal cortex of the in vitro isolated guinea pig brain. Epilepsy Res 130:21–26 Available at: http://dx.doi.org/10.1016/j.eplepsyres.2017.01.001.
Walker MC (2015) Hippocampal sclerosis: Causes and prevention. Semin Neurol 35:193–200.
Walther H, Lambert JDC, Jones RSG, Heinemann U, Hamon B (1986) Epileptiform activity in combined slices of the hippocampus, subiculum and entorhinal cortex during perfusion with low magnesium medium. Neurosci Lett 69:156–161.
Weiss SA, Alvarado-Rojas C, Bragin A, Behnke E, Fields T, Fried I, Engel J, Staba R (2016) Ictal onset patterns of local field potentials, high frequency oscillations, and unit activity in human mesial temporal lobe epilepsy. Epilepsia 57:111–121.
Whittington MA, Traub RD, Faulkner HJ, Stanford IM, Jeffers JGR (1997) Recurrent excitatory postsynaptic potentials induced by synchronized fast cortical oscillations. Proc Natl Acad Sci U S A 94:12198–12203.
Worrell GA, Gardner AB, Stead SM, Hu S, Goerss S, Cascino GJ, Meyer FB, Marsh R, Litt B (2008) High-frequency oscillations in human temporal lobe: Simultaneous microwire and clinical macroelectrode recordings. Brain 131:928–937.
Zandt MA Van, Naegele JR (2017) GABAergic Synapse Dysfunction and Repair in Temporal Lobe Epilepsy. Synaptic Plast.
Zhang L, Fan D, Wang Q (2017) Transition dynamics of a dentate gyrus-CA3 neuronal network during temporal lobe epilepsy. Front Comput Neurosci 11:1–14.
Zhang YF, Xiong TQ, Tan BH, Song Y, Li SL, Yang L Bin, Li YC (2014) Pilocarpine-induced epilepsy is associated with actin cytoskeleton reorganization in the mossy fiber-CA3 synapses. Epilepsy Res 108:379–389 Available at: http://dx.doi.org/10.1016/j.eplepsyres.2014.01.016.

Zijlmans M, Jiruska P, Zelmann R, Leijten FSS, Jefferys JGR, Gotman J (2012) High-frequency oscillations as a new biomarker in epilepsy. Ann Neurol 71:169–178.

FIGURES

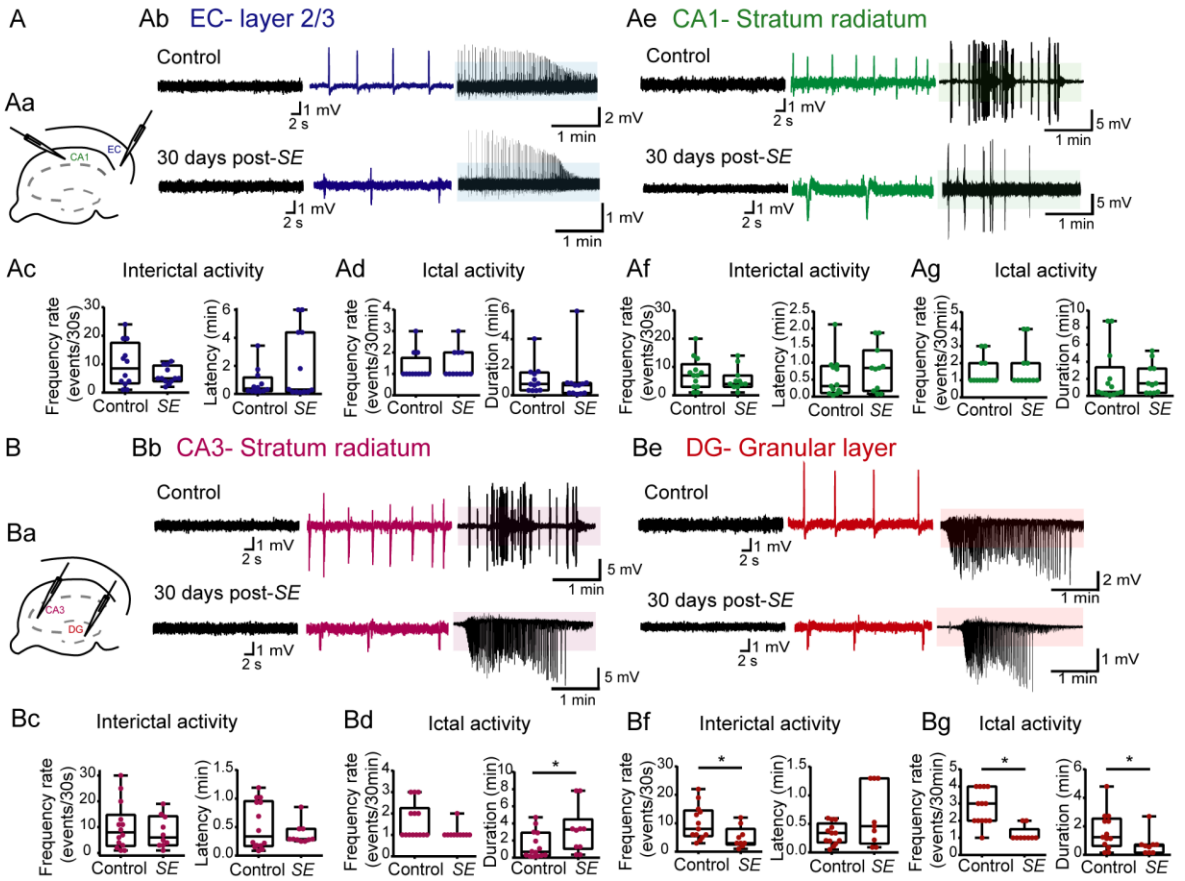

Figure 1. Dual extracellular recordings in hippocampal–EC slices from epileptic and control rats, at 30 days post-SE. Traces without epileptiform activity (left), with interictal activity (middle), and with ictal activity (right).

(Aa) Schematic representation of a horizontal hippocampal-EC slice, showing the locations of two extracellular recording electrodes in entorhinal cortex (EC, blue) and CA1 (green). n of animals: Control: 9, SE: 8.

(Ab) Representative local field potential (LFP) recordings (top) obtained from EC during application of 4-AP in a hippocampal-EC slice that generated interictal (trace in blue) and ictal discharges (outlined in blue).

(Ac) Boxplot illustrating the pooled data of frequency (number of events/30s; Mann–Whitney U test, U=57, P > 0.05) (left) and the latency for IEDs (min; Mann–Whitney U test, U=70, P > 0.05) (right); and (Ad) the frequency (number of events/30min; Mann–Whitney U test, U=66.5, P > 0.05) (left) and duration of Ictal events (min; Mann–Whitney U test, U=49, P > 0.05) (right). n of recordings: Control: 12, SE: 12; n of slices: Control:10, SE: 8.

(Ae) Representative local field potential recordings (top) obtained from CA1 during application of 4-AP in a hippocampal-EC slice that generated interictal (trace in green) and ictal discharges (outlined in green).

(Af) Boxplot illustrating the pooled data of frequency (number of events/30s; Mann–Whitney U test, U=55.5, P > 0.05) (left) and latency for IEDs (min; Mann–Whitney U test, U=58.5, P > 0.05) (right); and (Ag) frequency (number of events/30min; Mann–Whitney U test, U=65.5, P > 0.05) (left) and duration of Ictal events (min; Mann–Whitney U test, U=54.4, P > 0.05) (right). n of recordings: Control: 13, SE: 11; n of slices: Control: 11, SE: 7.

(Ba) Schematic representation of a horizontal hippocampal-EC slice, showing the locations of two extracellular recording electrodes in CA3 (pink) and dentate gyrus (DG, red).

(Bb) Representative local field potential recordings (top) obtained from CA3 during application of 4-AP in a hippocampal-EC slice that generated interictal (trace in pink) and ictal discharges (outlined in pink). **(Bc)** Boxplot illustrating the pooled data of frequency (number of events/30s; Mann–Whitney U test, U=65, P > 0.05) (left) and the latency for IEDs (min; Mann–Whitney U test, U=66, P > 0.05) (right); and **(Bd)** the frequency (number of events/30min; Mann–Whitney U test, U=45.5, P > 0.05) (left) and duration of Ictal events (min; Mann–Whitney U test, U=34, *P < 0.05) (right). n of recordings: Control: 14, SE:10; n of slices: Control: 9, SE: 6.
(Be) Representative local field potential recordings (top) obtained from DG during application of 4-AP in a hippocampal-EC slice that generated interictal (trace in red) and ictal discharges (outlined in orange).
(Bf) Boxplot illustrating the pooled data of frequency (number of events/30s; Mann–Whitney U test, U=24, *P < 0.05) (left) and the latency for IEDs (min; Mann–Whitney U test, U=41.5, *P > 0.05) (right); and (Bd) the frequency (number of events/30min; Mann–Whitney U test, U=10.50, *P < 0.05) (left) and duration of Ictal events (min; Mann–Whitney U test, U=26.5, *P < 0.05) (right). n of recordings: Control: 13, SE: 9; n of slices: Control: 8, SE: 7.

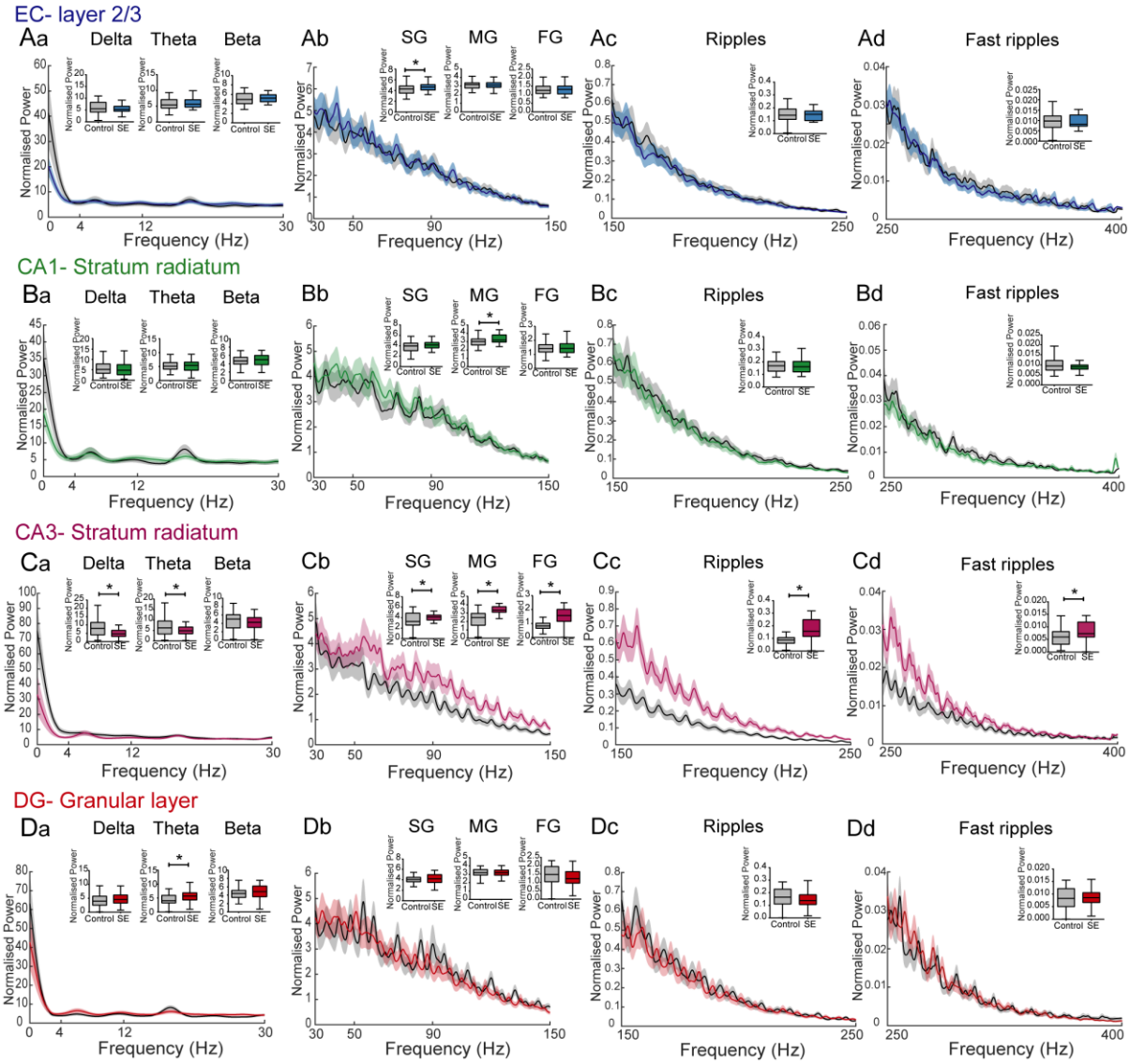

Figure 2. Power spectral densities of frequencies between 0 and 400 Hz in hippocampal-EC slices from epileptic and control animals, at 30 days post-SE induction. Control group (n of epoch: 45-50; n of animals: 9); Epileptic group (n of epoch: 46-50; n of animals: 8). SG: Slow gamma; MG: Middle gamma; FG: Fast gamma.

(Aa) Delta, theta, beta frequency bands in EC of control and epileptic groups. Data are presented as mean ± SD. Inset, box-and-whiskers plot illustrating the pooled data for control and epileptic groups. Unpaired t-test or Mann–Whitney U test, $P > 0.05$.

(Ab) Slow-, middle- and fast gamma frequency bands in EC of control and epileptic groups, showing a higher power of slow gamma in slices from epileptic animals, compared to controls ($t=2.39$; $^*P < 0.05$). Data are presented as mean ± SD. Inset, box-and-whiskers plot illustrating the pooled data for control and epileptic groups. Unpaired t-test.

(Ac) Ripples frequency band in EC of control and epileptic groups. Data are presented as mean ± SD. Inset, box-and-whiskers plot illustrating the pooled data for control and epileptic groups. Mann–Whitney U test, $P > 0.05$.

(Ad) Fast ripples frequency band in EC of control and epileptic groups. Data are presented as mean ± SD. Inset, box-and-whiskers plot illustrating the pooled data for control and epileptic groups. Mann–Whitney U test, $P > 0.05$.

(Ba) Delta, theta, beta frequency bands in CA1 of control and epileptic groups. Data are presented as mean ± SD. Inset, box-and-whiskers plot illustrating the pooled data for control and epileptic groups. Unpaired t-test or Mann–Whitney U test, $P > 0.05$.

(Bb) Slow-, middle- and fast gamma frequency bands in CA1 of control and epileptic groups, showing a higher power of middle gamma oscillation in CA1 of slices from epileptic animals, compared to controls (Mann–Whitney U test, U=886; *P < 0.05). Data are presented as mean ± SD. Inset, box-and-whiskers plot illustrating the pooled data for control and epileptic groups.
(Bc) Ripples frequency band in CA1 of control and epileptic groups. Data are presented as mean ± SD. Inset, box-and-whiskers plot illustrating the pooled data for control and epileptic groups. Mann–Whitney U test, P > 0.05.
(Bd) Fast ripples frequency band in CA1 of control and epileptic groups. Data are presented as mean ± SD. Inset, box-and-whiskers plot illustrating the pooled data for control and epileptic groups. Unpaired t-test, P > 0.05.
(Ca) Delta, theta, beta frequency bands in CA3 of control and epileptic groups, showing a lower power of delta (Unpaired t-test, t=4.24; *P < 0.05) and theta (Unpaired t-test, t=2.59; *P < 0.05) in CA3 of slices from epileptic animals, than controls. Data are presented as mean ± SD. Inset, box-and-whiskers plot illustrating the pooled data for control and epileptic groups.
(Cb) Slow-, middle- and fast gamma frequency bands in CA3 of control and epileptic groups, illustrating a higher power of slow- (Unpaired t-test, t=2.68; *P < 0.05), middle- (Unpaired t-test, t=6.87; *P < 0.05) and fast- gamma (Unpaired t-test, t=6.45; *P < 0.05) in CA3 of slices from epileptic animals than controls. Data are presented as mean ± SD. Inset, box-and-whiskers plot illustrating the pooled data for control and epileptic groups.
(Cc) Ripples frequency band in CA3 of control and epileptic groups. Slices from epileptic animals presented a higher power of ripples than controls (Mann–Whitney U test, U= 300; *P < 0.05). Data are presented as mean ± SD. Inset, box-and-whiskers plot illustrating the pooled data for control and epileptic groups.
(Cd) Fast ripples frequency band in CA3 of control and epileptic groups. Slices from epileptic animals presented a higher power of fast ripples than controls (Mann–Whitney U test, U= 805; *P < 0.05). Data are presented as mean ± SD. Inset, box-and-whiskers plot illustrating the pooled data for control and epileptic groups.
(Da) Delta, theta, beta frequency bands in DG of control and epileptic groups. Slices from epileptic animals presented a higher power of theta (Unpaired t-test, t=2.55; *P < 0.05). Data are presented as mean ± SD. Inset, box-and-whiskers plot illustrating the pooled data for control and epileptic groups.
(Db) Slow-, middle- and fast gamma frequency bands in DG of control and epileptic groups. Data are presented as mean ± SD. Inset, box-and-whiskers plot illustrating the pooled data for control and epileptic groups. Unpaired t-test or Mann–Whitney U test, P > 0.05.
(Dc) Ripples frequency band in DG of control and epileptic groups. Data are presented as mean ± SD. Inset, box-and-whiskers plot illustrating the pooled data for control and epileptic groups. Unpaired t-test, P > 0.05.
(Dd) Fast ripples frequency band in DG of control and epileptic groups. Data are presented as mean ± SD. Inset, box-and-whiskers plot illustrating the pooled data for control and epileptic groups. Unpaired t-test, P > 0.05.

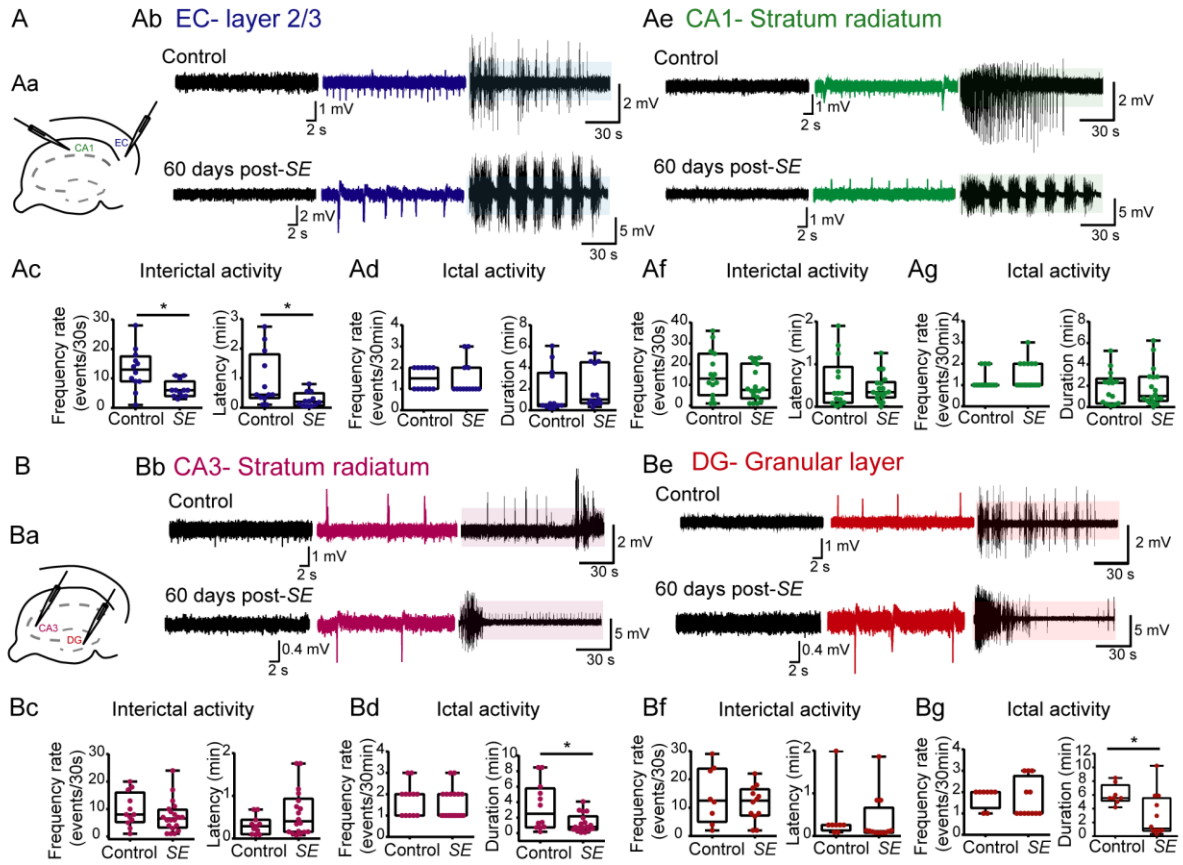

Figure 3. Dual extracellular recordings in hippocampal–EC slices from epileptic and control rats, at 60 days post-SE induction. Traces without epileptiform activity (left), interictal activity (middle), and ictal activity (left).

(Aa) Schematic representation of a horizontal hippocampal-EC slice, showing the locations of two extracellular recording electrodes in entorhinal cortex (EC, blue) and CA1 (green). n of animals: Control: 8, SE: 9.

(Ab) Representative local field potential recordings (top) obtained from EC during application of 4A-P in a hippocampal-EC slice that generated interictal (trace in blue) and ictal discharges (outlined in blue).

(Ac) Boxplot illustrating the pooled data of frequency (number of events/30s; Mann–Whitney U test, U=28, *P < 0.05) (left) and the latency for IEDs (min; Mann–Whitney U test, U=33, *P < 0.05) (right); and **(Ad)** the frequency (number of events/30min; Mann–Whitney U test, U=69, P > 0.05) (left) and duration of Ictal events (min; Mann–Whitney U test, U=51, P > 0.05) (right). n of recordings: Control: 12, SE: 12-13; n of slices: Control: 9, SE: 10.

(Ae) Representative field potential recordings (top) obtained from CA1 during application of 4-AP in a hippocampal-EC slice that generated interictal (trace in green) and ictal discharges (outlined in green).

(Af) Boxplot illustrating the pooled data of frequency (number of events/30s; Mann–Whitney U test, U=100, P > 0.05) (left) and latency for IEDs (min; Mann–Whitney U test, U=116, P > 0.05) (right); and **(Ag)** frequency (number of events/30min; Mann–Whitney U test, U=115.5, P > 0.05) (left) and duration of Ictal events (min; Mann–Whitney U test, U=134.5, P > 0.05) (right). n recordings: Control: 14-15, SE: 18; n slices: Control: 10, SE: 10.

(Ba) Schematic representation of a horizontal hippocampal-EC slice, showing the locations of two extracellular recording electrodes in CA3 (pink) and dentate gyrus (DG, red). n animals: Control: 9; SE: 9.

(Bb) Representative field potential recordings (top) obtained from CA3 during application of 4A-P in a hippocampal-EC slice that generated interictal (trace in pink) and ictal discharges (outlined in pink).

(Bc) Boxplot illustrating the pooled data of frequency (number of events/30s; Mann–Whitney U test, U=90.5, P > 0.05) (left) and the latency for IEDs (min; Mann–Whitney U test, U=70.5, P > 0.05) (right); and **(Bd)** the frequency (number of events/30min; Mann–Whitney U test, U=97, P > 0.05) (left) and

duration of Ictal events (min; Mann–Whitney U test, U=56, *P < 0.05) (right). n recordings: Control: 11-12; SE: 18-20; n slices: Control: 10; SE: 10.
(Be) Representative field potential recordings (top) obtained from DG during application of 4A-P in a hippocampal-EC slice that generated interictal (trace in red) and ictal discharges (outlined in orange).
(Bf) Boxplot illustrating the pooled data of frequency (number of events/30s; Mann–Whitney U test, U=41 P > 0.05) (left) and the latency for IEDs (min; Mann–Whitney U test, U=31, P > 0.05) (right); and **(Bd)** the frequency (number of events/30min; Mann–Whitney U test, U=41, P > 0.05) (left) and duration of Ictal events (min; Mann–Whitney U test, U=19, *P < 0.05) (right). n recordings: Control: 8, SE: 12; n slices: Control: 9, SE: 8.

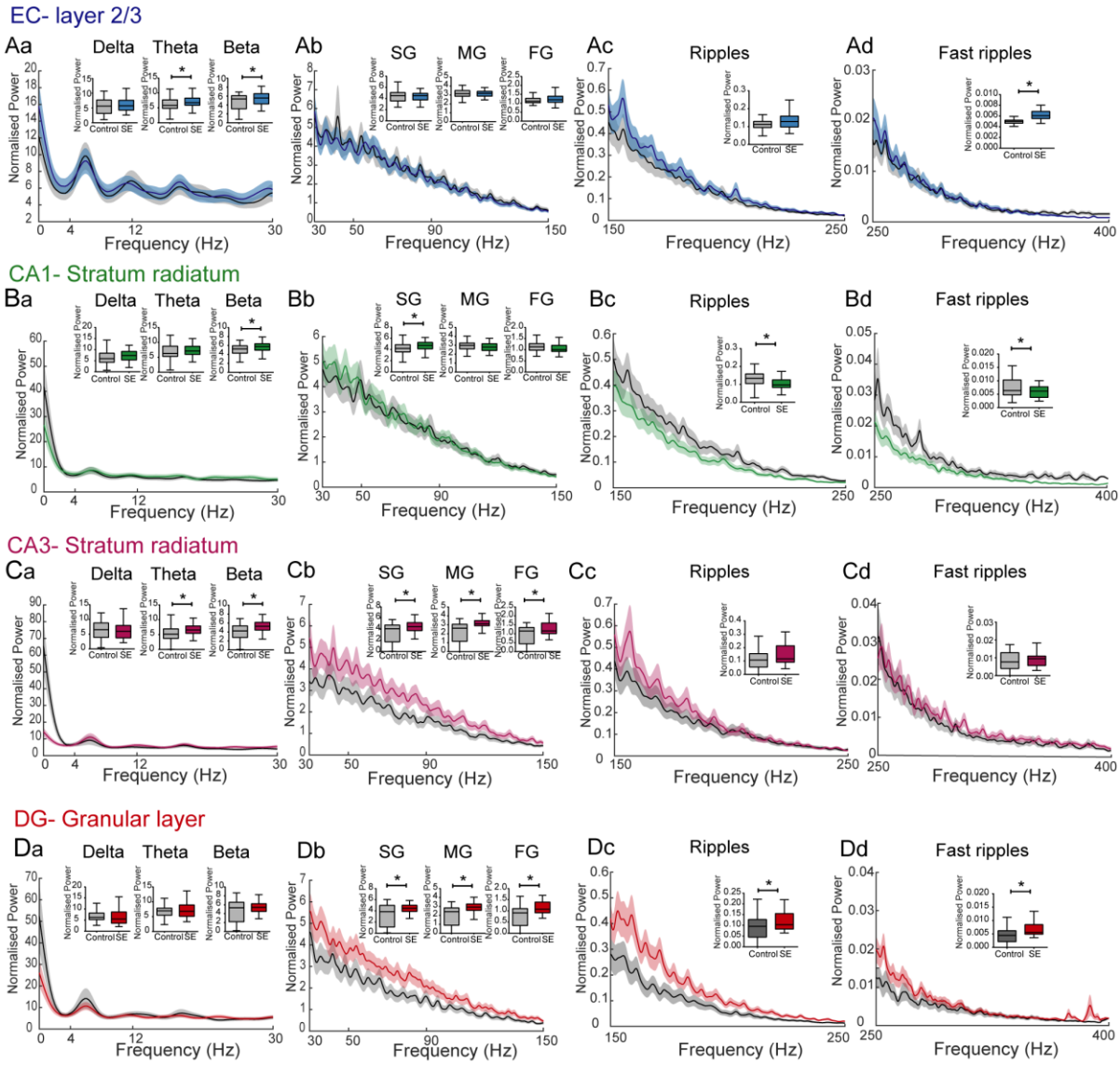

Figure 4. Power spectral densities of frequencies between 0 and 400 Hz in hippocampal-EC slices from epileptic and control animals, at 60 days post-SE induction. Control group (n of epoch: 35-50; n of animals: 9); Epileptic group (n of epoch: 30-50; n of animals: 8-9). SG: Slow gamma; MG: Middle gamma; FG: Fast gamma.

(Aa) Delta, theta, beta frequency bands in EC of control and epileptic groups. Power of theta (Unpaired t-test, t=2.04; *P < 0.05), and beta (Unpaired t-test, t=2.35; *P < 0.05) was higher in EC of slices from epileptic animals than control slices. Data are presented as mean ± SD. Inset, box-and-whiskers plot illustrating the pooled data for control and epileptic groups.

(Ab) Slow-, middle- and fast gamma frequency bands in EC of control and epileptic groups. Data are presented as mean ± SD. Inset, box-and-whiskers plot illustrating the pooled data for control and epileptic groups. Unpaired t-test or Mann–Whitney U test, P > 0.05.

(Ac) Ripples frequency band in EC of control and epileptic groups. Data are presented as mean ± SD. Inset, box-and-whiskers plot illustrating the pooled data for control and epileptic groups. Mann–Whitney U test, P > 0.05.

(Ad) Fast ripples frequency band in EC of control and epileptic groups. Data are presented as mean ± SD. Inset, box-and-whiskers plot illustrating the pooled data for control and epileptic groups. Unpaired t-test, t=6.88; *P < 0.05.

(Ba) Delta, theta, beta frequency bands in CA1 of control and epileptic groups. Data are presented as mean ± SD. Power of beta oscillation was higher in CA1 of slices from epileptic animals than control slices (Unpaired t-test, t=2.50; *P < 0.05). Inset, box-and-whiskers plot illustrating the pooled data for control and epileptic groups.

(Bb) Slow-, middle- and fast gamma frequency bands in CA1 of control and epileptic groups. Data are presented as mean ± SD. Power of slow gamma oscillation was higher in CA1 of slices from epileptic animals than control slices (Unpaired t-test, t=2.36; *P < 0.05). Inset, box-and-whiskers plot illustrating the pooled data for control and epileptic groups.
(Bc) Ripples frequency band in CA1 of control and epileptic groups. Data are presented as mean ± SD. Inset, box-and-whiskers plot illustrating the pooled data for control and epileptic groups. Mann–Whitney U test, U=687; *P < 0.05.
(Bd) Fast ripples frequency band in CA1 of control and epileptic groups. Data are presented as mean ± SD. Inset, box-and-whiskers plot illustrating the pooled data for control and epileptic groups. Mann–Whitney U test, U=746.5; *P < 0.05.
(Ca) Delta, theta, beta frequency bands in CA3 of control and epileptic groups. A higher power of theta (Mann–Whitney U test, U=801; *P <0.05) and beta (Unpaired t-test, t=3.81; *P <0.05) were found in CA3 of slices from epileptic animals, when compared to controls. Data are presented as mean ± SD. Inset, box-and-whiskers plot illustrating the pooled data for control and epileptic groups.
(Cb) Slow-, middle- and fast gamma frequency bands in CA3 of control and epileptic groups. Power of slow- (Mann–Whitney U test, U=846; *P <0.05), middle- (Mann–Whitney U test, U=635; *P <0.05) and fast gamma (Mann–Whitney U test, U=917.5; *P <0.05) were higher in the epileptic group, when compared to control group. Data are presented as mean ± SD. Inset, box-and-whiskers plot illustrating the pooled data for control and epileptic groups.
(Cc) Ripples frequency band in CA3 of control and epileptic groups. Data are presented as mean ± SD. Inset, box-and-whiskers plot illustrating the pooled data for control and epileptic groups. Mann–Whitney U test, P > 0.05.
(Cd) Fast ripples frequency band in CA3 of control and epileptic animals. Data are presented as mean ± SD. Inset, box-and-whiskers plot illustrating the pooled data for control and epileptic groups. Mann–Whitney U test, P > 0.05.
(Da) Delta, theta, beta frequency bands in DG of control and epileptic groups. Data are presented as mean ± SD. Inset, box-and-whiskers plot illustrating the pooled data for control and epileptic groups. Unpaired t-test or Mann–Whitney U test, P > 0.05.
(Db) Slow-, middle- and fast gamma frequency bands in DG of control and epileptic groups. Slices from epileptic animals had a higher power of slow- (Mann–Whitney U test, U=909; *P < 0.05), middle- (Mann–Whitney U test, U=646; *P < 0.05), and fast gamma oscillations (Mann–Whitney U test, U=702; *P < 0.05) than control slices. Data are presented as mean ± SD. Inset, box-and-whiskers plot illustrating the pooled data for control and epileptic groups.
(Dc) Ripples frequency band in DG of control and epileptic groups. Data are presented as mean ± SD. Inset, box-and-whiskers plot illustrating the pooled data for control and epileptic groups. Mann–Whitney U test, U=868; *P < 0.05.
(Dd) Fast ripples frequency band in DG of control and epileptic groups. Data are presented as mean ± SD. Inset, box-and-whiskers plot illustrating the pooled data for control and epileptic groups. Mann–Whitney U test, U=457.5; *P < 0.05.

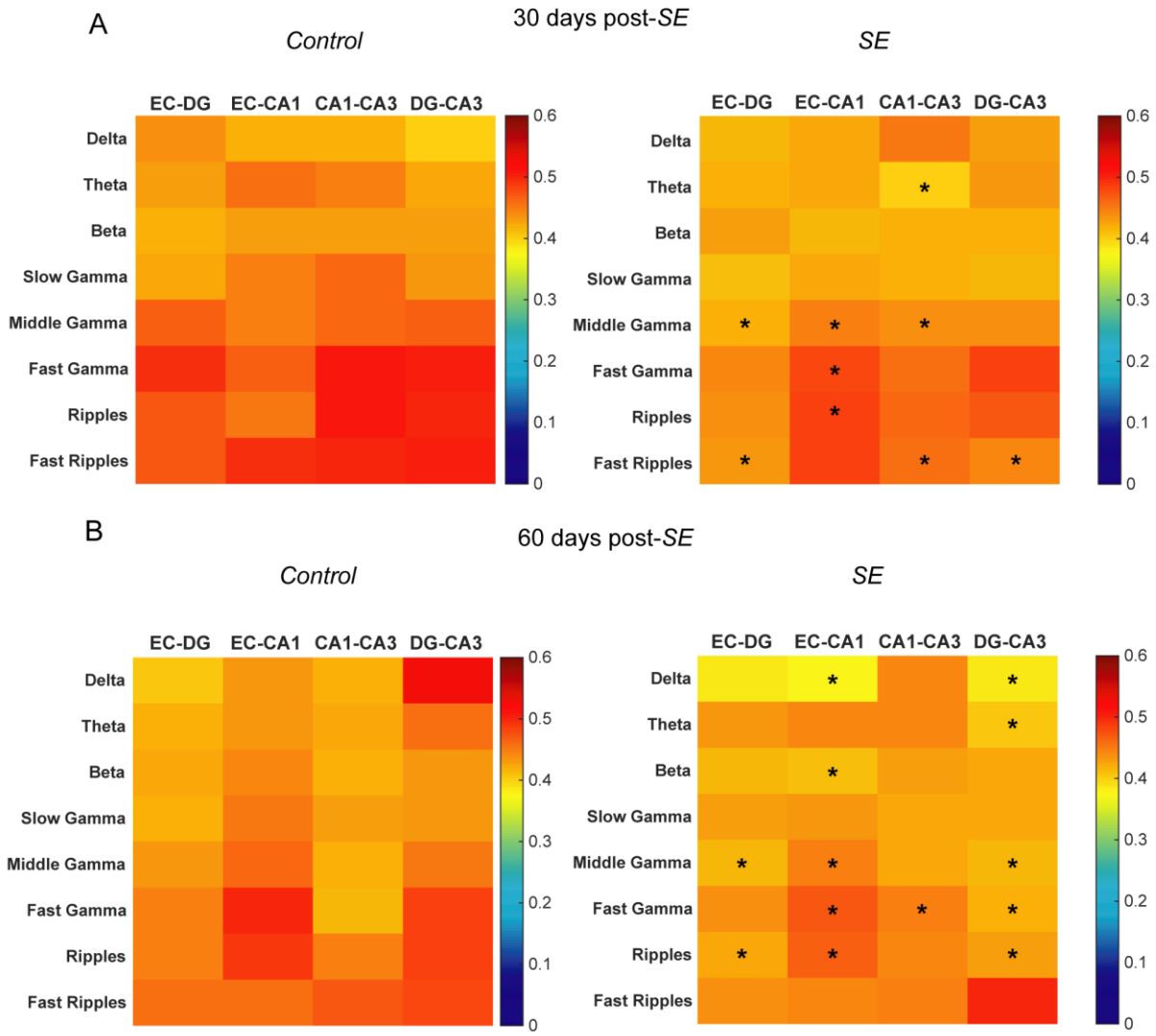

Figure 5. Phase coherence matrices from control and epileptic groups, at 30- and 60-days post-SE induction. The x axis is representing the respective pair of electrodes recorded (EC-DG, EC-CA1, CA1-CA3, DG-CA3), while y axis is showing the mean coherence for all frequency's bands. Warmer colors represent higher coherence. Unpaired t-test or Mann-Whitney test; * $P < 0.05$; differences from control group.
(A) Control and epileptic groups at 30 days post-SE (Control: n of epoch: 20-25, n of animals: 9, SE: n of epoch: 24-25, n of animals: 8).
(B) Control and epileptic groups at 60 days post-SE induction (Control: n of epoch: 20-25, n of animals: 8, SE: n of epoch: 20-25, n of animals: 9).

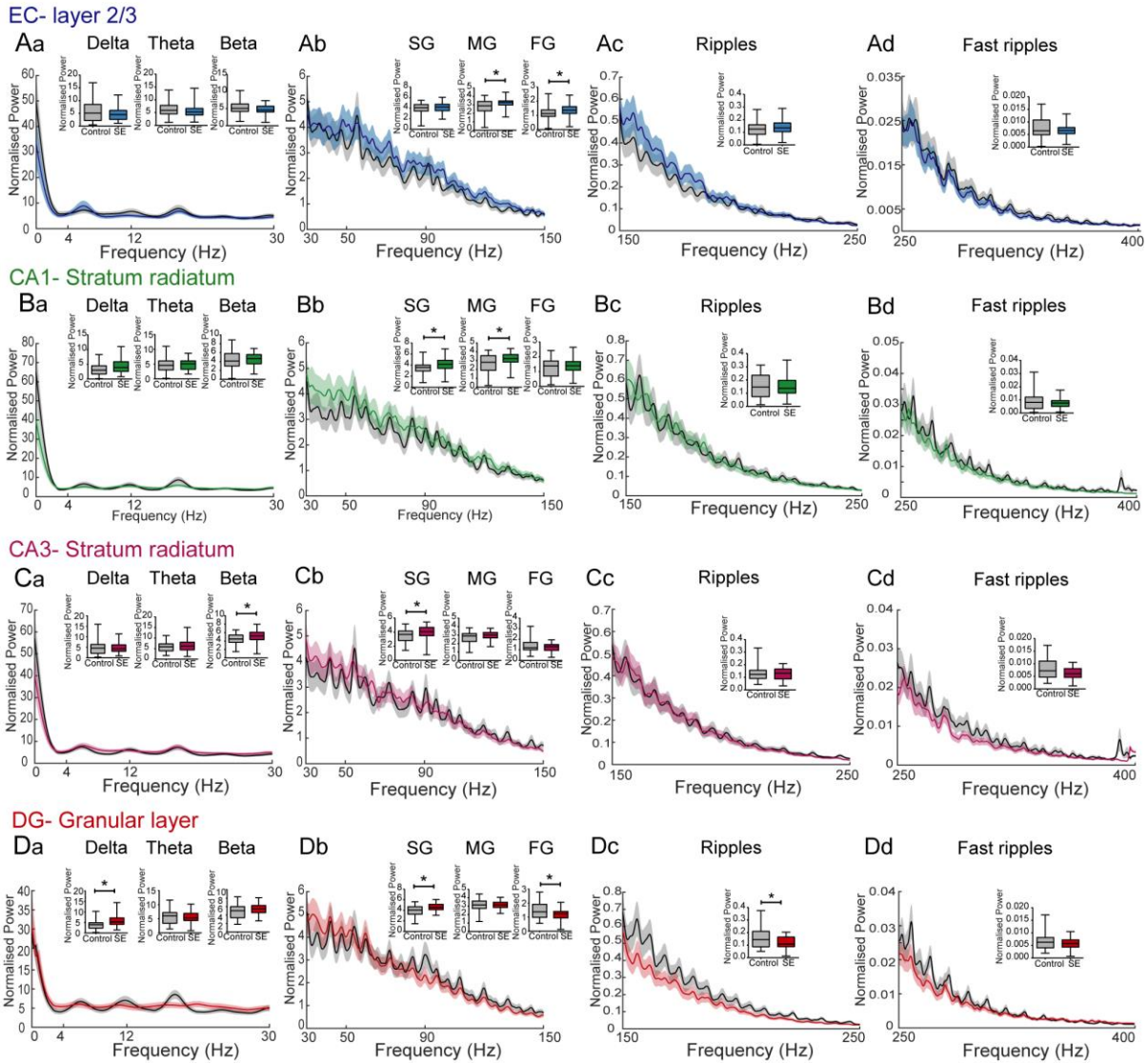

Figure 6. Power spectral densities of frequencies between 0 and 400 Hz in hippocampal-EC slices from epileptic and control animals, during spontaneous network activity, at 30 days post-SE induction. Control group (n of epoch: 30-50; n of animals: 8-9); Epileptic group (n of epoch: 35-50; n of animals: 9). SG: Slow gamma; MG: Middle gamma; FG: Fast gamma.

(Aa) Delta, theta, beta frequency bands in EC of control and epileptic groups. Data are presented as mean ± SD. Inset, box-and-whiskers plot illustrating the pooled data for control and epileptic groups. Unpaired t-test or Mann–Whitney U test, $P > 0.05$.

(Ab) Slow-, middle- and fast gamma frequency bands in EC of control and epileptic groups. Power of middle- (Unpaired t-test, $t=3.45$; $^*P < 0.05$) and fast- gamma oscillation (Unpaired t-test, $t=2.60$; $^*P < 0.05$) were higher in EC of slices from epileptic animals than controls. Data are presented as mean ± SD. Inset, box-and-whiskers plot illustrating the pooled data for control and epileptic groups.

(Ac) Ripples frequency band in EC of control and epileptic groups. Data are presented as mean ± SD. Inset, box-and-whiskers plot illustrating the pooled data for control and epileptic groups. Unpaired t-test, $P > 0.05$.

(Ad) Fast ripples frequency band in EC of control and epileptic groups. Data are presented as mean ± SD. Inset, box-and-whiskers plot illustrating the pooled data for control and epileptic groups. Unpaired t-test, $P > 0.05$.

(Ba) Delta, theta, beta frequency bands in CA1 of control and epileptic groups. Data are presented as mean ± SD. Inset, box-and-whiskers plot illustrating the pooled data for control and epileptic groups. Unpaired t-test or Mann–Whitney U test, $P > 0.05$.

(Bb) Slow-, middle- and fast gamma frequency bands in CA1 of control and epileptic groups. Slices from epileptic groups had higher Power of slow- (Mann–Whitney U test, $U=752$; $^*P < 0.05$) and middle

oscillations (Unpaired t-test, t=3.10; *P < 0.05) than control slices. Data are presented as mean ± SD. Inset, box-and-whiskers plot illustrating the pooled data for control and epileptic groups.
(Bc) Ripples frequency band in CA1 of control and epileptic groups. Data are presented as mean ± SD. Inset, box-and-whiskers plot illustrating the pooled data for control and epileptic groups. Unpaired t-test, P > 0.05.
(Bd) Fast ripples frequency band in CA1 of control and epileptic groups. Data are presented as mean ± SD. Inset, box-and-whiskers plot illustrating the pooled data for control and epileptic groups. Mann–Whitney U test, P > 0.05.
(Ca) Delta, theta, beta frequency bands in CA3 of control and epileptic groups. Power of beta oscillations was higher in slices from epileptic animals (Unpaired t-test, t=2.68; *P < 0.05) when compared to control slices. Data are presented as mean ± SD. Inset, box-and-whiskers plot illustrating the pooled data for control and epileptic groups.
(Cb) Slow-, middle- and fast gamma frequency bands in CA3 of control and epileptic groups. Power of slow gamma oscillations was higher in slices from epileptic animals (Unpaired t-test, t=2.40; *P < 0.05) when compared to control slices. Data are presented as mean ± SD. Inset, box-and-whiskers plot illustrating the pooled data for control and epileptic groups.
(Cc) Ripples frequency band in CA3 of control and epileptic groups. Data are presented as mean ± SD. Inset, box-and-whiskers plot illustrating the pooled data for control and epileptic groups. Mann–Whitney U test, P > 0.05.
(Cd) Fast ripples frequency band in CA3 of control and epileptic groups. Data are presented as mean ± SD. Inset, box-and-whiskers plot illustrating the pooled data for control and epileptic groups. Mann–Whitney U test, P > 0.05.
(Da) Delta, theta, beta frequency bands in DG of control and epileptic groups. Power of delta oscillations was higher in slices from epileptic animals (Mann–Whitney U test, U=726; *P < 0.05) than control slices. Data are presented as mean ± SD. Inset, box-and-whiskers plot illustrating the pooled data for control and epileptic groups.
(Db) Slow-, middle- and fast gamma frequency bands in DG of control and epileptic groups. Power of slow gamma was higher (Unpaired t-test, t=3.92; *P < 0.05); and power of fast gamma oscillations was lower in slices from epileptic animals (Mann–Whitney U test, U=932; *P < 0.05), in comparison to controls. Data are presented as mean ± SD. Inset, box-and-whiskers plot illustrating the pooled data for control and epileptic groups.
(Dc) Ripples frequency band in DG of control and epileptic groups. Data are presented as mean ± SD. Inset, box-and-whiskers plot illustrating the pooled data for control and epileptic groups. Mann–Whitney U test, U=933; *P < 0.05.
(Dd) Fast ripples frequency band in DG of control and epileptic animals. Data are presented as mean ± SD. Inset, box-and-whiskers plot illustrating the pooled data for control and epileptic groups. Mann–Whitney U test, U=1112; *P < 0.05.

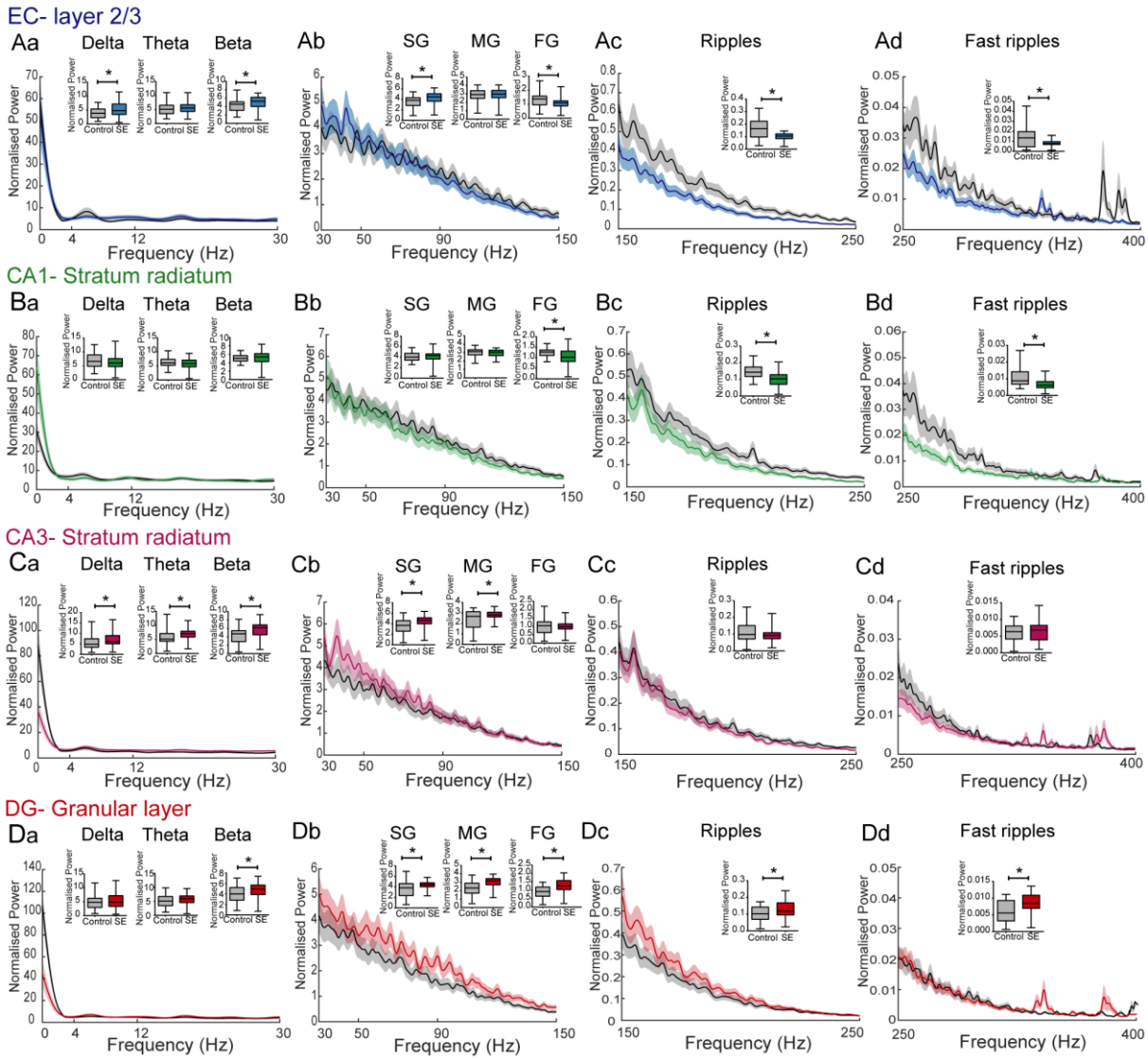

Figure 7. Power spectral densities of frequencies between 0 and 400 Hz in hippocampal-EC slices from epileptic and control animals, during spontaneous network activity, at 60 days post-SE induction. Control group (n of epoch: 30-50; n of animals: 8-9); Epileptic group (n of epoch: 35-50; n of animals: 9). SG: Slow gamma; MG: Middle gamma; FG: Fast gamma.

(Aa) Delta, theta, beta frequency bands in EC of control and epileptic groups. Higher power of delta (Mann–Whitney U test, U=874; *P < 0.05), theta (Unpaired t-test, t=1.0; *P < 0.05) and beta (Mann–Whitney U test, U=877; *P < 0.05) were found in slices from epileptic animals, when compared to controls. Data are presented as mean ± SD. Inset, box-and-whiskers plot illustrating the pooled data for control and epileptic groups.

(Ab) Slow-, middle- and fast gamma frequency bands in EC of control and epileptic groups. Higher power of slow gamma (Unpaired t-test, t=3.02; *P < 0.05), and lower power of fast gamma (Mann–Whitney U test, U=794; *P < 0.05) were found in slices from epileptic animals, when compared to controls. Data are presented as mean ± SD. Inset, box-and-whiskers plot illustrating the pooled data for control and epileptic groups.

(Ac) Ripples frequency band in EC of control and epileptic. Data are presented as mean ± SD. Inset, box-and-whiskers plot illustrating the pooled data for control and epileptic groups. Unpaired t-test, t=5.38; *P < 0.05.

(Ad) Fast ripples frequency band in EC of control and epileptic groups. Data are presented as mean ± SD. Inset, box-and-whiskers plot illustrating the pooled data for control and epileptic groups. Mann–Whitney U test, U=790; *P < 0.05.

(Ba) Delta, theta, beta frequency bands in CA1 of control and epileptic groups. Data are presented as mean ± SD. Inset, box-and-whiskers plot illustrating the pooled data for control and epileptic groups. Unpaired t-test or Mann–Whitney U test, $P > 0.05$.
(Bb) Slow-, middle- and fast gamma frequency bands in CA1 of control and epileptic groups. Power of fast gamma oscillation was lower in slices from epileptic animals (Unpaired t-test, $t=3.21$; $^*P < 0.05$), than in controls. Data are presented as mean ± SD. Inset, box-and-whiskers plot illustrating the pooled data for control and epileptic groups.
(Bc) Ripples frequency band in CA1 of control and epileptic groups. Data are presented as mean ± SD. Inset, box-and-whiskers plot illustrating the pooled data for control and epileptic groups. Unpaired t-test, $t=4.75$; $^*P < 0.05$.
(Bd) Fast ripples frequency band in CA1 of control and epileptic groups. Data are presented as mean ± SD. Inset, box-and-whiskers plot illustrating the pooled data for control and epileptic groups. Mann-Whitney test, $U=503$; $^*P < 0.05$.
(Ca) Delta, theta, beta frequency bands in CA3 of control and epileptic groups. Power of delta (Mann-Whitney test, $U=896$; $^*P < 0.05$), theta (Unpaired t-test, $t=3.02$; $^*P < 0.05$), beta (Unpaired t-test, $t=3.89$; $^*P < 0.05$) bands were higher in slices from epileptic animals, than control slices. Data are presented as mean ± SD. Inset, box-and-whiskers plot illustrating the pooled data for control and epileptic groups.
(Cb) Slow-, middle- and fast gamma frequency bands in CA3 of control and epileptic groups. Power of slow- (Mann-Whitney test, $U=711$; $^*P < 0.05$), and middle (Mann-Whitney test, $U=912$; $^*P < 0.05$) gamma bands were higher in slices from epileptic animals, than control slices. Data are presented as mean ± SD. Inset, box-and-whiskers plot illustrating the pooled data for control and epileptic groups.
(Cc) Ripples frequency band in CA3 of control and epileptic groups. Data are presented as mean ± SD. Inset, box-and-whiskers plot illustrating the pooled data for control and epileptic groups. Mann-Whitney test, $P > 0.05$.
(Cd) Fast ripples frequency band in CA3 of control and epileptic groups. Data are presented as mean ± SD. Inset, box-and-whiskers plot illustrating the pooled data for control and epileptic groups. Unpaired t-test, $P > 0.05$.
(Da) Delta, theta, beta frequency bands in DG of control and epileptic groups. Slices from epileptic animals had higher power of beta (Unpaired t-test, $t=2.63$; $^*P < 0.05$) than control slices. Data are presented as mean ± SD. Inset, box-and-whiskers plot illustrating the pooled data for control and epileptic groups.
(Db) Slow-, middle- and fast gamma frequency bands in DG of control and epileptic groups. Power of slow- (Mann-Whitney test, $U=816$; $^*P < 0.05$), middle- (Unpaired t-test, $t=5.37$; $^*P < 0.05$), and fast- (Unpaired t-test, $t=4.72$; $^*P < 0.05$) gamma were higher in slices from epileptic animals than control slices. Data are presented as mean ± SD. Inset, box-and-whiskers plot illustrating the pooled data for control and epileptic groups.
(Dc) Ripples frequency band in DG of control and epileptic groups. Data are presented as mean ± SD. Inset, box-and-whiskers plot illustrating the pooled data for control and epileptic groups. Unpaired t-test, $t=2.80$; $^*P < 0.05$.
(Dd) Fast ripples frequency band in DG of control and epileptic groups. Data are presented as mean ± SD. Inset, box-and-whiskers plot illustrating the pooled data for control and epileptic groups. Mann-Whitney test, $U=744$; $^*P < 0.05$.

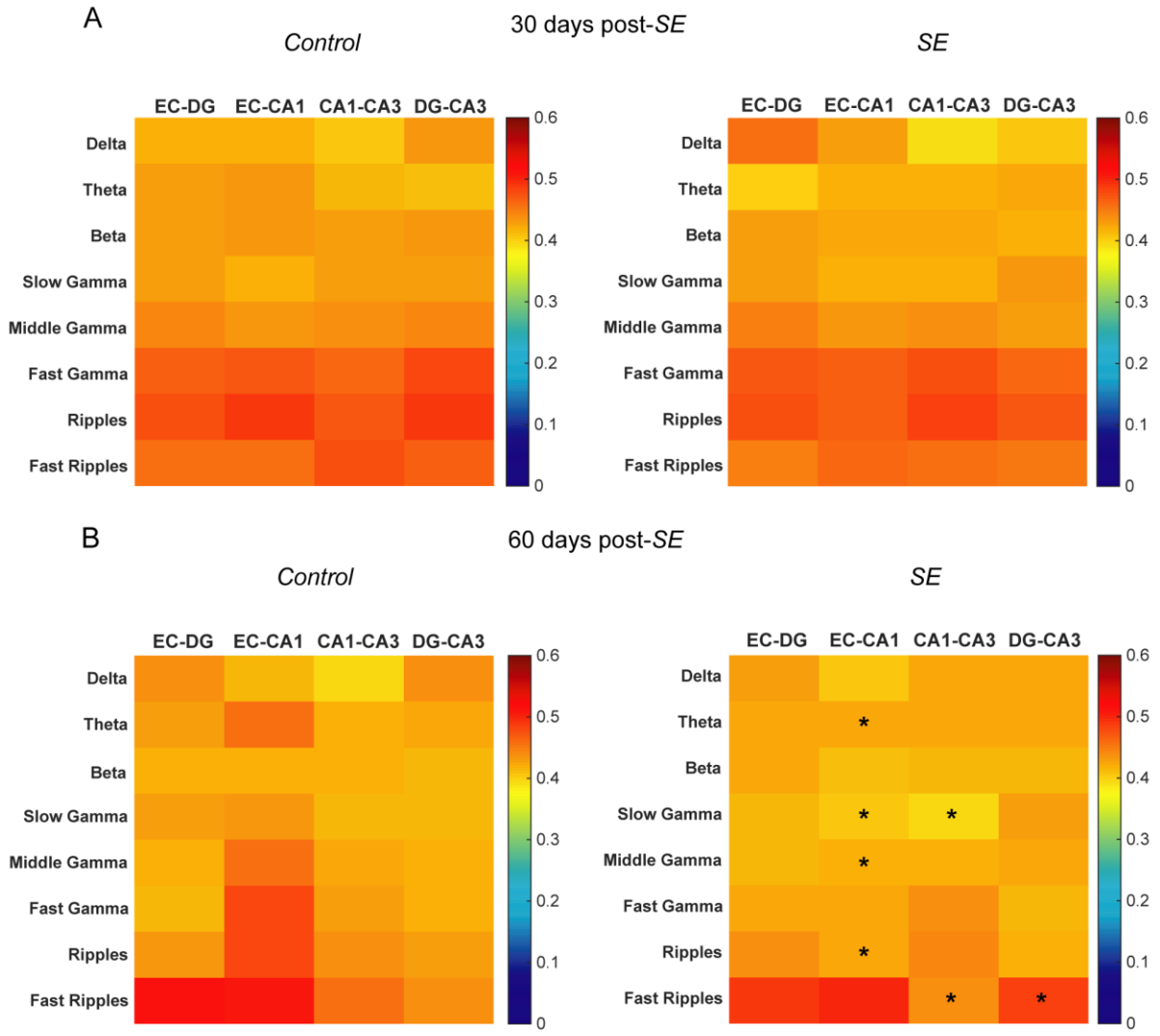

Figure 8. Phase coherence matrices from control and epileptic groups, during spontaneous network activity, at 30- and 60-days post-SE induction. The x axis is representing the respective pair of electrodes recorded (EC-DG, EC-CA1, CA1-CA3, DG-CA3), while y axis is showing the mean coherence for all frequency's bands. Warmer colors represent higher coherence. Unpaired t-test or Mann-Whitney test; * P < 0.05; differences from control group.
(A) Control and epileptic groups at 30 days post-SE (Control: n of epoch: 20-25, n of animals: 8, SE: n of epoch: 20-25, n of animals: 9).
(B) Control and epileptic groups at 60 days post-SE induction (Control: n of epoch: 20-25, n of animals: 8, SE: n of epoch: 20-25, n of animals: 9).

SUPPLEMENTARY INFORMATION

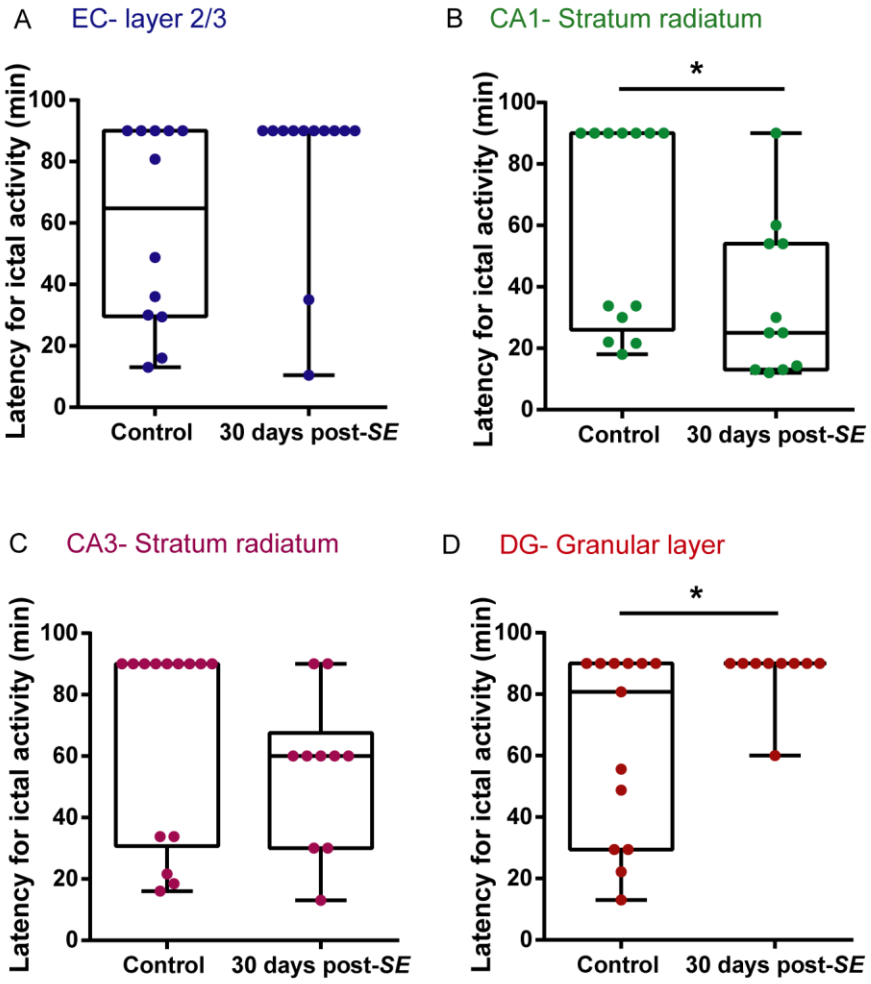

Figure S1. Latency for the first ictal discharge in hippocampal–EC slices from epileptic and control rats, at 30 days post-SE. (A) EC, **(B)** CA1, **(C)** CA3 and **(D)** DG. Mann–Whitney U test, *P < 0.05.

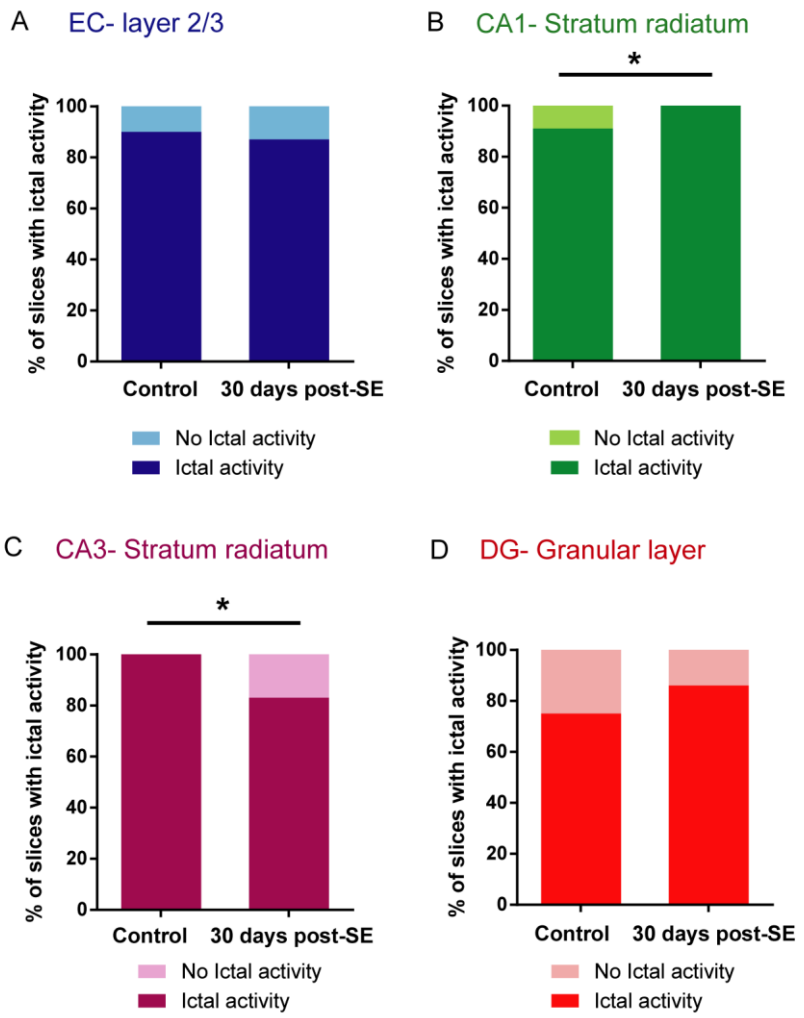

Figure S2. Percentage of slices generating ictal discharges after 4-AP bath application, at 30 days post-SE. (A) EC, **(B)** CA1, **(C)** CA3 and **(D)** DG. EC Control: 90% (9/10 slices), EC SE: 87.5% (7/8 slices); CA1 Control: 90.9% (10/11 slices), CA1 SE: 100% (7/7 slices); CA3 Control: 100% (9/9 slices), CA3 SE: 83.3% (5/6 slices); DG Control: 75% (6/8 slices), DG SE: 85.7% (6/7 slices). *P < 0.05, Fisher's exact test.

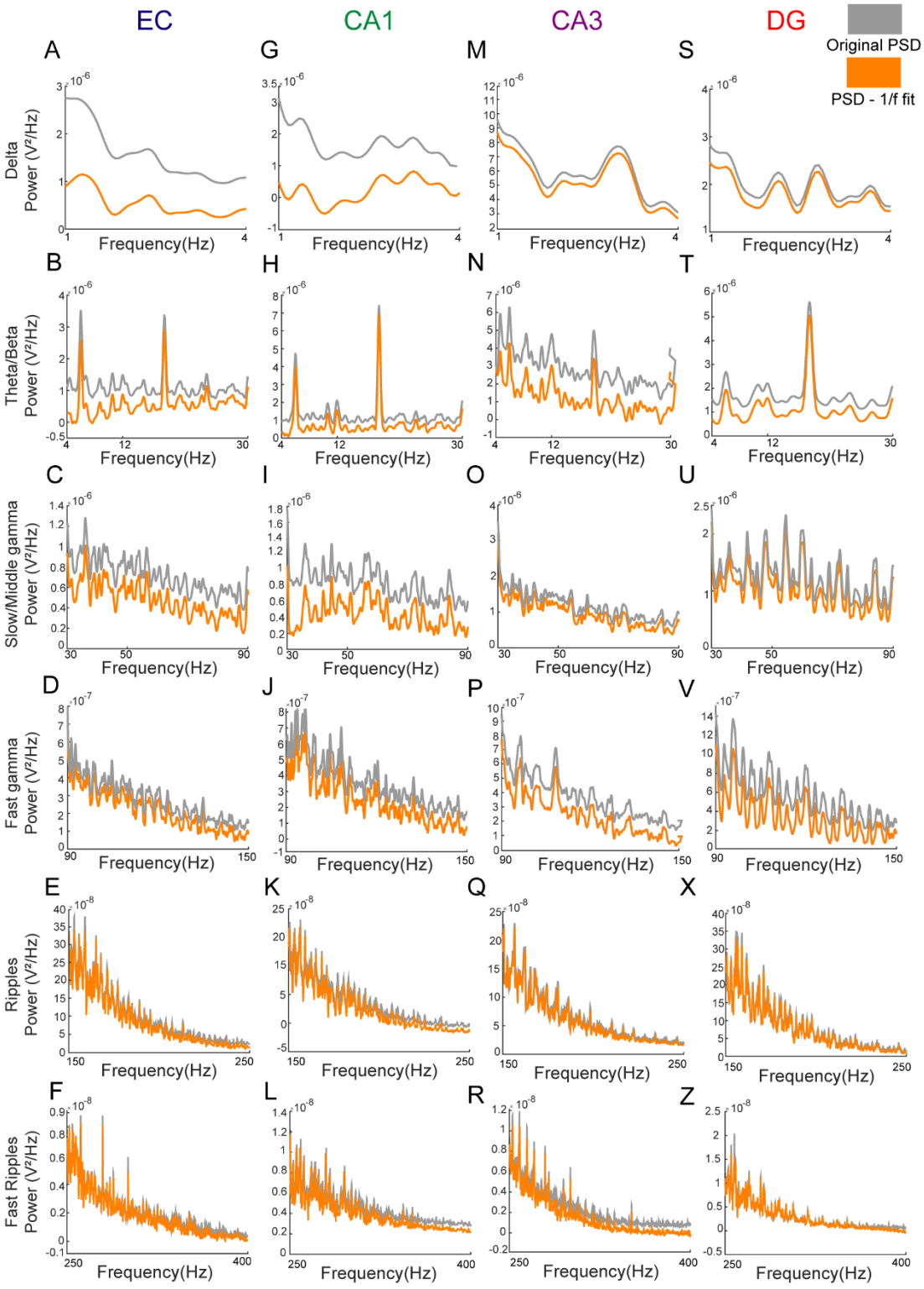

Figure S3. Original PSD (grey) containing aperiodic activity and the 1/f fit removal from PSD (orange) of 4-AP-bathed control slices for all frequency bands in each hippocampal formation region. (A-F) EC, **(G-L)** CA1, **(M-R)** CA3 and **(T-Z)** DG.

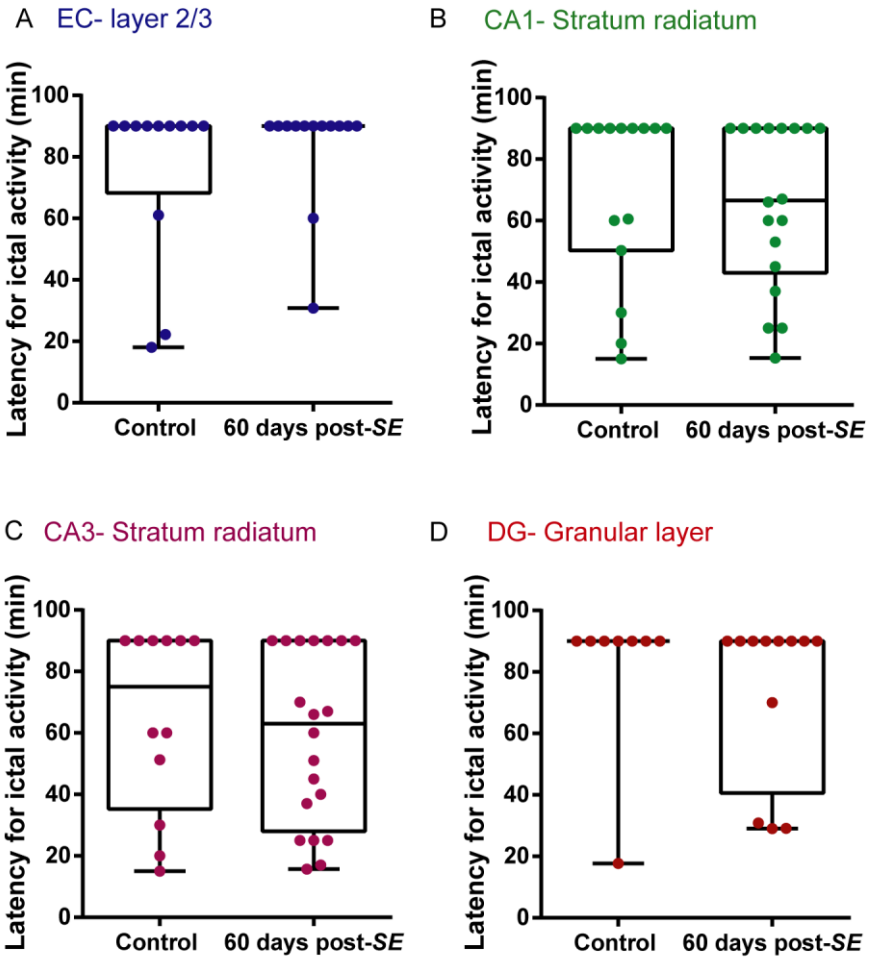

Figure S4. Latency for the first ictal discharge in hippocampal–EC slices from epileptic and control rats, at 60 days post-*SE*. (A) EC, **(B)** CA1, **(C)** CA3 and **(D)** DG. Mann–Whitney U test, *P < 0.05.

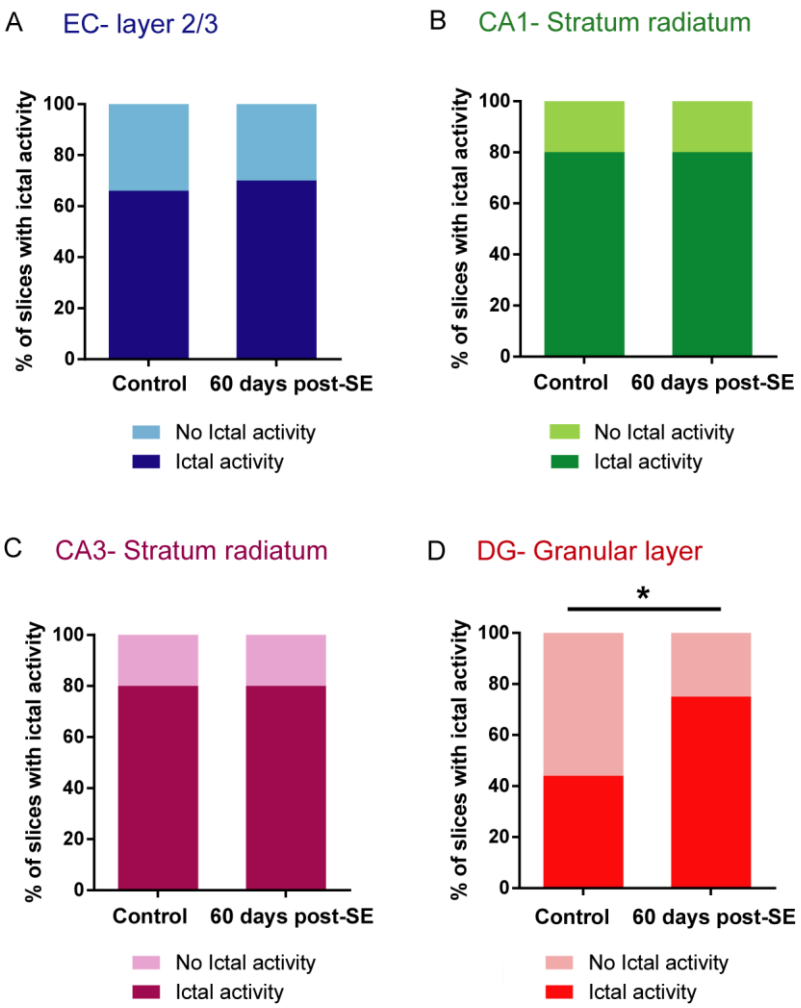

Figure S5. Percentage of slices generating ictal discharges after 4-AP bath application, at 60 days post-*SE*. (A) EC, **(B)** CA1, **(C)** CA3 and **(D)** DG. EC Control: 66% (6/9 slices), EC SE: 70% (7/10 slices); CA1 Control: 80% (8/10 slices), CA1 SE: 80% (8/10 slices); CA3 Control: 80% (8/10 slices), CA3 SE: 80% (8/10 slices); DG Control: 44.4% (4/9 slices), DG SE: 75% (6/8 slices). *P < 0.05, Fisher's exact test.

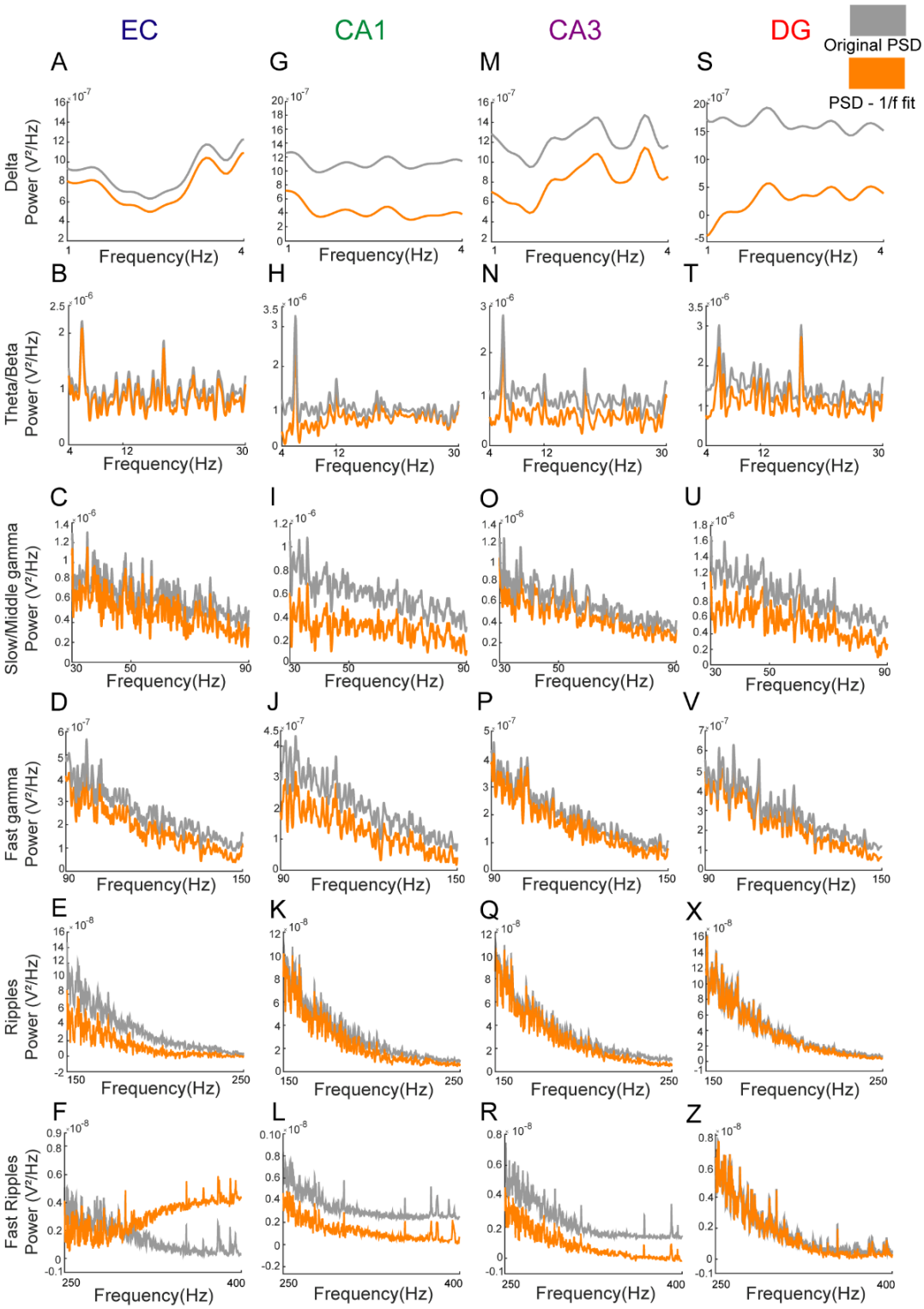

Figure S6. Original PSD (grey) containing aperiodic activity and the 1/f fit removal from PSD (orange) during spontaneous network activity of control slices for all frequency bands in each hippocampal formation region. (A-F) EC, **(G-L)** CA1, **(M-R)** CA3 and **(T-Z)** DG.

Table S1. Characteristics of 4-AP-induced epileptiform activity in EC, CA1, CA3 and DG at 30- and 60-days post-*SE* induction.

		IEDs		*IDs*		
Region	**Group**	**Frequency (events/30s)**	**Latency (min)**	**Frequency (events/30min)**	**Latency (min)**	**Duration (min)**
			30 days post-SE			
EC	**Control**	9.75±7.80	0.79±0.97	1.33±0.65	58.6±32.4	1.14±1.04
	SE	6.00±2.98	1.99±2.45	1.41±0.66	78.7±26.7	0.96±1.62
CA1	**Control**	7.61±5.50	0.54±0.58	1.46±0.77	60.7±33.2	2.21±3.16
	SE	5.63±3.95	0.82±0.65	1.72±1.19	**35.4±25.5[a]**	2.00±1.80
CA3	**Control**	10.2±9.08	0.52±0.41	1.64±0.84	66.6±32.8	1.45±1.57
	SE	8.10±6.10	0.37±0.18	1.10±0.31	55.3±24.9	**3.21±2.71[a]**
DG	**Control**	1.65±1.30	0.32±0.18	2.76±1.01	63.0±30.7	1.69±1.30
	SE	**0.72±0.78[a]**	**0.72±0.78[a]**	**1.22±0.44[b]**	**86.6±10.0[a]**	**0.72±0.78[a]**
			60 days post-SE			
EC	**Control**	13.0±7.15	0.94±0.91	1.50±0.52	75.9±27.3	1.76±2.10
	SE	**6.33±2.80[b]**	**0.26±0.24[a]**	1.46±0.77	83.1 ±17.7	**2.05 ±1.90[d]**
CA1	**Control**	**15.00±11.05[c]**	0.54±0.59	1.20±0.41	69.7±28.4	1.86±1.52
	SE	10.2±8.19	0.44±0.31	1.38±0.60	**65.1±26.6[d]**	1.86±1.77
CA3	**Control**	9.66 ±6.09	0.31±0.21	1.75±0.75	66.6±32.8	**3.44 ±3.04[c]**
	SE	7.35 ±5.72	0.59±0.54	1.50±0.68	**58.6±28.2[d]**	**1.29±1.15[a]**
DG	**Control**	14.38 ±9.92	0.43±0.63	**1.75±0.46[c]**	80.9±25.5	**6.02 ±1.44[c]**
	SE	**11.50 ±6.24[d]**	0.37±0.54	1.66±0.88	73.2±26.9	**2.94±3.09[ad]**

Data are expressed as mean±SD. [a] $P < 0.05$; difference from control group; [b] $P < 0.001$; difference from control group; [c] $P < 0.05$; difference from control 30 days post-*SE*; [d] $P < 0.05$; difference from SE 30 days post-*SE*. *IEDs*: Interictal events discharges; *IDs*: Ictal events. EC: entorhinal cortex; DG: dentate gyrus

Table S2. PSD of different oscillations, under 4-AP induced hyperexcitability, in EC, CA1, CA3 and DG at 30- and 60 days post-*SE.*

Region	Group	Delta	Theta	Beta	Slow gamma	Middle gamma	Fast gamma	Ripples	Fast Ripples
					30 days post-SE				
EC	**Control**	5.92±3.48	5.38±2.07	4.84±1.70	4.25±0.95	3.08±0.42	1.33 ±0.29	0.15±0.06	0.009±0.003
	SE	5.63±1.86	5.94±1.53	5.22±0.94	**4.67±0.73[a]**	3.10±0.40	1.30±0.28	0.14±0.03	0.009±0.002
CA1	**Control**	5.79±3.40	5.34±2.03	4.64±1.34	3.78±1.04	2.97±0.66	1.44±0.45	0.17 ±0.06	0.010±0.003
	SE	5.61±3.54	5.24±1.87	4.83±1.35	4.04±0.70	**3.32±0.50[b]**	1.51±0.49	0.16 ±0.06	0.009±0.001
CA3	**Control**	5.61±3.54	6.80±4.07	4.58±2.01	3.46±1.43	2.31±0.91	0.88±0.44	0.09±0.04	0.006±0.003
	SE	**4.93±2.45[d]**	**5.06±2.35[a]**	4.17±1.57	**4.06±0.57[b]**	**3.35±0.52[d]**	**1.54±0.55[d]**	**0.17±0.07[d]**	**0.008±0.003[b]**
DG	**Control**	4.35±2.66	4.33±2.00	4.20±1.78	4.02±0.63	3.14 ±0.57	1.40±0.62	0.16±0.07	0.008±0.008
	SE	4.86±2.51	**5.40±2.17[a]**	4.72±1.66	4.10±1.23	3.21±0.43	1.28±0.51	0.15±0.07	0.008±0.003
					60 days post-SE				
EC	**Control**	5.44±2.63	6.24±2.34	4.65±1.84	4.16±1.39	3.17±0.41	1.17 ±0.40	0.11±0.04	0.004±0.0005
	SE	6.23±2.56	**7.08±1.72[a]**	**5.42±1.37[a]**	4.34±0.81	3.15±0.35	1.25±0.32	0.13±0.05	**0.006±0.0007[c]**
CA1	**Control**	6.57±3.20	6.90±2.42	5.03±1.53	4.10±1.17	2.89±0.55	1.13±0.26	0.13 ±0.04	0.007±0.003
	SE	7.45±2.79	7.27±1.98	**5.71±1.16[a]**	**4.59±0.90[a]**	2.80±0.49	1.06±0.23	**0.10 ±0.03[b]**	**0.005±0.002[a]**
CA3	**Control**	6.62 ±2.96	5.31±2.58	3.98±1.88	3.30±1.79	2.17±1.19	0.92±0.52	0.11±0.07	0.008±0.006
	SE	**6.14±2.76[a]**	**6.89±2.23[b]**	**5.26±1.42[b]**	**4.48±1.00[b]**	**3.15±0.48[c]**	**1.28±0.41[a]**	0.14±0.07	0.009±0.004
DG	**Control**	6.78±2.92	6.56±2.48	4.69±2.41	3.32±1.93	1.99 ±1.10	0.77±0.43	0.08±0.05	0.004±0.003
	SE	6.48±3.49	7.36±2.61	5.38±1.20	**4.43±0.82[a]**	2.92±0.53c	**1.14±0.29[b]**	**0.11±0.04[a]**	**0.006±0.002[b]**

Data are expressed as mean±SD. [a] $P < 0.05$, difference from control group; [b] $P < 0.01$, difference from control group; [c] $P < 0.001$, difference from control group, [d] $P < 0.0001$, difference from control group. EC: entorhinal cortex; DG: dentate gyrus

Table S3. **Mean phase coherence of different oscillations, under 4-AP induced hyperexcitability, between EC, CA1, CA3 and DG, at 30- and 60- days post-*SE***.

Region	Group	Delta	Theta	Beta	Slow gamma	Middle gamma	Fast gamma	Ripples	Fast Ripples
					30 days post-SE				
EC-DG	**Control**	0.44±0.09	0.43±0.05	0.41±0.04	0.41±0.03	0.46±0.07	0.49±0.09	0.47±0.07	0.47±0.02
	SE	0.41±0.09	0.42±0.05	0.42±0.05	0.40±0.03	**0.41±0.02[a]**	0.44±0.03	0.43±0.01	**0.43±0.01[d]**
EC-CA1	**Control**	0.41±0.09	0.45±0.05	0.42±0.03	0.44±0.05	0.41±0.02	0.40±0.02	0.41±0.01	0.49±0.04
	SE	0.42±0.08	0.42±0.06	0.41±0.03	0.42±0.04	**0.44±0.04[a]**	**0.48±0.06[d]**	**0.48±0.05[d]**	0.48±0.05
CA1-CA3	**Control**	0.41±0.08	0.44±0.05	0.43±0.04	0.45±0.07	0.40±0.02	0.43±0.03	0.45±0.03	0.50±0.06
	SE	0.45±0.12	**0.40±0.05[b]**	0.42±0.03	0.42±0.02	**0.43±0.04[b]**	0.45±0.06	0.46±0.04	**0.45±0.03[a]**
DG-CA3	**Control**	0.39±0.10	0.42±0.05	0.42±0.02	0.43±0.05	0.45±0.05	0.48±0.07	0.49±0.08	0.50±0.06
	SE	0.43±0.10	0.43±0.05	0.41±0.03	0.41±0.03	0.44±0.02	0.48±0.05	0.47±0.04	**0.44±0.01[d]**
					60 days post-SE				
EC-DG	**Control**	0.40±0.09	0.41±0.05	0.42±0.03	0.41±0.03	0.43±0.03	0.44±0.04	0.44±0.03	0.43±0.02
	SE	0.38±0.09	0.43±0.06	0.41±0.02	0.42±0.03	**0.41±0.02[a]**	0.43±0.02	**0.42±0.01[a]**	0.44±0.02
EC-CA1	**Control**	0.43±0.11	0.43±0.06	0.44±0.03	0.45±0.04	0.46±0.06	0.49±0.09	0.47±0.07	0.44±0.02
	SE	**0.37±0.08[a]**	0.44±0.05	**0.40±0.03[c]**	0.43±0.03	**0.42±0.05[b]**	**0.41±0.01[b]**	**0.42±0.01[b]**	0.44±0.02
CA1-CA3	**Control**	0.42±0.08	0.42±0.05	0.41±0.04	0.42±0.03	0.41±0.02	0.41±0.01	0.44±0.02	0.44±0.01
	SE	0.44±0.12	0.44±0.07	0.43±0.05	0.42±0.03	0.42±0.03	**0.44±0.02[c]**	0.44±0.03	0.44±0.02
DG-CA3	**Control**	0.52±0.14	0.45±0.07	0.43±0.05	0.43±0.03	0.45±0.04	0.48±0.06	0.48±0.05	0.47±0.04
	SE	**0.38±0.09[c]**	**0.40±0.05[b]**	0.42±0.04	0.42±0.04	**0.41±0.02[c]**	**0.41±0.02[d]**	**0.42±0.02[d]**	0.49±0.06

Data are expressed as mean±SD. [a] $P < 0.05$, difference from control group; [b] $P < 0.01$, difference from control group; [c] $P < 0.001$, difference from control group; [d] $P < 0.0001$, difference from control group. EC: entorhinal cortex; DG: dentate gyrus

Table S4. **PSD of different oscillations in EC, CA1, CA3 and DG in absence of 4-AP, at 30- and 60-days post-*SE*.**

Region	Group	Delta	Theta	Beta	Slow gamma	Middle gamma	Fast gamma	Ripples	Fast Ripples
					30 days post-SE				
EC	**Control**	5.55±3.91	6.36±2.73	5.22±1.97	3.83±1.16	2.70±0.84	1.15±0.43	0.12±0.06	0.007±0.004
	SE	4.94±2.80	5.57±2.42	4.73±1.27	4.11±0.85	**3.20±0.59[c]**	**1.37±0.40[a]**	0.14±0.05	0.006±0.002
CA1	**Control**	3.43±2.14	4.73±2.49	4.27±2.09	3.37±1.09	2.65±1.08	1.28±0.62	0.15±0.09	0.008±0.006
	SE	4.21±2.28	4.89±1.83	4.54±1.34	**4.11±1.12[b]**	**3.21±0.63[b]**	1.42±0.49	0.15±0.07	0.007±0.003
CA3	**Control**	5.01±3.58	5.77±2.25	4.42±1.23	3.51±0.97	2.69±0.72	1.35±0.62	0.13±0.06	0.007±0.004
	SE	4.96±2.63	6.50±2.62	**5.12±1.38[c]**	**3.98±0.97[a]**	2.94±0.50	1.26±0.37	0.13±0.04	0.006±0.002
DG	**Control**	4.00±2.52	5.79±2.59	4.89±1.66	3.96±0.88	3.14±0.67	1.47±0.60	0.16±0.08	0.007±0.003
	SE	**5.70±2.72[c]**	5.68±1.80	5.42±1.20	**4.59±0.69[c]**	3.14±0.43	**1.20±0.35[a]**	**0.11±0.04[a]**	0.006±0.002
					60 days post-SE				
EC	**Control**	3.97±1.82	5.17±2.09	4.24±1.37	3.65±0.89	2.85±0.69	1.34±0.50	0.16±0.07	0.015±0.011
	SE	**5.47±2.84[b]**	5.59±2.04	**4.94±1.66[b]**	**4.28±1.16[b]**	2.82±0.84	**1.09±0.42[b]**	**0.10±0.02[d]**	**0.008±0.003[b]**
CA1	**Control**	6.80±2.67	6.24±1.81	5.08±0.90	4.12±0.79	2.99±.0.45	1.23±0.20	0.14±0.04	0.010±0.005
	SE	6.04±2.65	5.59±1.95	5.02±1.71	3.99±1.34	2.94±0.41	**1.02±0.42[b]**	**0.10±0.04[d]**	**0.006±0.002[d]**
CA3	**Control**	5.48±3.15	5.64±2.53	4.34±1.67	3.54±1.26	2.37±0.86	0.99±0.44	0.10±0.05	0.005±0.002
	SE	**6.76±3.16[a]**	**6.98±1.85[b]**	**5.68±1.77[c]**	**4.46±1.15[c]**	**2.82±0.37[a]**	0.99±0.29	0.09±0.04	0.006±0.003
DG	**Control**	4.96±2.57	5.09±2.01	3.99±1.52	3.55±1.43	2.28±0.77	0.90±0.32	0.10±0.04	0.006±0.003
	SE	5.44±2.79	5.72±2.00	**4.77±1.43[b]**	**4.33±0.78[b]**	**3.04±0.60[d]**	**1.25±0.41[d]**	**0.12±0.04[b]**	**0.008±0.002[c]**

Data are expressed in mean±SD. [a] $P < 0.05$, *difference from control group; [b] $P < 0.01$, difference from control group; [c] $P < 0.001$, difference from control group; [d] $P < 0.0001$, difference from control group. EC: entorhinal cortex; DG: dentate gyrus

Table S5. Mean phase coherence of different oscillations in the EC, CA1, CA3 and DG in absence of 4-AP, at 30- and 60-days post-*SE* induction.

Region	Group	Delta	Theta	Beta	Slow gamma	Middle gamma	Fast gamma	Ripples	Fast Ripples
					30 days post-SE				
EC-DG	**Control**	0.41±0.07	0.42±0.05	0.43±0.03	0.43±0.03	0.44±0.02	0.46±0.04	0.47±0.06	0.45±0.03
	SE	0.45±0.08	0.39±0.07	0.43±0.05	0.42±0.03	0.44±0.03	0.47±0.04	0.47±0.04	0.44±0.03
EC-CA1	**Control**	0.41±0.09	0.43±0.07	0.43±0.04	0.41±0.03	0.43±0.03	0.47±0.06	0.48±0.07	0.45±0.03
	SE	0.42±0.08	0.41±0.04	0.42±0.03	0.41±0.04	0.43±0.02	0.46±0.04	0.46±0.02	0.46±0.02
CA1-CA3	**Control**	0.40±0.08	0.41±0.06	0.42±0.04	0.43±0.02	0.44±0.03	0.46±0.05	0.46±0.04	0.47±0.04
	SE	0.39±0.09	0.41±0.04	0.42±0.03	0.41±0.04	0.43±0.03	0.47±0.05	0.48±0.05	0.45±0.02
DG-CA3	**Control**	0.43±0.08	0.40±0.06	0.43±0.03	0.42±0.03	0.44±0.04	0.47±0.06	0.48±0.06	0.46±0.02
	SE	0.40±0.10	0.42±0.03	0.42±0.03	0.43±0.03	0.43±0.02	0.45±0.04	0.46±0.03	0.45±0.02
					60 days post-SE				
EC-DG	**Control**	0.43±0.09	0.43±0.06	0.42±0.05	0.42±0.02	0.42±0.02	0.41±0.02	0.43±0.02	0.51±0.02
	SE	0.43±0.10	0.42±0.05	0.42±0.03	0.41±0.02	0.41±0.02	0.42±0.02	0.44±0.02	0.49±0.03
EC-CA1	**Control**	0.41±0.07	0.45±0.06	0.42±0.01	0.43±0.04	0.46±0.05	0.48±0.09	0.46±0.02	0.49±0.04
	SE	0.40±0.11	**0.42±0.05**[a]	0.41±0.03	**0.40±0.03**[a]	**0.42±0.02**[b]	0.42±0.01	**0.42±0.01**[d]	0.50±0.05
CA1-CA3	**Control**	0.39±0.08	0.42±0.06	0.42±0.04	0.41±0.03	0.42±0.02	0.43±0.03	0.44±0.03	0.46±0.02
	SE	0.42±0.11	0.42±0.05	0.41±0.03	**0.39±0.02**[a]	0.41±0.03	0.44±0.02	0.44±0.03	**0.44±0.02**[a]
DG-CA3	**Control**	0.43±0.08	0.42±0.05	0.41±0.03	0.41±0.03	0.42±0.03	0.42±0.02	0.42±0.01	0.43±0.01
	SE	0.42±0.08	0.42±0.05	0.41±0.03	0.42±0.04	0.42±0.02	0.41±0.02	0.42±0.01	**0.48±0.04**[d]

Data are expressed in mean±SD. [a] $P < 0.05$, difference from control group; [b] $P < 0.01$, difference from control group; [c] $P < 0.001$, difference from control group; [d] $P < 0.0001$, difference from control group. EC: entorhinal cortex; DG: dentate gyrus

Capítulo II

GABAergic interneurons in epilepsy: More than a simple change in inhibition

Title: GABAergic Interneurons in Epilepsy: More than a simple change in inhibition

Joseane Righes Marafiga[1, 2], Mayara Vendramin Pasquetti[1, 2], Maria Elisa Calcagnotto[1, 2, 3]

[1]Neurophysiology and Neurochemistry of Neuronal Excitability and Synaptic Plasticity Laboratory, Department of Biochemistry, ICBS, Universidade Federal do Rio Grande do Sul, Porto Alegre, 90035-003, RS, Brazil

[2]Graduate Program in Biological Science: Biochemistry, Universidade Federal do Rio Grande do Sul, Porto Alegre, 90035-003, RS, Brazil

[3]Graduate Program in Neuroscience, Universidade Federal do Rio Grande do Sul, Porto Alegre, 90046-900, RS, Brazil

*Corresponding author: Maria Elisa Calcagnotto, MD, PhD

Address: NNNESP Lab., Department of Biochemistry, ICBS/UFRGS, R. Ramiro Barcelos 2600 Anexo 21111, Porto Alegre, RS 90035-003, Brazil.

Phone: +55 51 33085570

E-mail: elisa.calcagnotto@ufrgs.br

Abstract

The pathophysiology of epilepsy has been historically grounded on hyperexcitability attributed to the oversimplified imbalance between excitation (E) and inhibition (I) in the brain. The decreased inhibition is mostly attributed to deficits in gamma-aminobutyric acid-containing (GABAergic) interneurons, the main source of inhibition in the central nervous system. However, the cell diversity, the wide range of spatiotemporal connectivity and the distinct effects of the neurotransmitter GABA, especially during development must be considered to critically revisit the concept of hyperexcitability caused by decreased inhibition as a key characteristic in the development of epilepsy. Here, we will discuss that behind this known mechanism, there is a heterogeneity of GABAergic interneurons with distinct functions and sources, which have specific roles in controlling the neural network activity within the recruited microcircuit and altered network during the epileptogenic process.

Keywords: GABAergic system; interneurons; neuronal network; epilepsy; excitation-inhibition imbalance.

1. Introduction

Over the years, the physiopathology of epilepsy has been superficially grounded on the imbalance between excitation (E) and inhibition (I) (E-I) in the brain, presumably due to an increased excitation and reduced inhibition. However, the mechanisms underlying epileptogenesis include processes that range from genes and subcellular signaling cascades to complex neural circuits and neuronal plasticity [1, 2]. Although epileptiform activities and seizures could result from a shift in the balanced E-I [3-7], they are the tip of the iceberg in epilepsy and represent only an event in a complex process of epileptogenesis (Fig. 1). This process includes cellular diversity; synaptic spatiotemporal dynamics of interneuronal connectivity; synaptic reorganization of neuronal microcircuits modifying network synchrony and brain oscillations; and inhibition/excitation interaction, which could be either reinforced or weakened, besides the specific epilepsy etiology and associated comorbidities. Therefore, epileptogenesis are far more complex than the simply decreasing inhibition and increase excitation and different issues need to be considered. For example, the neurotransmitters involved in the process can induce paradoxical effects, especially during development; the antiepileptic drugs do not necessarily decrease or abolish seizures by decreasing excitation or increasing inhibition; and network excitability can be modulated not only by synaptic and intrinsic neuronal properties, but also by metabolic and signaling pathways [8]. In addition, the loss of a glutamatergic cell population, such as, the mossy cells in the hilus of the dentate gyrus of the hippocampus, can be involved on seizure generation instead of decreasing excitability [9]. Although excitatory cells are equally important in seizure generation and epilepsy, we will focus our effort in explore alterations in the inhibitory system.

The impact of impairment in inhibition on brain diseases, including epilepsy, has been consistently investigated [10-13]. Since gamma-aminobutyric acid-containing (GABAergic) interneurons are the main source of inhibition in the brain [14], the population diversity of these cells and their wide range of connectivity, distribution and density must be considered to understand the mechanisms underlying epilepsy [15, 16]. Therefore, the concept that a key point for the epilepsy development is hyperexcitability caused by decreased inhibition must be revisited.

2. Generation of interneuron diversity

Most of GABAergic interneurons in the cerebral cortex and hippocampus originate from three main progenitor regions in the embryonic subpallium: mainly from the caudal and medial ganglionic eminences (CGE and MGE), and a small percentage from the preoptic area (POA) [17-20]. The MGE produces 60% of the cortical and hippocampal interneurons, including fast-spiking parvalbumin (FS-PV)-expressing basket and chandelier cells; and somatostatin (SOM)-expressing interneurons with or without coexpression of either calretinin (CR), neuropeptide-Y (NPY), or reelin. The CGE generates about 30% of interneurons including cholecystokinin (CCK), CR, vasointestinal peptide (VIP), reelin, and neurogliaform cells [12]. The POA gives rise to a small population of multipolar GABAergic neocortical interneurons with rapid and adaptive firing neurons expressing reelin and/or NPY [19]. In addition, GABAergic neurons developed at later stages of human fetal period [21, 22] increase the cellular diversity of inhibitory neuron subtypes that eventually influence the cortical circuitry. These GABAergic interneurons play a central role in information processing by regulating neural activity and local circuits, and by synchronizing neural network

oscillations [23], through their inhibitory effects on excitatory and inhibitory neurons (Fig. 1).

3. Spatiotemporal dynamics of interneuronal connectivity

Different interneuron subtypes are positioned at subcellular domains to control network activity. In the cortex and hippocampus, inhibitory interneuron subtypes differ in their functional and temporal connectivity at distinct postsynaptic domains on pyramidal cells [24-26]. Together with the interneuronal network connectivity, the intrinsic properties of interneurons are particularly crucial to generate and control neuronal oscillations and plasticity [27]. At different time points, GABAergic afferents make synapses on distinct domains of pyramidal cells, dendrites or soma, and one specific domain of pyramidal cells can also receive synaptic contacts from distinct GABAergic interneurons [28]. For example, distal dendritic inhibition from distinct sources, induced essentially by non-fast spiking SOM-, NPY-expressing interneurons, regulates excitatory inputs and is able to inhibit calcium spikes, contributing differentially to dendritic computations and synaptic plasticity [25, 26]. Whereas perisomatic inhibition (i.e., soma, axon initial segment and thick proximal dendrites of cortical and hippocampal pyramidal cells), performed by FS-PV-expressing basket cells or CCK-expressing interneurons, is critical for controlling synchronous network activity [24, 28-33] (Fig. 1). For example, in the hippocampus, basket cells [34] strongly increase their firing rate and the discharges are phase-coupled to the oscillatory cycles of ripples [25] and are moderately coupled to the ascending phase of extracellular gamma oscillations in the pyramidal cell layer. Basket cells have the ability to gate precisely the timing of action potential generation [29, 35, 36]. Moreover, CCK-expressing cells fire at a theta phase when CA1 pyramidal cells start firing, and

during gamma oscillations, CCK-expressing cells fire just before CA1 pyramidal cells [37]. However, FS-PV-expressing interneurons can also innervate either axons [38] or dendrites of target cells with temporal differences [30, 39-41]. Consequently, the position of FS-PV-expressing interneurons seems to be crucial to regulate the output of excitatory circuits and local spiking activity. Different inhibitory interneuron subtypes, which conducted different oscillation patterns in the brain, intrinsically regulate network activity; and the coordinated spatiotemporal synaptic interaction between several classes of interneurons and pyramidal cells during network oscillations can actively generate and modulate inhibition, synchrony and plasticity at different developmental and behavioral states [25, 42]. Thus, GABAergic interneurons participate actively in regulating neuronal networks and brain oscillations [12, 43].

Deficits of GABAergic inputs at specific subcellular domain and timing, modifying the interneuronal circuitry, could affect brain oscillations, inhibition, synchrony and plasticity [25, 44-47]. Indeed, the epileptic brain is able to generate an oscillatory pattern in the network with different spatiotemporal synchronicity [48]. However, the GABAergic-mediated abnormalities are associated not only with epilepsy [15, 49]. Similar deficits in the GABAergic system are shared with several neurological and psychiatric disorders [50], such as, schizophrenia [51], anxiety [52], and autism spectrum disorder (ASD) [53], that present common mechanisms associated with epilepsy as we address below. Indeed, the concept of "interneuronopathy", implying the impaired development, migration or function of interneurons, has emerged as a possible physiopathological mechanism of these disorders [54-57]. Reductions of PV-, SOM- and Reelin-expressing interneurons and GABA transporter-I [58] and reduction in cortical interneuronal processes [59] are reported in schizophrenia, similar to what is observed in epilepsy [60]. Since PV-

expressing basket cells project to the perisomatic domain, controlling the output and synchrony of pyramidal neurons, impairment of cortical inhibition [61] and the disruption of synchronized firing activity of cortical neurons [62] has been reported in patients with schizophrenia. The impairment of neurotransmission mediated by GABAergic signaling is also implicated in the pathophysiology of anxiety [63]. A recent study had shown alteration of GABAergic signaling, decrease in GABAergic interneurons and an increase in $GABA_A$ receptor β3 subunit expression in the hippocampus, associated with anxiety-like behavior in epileptic mice [52]. Interestingly, MGE precursor cells grafted into hippocampus of newborn rats were able to modulate the inhibitory tone in the hippocampus, decreasing in the levels of anxiety of transplanted animals [64]. Also, studies indicate that GABAergic neurotransmission is altered in ASD in humans [65-67], and GABAergic interneuron number and positioning are altered, mainly PV- expressing cells in mouse models of ASD [68-70]. The interneuron subtypes affected vary across ASD models and may include PV, SOM, or NPY-expressing interneurons [71, 72]. Seizures and deficit of cortical inhibitory synaptic transmission had been recorded in some ASD models (unpublished data from our group). Therefore, concurrent epilepsy can be part of the deficits observed in ASD. However almost 40% the individuals with ASD develop epilepsy at different stages of life with different degrees of impairment and a greater number present epileptiform activity on the EEG without clinical epilepsy [73-76] and the cognitive deficits could be attribute to a pure ASD phenotype rather than an epilepsy-related comorbidity [57].

In fact, this pathophysiological mechanism of interneuronopathy which have implication on the connectivity and synchrony in the brain, have been shown to be associated with the in the clinical manifestation of these neurological and psychiatric

disorders such as cognitive or behavioral deficits and seizures [57, 77]. There is consistent evidence across studies that neurological and psychiatric disorders such as, schizophrenia and autism present reduction of neural synchronicity, and impaired cognitive functions, for example, perception, memory, attention, social cognition, suggesting that besides the impaired inhibition, the abnormal synchrony, caused by the E-I imbalance, could be involved in the onset of the cognitive dysfunctions. In epilepsy, besides seizures, cognitive or behavioral deficits could be a feature. However, the symptomatology is more complex, once it is dependent of the source of altered interneuronal connectivity, the epileptic focus and synchrony impairment (Fig. 1), that lead to specific cognitive deficits and seizure behavior [77].

4. Microcircuit with inhibitory motifs and brain oscillations

The GABAergic interneurons of different subtypes are involved in different microcircuit motifs, such as feed-forward inhibition, feedback inhibition and counter-inhibition (Fig. 1). Dysfunction in these microcircuits have been identified in epilepsy.

FS-PV-expressing basket cells, for example, are able to generate ripples oscillations (up to 200 Hz) by triggering synchronous firing of pyramidal cells and inhibitory postsynaptic events [78]. In addition, the intrinsic properties of FS-PV-expressing interneurons and fast kinetics of $GABA_A$ receptors are important to achieve precise timing for gamma oscillations in cortex and hippocampus [79-81]. Besides FS interneurons, SOM-expressing neurons activity also regulates gamma oscillations in visual cortex and in basal forebrain areas [82, 83]. Studies have shown that the activation of PV and SOM-expressing interneurons generates high-frequency oscillations (HFOs) [84], and that the perisomatic inhibition of basket cells in CA1 pyramidal cells is fundamental to generate gamma oscillations [78, 79, 85].

Strong activation of FS-PV-expressing cells or loss inhibition in the microcircuit could trigger epileptiform activity that recruits adjacent neural circuits [86-88]. PV-expressing interneurons appear to control the ictal event spread, even far from the epileptogenic focus, contributing to reduce the seizure generalization [89]. The impairment of perisomatic inhibition, caused by silencing PV-expressing interneurons, facilitates the development of spontaneous seizures [90]. In addition, altered activity of PV-expressing cells affects not only inhibitory, but also excitatory inputs to pyramidal neurons in the inhibitory microcircuits [91].

Besides changes in the strength of inhibition in the modified network activity, the displacement, number and size of interneurons also appears to contribute to rewire the microcircuit motifs, leading to epileptogenesis, abnormal brain oscillation pattern and neurodevelopmental deficits. Indeed, interneuronal displacement [49, 92, 93], reduction in cortical interneuronal processes [60], decrement of PV-expressing interneurons in the hippocampal CA1 and hilus [15, 16, 94-99] and SOM-expressing interneurons in the dentate gyrus [94, 100-104], aberrant synaptic reorganization and increased soma size of interneurons [105-108], have been reported in both animal models and patients with epilepsy. The decreased number of PV-expressing interneurons reduces the inhibition of pyramidal and granule cells, that in turn, can increase excitability not only locally, but also in other connected regions [94, 99, 109]. The decreased number of SOM interneurons in the hilus is directly correlated with the reduced inhibitory synaptic input to granule cells [101, 110]. Finally, the decreased density, increased soma size, axonal sprouting and reorganization with aberrant synaptic connections of SOM-expressing interneurons in the hippocampus not only reduces pyramidal cell excitability in the hippocampal CA1, but also affects other inhibitory interneurons. The result is a potentially build up disinhibited network [100]

with increased synchronization of pyramidal cell activity, leading to epileptiform activity [13, 111]. This reorganized circuitry could synchronize granule cell activity, disrupt network organization and increase excitation, despite the increment of GABAergic terminals, contributing to the inhibitory dysfunction in epilepsy.

5. GABAergic interneurons and hyperexcitability

The excitation and the inhibition, at different levels in the neuronal network, control the neuronal firing patterns and brain oscillations [112-116].

PV- and SOM-expressing interneurons, targeting different subcellular domains of pyramidal cells (Fig. 1), play important roles in E-I circuitry, and consequently, are involved in oscillations and epileptiform activity generation. The PV-expressing cells in the cortex maintain the gamma and beta bands across the cortical layers and, together with SOM-expressing cells, contribute to regulate delta oscillations in mice [117]. In addition, activation of PV- and SOM-expressing interneurons in the entorhinal cortex is able to trigger interictal and ictal discharges in mice, similar to temporal lobe epilepsy in humans [118].

During development, interneurons are critical for circuit formation and early network activity [45, 119] in both cortex and hippocampus. At the first postnatal week, interneurons and principal cells form excitatory circuits, even before the excitatory inputs become exclusively of the principal cells [120]. This is functionally significant, since the distribution of interneurons are fundamental to generate early network oscillations which, in turn, provide the necessary depolarization for glutamatergic synapses development via calcium influx through NMDA receptors [12, 121]. Although the immature excitatory currents are necessary for circuit development, they also increase the probability of the brain to develop seizures. Studies revealed that giant

depolarizing potential (GDP)-like events, characteristic of excitatory GABAergic synapses [120, 122], are present in the developing network. These GDP operate to synchronize electrical activity, to induce brain network development [121, 123, 124]. However, they increase the probability of seizure generation [122, 124].

Some studies have shown the potential involvement of inhibitory interneurons in seizure initiation and maintenance, with the increase of interneurons firing rates seconds to minutes before the seizure onset, in dentate gyrus, CA1, CA3 and hilus [125]. The activation of PV- and SOM-expressing interneurons targeting CA3 pyramidal cells can suppress epileptiform activity [28] and the inhibition of PV- and/or SOM-expressing interneurons, either individually or together, reduces seizure duration, while inhibiting PV-expressing interneurons increased seizure threshold [126].

The GABAergic inputs reduce network excitability and contribute essentially to the oscillatory patterning and synchronization of neural activity (as mentioned above). However, the impact of neural activity in target structures and enhanced GABAergic transmission may, in certain cases, facilitate seizures by inducing synchronization that can spread across neighboring networks [77]. Moreover, GABA-mediated hyperpolarization is essential for the development of synchronized low-frequency oscillations dependent of low-threshold calcium channels in absence seizures [127-129]. Therefore, such complex and varied mechanisms indicates that hyperexcitability in epilepsy goes beyond of simply decreasing inhibition.

Taking into account the essential participation of different interneurons of distinct origins in modulating neuronal network activity, for many years, intracerebral grafting of interneuronal precursor cells harvest from ganglionic eminences or derived from human embryonic stem cells have been used as an approach to restore inhibition

in different types of disease based-models, such as epilepsy [130-137]. Cell replacement studies using MGE precursors (the main source of PV- and SOM-expressing interneurons) showed considerable cell survival, differentiation, migration and functionally integration within the host neuronal network, and consequently rescuing the loss of inhibition [92, 130-133, 135, 138-147]. When MGE-precursor cells are grafted into the brain of animal models of epilepsy, seizure threshold increases, frequency and duration of epileptic seizures reduce, GABAergic inhibition and brain oscillations are restored [130, 132, 134, 142]. As mentioned, changes in GABAergic function impair synaptic plasticity and disrupt network organization and normal brain oscillations, affecting not only inhibitory, but also excitatory inputs to principal cells and interneurons. Interneuron precursor transplants have a potent impact over the seizures by restoring inhibition within the circuit, which presumably modifies the complex interactions between neuronal networks with distinct neuronal firing and dynamical evolution of synchronization.

The functional evaluation of interneurons on the reorganized network in epilepsy, and their readjusted pattern could help us to understand the intricate mechanism behind seizure generation and seizure control, further than the simple feature of decreasing and increasing inhibition.

Acknowledgments

This work was supported by Conselho Nacional de Desenvolvimento Científico e Tecnológico (CNPq), Brazil, no. 465671/2014-4 and Coordenação de Aperfeiçoamento de Pessoal de Nível Superior (CAPES).

Conflict of interest

The authors have no conflicts of interest to disclose.

References

[1] Noebels JL, Avoli M, Rogawski MA, Olsen RW, Delgado-Escueta AV. *Jasper's Basic Mechanisms of the Epilepsies*. *Fourth Edition* ed; 2012.

[2] Engel J. Excitation and inhibition in epilepsy. Can J Neurol Sci 1996;23: 167-74.

[3] Dichter MA, Ayala GF. Cellular mechanisms of epilepsy: a status report. Science 1987;237: 157-64.

[4] Galarreta M, Hestrin S. Frequency-dependent synaptic depression and the balance of excitation and inhibition in the neocortex. Nat Neurosci 1998;1: 587-94.

[5] Nelson SB, Turrigiano GG. Synaptic depression: a key player in the cortical balancing act. Nat Neurosci 1998;1: 539-41.

[6] Tasker JG, Dudek FE. Electrophysiology of GABA-mediated synaptic transmission and possible roles in epilepsy. Neurochem Res 1991;16: 251-62.

[7] Timofeev I, Grenier F, Steriade M. Contribution of intrinsic neuronal factors in the generation of cortically driven electrographic seizures. J Neurophysiol 2004;92: 1133-43.

[8] Shao LR, Habela CW, Stafstrom CE. Pediatric Epilepsy Mechanisms: Expanding the Paradigm of Excitation/Inhibition Imbalance. Children (Basel) 2019;6.

[9] Bui AD, Nguyen TM, Limouse C, Kim HK, Szabo GG, Felong S, Maroso M, Soltesz I. Dentate gyrus mossy cells control spontaneous convulsive seizures and spatial memory. Science 2018;359: 787-790.

[10] Olsen RW, Avoli M. GABA and epileptogenesis. Epilepsia 1997;38: 399-407.

[11] Treiman DM. GABAergic mechanisms in epilepsy. Epilepsia 2001;42 Suppl 3: 8-12.

[12] Pelkey KA, Chittajallu R, Craig MT, Tricoire L, Wester JC, McBain CJ. Hippocampal GABAergic Inhibitory Interneurons. Physiol Rev 2017;97: 1619-1747.

[13] Ye H, Kaszuba S. Inhibitory or excitatory? Optogenetic interrogation of the functional roles of GABAergic interneurons in epileptogenesis. J Biomed Sci 2017;24: 93.

[14] Kelsom C, Lu W. Development and specification of GABAergic cortical interneurons. Cell Biosci 2013;3: 19.

[15] Liu YQ, Yu F, Liu WH, He XH, Peng BW. Dysfunction of hippocampal interneurons in epilepsy. Neurosci Bull 2014;30: 985-998.

[16] Zhu Q, Ke W, He Q, Wang X, Zheng R, Li T, Luan G, Long YS, Liao WP, Shu Y. Laminar Distribution of Neurochemically-Identified Interneurons and Cellular Co-expression of Molecular Markers in Epileptic Human Cortex. Neurosci Bull 2018;34: 992-1006.

[17] Butt SJ, Fuccillo M, Nery S, Noctor S, Kriegstein A, Corbin JG, Fishell G. The temporal and spatial origins of cortical interneurons predict their physiological subtype. Neuron 2005;48: 591-604.

[18] Wonders C, Anderson SA. Cortical interneurons and their origins. Neuroscientist 2005;11: 199-205.

[19] Gelman DM, Marin O. Generation of interneuron diversity in the mouse cerebral cortex. Eur J Neurosci 2010;31: 2136-41.

[20] Tricoire L, Pelkey KA, Erkkila BE, Jeffries BW, Yuan X, McBain CJ. A blueprint for the spatiotemporal origins of mouse hippocampal interneuron diversity. J Neurosci 2011;31: 10948-70.
[21] Letinic K, Zoncu R, Rakic P. Origin of GABAergic neurons in the human neocortex. Nature 2002;417: 645-9.
[22] Arshad A, Vose LR, Vinukonda G, Hu F, Yoshikawa K, Csiszar A, Brumberg JC, Ballabh P. Extended Production of Cortical Interneurons into the Third Trimester of Human Gestation. Cereb Cortex 2016;26: 2242-2256.
[23] Mann EO, Paulsen O. Role of GABAergic inhibition in hippocampal network oscillations. Trends Neurosci 2007;30: 343-9.
[24] Freund TF, Buzsaki G. Interneurons of the hippocampus. Hippocampus 1996;6: 347-470.
[25] Klausberger T, Somogyi P. Neuronal diversity and temporal dynamics: the unity of hippocampal circuit operations. Science 2008;321: 53-7.
[26] Miles R, Tóth K, Gulyás AI, Hájos N, Freund TF. Differences between somatic and dendritic inhibition in the hippocampus. Neuron 1996;16: 815-23.
[27] Chen JL, Nedivi E. Highly specific structural plasticity of inhibitory circuits in the adult neocortex. Neuroscientist 2013;19: 384-93.
[28] Ledri M, Madsen MG, Nikitidou L, Kirik D, Kokaia M. Global optogenetic activation of inhibitory interneurons during epileptiform activity. J Neurosci 2014;34: 3364-77.
[29] Cobb SR, Buhl EH, Halasy K, Paulsen O, Somogyi P. Synchronization of neuronal activity in hippocampus by individual GABAergic interneurons. Nature 1995;378: 75-8.
[30] Miles R, Poncer JC. Paired recordings from neurones. Curr Opin Neurobiol 1996;6: 387-94.
[31] Marchionni I, Maccaferri G. Quantitative dynamics and spatial profile of perisomatic GABAergic input during epileptiform synchronization in the CA1 hippocampus. J Physiol 2009;587: 5691-708.
[32] Howard A, Tamas G, Soltesz I. Lighting the chandelier: new vistas for axo-axonic cells. Trends Neurosci 2005;28: 310-6.
[33] Contreras A, Hines DJ, Hines RM. Molecular Specialization of GABAergic Synapses on the Soma and Axon in Cortical and Hippocampal Circuit Function and Dysfunction. Front Mol Neurosci 2019;12: 154.
[34] Ylinen A, Bragin A, Nádasdy Z, Jandó G, Szabó I, Sik A, Buzsáki G. Sharp wave-associated high-frequency oscillation (200 Hz) in the intact hippocampus: network and intracellular mechanisms. J Neurosci 1995;15: 30-46.
[35] Mody I, Pearce RA. Diversity of inhibitory neurotransmission through GABA(A) receptors. Trends Neurosci 2004;27: 569-75.
[36] Mann EO, Suckling JM, Hajos N, Greenfield SA, Paulsen O. Perisomatic feedback inhibition underlies cholinergically induced fast network oscillations in the rat hippocampus in vitro. Neuron 2005;45: 105-17.
[37] Tukker JJ, Fuentealba P, Hartwich K, Somogyi P, Klausberger T. Cell type-specific tuning of hippocampal interneuron firing during gamma oscillations in vivo. J Neurosci 2007;27: 8184-9.
[38] Kawaguchi Y, Kubota Y. GABAergic cell subtypes and their synaptic connections in rat frontal cortex. Cereb Cortex 1997;7: 476-86.
[39] Klausberger T. GABAergic interneurons targeting dendrites of pyramidal cells in the CA1 area of the hippocampus. Eur J Neurosci 2009;30: 947-57.

[40] Leão RN, Mikulovic S, Leão KE, Munguba H, Gezelius H, Enjin A, Patra K, Eriksson A, Loew LM, Tort AB, Kullander K. OLM interneurons differentially modulate CA3 and entorhinal inputs to hippocampal CA1 neurons. Nat Neurosci 2012;15: 1524-30.
[41] Müller C, Remy S. Dendritic inhibition mediated by O-LM and bistratified interneurons in the hippocampus. Front Synaptic Neurosci 2014;6: 23.
[42] Kann O. The interneuron energy hypothesis: Implications for brain disease. Neurobiol Dis 2016;90: 75-85.
[43] Lodato S, Arlotta P. Generating neuronal diversity in the mammalian cerebral cortex. Annu Rev Cell Dev Biol 2015;31: 699-720.
[44] Cohen I, Navarro V, Clemenceau S, Baulac M, Miles R. On the origin of interictal activity in human temporal lobe epilepsy in vitro. Science 2002;298: 1418-21.
[45] Khalilov I, Le Van Quyen M, Gozlan H, Ben-Ari Y. Epileptogenic actions of GABA and fast oscillations in the developing hippocampus. Neuron 2005;48: 787-96.
[46] Konopaske GT, Sweet RA, Wu Q, Sampson A, Lewis DA. Regional specificity of chandelier neuron axon terminal alterations in schizophrenia. Neuroscience 2006;138: 189-96.
[47] Traub RD, Pais I, Bibbig A, Lebeau FE, Buhl EH, Garner H, Monyer H, Whittington MA. Transient depression of excitatory synapses on interneurons contributes to epileptiform bursts during gamma oscillations in the mouse hippocampal slice. J Neurophysiol 2005;94: 1225-35.
[48] de la Prida LM, Huberfeld G. Inhibition and oscillations in the human brain tissue in vitro. Neurobiol Dis 2019;125: 198-210.
[49] Calcagnotto ME, Paredes MF, Tihan T, Barbaro NM, Baraban SC. Dysfunction of synaptic inhibition in epilepsy associated with focal cortical dysplasia. J Neurosci 2005;25: 9649-57.
[50] Marín O. Interneuron dysfunction in psychiatric disorders. Nat Rev Neurosci 2012;13: 107-20.
[51] Nakazawa K, Zsiros V, Jiang Z, Nakao K, Kolata S, Zhang S, Belforte JE. GABAergic interneuron origin of schizophrenia pathophysiology. Neuropharmacology 2012;62: 1574-83.
[52] Zhu X, Yao Y, Li X, Dong J, Zhang A. Alteration of GABAergic signaling is associated with anxiety-like behavior in temporal lobe epilepsy mice. Prog Neuropsychopharmacol Biol Psychiatry 2019;93: 141-148.
[53] Tomassy GS, Morello N, Calcagno E, Giustetto M. Developmental abnormalities of cortical interneurons precede symptoms onset in a mouse model of Rett syndrome. J Neurochem 2014;131: 115-27.
[54] Kato M, Dobyns WB. X-linked lissencephaly with abnormal genitalia as a tangential migration disorder causing intractable epilepsy: proposal for a new term, "interneuronopathy". J Child Neurol 2005;20: 392-7.
[55] Sebe JY, Baraban SC. The promise of an interneuron-based cell therapy for epilepsy. Dev Neurobiol 2011;71: 107-17.
[56] Paterno R, Casalia M, Baraban SC. Interneuron deficits in neurodevelopmental disorders: Implications for disease pathology and interneuron-based therapies. Eur J Paediatr Neurol 2019.
[57] Katsarou AM, Moshé SL, Galanopoulou AS. Galanopoulou, Interneuronophaties and their role in the early life epilepsies and neurodevelopmental disorders. Epilepsia Open 2017;2: 284-306.
[58] Guidotti A, Auta J, Davis JM, Di-Giorgi-Gerevini V, Dwivedi Y, Grayson DR, Impagnatiello F, Pandey G, Pesold C, Sharma R, Uzunov D, Costa E, DiGiorgi

Gerevini V. Decrease in reelin and glutamic acid decarboxylase67 (GAD67) expression in schizophrenia and bipolar disorder: a postmortem brain study. Arch Gen Psychiatry 2000;57: 1061-9.
[59] Kalus P, Bondzio J, Federspiel A, Müller TJ, Zuschratter W. Cell-type specific alterations of cortical interneurons in schizophrenic patients. Neuroreport 2002;13: 713-7.
[60] Prince DA, Parada I, Scalise K, Graber K, Jin X, Shen F. Epilepsy following cortical injury: cellular and molecular mechanisms as targets for potential prophylaxis. Epilepsia 2009;50 Suppl 2: 30-40.
[61] Daskalakis ZJ, Christensen BK, Chen R, Fitzgerald PB, Zipursky RB, Kapur S. Evidence for impaired cortical inhibition in schizophrenia using transcranial magnetic stimulation. Arch Gen Psychiatry 2002;59: 347-54.
[62] Spencer KM, Nestor PG, Perlmutter R, Niznikiewicz MA, Klump MC, Frumin M, Shenton ME, McCarley RW. Neural synchrony indexes disordered perception and cognition in schizophrenia. Proc Natl Acad Sci U S A 2004;101: 17288-93.
[63] Nemeroff CB. The role of GABA in the pathophysiology and treatment of anxiety disorders. Psychopharmacol Bull 2003;37: 133-46.
[64] Romariz SA, Paiva DeS, Valente MF, Barnabé GF, Frussa-Filho R, Barbosa-Silva RC, Calcagnotto ME, Longo BM. Long-lasting anxiolytic effect of neural precursor cells freshly prepared but not neurosphere-derived cell transplantation in newborn rats. BMC Neurosci 2014;15: 94.
[65] Blatt GJ, Fitzgerald CM, Guptill JT, Booker AB, Kemper TL, Bauman ML. Density and distribution of hippocampal neurotransmitter receptors in autism: an autoradiographic study. J Autism Dev Disord 2001;31: 537-43.
[66] Fatemi SH, Halt AR, Stary JM, Kanodia R, Schulz SC, Realmuto GR. Glutamic acid decarboxylase 65 and 67 kDa proteins are reduced in autistic parietal and cerebellar cortices. Biol Psychiatry 2002;52: 805-10.
[67] Bozzi Y, Provenzano G, Casarosa S. Neurobiological bases of autism-epilepsy comorbidity: a focus on excitation/inhibition imbalance. Eur J Neurosci 2018;47: 534-548.
[68] Gogolla N, Leblanc JJ, Quast KB, Südhof TC, Fagiolini M, Hensch TK. Common circuit defect of excitatory-inhibitory balance in mouse models of autism. J Neurodev Disord 2009;1: 172-81.
[69] Rubenstein JL, Merzenich MM. Model of autism: increased ratio of excitation/inhibition in key neural systems. Genes Brain Behav 2003;2: 255-67.
[70] Rubinstein M, Han S, Tai C, Westenbroek RE, Hunker A, Scheuer T, Catterall WA. Dissecting the phenotypes of Dravet syndrome by gene deletion. Brain 2015;138: 2219-33.
[71] Sgadò P, Genovesi S, Kalinovsky A, Zunino G, Macchi F, Allegra M, Murenu E, Provenzano G, Tripathi PP, Casarosa S, Joyner AL, Bozzi Y. Loss of GABAergic neurons in the hippocampus and cerebral cortex of Engrailed-2 null mutant mice: implications for autism spectrum disorders. Exp Neurol 2013;247: 496-505.
[72] Fontes-Dutra M, Santos-Terra J, Deckmann I, Brum Schwingel G, Della-Flora Nunes G, Hirsch MM, Bauer-Negrini G, Riesgo RS, Bambini-Júnior V, Hedin-Pereira C, Gottfried C. Resveratrol Prevents Cellular and Behavioral Sensory Alterations in the Animal Model of Autism Induced by Valproic Acid. Front Synaptic Neurosci 2018;10: 9.
[73] Canitano R. Epilepsy in autism spectrum disorders. Eur Child Adolesc Psychiatry 2007;16: 61-6.

[74] Deonna T, Roulet E. Autistic spectrum disorder: evaluating a possible contributing or causal role of epilepsy. Epilepsia 2006;47 Suppl 2: 79-82.
[75] Parmeggiani A, Barcia G, Posar A, Raimondi E, Santucci M, Scaduto MC. Epilepsy and EEG paroxysmal abnormalities in autism spectrum disorders. Brain Dev 2010;32: 783-9.
[76] Jensen FE. Epilepsy as a spectrum disorder: Implications from novel clinical and basic neuroscience. Epilepsia 2011;52 Suppl 1: 1-6.
[77] Uhlhaas PJ, Singer W. Neural synchrony in brain disorders: relevance for cognitive dysfunctions and pathophysiology. Neuron 2006;52: 155-68.
[78] Buzsáki G, Silva FL. High frequency oscillations in the intact brain. Prog Neurobiol 2012;98: 241-9.
[79] Cardin JA, Carlén M, Meletis K, Knoblich U, Zhang F, Deisseroth K, Tsai LH, Moore CI. Driving fast-spiking cells induces gamma rhythm and controls sensory responses. Nature 2009;459: 663-7.
[80] Middleton S, Jalics J, Kispersky T, Lebeau FE, Roopun AK, Kopell NJ, Whittington MA, Cunningham MO. NMDA receptor-dependent switching between different gamma rhythm-generating microcircuits in entorhinal cortex. Proc Natl Acad Sci U S A 2008;105: 18572-7.
[81] Whittington MA, Traub RD. Interneuron diversity series: inhibitory interneurons and network oscillations in vitro. Trends Neurosci 2003;26: 676-82.
[82] Veit J, Hakim R, Jadi MP, Sejnowski TJ, Adesnik H. Cortical gamma band synchronization through somatostatin interneurons. Nat Neurosci 2017;20: 951-959.
[83] Espinosa N, Alonso A, Lara-Vasquez A, Fuentealba P. Basal forebrain somatostatin cells differentially regulate local gamma oscillations and functionally segregate motor and cognitive circuits. Sci Rep 2019;9: 2570.
[84] Stark E, Roux L, Eichler R, Senzai Y, Royer S, Buzsáki G. Pyramidal cell-interneuron interactions underlie hippocampal ripple oscillations. Neuron 2014;83: 467-480.
[85] Bartos M, Vida I, Frotscher M, Meyer A, Monyer H, Geiger JR, Jonas P. Fast synaptic inhibition promotes synchronized gamma oscillations in hippocampal interneuron networks. Proc Natl Acad Sci U S A 2002;99: 13222-7.
[86] Sun QQ, Huguenard JR, Prince DA. Reorganization of barrel circuits leads to thalamically-evoked cortical epileptiform activity. Thalamus Relat Syst 2005;3: 261-273.
[87] Paz JT, Bryant AS, Peng K, Fenno L, Yizhar O, Frankel WN, Deisseroth K, Huguenard JR. A new mode of corticothalamic transmission revealed in the Gria4(-/-) model of absence epilepsy. Nat Neurosci 2011;14: 1167-73.
[88] Paz JT, Huguenard JR. Microcircuits and their interactions in epilepsy: is the focus out of focus? Nat Neurosci 2015;18: 351-9.
[89] Sessolo M, Marcon I, Bovetti S, Losi G, Cammarota M, Ratto GM, Fellin T, Carmignoto G. Parvalbumin-Positive Inhibitory Interneurons Oppose Propagation But Favor Generation of Focal Epileptiform Activity. J Neurosci 2015;35: 9544-57.
[90] Drexel M, Romanov RA, Wood J, Weger S, Heilbronn R, Wulff P, Tasan RO, Harkany T, Sperk G. Selective Silencing of Hippocampal Parvalbumin Interneurons Induces Development of Recurrent Spontaneous Limbic Seizures in Mice. J Neurosci 2017;37: 8166-8179.
[91] Moore AK, Weible AP, Balmer TS, Trussell LO, Wehr M. Rapid Rebalancing of Excitation and Inhibition by Cortical Circuitry. Neuron 2018;97: 1341-1355.e6.

[92] Cobos I, Calcagnotto ME, Vilaythong AJ, Thwin MT, Noebels JL, Baraban SC, Rubenstein JL. Mice lacking Dlx1 show subtype-specific loss of interneurons, reduced inhibition and epilepsy. Nat Neurosci 2005;8: 1059-68.
[93] Barinka F, Druga R, Marusic P, Krsek P, Zamecnik J. Calretinin immunoreactivity in focal cortical dysplasias and in non-malformed epileptic cortex. Epilepsy Res 2010;88: 76-86.
[94] Wittner L, Eross L, Czirják S, Halász P, Freund TF, Maglóczky Z. Surviving CA1 pyramidal cells receive intact perisomatic inhibitory input in the human epileptic hippocampus. Brain 2005;128: 138-52.
[95] Tóth K, Eross L, Vajda J, Halász P, Freund TF, Maglóczky Z. Loss and reorganization of calretinin-containing interneurons in the epileptic human hippocampus. Brain 2010;133: 2763-77.
[96] Dinocourt C, Petanjek Z, Freund TF, Ben-Ari Y, Esclapez M. Loss of interneurons innervating pyramidal cell dendrites and axon initial segments in the CA1 region of the hippocampus following pilocarpine-induced seizures. J Comp Neurol 2003;459: 407-25.
[97] Papp P, Kovács Z, Szocsics P, Juhász G, Maglóczky Z. Alterations in hippocampal and cortical densities of functionally different interneurons in rat models of absence epilepsy. Epilepsy Res 2018;145: 40-50.
[98] Huusko N, Römer C, Ndode-Ekane XE, Lukasiuk K, Pitkänen A. Loss of hippocampal interneurons and epileptogenesis: a comparison of two animal models of acquired epilepsy. Brain Struct Funct 2015;220: 153-91.
[99] Sun C, Mtchedlishvili Z, Bertram EH, Erisir A, Kapur J. Selective loss of dentate hilar interneurons contributes to reduced synaptic inhibition of granule cells in an electrical stimulation-based animal model of temporal lobe epilepsy. J Comp Neurol 2007;500: 876-93.
[100] Maglóczky Z, Freund TF. Impaired and repaired inhibitory circuits in the epileptic human hippocampus. Trends Neurosci 2005;28: 334-40.
[101] Robbins RJ, Brines ML, Kim JH, Adrian T, de Lanerolle N, Welsh S, Spencer DD. A selective loss of somatostatin in the hippocampus of patients with temporal lobe epilepsy. Ann Neurol 1991;29: 325-32.
[102] Sundstrom LE, Brana C, Gatherer M, Mepham J, Rougier A. Somatostatin- and neuropeptide Y-synthesizing neurones in the fascia dentata of humans with temporal lobe epilepsy. Brain 2001;124: 688-97.
[103] Kobayashi M, Buckmaster PS. Reduced inhibition of dentate granule cells in a model of temporal lobe epilepsy. J Neurosci 2003;23: 2440-52.
[104] Cossart R, Dinocourt C, Hirsch JC, Merchan-Perez A, De Felipe J, Ben-Ari Y, Esclapez M, Bernard C. Dendritic but not somatic GABAergic inhibition is decreased in experimental epilepsy. Nat Neurosci 2001;4: 52-62.
[105] Wittner L, Maglóczky Z. Synaptic Reorganization of the Perisomatic Inhibitory Network in Hippocampi of Temporal Lobe Epileptic Patients. Biomed Res Int 2017;2017: 7154295.
[106] Wittner L, Maglóczky Z, Borhegyi Z, Halász P, Tóth S, Eross L, Szabó Z, Freund TF. Preservation of perisomatic inhibitory input of granule cells in the epileptic human dentate gyrus. Neuroscience 2001;108: 587-600.
[107] Peng Z, Zhang N, Wei W, Huang CS, Cetina Y, Otis TS, Houser CR. A reorganized GABAergic circuit in a model of epilepsy: evidence from optogenetic labeling and stimulation of somatostatin interneurons. J Neurosci 2013;33: 14392-405.
[108] Zhang W, Yamawaki R, Wen X, Uhl J, Diaz J, Prince DA, Buckmaster PS. Surviving hilar somatostatin interneurons enlarge, sprout axons, and form new

synapses with granule cells in a mouse model of temporal lobe epilepsy. J Neurosci 2009;29: 14247-56.
[109] Wick ZC, Leintz CH, Xamonthiene C, Huang BH, Krook-Magnuson E. Axonal sprouting in commissurally projecting parvalbumin-expressing interneurons. J Neurosci Res 2017;95: 2336-2344.
[110] de Lanerolle NC, Kim JH, Robbins RJ, Spencer DD. Hippocampal interneuron loss and plasticity in human temporal lobe epilepsy. Brain Res 1989;495: 387-95.
[111] Fujiwara-Tsukamoto Y, Isomura Y, Kaneda K, Takada M. Synaptic interactions between pyramidal cells and interneurone subtypes during seizure-like activity in the rat hippocampus. J Physiol 2004;557: 961-79.
[112] Steriade M, Timofeev I, Grenier F. Natural waking and sleep states: a view from inside neocortical neurons. J Neurophysiol 2001;85: 1969-85.
[113] Timofeev I, Grenier F, Steriade M. Impact of intrinsic properties and synaptic factors on the activity of neocortical networks in vivo. J Physiol Paris 2000;94: 343-55.
[114] Timofeev I, Grenier F, Steriade M. Disfacilitation and active inhibition in the neocortex during the natural sleep-wake cycle: an intracellular study. Proc Natl Acad Sci U S A 2001;98: 1924-9.
[115] Haider B, Häusser M, Carandini M. Inhibition dominates sensory responses in the awake cortex. Nature 2013;493: 97-100.
[116] Steriade M. Impact of network activities on neuronal properties in corticothalamic systems. J Neurophysiol 2001;86: 1-39.
[117] Kuki T, Fujihara K, Miwa H, Tamamaki N, Yanagawa Y, Mushiake H. Contribution of parvalbumin and somatostatin-expressing GABAergic neurons to slow oscillations and the balance in beta-gamma oscillations across cortical layers. Front Neural Circuits 2015;9: 6.
[118] Yekhlef L, Breschi GL, Lagostena L, Russo G, Taverna S. Selective activation of parvalbumin- or somatostatin-expressing interneurons triggers epileptic seizurelike activity in mouse medial entorhinal cortex. J Neurophysiol 2015;113: 1616-30.
[119] Luhmann HJ, Kirischuk S, Sinning A, Kilb W. Early GABAergic circuitry in the cerebral cortex. Curr Opin Neurobiol 2014;26: 72-8.
[120] Ben-Ari Y, Cherubini E, Corradetti R, Gaiarsa JL. Giant synaptic potentials in immature rat CA3 hippocampal neurones. J Physiol 1989;416: 303-25.
[121] Ben-Ari Y, Gaiarsa JL, Tyzio R, Khazipov R. GABA: a pioneer transmitter that excites immature neurons and generates primitive oscillations. Physiol Rev 2007;87: 1215-84.
[122] Ben-Ari Y. Excitatory actions of gaba during development: the nature of the nurture. Nat Rev Neurosci 2002;3: 728-39.
[123] Allène C, Cattani A, Ackman JB, Bonifazi P, Aniksztejn L, Ben-Ari Y, Cossart R. Sequential generation of two distinct synapse-driven network patterns in developing neocortex. J Neurosci 2008;28: 12851-63.
[124] Nardou R, Ferrari DC, Ben-Ari Y. Mechanisms and effects of seizures in the immature brain. Semin Fetal Neonatal Med 2013;18: 175-84.
[125] Toyoda I, Fujita S, Thamattoor AK, Buckmaster PS. Unit Activity of Hippocampal Interneurons before Spontaneous Seizures in an Animal Model of Temporal Lobe Epilepsy. J Neurosci 2015;35: 6600-18.
[126] Khoshkhoo S, Vogt D, Sohal VS. Dynamic, Cell-Type-Specific Roles for GABAergic Interneurons in a Mouse Model of Optogenetically Inducible Seizures. Neuron 2017;93: 291-298.

[127] McCormick DA, Williamson A. Convergence and divergence of neurotransmitter action in human cerebral cortex. Proc Natl Acad Sci U S A 1989;86: 8098-102.
[128] Huguenard JR, Prince DA. Intrathalamic rhythmicity studied in vitro: nominal T-current modulation causes robust antioscillatory effects. J Neurosci 1994;14: 5485-502.
[129] Ulrich D, Huguenard JR. Gamma-aminobutyric acid type B receptor-dependent burst-firing in thalamic neurons: a dynamic clamp study. Proc Natl Acad Sci U S A 1996;93: 13245-9.
[130] Hsieh JY, Baraban SC. Medial Ganglionic Eminence Progenitors Transplanted into Hippocampus Integrate in a Functional and Subtype-Appropriate Manner. eNeuro 2017;4.
[131] Upadhya D, Hattiangady B, Castro OW, Shuai B, Kodali M, Attaluri S, Bates A, Dong Y, Zhang SC, Prockop DJ, Shetty AK. Human induced pluripotent stem cell-derived MGE cell grafting after status epilepticus attenuates chronic epilepsy and comorbidities via synaptic integration. Proc Natl Acad Sci U S A 2019;116: 287-296.
[132] Casalia ML, Howard MA, Baraban SC. Persistent seizure control in epileptic mice transplanted with gamma-aminobutyric acid progenitors. Ann Neurol 2017;82: 530-542.
[133] Zipancic I, Calcagnotto ME, Piquer-Gil M, Mello LE, Alvarez-Dolado M. Transplant of GABAergic precursors restores hippocampal inhibitory function in a mouse model of seizure susceptibility. Cell Transplant 2010;19: 549-64.
[134] Paiva DS, Romariz SAA, Valente MF, Moraes LB, Covolan L, Calcagnotto ME, Monteiro Longo B. Transplantation of inhibitory precursor cells from medial ganglionic eminence produces distinct responses in two different models of acute seizure induction. Epilepsy Behav 2017;70: 125-130.
[135] Lee H, Yun S, Kim IS, Lee IS, Shin JE, Park SC, Kim WJ, Park KI. Human fetal brain-derived neural stem/progenitor cells grafted into the adult epileptic brain restrain seizures in rat models of temporal lobe epilepsy. PLoS One 2014;9: e104092.
[136] Zhu Q, Naegele JR, Chung S. Cortical GABAergic Interneuron/Progenitor Transplantation as a Novel Therapy for Intractable Epilepsy. Front Cell Neurosci 2018;12: 167.
[137] Backofen-Wehrhahn B, Gey L, Bröer S, Petersen B, Schiff M, Handreck A, Stanslowsky N, Scharrenbroich J, Weißing M, Staege S, Wegner F, Niemann H, Löscher W, Gernert M. Anticonvulsant effects after grafting of rat, porcine, and human mesencephalic neural progenitor cells into the rat subthalamic nucleus. Exp Neurol 2018;310: 70-83.
[138] Alvarez-Dolado M, Calcagnotto ME, Karkar KM, Southwell DG, Jones-Davis DM, Estrada RC, Rubenstein JL, Alvarez-Buylla A, Baraban SC. Cortical inhibition modified by embryonic neural precursors grafted into the postnatal brain. J Neurosci 2006;26: 7380-9.
[139] Howard MA, Baraban SC. Synaptic integration of transplanted interneuron progenitor cells into native cortical networks. J Neurophysiol 2016;116: 472-8.
[140] Hunt RF, Baraban SC. Interneuron Transplantation as a Treatment for Epilepsy. Cold Spring Harb Perspect Med 2015;5.
[141] Hunt RF, Girskis KM, Rubenstein JL, Alvarez-Buylla A, Baraban SC. GABA progenitors grafted into the adult epileptic brain control seizures and abnormal behavior. Nat Neurosci 2013;16: 692-7.

[142] Howard MA, Rubenstein JL, Baraban SC. Bidirectional homeostatic plasticity induced by interneuron cell death and transplantation in vivo. Proc Natl Acad Sci U S A 2014;111: 492-7.
[143] Baraban SC, Southwell DG, Estrada RC, Jones DL, Sebe JY, Alfaro-Cervello C, García-Verdugo JM, Rubenstein JL, Alvarez-Buylla A. Reduction of seizures by transplantation of cortical GABAergic interneuron precursors into Kv1.1 mutant mice. Proc Natl Acad Sci U S A 2009;106: 15472-7.
[144] Calcagnotto ME, Zipancic I, Piquer-Gil M, Mello LE, Alvarez-Dolado M. Grafting of GABAergic precursors rescues deficits in hippocampal inhibition. Epilepsia 2010;51 Suppl 3: 66-70.
[145] Henderson KW, Gupta J, Tagliatela S, Litvina E, Zheng X, Van Zandt MA, Woods N, Grund E, Lin D, Royston S, Yanagawa Y, Aaron GB, Naegele JR. Long-term seizure suppression and optogenetic analyses of synaptic connectivity in epileptic mice with hippocampal grafts of GABAergic interneurons. J Neurosci 2014;34: 13492-504.
[146] Anderson S, Baraban S. Cell Therapy Using GABAergic Neural Progenitors. In: Noebels JL AM, Rogawski MA , Olsen RW , Delgado-Escueta AV., editor. Source Jasper's Basic Mechanisms of the Epilepsies [Internet] 4th ed; 2012.
[147] Hammad M, Schmidt SL, Zhang X, Bray R, Frohlich F, Ghashghaei HT. Transplantation of GABAergic Interneurons into the Neonatal Primary Visual Cortex Reduces Absence Seizures in Stargazer Mice. Cereb Cortex 2015;25: 2970-9.

Figures

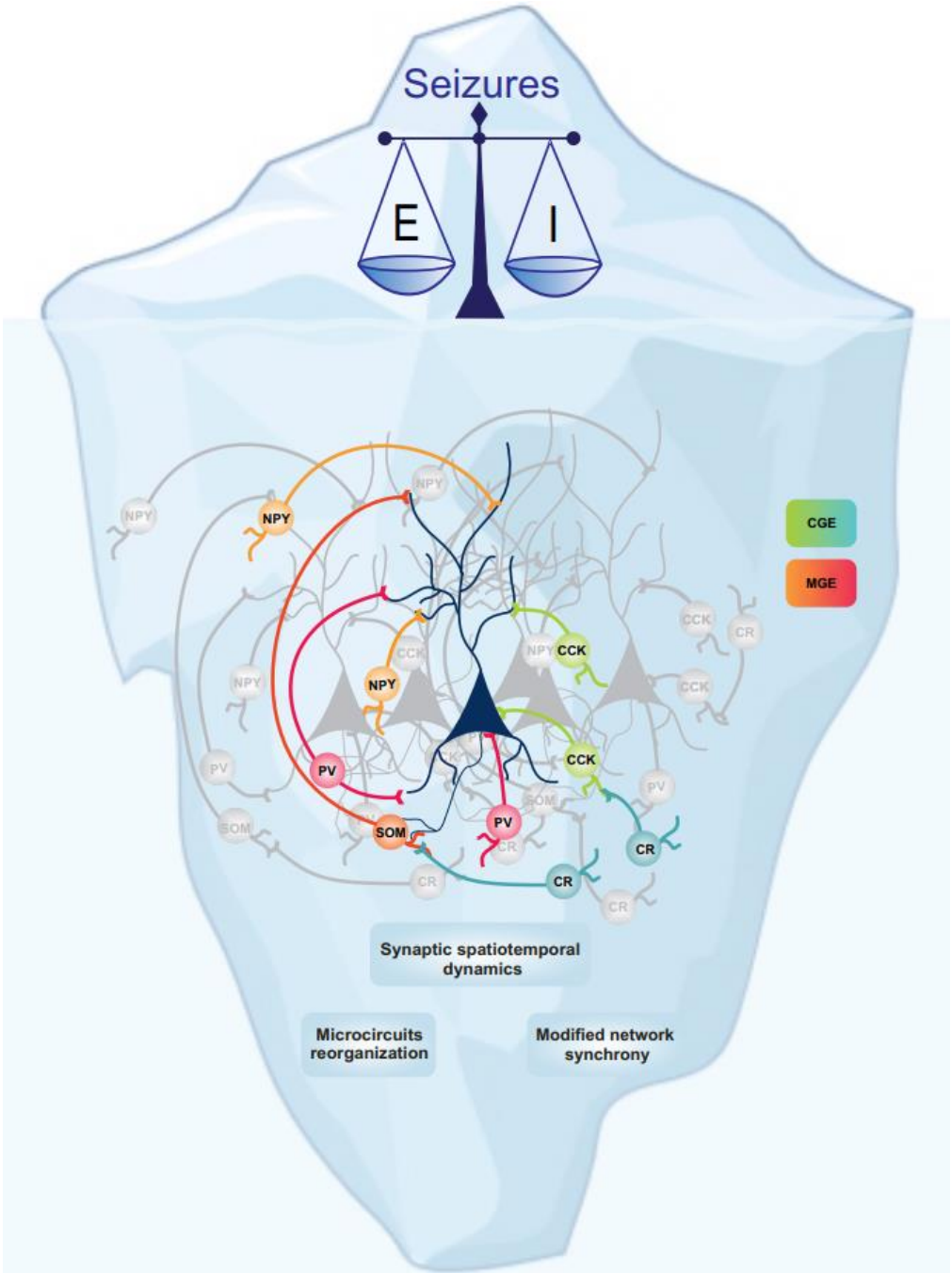

Figure 1: Top: Seizures and the shift in the balanced of excitation (E) and inhibition (I) are the tip of the iceberg in epilepsy and represent only an event in a complex process of epileptogenesis. Bottom: The cellular diversity represented by different GABAergic interneuron subtypes originated from caudal and medial ganglionic eminences (CGE: blue/green and MGE: orange/red) that make synapse on distinct domains of pyramidal cells and one specific domain of pyramidal cells receiving synaptic contacts from distinct GABAergic interneurons (Synaptic spatiotemporal dynamics of interneuronal connectivity). Distal dendritic inhibition is performed by SOM-, NPY-expressing interneurons, whereas FS-PV-expressing basket cells or CCK-expressing interneurons perform perisomatic inhibition. PV-expressing also make synapses at the dendrites of pyramidal cells. CR-expressing cells make synapses with interneurons at dendritic domain. The diversity of GABAergic interneurons is involved synaptic reorganization of different neuronal microcircuits recruited during the epileptogenic process.

PARTE III- DISCUSSÃO E CONCLUSÕES

DISCUSSÃO

1 Aumento da hiperexcitabilidade induzida por 4-AP

Estudos *in vitro* realizados em preparações de fatias cerebrais com as conexões intactas são amplamente utilizados (Avoli e Jefferys, 2016) e demonstram que, após a perfusão com 4-AP, iniciam-se eventos com padrões de atividade epileptiforme, que se assemelham às crises límbicas que ocorrem em pacientes com ELT (Avoli *et al.*, 2002; Gonzalez-Sulser *et al.*, 2011; Dulla *et al.*, 2018). Neste trabalho, associamos o uso do modelo *in vivo* de epilepsia induzida por pilocarpina, que mimetiza de forma similar as alterações fisiopatológicas crônicas da ELT (Garrido Sanabria *et al.*, 2002; Curia *et al.*, 2008), com o modelo *in vitro* de epilepsia induzido por 4-AP, utilizando fatias de hipocampo com CE (hipocampo-CE), que possui como vantagem produzir uma sincronização da rede enquanto preserva a inibição GABAérgica (Perreault e Avoli, 1991; Avoli *et al.*, 1996; Barbarosie e Avoli, 1997; Calcagnotto, Barbarosie e Avoli, 2000; Gafurov e Bausch, 2013). Dessa forma, podemos investigar as alterações decorrentes da ELT na geração de atividade epileptiforme em funções específicas de estruturas límbicas e o envolvimento do sistema GABAérgico. Os detalhes da metodologia empregada podem ser encontrados no ANEXO 2.

A atividade de potencial de campo, registrada através do EEG ou de registros extracelulares *in vitro*, contém características importantes para a identificação de condições cerebrais fisiológicas e patológicas em andamento (Olejniczak, 2006; Buzsáki, Anastassiou e Koch, 2012). A caracterização de eventos epileptiformes em particular, fornece informações fundamentais sobre os mecanismos que conduzem à

geração de eventos patológicos, assim como a sincronização anormal e hiperexcitabilidade de conjuntos neuronais (Avoli *et al.*, 2002; Avoli, 2014; Dulla *et al.*, 2018).

Os eventos epileptiformes do tipo interictal foram um dos primeiros eventos epileptiformes a serem reproduzidos *in vitro* em preparações de fatias cerebrais (Galvan, Grafe e Bruggencate, 1982; Voskuyl e Albus, 1985), e podem ser identificados em fatias cerebrais obtidas de pacientes submetidos à cirurgia para ELT refratária (Avoli *et al.*, 2005), fatias de hipocampo-CE de animais naive (Barbarosie e Avoli, 1997; Calcagnotto, Barbarosie e Avoli, 2000) e de animais epilépticos (D'Antuono *et al.*, 2002; Panuccio *et al.*, 2010). Desde então, esses estudos comprovam que os eventos interictais estão envolvidos no desenvolvimento da epileptogênese (Staba *et al.*, 2002; Lévesque, Salami, *et al.*, 2018), são preditivos de crises epilépticas e epilepsia (Jacobs *et al.*, 2008, 2016; Schevon *et al.*, 2009; Chauvière *et al.*, 2012), e podem ser utilizados como prognóstico de tratamento e remissão da ELT (Fedele *et al.*, 2017; Shah *et al.*, 2019).

No presente trabalho, as fatias hipocampais de ratos epilépticos, 30 dias após o *SE*, perfundidas com 4-AP, apresentaram uma diminuição da latência para a geração de eventos ictais quando comparado ao grupo controle, sugerindo que CA1 possui uma maior suscetibilidade à ictogênese, a qual pode estar correlacionada com o aumento da excitabilidade nessa região (Figura 7). A área CA1 do hipocampo é uma das regiões mais vulneráveis em pacientes com epilepsia, e em modelos animais de ELT (Lehmann *et al.*, 2000; Scharfman, 2007; Navidhamidi, Ghasemi e Mehranfard, 2017), a qual apresenta morte celular e perda sináptica (Turski *et al.*, 1983), aumento do input glutamatérgico como resultado do brotamento axonal de células piramidais (Esclapez *et al.*, 1999; Lehmann *et al.*, 2000; Smith e Dudek, 2001),

diminuição do input GABAérgico induzido por perda de interneurônios (Cossart *et al.*, 2001; Smith e Dudek, 2001; Dinocourt *et al.*, 2003), e alteração de propriedades intrínsecas de células piramidais e interneurônios de CA1 (Yaari e Beck, 2002; Dugladze *et al.*, 2007). Algumas dessas modificações ocorrem durante o período latente, provavelmente como uma consequência direta do *SE* (Dinocourt *et al.*, 2003), e durante o estágio crônico tais alterações são mantidas e muitas vezes exacerbadas (Smith e Dudek, 2001; Gorter e Lopes da Silva, 2002), contribuindo para o aumento da excitabilidade em CA1. Dessa forma, a hiperexcitabilidade pode constituir um fator decisivo para a geração e propagação de atividade epileptiforme *in vitro*. No entanto, 60 dias após o *SE*, não observamos alterações na geração de eventos interictais e ictais em CA1 de fatias oriundas de animais epilépticos. Portanto, em um período avançado da epileptogênese (60 dias após o *SE*), as alterações na suscetibilidade à ictogênese não foram observadas, sugerindo que os mecanismos envolvendo hiperexcitabilidade em CA1 foram interrompidos ou compensados, possivelmente correlacionado com mudanças neuronais plásticas dependentes da idade e da condição epiléptica prolongada (Gorter e Lopes da Silva, 2002; Panuccio *et al.*, 2010). Dessa forma mais estudos são necessários afim de elucidar os mecanismos subjacentes à condição epiléptica já estabelecida em CA1.

De maneira oposta, a região CA3 das fatias de hipocampo-CE de animais epilépticos aos 30 dias após o *SE*, foram menos suscetíveis à geração de eventos ictais induzidos por 4-AP, do que as fatias de hipocampo-CE de animais controle, pareados por idade. No entanto, os eventos ictais tiveram maior duração no grupo epiléptico quando comparado aos controles. Esta duração foi reduzida aos 60 dias após o *SE* em comparação aos 30 dias após o *SE*, mas não apresentou diferença do respectivo grupo controle (pareado pela idade). Em fatias hipocampais oriundas de

pacientes com ELT refratária, CA3 também teve menor suscetibilidade em gerar atividade epileptiforme (Reyes-Garcia *et al.*, 2018), assim como em fatias de hipocampo oriundos de animais com epilepsia induzida por pilocarpina, onde os eventos interictais apresentaram menor frequência quando comparado ao grupo controle (Nagao, Massimo e Gloor, 1994; Panuccio *et al.*, 2010). Com relação às alterações anatômicas em CA3 decorrentes da epileptogênese, estudos demonstram uma modesta perda neuronal em animais tratados com pilocarpina (Turski *et al.*, 1983; Esclapez *et al.*, 1999). Dessa forma, as alterações funcionais encontradas em CA3 podem estar correlacionadas com o grau de comprometimento anatômico e estrutural desse microcircuito, mas também podem refletir o papel de CA3 no controle da progressão do processo epileptogênico e estabelecimento crônico da epilepsia (Barbarosie e Avoli, 1997). Apesar de CA3 ser fundamental na geração de um circuito excitatório aberrante durante a epileptogênese parece que o microcircuito não é afetado (Navidhamidi, Ghasemi e Mehranfard, 2017).

Alterações celulares e moleculares desencadeadas pela epileptogênese também são encontradas no GD e no CE (Gorter e Lopes da Silva, 2002; Buckmaster, Kobayashi e Wen, 2003; Kobayashi e Buckmaster, 2003; Dengler e Coulter, 2016; Nakahara *et al.*, 2018). O GD desempenha um papel fundamental no controle da propagação de atividade epileptiforme do CE para o hipocampo (Barbarosie *et al.*, 2000; Hsu, 2007). No entanto, conforme descrito por estudos em pacientes com ELT e em modelos animais de epilepsia induzida por pilocarpina, as alterações fisiopatológicas no GD tem sido correlacionadas com a modificação da função de controle de entrada de eventos patológicos para o hipocampo, contribuindo assim para o desenvolvimento de epilepsia (Scharfman, 2019). Nesse trabalho, o GD de fatias de animais epilépticos, 30 dias após o *SE*, apresentou maior latência e menor

duração de eventos ictais, e menor frequência de eventos interictais do que os controles. Dessa forma, esses resultados indicam que a função de controle do GD permanece intacta no período inicial da epilepsia induzida por pilocarpina. No entanto, aos 60 dias após o *SE*, a suscetibilidade para a geração de eventos ictais foi maior no GD de animais epilépticos quando comparada ao grupo controle, e a duração dos eventos ictais foi maior quando comparada ao grupo de 30 dias após o *SE* (Figura 7). O aumento da ictogênese no GD aos 60 dias após o *SE* pode ser atribuído à uma alteração nas propriedades intrínsecas e de rede das células granulares (Dengler e Coulter, 2016; Kelly e Beck, 2017), e à redução do *input* inibitório sobre as células granulares (Sloviter, 1987; Kobayashi e Buckmaster, 2003), refletindo uma perturbação funcional dessa região, que passa a facilitar o desenvolvimento da epilepsia.

Outras estruturas temporais mesiais, além do hipocampo, estão envolvidas na fisiopatologia da ELT e, em particular, o CE é capaz de gerar eventos epileptiformes *in vitro*, possuindo um limiar inferior na geração desses eventos, quando comparado ao hipocampo (Panuccio *et al.*, 2010; Ren *et al.*, 2014). A atividade epileptiforme induzida por 4-AP no CE de fatias de hipocampo-CE de animais epilépticos, 30 dias após o *SE*, foi semelhante em ambos os grupos. Aos 60 dias após o *SE*, o CE das fatias de animais epilépticos tiveram menor latência para a geração de eventos interictais, no entanto esses eventos foram menos frequentes do que no grupo controle; e os eventos ictais apresentaram maior frequência quando comparados ao grupo controle (Figura 7). Apesar do CE apresentar morte celular em modelos de ELT, evidências demonstram o aumento da excitabilidade celular nessa região (Kobayashi e Buckmaster, 2003; Tolner *et al.*, 2007), a qual pode estar envolvida na menor latência para a geração de eventos interictais e no aumento da frequência de eventos

ictais, contribuindo para o estabelecimento da ictogênese. Por outro lado, a diminuição da frequência dos eventos interictais ainda pode ser afetada pela alteração e perda celular no CE de fatias de animais epilépticos, preferencialmente na camada III, observada em humanos e em modelo animal de epilepsia induzida por pilocarpina, (Du *et al.*, 1993, 1995). Além disso, outra hipótese é que a diminuição na frequência de eventos interictais pode ser decorrente de uma ruptura no circuito hipocampo-CE, acarretando na alteração na propagação de eventos interictais, oriundos de CA3, via CA1 e subículo, para o CE (Avoli *et al.*, 1996; Barbarosie e Avoli, 1997).

A caracterização *in vitro* da atividade epileptiforme no modelo animal de epilepsia induzida por pilocarpina reforça o papel singular de cada uma das regiões da formação hipocampal. Enfatizamos que o CE é crucial para a geração e modulação dos eventos ictais e interictais, principalmente 60 dias após o *SE*; CA1 apresenta maior suscetibilidade a ictogênese 30 dias após o *SE*; CA3 possui menores déficits funcionais decorrentes da ELT, sugerindo que essa região pode conduzir a atividade patológica no circuito hipocampo-CE; e por fim o GD, que controla a hiperexcitabilidade durante a epileptogênese em um período inicial, no entanto perde essa função quando a epilepsia é estabelecida.

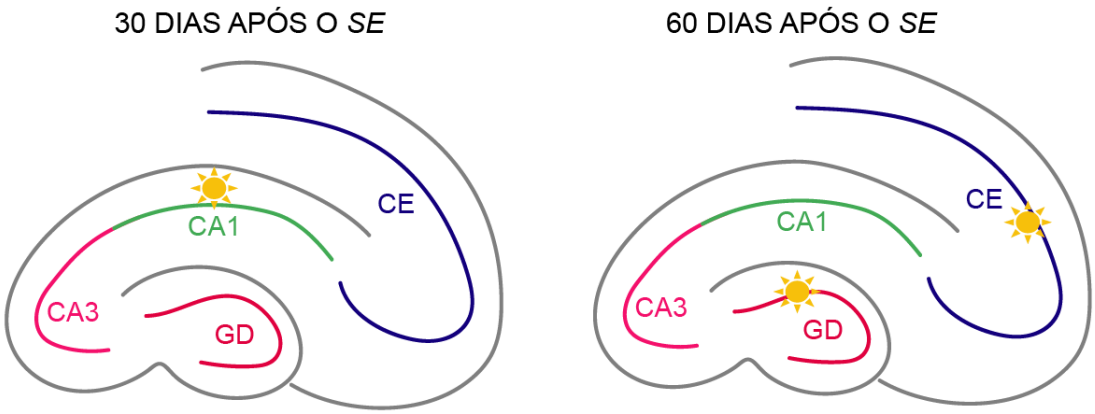

Figura 7 Representação gráfica de fatias de hipocampo e CE de animais epilépticos durante a perfusão com 4-AP, 30 e 60 dias após o *SE*. O aumento da hiperexcitabilidade induzida por 4-AP foi observado em CA1 de fatias de animais epilépticos, 30 dias após *SE*; e no CE e DG de fatias de animais epilépticos, 60 dias após *SE*; ambos comparados ao grupo controle pareado por idade. *SE*: Status

Epilepticus; 4-AP: 4-aminopiridina; CE: Córtex Entorrinal; GD: Giro Denteado. Criado em Adobe Illustrator®.

2 Alterações na potência espectral das oscilações durante a hiperexcitabilidade induzida por 4-AP

Inúmeros estudos apontam a relação entre ELT e redes cerebrais funcionalmente anormais (Bernhardt et al., 2013; Kramer e Cash, 2012; Shah et al., 2019). Considerando que a atividade neuronal anormal não ocorre em um neurônio isolado, pelo contrário, resulta da atividade patológica de um conjunto de neurônios, propõe-se que as crises epilépticas são decorrentes de uma alteração funcional dos microcircuitos neuronais, e que a ELT é resultante das alterações fisiopatológicas e funcionais da rede neuronal (Kramer e Cash, 2012; González Otárula e Schuele, 2020).

A atividade oscilatória classificada em diferentes faixas de frequência pode refletir a função dos vários circuitos neuronais cerebrais (Buzsáki, 2006; Colgin, 2016), e a sua alteração constitui uma característica crucial para a identificação de processos fisiopatológicos (Scharfman, 2007; Colgin, 2011). A análise de potência espectral dos traçados interictais (sem eventos interictais) demonstrou que a região CA3 de fatias de hipocampo-CE de animais epilépticos, 30 dias após o *SE*, teve menor potência das oscilações delta e teta, do que os controles. A diminuição do ritmo teta do hipocampo também é observada após eventos interictais em pacientes com ELT (Fu et al., 2018), e em modelo animal de epilepsia induzida por pilocarpina nos estágios latente e crônico (Ge et al., 2013; Pasquetti et al., 2019), sugerindo que os eventos interictais têm um impacto relevante no ritmo teta na epilepsia. Porém, observamos que as fatias de hipocampo-CE dos animais epilépticos apresentaram uma maior potência da oscilação teta no GD 30 dias após o *SE*, e no CE e CA3 aos

60 dias após o *SE,* quando comparados aos controles. A maior potência de teta encontrada em regiões da formação hipocampal pode ser atribuída à um mecanismo compensatório, onde o aumento da potência de oscilações de baixa frequência contrabalançam o aumento das HFOs, devido ao aumento de atividade excitatória desencadeada por uma disfunção GABAérgica (Genovesi *et al.*, 2011). Portanto, a heterogeneidade da potência do ritmo teta nas fatias de hipocampo-CE podem refletir a reorganização neural no dois períodos de epileptogênese (Curia *et al.*, 2008).

As oscilações beta contribuem para a geração de eventos epileptiformes durante a epileptogênese, e são extremamente importantes para a sincronização de longo alcance (Traub *et al.*, 1996; Whittington *et al.*, 1997). Nós demonstramos que as fatias de hipocampo-CE de animais epilépticos tiveram maior potência de beta em CE, CA1 e CA3, em 60 dias após o *SE*, mas não aos 30 dias após o *SE,* quando comparado ao respectivo grupo controle. Este aumento na potência de beta somente durante estágios crônicos da epilepsia pode estar correlacionado com mecanismos de estabelecimento da epilepsia, e a geração de eventos epileptiformes recorrentes. Em pacientes com ELT, há aumento da potência da oscilação beta no período pré-ictal (Sorokin, Paz e Huguenard, 2016); além disso em um modelo experimental de crises de ausência, foi demonstrado que o aumento da potência da oscilação beta está correlacionado com a suscetibilidade de gerar crises epilépticas (Glaba *et al.*, 2020).

As oscilações gama também possuem uma estreita relação com a geração de atividade epileptiforme *in vitro* (Quilichini *et al.*, 2012). Aos 30 dias após o *SE*, encontramos maior potência de gama lento em CE, gama médio em CA1 e gama lento, médio e rápido em CA3 das fatias de hipocampo-CE de animais epilépticos, quando comparado aos controles. Aos 60 dias após o *SE*, encontramos maior

potência de todas as bandas de frequência gama em CA3 e GD, e gama lento em CA1 de fatias de hipocampo-CE de animais epilépticos, do que em fatias de controle. Assim, observamos que em diferentes estágios da epileptogênese, após um segundo insulto de hiperexcitabilidade induzido por 4-AP, ocorre uma alteração na potência das oscilações gama na formação hipocampal, principalmente em CA3 e CA1; ressaltando o papel das oscilações gama como um potencial biomarcador para a identificação da rede neuronal patológica com geração de eventos interictais no cérebro (Ren *et al.*, 2015).

Não apenas gama, mas também oscilações mais rápidas estão envolvidas na geração de atividade epileptiforme (Hamidi, Lévesque e Avoli, 2014; Salami, Levesque, *et al.*, 2014), e tanto HFOs quanto as oscilações gama são identificadas no EEG de pacientes com ELT e modelos animais de epilepsia induzida por ácido caínico ou pilocarpina (Bragin *et al.*, 2004; Lévesque *et al.*, 2011; Pearce *et al.*, 2013; Ewell *et al.*, 2019; Jacobs e Zijlmans, 2020). Aqui, demonstramos que as HFOs podem ser detectadas nos intervalos de eventos interictais em fatias de hipocampo-CE. Evidências demonstram que as HFOs, denominadas ripples (150-250 Hz) e fast ripples (250-500 Hz) associadas a eventos interictais são excelentes biomarcadores da epileptogênese (Zijlmans *et al.*, 2011; Salami, Levesque, *et al.*, 2014; Jacobs *et al.*, 2016; Lévesque, Salami, *et al.*, 2018; Thomschewski, Hincapié e Frauscher, 2019). Aos 30 dias após o *SE*, a região CA3 de fatias de hipocampo-CE de animais epilépticos apresentou maior potência de HFOs. Alterações da atividade oscilatória de alta frequência em CA3, aos 30 dias após o *SE*, pode demonstrar a relevância dessa região específica na progressão da epileptogênese e estabelecimento da ictogênese. Aos 60 dias após o *SE*, o CE apresentou maior potência de ripples, e o GD, maior potência de ambas HFOs. Assim, as HFOs tiveram maior potência nas

redes neuronais de animais epilépticos com um segundo insulto de hiperexcitabilidade, possivelmente refletindo os mecanismos anormais de sincronização neuronal desses microcircuitos (Jefferys *et al.*, 2012). Dessa forma, consideramos que a maior potência das HFOs pode ter um valor preditivo de formação de redes epileptogênicas, como na área CA3 do hipocampo aos 30 dias após o *SE*; e de alvos específicos de epileptogênese, como no CE e GD aos 60 dias após o *SE* (Fedele *et al.*, 2017; Jacobs e Zijlmans, 2020). As alterações da atividade oscilatória na formação hipocampal de animais epilépticos, 30 e 60 dias após o *SE*, estão resumidas na Figura 8.

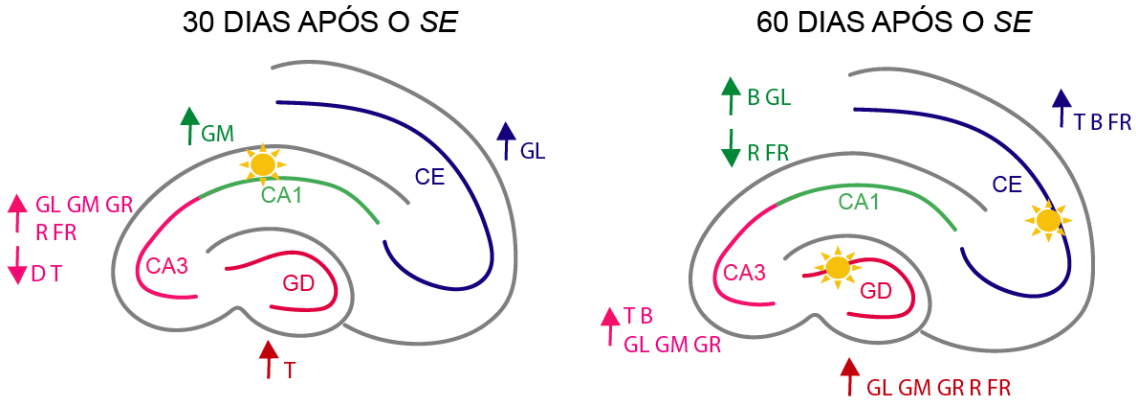

Figura 8 Alterações na densidade espectral de potência em fatias de hipocampo e CE de animais epilépticos durante a perfusão com 4-AP, 30 e 60 dias após o *SE* (comparados ao grupo controle pareado por idade). O sol representa o aumento da hiperexcitabilidade induzida por 4-AP , 30 e 60 dias após o *SE*. *SE*: Status Epilepticus; CE: Córtex Entorrinal; GD: Giro Denteado; D: Delta; T: Teta; B: Beta; GL: Gama lento; GM: Gama médio; GR: Gama rápido, R: Ripples; FR: Fast ripples.
↑: aumento; ↓: diminuição. Criado em Adobe Illustrator®.

3 Alterações na sincronia de oscilações entre diferentes regiões da formação hipocampal durante a hiperexcitabilidade induzida por 4-AP

Atividades neuronais sincronizadas de diferentes áreas cerebrais exercem uma grande influência na capacidade de interação entre circuitos, e fornecem um mecanismo para o processamento e propagação da informação (Buzsaki e Draguhn, 2004; Buzsáki e Watson, 2012; Igarashi *et al.*, 2014; Colgin, 2016; Malkov *et al.*, 2021). Neste estudo, a análise de coerência de fase pode revelar a atividade

sincronizada entre regiões distintas do circuito hipocampo-CE em bandas de frequência específicas, e pode enfatizar a atividade oscilatória síncrona entre regiões específicas (Horwitz, 2003), fundamental para o desenvolvimento e estabelecimento da ELT.

As fatias de hipocampo-CE de animais epilépticos perfundidas com 4-AP, 30 dias após o *SE*, apresentaram uma maior coerência de fase das oscilações gama entre CA1-CA3, quando comparados aos controles pareados por idade. No entanto, aos 60 dias após o *SE*, observamos uma menor coerência de fase de gama lento e/ou gama médio entre CE-DG, CE-CA1 e GD-CA3 de fatias de hipocampo-CE de animais epilépticos, comparado aos controles. Esses resultados sugerem que, as oscilações gama estão sincronizadas, no início da fase crônica da epileptogênese em fatias de hipocampo-CE de animais epilépticos, contribuindo para a ictogênese (Figura 9). No entanto, na condição epiléptica estabelecida aos 60 dias após o *SE*, a sincronização das oscilações gama está reduzida, podendo ser decorrente das alterações funcionais e estruturais resultantes da epilepsia, como por exemplo, perda de interneurônios, maturação anormal de células granulares e brotamento de fibras musgosas (Scharfman, 2019; Lybrand *et al.*, 2021).

Referente às HFOs, observamos uma maior coerência de fase entre CE-CA1, 30 dias após o *SE* (Figura 9). A presença de HFOs durante a epileptogênese pode indicar a reorganização da rede patológica, a qual pode apresentar danos funcionais e estruturais importantes no circuito do hipocampo-CE, contribuindo para o estabelecimento da ELT (Bragin *et al.*, 2004; Lévesque *et al.*, 2011; Lévesque, Shiri, *et al.*, 2018), mas também pode indicar a continuidade de uma rede irreversivelmente patológica, síncrona e hiperexcitável. Aos 60 dias após o *SE*, também encontramos uma maior coerência de fase de HFOs entre CA3-CA1 das fatias de hipocampo-CE

de animais epilépticos (Figura 9). Conforme relatado por vários estudos, as HFOs também podem ser utilizadas como fator decisivo para o diagnóstico, tratamento cirúrgico e prognóstico de pacientes com epilepsia (Jacobs *et al.*, 2008; Fujiwara *et al.*, 2012; Fedele *et al.*, 2017), dessa forma, em modelos que mimetizam períodos crônicos da epilepsia, a detecção do aumento de HFOs é esperada.

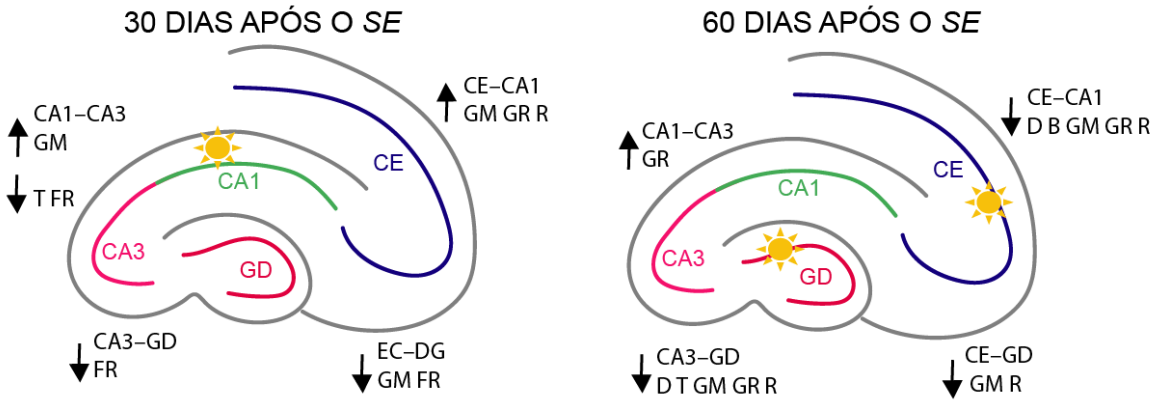

Figura 9 Alterações na coerência de fase em fatias de hipocampo e CE de animais epilépticos durante a perfusão com 4-AP, 30 e 60 dias após o *SE* (comparados ao grupo controle pareado por idade). O sol representa o aumento da hiperexcitabilidade induzida por 4-AP , 30 e 60 dias após o *SE*. *SE*: Status Epilepticus; CE: Córtex Entorrinal; GD: Giro Denteado; D: Delta; T: Teta; B: Beta; GL: Gama lento; GM: Gama médio; GR: Gama rápido, R: Ripples; FR: Fast ripples. ↑: aumento; ↓: diminuição. Criado em Adobe Illustrator®.

4 Alterações na potência espectral das oscilações durante a atividade espontânea da rede

A atividade neuronal espontânea da rede também se propaga através dos circuitos neuronais em padrões oscilatórios específicos (Kerschensteiner, 2014; Colgin, 2016). Embora não tenha sido registrada atividade epileptiforme nas fatias de hipocampo-CE durante a perfusão com ACSF, a análise dos trechos da atividade espontânea da rede relevou maior potência das oscilações gama em CE, CA1, CA3 e GD em fatias de hipocampo-CE de animais epilépticos, 30 e 60 dias após o *SE*, quando comparado aos respectivos controles (Figura 10). Essa alteração na potência das oscilações gama foi semelhante ao que observamos nas fatias de hipocampo-CE de animais epilépticos durante a perfusão com ACSF e 4-AP, sugerindo que a

mudança na atividade oscilatória na faixa de frequência gama pode refletir os processos patológicos em andamento, que contribuem para a ictogênese (Goldberg e Coulter, 2013; Sato *et al.*, 2017). Evidências demonstram o aumento das oscilações gama em áreas do cérebro associada a crises epilépticas em pacientes e modelos animais de epilepsia (Hughes, 2008; de Curtis e Gnatkovsky, 2009). Portanto, estes resultados reinforçam que as oscilações gama são biomarcadores úteis para a epileptogênese.

As HFOs, também referidas como importantes marcadores de processos patológicos em andamento e da epileptogênese, foram encontradas nas fatias de hipocampo-CE de animais epilépticos, durante a atividade espontânea da rede. No entanto, observamos maior potência de ripples e fast ripples somente no GD aos 60 dias após o *SE*, quando comparado ao grupo controle (Figura 10). Dessa forma, na ausência de um segundo insulto de hiperexcitabilidade, e considerando que somente processos patológicos em decurso e a excitabilidade anormal da rede estão sendo avaliadas nesse protocolo experimental, esse resultado demonstra que o GD representa uma área crucial para o processo epileptogênico. O GD foi a única região com aumento de HFOs *per se*, o que pode ser considerado um biomarcador da perda de controle sobre os inputs para hipocampo.

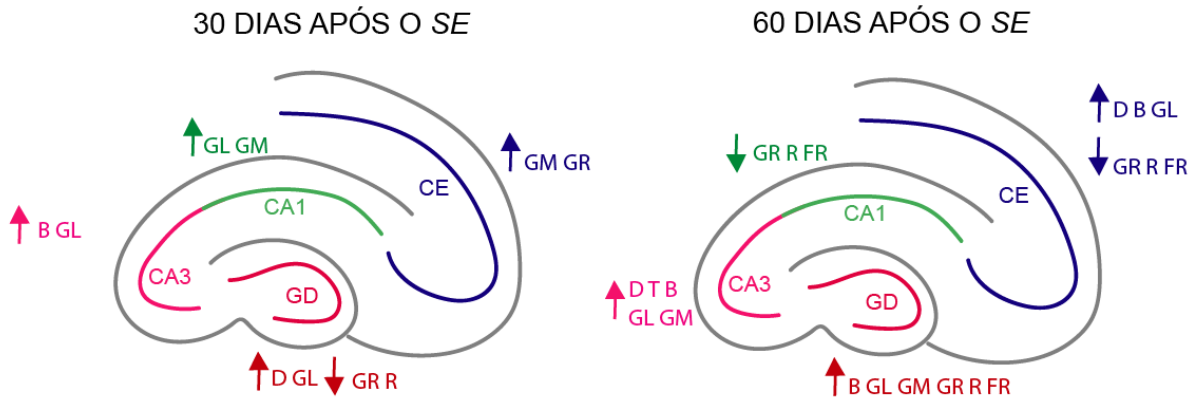

Figura 10 Alterações na densidade espectral de potência em fatias de hipocampo e CE de animais epilépticos durante a atividade espontânea da rede, 30 e 60 dias após o *SE* (comparados ao grupo

controle pareado por idade). *SE*: Status Epilepticus; CE: Córtex Entorrinal; GD: Giro Denteado; D: Delta; T: Teta; B: Beta; GL: Gama lento; GM: Gama médio; GR: Gama rápido, R: Ripples; FR: Fast ripples. ↑: aumento; ↓: diminuição. Criado em Adobe Illustrator®.

5 Alterações na sincronia das oscilações durante a atividade espontânea da rede

Aos 30 dias após o *SE*, os grupos *SE* e controle não apresentaram nenhuma diferença na coerência de fase entre as oscilações durante a atividade de rede espontânea. No entanto, aos 60 dias após o *SE,* a coerência de fase foi maior nas oscilações de alta frequência entre GD-CA3 das fatias hipocampais-CE de animais epilépticos (Figura 11). Na ausência de 4-AP, o GD também apresentou maior potência das oscilações rápidas, demonstrando que a atividade espontânea da rede apresenta alterações oscilatórias decorrente da reorganização sináptica e estrutural no modelo de epilepsia induzida por pilocarpina (Garrido Sanabria *et al.*, 2002). Consequentemente, é provável que ocorram alterações na conectividade no circuito hipocampo-CE de fatias de animais epilépticos. De fato, o GD e CA3 sofrem mudanças morfológicas e funcionais que contribuem para a epileptogênese (Zhang, Fan e Wang, 2017), e por meio da análise de coerência em fatias de hipocampo-CE foi possível identificar uma específica e importante alteração da conectividade entre esses microcircuitos, influenciando assim o desenvolvimento de redes hiperexcitáveis e geradoras de crises (Figura 11).

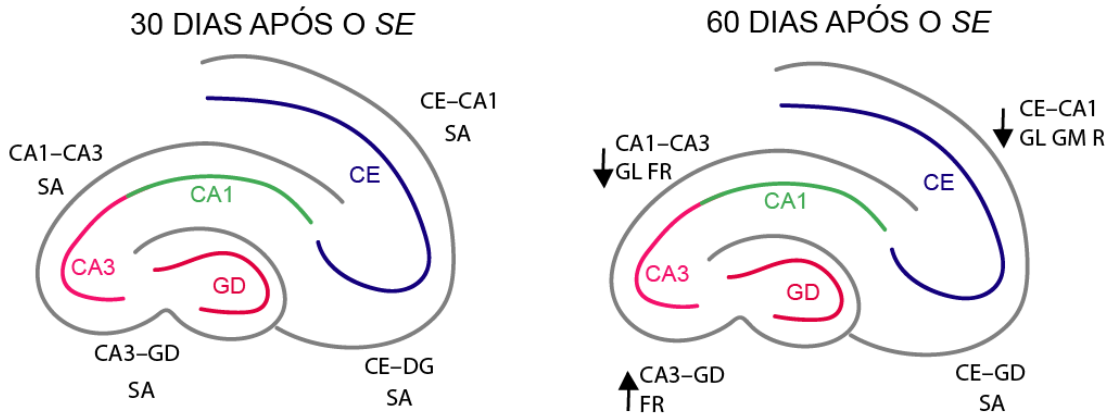

Figura 11 Alterações na coerência de fase em fatias de hipocampo e CE de animais epilépticos durante a atividade espontânea da rede, 30 e 60 dias após o *SE* (comparados ao grupo controle pareado por idade). *SE*: Status Epilepticus; CE: Córtex Entorrinal; GD: Giro Denteado; D: Delta; T: Teta; B: Beta; GL: Gama lento; GM: Gama médio; GR: Gama rápido, R: Ripples; FR: Fast ripples; SA: sem alterações. ↑: aumento; ↓: diminuição. Criado em Adobe Illustrator®.

6 O sistema GABAérgico e as epilepsias

A importância da inibição mediada pelo GABA no encéfalo normal e sua função em doenças decorrentes do desequilíbrio de excitação/inibição, como a epilepsia, são bem aceitos, graças ao conhecimento cada vez maior da fisiologia do SNC, os progressos da genética e demais avanços científicos (Genovesi *et al.*, 2011; Ben-Ari *et al.*, 2012; Liu *et al.*, 2014; Magloire *et al.*, 2019; Tang, Jaenisch e Sur, 2021; Zhang *et al.*, 2021). No entanto, é importante ressaltar que a sinalização GABAérgica possui uma gama de funções que não se resumem apenas na inibição dos circuitos.

Os interneurônios GABAérgicos são reconhecidos com base nos seus padrões de disparo, perfis de expressão molecular, e suas inervações de domínios subcelulares distintos em células piramidais (Ascoli *et al.*, 2008). Desse modo, desempenham um papel central na regulação da atividade hipocampal e cortical através dos seus efeitos inibitórios em neurônios excitatórios, formando um sistema de controle altamente eficiente, e regulando a sensibilidade do circuito neuronal (Kepecs e Fishell, 2014). Além disso, o controle da geração de padrões oscilatórios promovido pelos interneurônios podem se revelar muito mais importante do que a

inibição em si , promovendo a sincronização neuronal e facilitando a geração de crises epilépticas (Cobb *et al.*, 1995; Avoli e de Curtis, 2011; Khazipov, 2016).

Os mecanismos envolvidos na geração de crises epilépticas são complexos, e não podem ser resumidos como um prejuízo ou colapso do sistema inibitório. O envolvimento do sistema GABAérgico na fisiopatologia da epilepsia é evidente, uma vez que a ruptura da rede sináptica e a reorganização das redes neuronais no córtex e no hipocampo na epileptogênese inclui a perda ou alterações intrísinsecas de interneurônios GABAérgicos (Liu *et al.*, 2014). Portanto, definir as populações neuronais, seu perfil de expressão molecular, conexões sinápticas e atividade temporal, juntamente com a alteração da atividade desses tipos celulares, nos permite compreender de forma mais clara o papel da sinalização inibitória no desenvolvimento de redes patológicas.

CONCLUSÕES

Neste trabalho foi possível identificar alterações nos padrões oscilatórios em fatias de hipocampo-CE de animais epilépticos durante um segundo insulto de hiperexcitabilidade induzido por 4-AP, mas também durante a atividade espontânea da rede neuronal, em dois períodos da epileptogênese. A caracterização dos padrões de atividade epileptiforme e das oscilações hipocampais em cada região da formação hipocampal durante o período interictal é decisivo para entender o processo de geração das crises epilépticas. No entanto, a identificação de alterações oscilatórias *in vitro* durante um período de atividade espontânea da rede na ausência de atividade epileptiforme, ressalta que este circuito neuronal mantém uma progressão gradual de alterações que também contribuem para a geração de crises epilépticas.

É importante ressaltar que a reorganização dos circuitos neurais na ELT inclui uma série de modificações estruturais e funcionais, que não se resumem a um prejuízo ou dano dos componentes do sistema GABAérgico. Em vista disso, a investigação minusciosa das alterações excitatórias e inibitórias da rede neuronal pode contribuir para o entendimento dos mecanismos envolvidos no desenvolvimento, progressão da epileptogênese e ictogênese. Em particular, elucidar a função dos interneurônios na rede neuronal aberrante é crucial para a compreensão que a ELT não é exclusivamente decorrente de um desequilíbrio entre excitação e inibição, com ênfase em um prejuízo no sistema GABAérgico.

FINANCIAMENTO

O presente trabalho foi realizado com apoio do Conselho Nacional de Desenvolvimento Científico e Tecnológico (CNPq) e da Coordenação de Aperfeiçoamento de Pessoal de Nível Superior - Brasil (CAPES).

REFERÊNCIAS

Ahmad, S., Khanna, R. e Sani, S. (2020) “Surgical Treatments of Epilepsy”, *Seminars in Neurology*, 40(6), p. 696–707. doi: 10.1055/s-0040-1719072.

Arabadzisz, D. *et al.* (2005) “Epileptogenesis and chronic seizures in a mouse model of temporal lobe epilepsy are associated with distinct EEG patterns and selective neurochemical alterations in the contralateral hippocampus”, *Experimental Neurology*, 194(1), p. 76–90. doi: 10.1016/j.expneurol.2005.01.029.

Ascoli, G. A. *et al.* (2008) “Petilla terminology: Nomenclature of features of GABAergic interneurons of the cerebral cortex”, *Nature Reviews Neuroscience*, 9(7), p. 557–568. doi: 10.1038/nrn2402.

Avoli, M. *et al.* (1996) “Synchronous GABA-mediated potentials and epileptiform discharges in the rat limbic system in vitro”, *Journal of Neuroscience*, 16(12), p. 3912–3924. doi: 10.1523/jneurosci.16-12-03912.1996.

Avoli, M. *et al.* (2002) “Network and pharmacological mechanisms leading to epileptiform synchronization in the limbic system in vitro”, *Progress in Neurobiology*, 68(3), p. 167–207. doi: 10.1016/S0301-0082(02)00077-1.

Avoli, M. *et al.* (2005) “Cellular and molecular mechanisms of epilepsy in the human brain”, *Progress in Neurobiology*, 77(3), p. 166–200. doi: 10.1016/j.pneurobio.2005.09.006.

Avoli, M. (2014) “Mechanisms of Epileptiform Synchronization in Cortical Neuronal Networks”, *Current Medicinal Chemistry*, 21(6), p. 653–662. doi: 10.2174/09298673206613119151136.

Avoli, M. e de Curtis, M. (2011) “GABAergic synchronization in the limbic system and

its role in the generation of epileptiform activity", *Progress in Neurobiology*, 95(2), p. 104–132. doi: 10.1016/j.pneurobio.2011.07.003.

Avoli, M. e Jefferys, J. G. R. (2015) "Models of drug-induced epileptiform synchronization in vitro", *Journal of Neuroscience Methods*, 260, p. 26–32. doi: 10.1016/j.jneumeth.2015.10.006.

Avoli, M. e Jefferys, J. G. R. (2016) "Models of drug-induced epileptiform synchronization in vitro", *Journal of Neuroscience Methods*, 260(1959), p. 26–32. doi: 10.1016/j.jneumeth.2015.10.006.

Barbarosie, M. *et al.* (2000) "CA3-released entorhinal seizures disclose dentate gyrus epileptogenicity and unmask a temporoammonic pathway", *Journal of Neurophysiology*, 83(3), p. 1115–1124. doi: 10.1152/jn.2000.83.3.1115.

Barbarosie, M. *et al.* (2002) "Masking synchronous GABA-mediated potentials controls limbic seizures", *Epilepsia*, 43(12), p. 1469–1479. doi: 10.1046/j.1528-1157.2002.17402.x.

Barbarosie, M. e Avoli, M. (1997) "CA3-driven hippocampal-entorhinal loop controls rather than sustains in vitro limbic seizures", *Journal of Neuroscience*, 17(23), p. 9308–9314. doi: 10.1523/jneurosci.17-23-09308.1997.

Bartolomei, F. *et al.* (2001) "Neural networks involving the medial temporal structures in temporal lobe epilepsy", *Clinical Neurophysiology*, 112(9), p. 1746–1760. doi: 10.1016/S1388-2457(01)00591-0.

Belluscio, M. A. *et al.* (2012) "Cross-frequency phase-phase coupling between theta and gamma oscillations in the hippocampus", *Journal of Neuroscience*, 32(2), p. 423–435. doi: 10.1523/JNEUROSCI.4122-11.2012.

Ben-Ari, Y. *et al.* (2007) "GABA: A pioneer transmitter that excites immature neurons

and generates primitive oscillations", *Physiological Reviews*, 87(4), p. 1215–1284. doi: 10.1152/physrev.00017.2006.

Ben-Ari, Y. *et al.* (2012) "The GABA excitatory/inhibitory shift in brain maturation and neurological disorders", *Neuroscientist*, 18(5), p. 467–486. doi: 10.1177/1073858412438697.

Berg, A. T. *et al.* (2010) "Revised terminology and concepts for organization of seizures and epilepsies: Report of the ILAE Commission on Classification and Terminology, 2005-2009", *Epilepsia*, 51(4), p. 676–685. doi: 10.1111/j.1528-1167.2010.02522.x.

Bertram, E. H. (2009) "Temporal lobe epilepsy: Where do the seizures really begin?", *Epilepsy & Behavior*, 14(1), p. 32–37. doi: 10.1016/j.yebeh.2008.09.017.

Biagini, G. *et al.* (2005) "Impaired activation of CA3 pyramidal neurons in the epileptic hippocampus", *NeuroMolecular Medicine*, 7(4), p. 325–342. doi: 10.1385/NMM:7:4:325.

Blümcke, I. *et al.* (2013) "International consensus classification of hippocampal sclerosis in temporal lobe epilepsy: A Task Force report from the ILAE Commission on Diagnostic Methods", *Epilepsia*, 54(7), p. 1315–1329. doi: 10.1111/epi.12220.

Blümcke, I., Mrcpath, M. T. e Wiestler, D. (2002) "Blümcke, Mrcpath, Wiestler_Ammon ' s Horn Sclerosis A Maldevelopmental Disorder Associated with Temporal Lobe Epilepsy.pdf", 1.

Boido, D. *et al.* (2014) "Network dynamics during the progression of seizure-like events in the hippocampal-parahippocampal regions", *Cerebral Cortex*, 24(1), p. 163–173. doi: 10.1093/cercor/bhs298.

Bortel, A. *et al.* (2010) "Convulsive status epilepticus duration as determinant for

epileptogenesis and interictal discharge generation in the rat limbic system", *Neurobiology of Disease*, 40(2), p. 478–489. doi: 10.1016/j.nbd.2010.07.015.

Boyett, J. M. e Buckmaster, P. S. (2001) "Somatostatin-immunoreactive interneurons contribute to lateral inhibitory circuits in the dentate gyrus of control and epileptic rats", *Hippocampus*, 11(4), p. 418–422. doi: 10.1002/hipo.1056.abs.

Bragin, A., Engel, J., Wilson, C. L., Fried, I. e Buzsáki, G. (1999) "High-frequency oscillations in human brain", *Hippocampus*, 9(2), p. 137–142. doi: 10.1002/(SICI)1098-1063(1999)9:2<137::AID-HIPO5>3.0.CO;2-0.

Bragin, A., Engel, J., Wilson, C. L., Fried, I. e Mathern, G. W. (1999) "Hippocampal and entorhinal cortex high-frequency oscillations (100-500 Hz) in human epileptic brain and in kainic acid-treated rats with chronic seizures", *Epilepsia*, 40(2), p. 127–137. doi: 10.1111/j.1528-1157.1999.tb02065.x.

Bragin, A. *et al.* (2002) "Local generation of fast ripples in epileptic brain", *Journal of Neuroscience*, 22(5), p. 2012–2021. doi: 10.1523/jneurosci.22-05-02012.2002.

Bragin, A. *et al.* (2004) "High-frequency oscillations after status epilepticus: Epileptogenesis and seizure genesis", *Epilepsia*, 45(9), p. 1017–1023. doi: 10.1111/j.0013-9580.2004.17004.x.

Broggini, A. C. S. *et al.* (2016) "Pre-ictal increase in theta synchrony between the hippocampus and prefrontal cortex in a rat model of temporal lobe epilepsy", *Experimental Neurology*, 279, p. 232–242. doi: 10.1016/j.expneurol.2016.03.007.

Buckle, P. e Haas, H. (1982) "Enhancement of synaptic transmission by 4-aminopyridine in hippocampal slices oh the rat", p. 109–122.

Buckmaster, P. S., Kobayashi, M. e Wen, X. (2003) "Reduced Inhibition and Increased Output of Layer II Neurons in the Medial Entorhinal Cortex in a Model of Temporal

Lobe Epilepsy", *Journal of Neuroscience*, 23(24), p. 8471–8479.

Buzsáki, G. (2006) *Rhythms of the Brain*. Oxford University Press, Inc. doi: 10.1093/acprof:oso/9780195301069.001.0001.

Buzsáki, G., Anastassiou, C. A. e Koch, C. (2012) "The origin of extracellular fields and currents-EEG, ECoG, LFP and spikes", *Nature Reviews Neuroscience*, 13(6), p. 407–420. doi: 10.1038/nrn3241.

Buzsaki, G. e Draguhn, A. (2004) "Neuronal Oscillations in Cortical Networks", *Science*, 304(June), p. 1926–1929. Available at: http://science.sciencemag.org/.

Buzsáki, G. e Watson, B. O. (2012) "Brain rhythms and neural syntax: Implications for efficient coding of cognitive content and neuropsychiatric disease", *Dialogues in Clinical Neuroscience*, 14(4), p. 345–367. doi: 10.31887/dcns.2012.14.4/gbuzsaki.

Calcagnotto, M. E., Barbarosie, M. e Avoli, M. (2000) "Hippocampus-entorhinal cortex loop and seizure generation in the young rodent limbic system", *Journal of Neurophysiology*, 83(5), p. 3183–3187. doi: 10.1152/jn.2000.83.5.3183.

Cappaert, N. L. M., Van Strien, N. M. e Witter, M. P. (2015) *Hippocampal Formation*. Fourth Edi, *The Rat Nervous System: Fourth Edition*. Fourth Edi. Elsevier Inc. doi: 10.1016/B978-0-12-374245-2.00020-6.

Castro, O. W. *et al.* (2011) "Comparative neuroanatomical and temporal characterization of FluoroJade-positive neurodegeneration after status epilepticus induced by systemic and intrahippocampal pilocarpine in Wistar rats", *Brain Research*, 1374, p. 43–55. doi: 10.1016/j.brainres.2010.12.012.

Cavalheiro, E. A. *et al.* (2006) "The Pilocarpine Model of Seizures", *Models of Seizures and Epilepsy*, p. 433–448. doi: 10.1016/B978-012088554-1/50037-2.

Cendes, F. *et al.* (2014) “Epilepsies associated with hippocampal sclerosis”, *Acta Neuropathologica*, 128(1), p. 21–37. doi: 10.1007/s00401-014-1292-0.

Chatzikonstantinou, A. (2014) “Epilepsy and the hippocampus”, *The Hippocampus in Clinical Neuroscience*, 34, p. 121–142. doi: 10.1159/000356435.

Chauvière, L. *et al.* (2009) “Early deficits in spatial memory and theta rhythm in experimental temporal lobe epilepsy”, *Journal of Neuroscience*, 29(17), p. 5402–5410. doi: 10.1523/JNEUROSCI.4699-08.2009.

Chauvière, L. *et al.* (2012) “Changes in interictal spike features precede the onset of temporal lobe epilepsy”, *Annals of Neurology*, 71(6), p. 805–814. doi: 10.1002/ana.23549.

Chen, L. L. *et al.* (2013) “One hour of pilocarpine-induced status epilepticus is sufficient to develop chronic epilepsy in mice, and is associated with mossy fiber sprouting but not neuronal death”, *Neuroscience Bulletin*, 29(3), p. 295–302. doi: 10.1007/s12264-013-1310-6.

Chvojka, J. *et al.* (2019) “The role of interictal discharges in ictogenesis — A dynamical perspective”, *Epilepsy and Behavior*, p. 106591. doi: 10.1016/j.yebeh.2019.106591.

Cobb, S. *et al.* (1995) “Synchronization of neuronal activity in hippocampus by individual GABAergic interneurons”, *Nature*, 378(7), p. 603–605.

Codadu, N. K. *et al.* (2019) “Divergent paths to seizure-like events”, *Physiological Reports*, 7(19), p. 1–15. doi: 10.14814/phy2.14226.

Codadu, N. K., Parrish, R. R. e Trevelyan, A. J. (2019) “Region-specific differences and areal interactions underlying transitions in epileptiform activity”, *Journal of Physiology*, 597(7), p. 2079–2096. doi: 10.1113/JP277267.

Colgin, L. L. *et al.* (2009) “Frequency of gamma oscillations routes flow of information in the hippocampus”, *Nature*, 462(7271), p. 353–357. doi: 10.1038/nature08573.

Colgin, L. L. (2011) “Oscillations and hippocampal-prefrontal synchrony”, *Current Opinion in Neurobiology*, 21(3), p. 467–474. doi: 10.1016/j.conb.2011.04.006.

Colgin, L. L. (2016) “Rhythms of the hippocampal network”, *Nature Reviews Neuroscience*, 17(4), p. 239–249. doi: 10.1038/nrn.2016.21.

Cossart, R. *et al.* (2001) “GABAergic inhibition is decreased in experimental epilepsy”, *Nature Neuroscience*, 4(1), p. 52–62.

Cotic, M. *et al.* (2013) “Synchrony of high frequency oscillations in the human epileptic brain”, *Proceedings of the Annual International Conference of the IEEE Engineering in Medicine and Biology Society, EMBS*, p. 5582–5585. doi: 10.1109/EMBC.2013.6610815.

Cotic, M. *et al.* (2015) “Mapping the coherence of ictal high frequency oscillations in human extratemporal lobe epilepsy”, *Epilepsia*, 56(3), p. 393–402. doi: 10.1111/epi.12918.

Di Cristo, G. *et al.* (2018) “KCC2, epileptiform synchronization, and epileptic disorders”, *Progress in Neurobiology*, 162, p. 1–16. doi: 10.1016/j.pneurobio.2017.11.002.

Cross, D. J. e Cavazos, J. E. (2007) “Synaptic reorganization in subiculum and CA3 after early-life status epilepticus in the kainic acid rat model”, *Epilepsy Research*, 73(2), p. 156–165. doi: 10.1016/j.eplepsyres.2006.09.004.

Curia, G. *et al.* (2008) “The pilocarpine model of temporal lobe epilepsy”, *Journal of Neuroscience Methods*, 172(2), p. 143–157. doi: 10.1016/j.jneumeth.2008.04.019.

Curia, G. *et al.* (2014) “Pathophysiogenesis of Mesial Temporal Lobe Epilepsy: Is Prevention of Damage Antiepileptogenic?”, *Current Medicinal Chemistry*, 21(6), p. 663–688. doi: 10.2174/09298673206613119152201.

de Curtis, M. e Avanzini, G. (2001) “Interictal spikes in focal epileptogenesis”, 63, p. 541–567.

de Curtis, M. e Gnatkovsky, V. (2009) “Reevaluating the mechanisms of focal ictogenesis: The role of low-voltage fast activity.”, *Epilepsia*, 50(12), p. 2514–2525. doi: 10.1111/j.1528-1167.2009.02249.x.

de Curtis, M., Jefferys, J. G. R. e Avoli, M. (2013) “Interictal Epileptiform Discharges in Partial Epilepsy”, *Jasper’s Basic Mechanisms of the Epilepsies*, p. 213–227. doi: 10.1093/med/9780199746545.003.0017.

Cymerblit-Sabba, A. e Schiller, Y. (2010) “Network dynamics during development of pharmacologically induced epileptic seizures in rats in vivo”, *Journal of Neuroscience*, 30(5), p. 1619–1630. doi: 10.1523/JNEUROSCI.5078-09.2010.

D’Antuono, M. *et al.* (2002) “Limbic network interactions leading to hyperexcitability in a model of temporal lobe epilepsy”, *Journal of Neurophysiology*, 87(1), p. 634–639. doi: 10.1152/jn.00351.2001.

D’Antuono, M. *et al.* (2010) “Antiepileptic drugs abolish ictal but not interictal epileptiform discharges in vitro”, *Epilepsia*, 51(3), p. 423–431. doi: 10.1111/j.1528-1167.2009.02273.x.

Dang-Vu, T. T. *et al.* (2008) “Spontaneous neural activity during human slow wave sleep”, *Proceedings of the National Academy of Sciences of the United States of America*, 105(39), p. 15160–15165. doi: 10.1073/pnas.0801819105.

Danzer, S. C. *et al.* (2010) “Structural plasticity of dentate granule cell mossy fibers

during the development of limbic epilepsy", *Hippocampus*, 20(1), p. 113–124. doi: 10.1002/hipo.20589.

Dengler, C. G. e Coulter, D. A. (2016) "Normal and epilepsy-associated pathologic function of the dentate gyrus", *Progress in Brain Research*, 226, p. 155–178. doi: 10.1016/bs.pbr.2016.04.005.

Devinsky, O. *et al.* (2016) "Sudden unexpected death in epilepsy: epidemiology, mechanisms, and prevention", *The Lancet Neurology*, 15(10), p. 1075–1088. doi: 10.1016/S1474-4422(16)30158-2.

Devinsky, O. *et al.* (2018) "Epilepsy", *Nature Reviews Disease Primers*, 4(May). doi: 10.1038/nrdp.2018.24.

Dinocourt, C. *et al.* (2003) "Loss of interneurons innervating pyramidal cell dendrites and axon initial segments in the CA1 region of the hippocampus following pilocarpine-induced seizures", *Journal of Comparative Neurology*, 459(4), p. 407–425. doi: 10.1002/cne.10622.

Dipoppa, M., Szwed, M. e Gutkin, B. S. (2016) "Controlling working memory operations by selective gating: The roles of oscillations and synchrony", *Advances in Cognitive Psychology*, 12(4), p. 209–232. doi: 10.5709/acp-0199-x.

Du, F. *et al.* (1993) "Preferential neuronal loss in layer III of the entorhinal cortex in patients with temporal lobe epilepsy", *Epilepsy Research*, 16(3), p. 223–233. doi: 10.1016/0920-1211(93)90083-J.

Du, F. *et al.* (1995) "Preferential neuronal loss in layer III of the medial entorhinal cortex in rat models of temporal lobe epilepsy", *Journal of Neuroscience*, 15(10), p. 6301–6313. doi: 10.1523/jneurosci.15-10-06301.1995.

Dudek, F. E. (2020) "Loss of GABAergic Interneurons in Seizure-Induced

Epileptogenesis—Two Decades Later and in a More Complex World", *Epilepsy Currents*, 20(6_suppl), p. 70S-72S. doi: 10.1177/1535759720960464.

Dugladze, T. *et al.* (2007) "Impaired hippocampal rhythmogenesis in a mouse model of mesial temporal lobe epilepsy", *Proceedings of the National Academy of Sciences of the United States of America*, 104(44), p. 17530–17535. doi: 10.1073/pnas.0708301104.

Dulla, C. G. *et al.* (2018) "How do we use in vitro models to understand epileptiform and ictal activity? A report of the TASK1-WG4 group of the ILAE/AES Joint Translational Task Force", *Epilepsia Open*, 3(4), p. 460–473. doi: 10.1002/epi4.12277.

Dupret, D., Pleydell-Bouverie, B. e Csicsvari, J. (2008) "Inhibitory interneurons and network oscillations", *Proceedings of the National Academy of Sciences of the United States of America*, 105(47), p. 18079–18080. doi: 10.1073/pnas.0810064105.

Esclapez, M. *et al.* (1999) "Newly formed excitatory pathways provide a substrate for hyperexcitability in experimental temporal lobe epilepsy", *Journal of Comparative Neurology*, 408(4), p. 449–460. doi: 10.1002/(SICI)1096-9861(19990614)408:4<449::AID-CNE1>3.0.CO;2-R.

Espinosa-Jovel, C. *et al.* (2018) "Epidemiological profile of epilepsy in low income populations", *Seizure*, 56, p. 67–72. doi: 10.1016/j.seizure.2018.02.002.

Ewell, L. A. *et al.* (2019) "The impact of pathological high-frequency oscillations on hippocampal network activity in rats with chronic epilepsy", *eLife*, 8, p. 1–24. doi: 10.7554/eLife.42148.

Falco-Walter, J. J., Scheffer, I. E. e Fisher, R. S. (2018) "The new definition and classification of seizures and epilepsy", *Epilepsy Research*, 139(July 2017), p. 73–79. doi: 10.1016/j.eplepsyres.2017.11.015.

Fedele, T. *et al.* (2017) “Resection of high frequency oscillations predicts seizure outcome in the individual patient”, *Scientific Reports*, 7(1), p. 1–10. doi: 10.1038/s41598-017-13064-1.

Fiest, K. M. *et al.* (2017) “Prevalence and incidence of epilepsy: A systematic review and meta-analysis of international studies”, *Neurology*, 89(6), p. 641. doi: 10.1212/WNL.0000000000004205.

Fisher, R. S. *et al.* (2005) “Epileptic Seizures and Epilepsy: Definitions Proposed by the International League Against Epilepsy (ILAE) and the International Bureau for Epilepsy (IBE)”, *Epilepsia*, 46(10), p. 1701–1702. doi: 10.1111/j.1528-1167.2005.00273_4.x.

Fisher, R. S. *et al.* (2014) “ILAE Official Report: A practical clinical definition of epilepsy”, *Epilepsia*, 55(4), p. 475–482. doi: 10.1111/epi.12550.

Fisher, R. S. *et al.* (2017) “Operational classification of seizure types by the International League Against Epilepsy: Position Paper of the ILAE Commission for Classification and Terminology”, *Epilepsia*, 58(4), p. 522–530. doi: 10.1111/epi.13670.

Fisher, R. S., Scharfman, H. E. e deCurtis, M. (2014) “How Can We Identify Ictal and Interictal Abnormal Activity?”, p. 3–23. doi: 10.1007/978-94-017-8914-1_1.

Fries, P. (2005) “A mechanism for cognitive dynamics: Neuronal communication through neuronal coherence”, *Trends in Cognitive Sciences*, 9(10), p. 474–480. doi: 10.1016/j.tics.2005.08.011.

Fries, P. (2015) “Rhythms for Cognition: Communication through Coherence”, *Neuron*, 88(1), p. 220–235. doi: 10.1016/j.neuron.2015.09.034.

Fries, P., Nikolić, D. e Singer, W. (2007) “The gamma cycle”, *Trends in Neurosciences*, 30(7), p. 309–316. doi: 10.1016/j.tins.2007.05.005.

Fu, X. *et al.* (2018) “Negative effects of interictal spikes on theta rhythm in human temporal lobe epilepsy”, *Epilepsy & Behavior*, 87, p. 207–211. doi: 10.1016/j.yebeh.2018.07.014.Negative.

Fujiwara, H. *et al.* (2012) “Resection of ictal high-frequency oscillations leads to favorable surgical outcome in pediatric epilepsy”, *Epilepsia*, 53(9), p. 1607–1617. doi: 10.1111/j.1528-1167.2012.03629.x.

De Furtado, M. A. *et al.* (2002) “Behavioral, morphologic, and electroencephalographic evaluation of seizures induced by intrahippocampal microinjection of pilocarpine”, *Epilepsia*, 43(SUPPL. 5), p. 37–39. doi: 10.1046/j.1528-1157.2002.043s2037.x.

Gafurov, B. e Bausch, S. B. (2013) “GABAergic transmission facilitates ictogenesis and synchrony between CA3, hilus, and dentate gyrus in slices from epileptic rats”, *Journal of Neurophysiology*, 110(2), p. 441–455. doi: 10.1152/jn.00679.2012.

Galvan, M., Grafe, P. e Bruggencate, G. Ten (1982) “Convulsant actions of 4-aminopyridine on the guinea-pig olfactory cortex slice”, *Brain Research*, 241(1), p. 75–86. doi: 10.1016/0006-8993(82)91230-6.

Garrido Sanabria, E. R. *et al.* (2002) “Damage, reorganization, and abnormal neocortical hyperexcitability in the pilocarpine model of temporal lobe epilepsy”, *Epilepsia*, 43(SUPPL. 5), p. 96–106. doi: 10.1046/j.1528-1157.43.s.5.31.x.

Ge, M. *et al.* (2013) “Transient impact of spike on theta rhythm in temporal lobe epilepsy”, *Experimental Neurology*, 250, p. 136–142. doi: 10.1016/j.expneurol.2013.09.023.

Genovesi, S. *et al.* (2011) “GABAergic Dysfunction in Autism and Epilepsy”, in *Autism - A Neurodevelopmental Journey from Genes to Behaviour*. doi: 10.5772/17387.

Glaba, P. *et al.* (2020) “Changes in Interictal Pretreatment and Posttreatment EEG in

Childhood Absence Epilepsy", *Frontiers in Neuroscience*, 14(March), p. 1–9. doi: 10.3389/fnins.2020.00196.

Goddard, G. V. (1967) "Development of Epileptic Seizures through Brain Stimulation at Low Intensity", *Nature Publishing Group*, 214, p. 1020–1021.

Goldberg, E. M. e Coulter, D. A. (2013) "Mechanisms of epileptogenesis: A convergence on neural circuit dysfunction", *Nature Reviews Neuroscience*, 14(5), p. 337–349. doi: 10.1038/nrn3482.

Gonzalez-Sulser, A. *et al.* (2011) "The 4-aminopyridine in vitro epilepsy model analyzed with a perforated multi-electrode array", 60((7-8)), p. 1142–1153. doi: 10.1016/j.neuropharm.2010.10.007.THE.

González Otárula, K. A. e Schuele, S. (2020) "Networks in Temporal Lobe Epilepsy", *Neurosurgery Clinics of North America*, 31(3), p. 309–317. doi: 10.1016/j.nec.2020.02.001.

Gorter, J. A. e Lopes da Silva, F. H. (2002) "Abnormal plastic changes in a rat model for mesial temporal lobe epilepsy: A short review", *Progress in Brain Research*, 138, p. 61–72. doi: 10.1016/S0079-6123(02)38071-3.

Goutagny, R. *et al.* (2013) "Alterations in hippocampal network oscillations and theta-gamma coupling arise before Aβ overproduction in a mouse model of Alzheimer's disease", *European Journal of Neuroscience*, 37(12), p. 1896–1902. doi: 10.1111/ejn.12233.

Grasse, D. W., Karunakaran, S. e Moxon, K. A. (2013) "Neuronal synchrony and the transition to spontaneous seizures", *Experimental Neurology*, 248, p. 72–84. doi: 10.1016/j.expneurol.2013.05.004.

Greenfield, L. J. (2013) "Molecular mechanisms of antiseizure drug activity at GABAA

receptors”, *Seizure*, 22(8), p. 589–600. doi: 10.1016/j.seizure.2013.04.015.

Haas, C. A. *et al.* (2002) “Role for reelin in the development of granule cell dispersion in temporal lobe epilepsy”, *Journal of Neuroscience*, 22(14), p. 5797–5802. doi: 10.1523/jneurosci.22-14-05797.2002.

Hamidi, S. ., Lévesque, M. . e Avoli, M. (2014) “Epileptiform synchronization and high-frequency oscillations in brain slices comprising piriform and entorhinal cortices”, *Neuroscience*, 281, p. 258–268. doi: 10.1016/j.neuroscience.2014.09.065.

Hamilton, S. E. *et al.* (1997) “Disruption of the m1 receptor gene ablates muscarinic receptor-dependent M current regulation and seizure activity in mice”, *Proceedings of the National Academy of Sciences of the United States of America*, 94(24), p. 13311–13316. doi: 10.1073/pnas.94.24.13311.

Hammond, C. (2015) *The adult hippocampal network*. Fourth Edi, *Cellular and Molecular Neurophysiology: Fourth Edition*. Fourth Edi. Elsevier Ltd. doi: 10.1016/B978-0-12-397032-9.00019-4.

Hansen, S. L., Sperling, B. B. e Sánchez, C. (2004) “Anticonvulsant and antiepileptogenic effects of GABAA receptor ligands in pentylenetetrazole-kindled mice”, *Progress in Neuro-Psychopharmacology and Biological Psychiatry*, 28(1), p. 105–113. doi: 10.1016/j.pnpbp.2003.09.026.

Heinemann, U., Kann, O. e Schuchmann, S. (2006) “An Overview of In Vitro Seizure Models in Acute and Organotypic Slices”, in *Models of Seizures and Epilepsy*, p. 35–44.

Herweg, N. A., Solomon, E. A. e Kahana, M. J. (2020) “Theta Oscillations in Human Memory”, *Trends in Cognitive Sciences*, 24(3), p. 208–227. doi: 10.1016/j.tics.2019.12.006.

Heuzeroth, H. *et al.* (2019) “The 4-aminopyridine model of acute seizures in vitro elucidates efficacy of new antiepileptic drugs”, *Frontiers in Neuroscience*, 13(JUN), p. 1–12. doi: 10.3389/fnins.2019.00677.

Horwitz, B. (2003) “The elusive concept of brain connectivity”, *NeuroImage*, 19(2), p. 466–470. doi: 10.1016/S1053-8119(03)00112-5.

Hsu, D. (2007) “The dentate gyrus as a filter or gate: a look back and a look ahead”, *Progress in Brain Research*, 163, p. 601–613. doi: 10.1016/S0079-6123(07)63032-5.

Huberfeld, G. *et al.* (2011) “Distinct mechanisms mediate interictal and pre-ictal discharges in human temporal lobe epilepsy”, *Epilepsy Currents*, 11(6), p. 200–202. doi: 10.5698/1535-7511-11.6.200.

Hughes, J. R. (2008) “Gamma, fast, and ultrafast waves of the brain: Their relationships with epilepsy and behavior”, *Epilepsy and Behavior*, 13(1), p. 25–31. doi: 10.1016/j.yebeh.2008.01.011.

Hunt, R. F. e Baraban, S. C. (2015) “Interneuron transplantation as a treatment for epilepsy”, *Cold Spring Harbor Perspectives in Medicine*, 5(12). doi: 10.1101/cshperspect.a022376.

Igarashi, K. M. *et al.* (2014) “Coordination of entorhinal-hippocampal ensemble activity during associative learning”, *Nature*, 510(7503), p. 143–147. doi: 10.1038/nature13162.

Insausti, R. e Amaral, D. G. (2003) *Hippocampal Formation*. THIRD EDIT, *The Human Nervous System: Second Edition*. THIRD EDIT. Elsevier, Inc. doi: 10.1016/B978-012547626-3/50024-7.

Jacobs, J. *et al.* (2008) “Interictal high-frequency oscillations (80-500 Hz) are an indicator of seizure onset areas independent of spikes in the human epileptic brain”,

Epilepsia, 49(11), p. 1893–1907. doi: 10.1111/j.1528-1167.2008.01656.x.

Jacobs, J. *et al.* (2016) “The identification of distinct high-frequency oscillations during spikes delineates the seizure onset zone better than high-frequency spectral power changes”, *Clinical Neurophysiology*, 127(1), p. 129–142. doi: 10.1016/j.clinph.2015.04.053.

Jacobs, J. e Zijlmans, M. (2020) “HFO to Measure Seizure Propensity and Improve Prognostication in Patients With Epilepsy”, *Epilepsy Currents*, 20(6), p. 338–347. doi: 10.1177/1535759720957308.

Jacoby, A. (2008) “Epilepsy and stigma: An update and critical review”, *Current Neurology and Neuroscience Reports*, 8(4), p. 339–344. doi: 10.1007/s11910-008-0052-8.

Jahangir, M. *et al.* (2021) “GABAergic System Dysfunction and Challenges in Schizophrenia Research”, *Frontiers in Cell and Developmental Biology*, 9(May), p. 1–12. doi: 10.3389/fcell.2021.663854.

Janszky, J. *et al.* (2005) “Temporal lobe epilepsy with hippocampal sclerosis: Predictors for long-term surgical outcome”, *Brain*, 128(2), p. 395–404. doi: 10.1093/brain/awh358.

Jarero-Basulto, J. J. *et al.* (2018) “Interactions between epilepsy and plasticity”, *Pharmaceuticals*, 11(1), p. 1–18. doi: 10.3390/ph11010017.

Jefferys, J. G. R. *et al.* (2012) “Mechanisms of physiological and epileptic HFO generation”, *Progress in Neurobiology*, 98(3), p. 250–264. doi: 10.1016/j.pneurobio.2012.02.005.

Jiménez-Balado, J. e Eich, T. S. (2021) “GABAergic dysfunction, neural network hyperactivity and memory impairments in human aging and Alzheimer’s disease”,

Seminars in Cell and Developmental Biology, 116, p. 146–159. doi: 10.1016/j.semcdb.2021.01.005.

Jirsch, J. D. *et al.* (2006) “High-frequency oscillations during human focal seizures”, *Brain*, 129(6), p. 1593–1608. doi: 10.1093/brain/awl085.

Jiruska, P. *et al.* (2013) “Synchronization and desynchronization in epilepsy: Controversies and hypotheses”, *Journal of Physiology*, 591(4), p. 787–797. doi: 10.1113/jphysiol.2012.239590.

Jones, R. S. G. e Lambert, J. D. C. (1990) “The role of excitatory amino acid receptors in the propagation of epileptiform discharges from the entorhinal cortex to the dentate gyrus in vitro”, *Experimental Brain Research*, 80(2), p. 310–322. doi: 10.1007/BF00228158.

Kandel, E. *et al.* (2014) *Princípios de Neurociências*. 5º ed.

Kandratavicius, L. *et al.* (2014) “Animal models of epilepsy: use and limitations”, *Neuropsychiatric Disease and Treatment*, p. 1693–1705.

Kelly, T. e Beck, H. (2017) “Functional properties of granule cells with hilar basal dendrites in the epileptic dentate gyrus”, *Epilepsia*, 58(1), p. 160–171. doi: 10.1111/epi.13605.

Kepecs, A. e Fishell, G. (2014) “Interneuron cell types are fit to function”, *Nature*, 505(7483), p. 318–326. doi: 10.1038/nature12983.

Kerschensteiner, D. (2014) “Spontaneous network activity and synaptic development”, *Neuroscientist*, 20(3), p. 272–290. doi: 10.1177/1073858413510044.

Kessler, K., Seymour, R. A. e Rippon, G. (2016) “Brain oscillations and connectivity in autism spectrum disorders (ASD): new approaches to methodology, measurement

and modelling", *Neuroscience and Biobehavioral Reviews*, 71, p. 601–620. doi: 10.1016/j.neubiorev.2016.10.002.

Khazipov, R. *et al.* (2004) "Developmental changes in GABAergic actions and seizure susceptibility in the rat hippocampus", *European Journal of Neuroscience*, 19(3), p. 590–600. doi: 10.1111/j.0953-816X.2003.03152.x.

Khazipov, R. (2016) "GABAergic synchronization in epilepsy", *Cold Spring Harbor Perspectives in Medicine*, 6(2), p. 1–14. doi: 10.1101/cshperspect.a022764.

Khazipov, R. e Holmes, G. L. (2003) "Synchronization of kainate-induced epileptic activity via GABAergic inhibition in the superfused rat hippocampus in vivo", *Journal of Neuroscience*, 23(12), p. 5337–5341. doi: 10.1523/jneurosci.23-12-05337.2003.

Kilb, W. (2012) "Development of the GABAergic system from birth to adolescence", *Neuroscientist*, 18(6), p. 613–630. doi: 10.1177/1073858411422114.

Kitchigina, V. F. (2018) "Alterations of Coherent Theta and Gamma Network Oscillations as an Early Biomarker of Temporal Lobe Epilepsy and Alzheimer's Disease", *Frontiers in Integrative Neuroscience*, 12(August), p. 1–15. doi: 10.3389/fnint.2018.00036.

Kitchigina, V. F. e Butuzova, M. V. (2009) "Theta activity of septal neurons during different epileptic phases: The same frequency but different significance?", *Experimental Neurology*, 216(2), p. 449–458. doi: 10.1016/j.expneurol.2009.01.001.

Klausberger, T. e Somogyi, P. (2008) "Neuronal diversity and temporal dynamics: The unity of hippocampal circuit operations", *Science*, 321(5885), p. 53–57. doi: 10.1126/science.1149381.

Klimesch, W., Sauseng, P. e Hanslmayr, S. (2007) "EEG alpha oscillations: The inhibition-timing hypothesis", *Brain Research Reviews*, 53(1), p. 63–88. doi:

10.1016/j.brainresrev.2006.06.003.

Knyazev, G. G. (2012) “EEG delta oscillations as a correlate of basic homeostatic and motivational processes”, *Neuroscience and Biobehavioral Reviews*, 36(1), p. 677–695. doi: 10.1016/j.neubiorev.2011.10.002.

Kobayashi, M. e Buckmaster, P. S. (2003) “Reduced inhibition of dentate granule cells in a model of temporal lobe epilepsy”, *Journal of Neuroscience*, 23(6), p. 2440–2452. doi: 10.1523/jneurosci.23-06-02440.2003.

Köhling, R. *et al.* (2000) “Ictal epileptiform activity is facilitated by hippocampal GABA(A) receptor-mediated oscillations”, *Journal of Neuroscience*, 20(18), p. 6820–6829. doi: 10.1523/jneurosci.20-18-06820.2000.

Kramer, M. A. e Cash, S. S. (2012) “Epilepsy as a disorder of cortical network organization”, *Neuroscientist*, 18(4), p. 360–372. doi: 10.1177/1073858411422754.

Kucewicz, M. T. *et al.* (2014) “High frequency oscillations are associated with cognitive processing in human recognition memory”, *Brain*, 137(8), p. 2231–2244. doi: 10.1093/brain/awu149.

Lazzarotto, G. *et al.* (2021) “Effect of Memantine on Pentylenetetrazol-induced Seizures and EEG Profile in Animal Model of Cortical Malformation”, *Neuroscience*, 457, p. 114–124. doi: 10.1016/j.neuroscience.2020.12.039.

Ledri, M. *et al.* (2014) “Global optogenetic activation of inhibitory interneurons during epileptiform activity”, *Journal of Neuroscience*, 34(9), p. 3364–3377. doi: 10.1523/JNEUROSCI.2734-13.2014.

Lehmann, T. N. *et al.* (2000) “Alterations of neuronal connectivity in area CA1 of hippocampal slices from temporal lobe epilepsy patients and from pilocarpine-treated epileptic rats”, *Epilepsia*, 41(SUPPL. 6), p. 190–194. doi: 10.1111/j.1528-

1157.2000.tb01580.x.

Leite, J. P., Garcia-Cairasco, N. e Cavalheiro, E. A. (2002) “New insights from the use of pilocarpine and kainate models”, *Epilepsy Research*, 50(1–2), p. 93–103. Available at: http://ovidsp.ovid.com/ovidweb.cgi?T=JS&PAGE=reference&D=emed5&NEWS=N&AN=2002288054.

Lévesque;, M. e Avoli, M. (2013) “The kainic acid models of temporal lobe epilepsy”, *Neurosci Biobehav Rev.*, 37(2), p. 2887–2899. doi: 10.1523/ENEURO.0337-20.2021.

Lévesque, M. *et al.* (2011) “High-frequency (80-500Hz) oscillations and epileptogenesis in temporal lobe epilepsy”, *Neurobiology of Disease*, 42(3), p. 231–241. doi: 10.1016/j.nbd.2011.01.007.

Lévesque, M. *et al.* (2012) “Two seizure-onset types reveal specific patterns of high-frequency oscillations in a model of temporal lobe epilepsy”, *Journal of Neuroscience*, 32(38), p. 13264–13272. doi: 10.1523/JNEUROSCI.5086-11.2012.

Lévesque, M. *et al.* (2017) “High-frequency oscillations and mesial temporal lobe epilepsy”, *Neuroscience Letters*, 667, p. 66–74. doi: 10.1016/j.neulet.2017.01.047.

Lévesque, M., Shiri, Z., *et al.* (2018) “High-frequency oscillations and mesial temporal lobe epilepsy”, *Neuroscience Letters*, 667, p. 66–74. doi: 10.1016/j.neulet.2017.01.047.

Lévesque, M., Salami, P., *et al.* (2018) “Interictal oscillations and focal epileptic disorders”, *European Journal of Neuroscience*, 48(8), p. 2915–2927. doi: 10.1111/ejn.13628.

Lévesque, M. e Avoli, M. (2021) “The subiculum and its role in focal epileptic disorders”, *Reviews in the Neurosciences*, 32(3), p. 249–273. doi: 10.1515/revneuro-

2020-0091.

Lévesque, M., Avoli, M. e Bernard, C. (2016) “Animal models of temporal lobe epilepsy following systemic chemoconvulsant administration”, *Journal of Neuroscience Methods*, 260, p. 45–52. doi: 10.1016/j.jneumeth.2015.03.009.

Lévesque, M., Behr, C. e Avoli, M. (2015) “The anti-ictogenic effects of levetiracetam are mirrored by interictal spiking and high-frequency oscillation changes in a model of temporal lobe epilepsy”, *Seizure*, 25, p. 18–25. doi: 10.1016/j.seizure.2014.11.008.

Levira, F. *et al.* (2017) “Premature mortality of epilepsy in low- and middle-income countries: A systematic review from the Mortality Task Force of the International League Against Epilepsy”, *Epilepsia*, 58(1), p. 6–16. doi: 10.1111/epi.13603.

Lisgaras, C. P., Mikroulis, A. e Psarropoulou, C. (2021) “Region-specific Effects of Early-life Status Epilepticus on the Adult Hippocampal CA3 – Medial Entorhinal Cortex Circuitry In vitro: Focus on Interictal Spikes and Concurrent High-frequency Oscillations”, *Neuroscience*, 466, p. 235–247. doi: 10.1016/j.neuroscience.2021.04.030.

Liu, J. S. *et al.* (2013) “Spatiotemporal dynamics of high-K+-induced epileptiform discharges in hippocampal slice and the effects of valproate”, *Neuroscience Bulletin*, 29(1), p. 28–36. doi: 10.1007/s12264-013-1304-4.

Liu, Y. Q. *et al.* (2014) “Dysfunction of hippocampal interneurons in epilepsy”, *Neuroscience Bulletin*, 30(6), p. 985–998. doi: 10.1007/s12264-014-1478-4.

Luhmann, H. J., Fukuda, A. e Kilb, W. (2015) “Control of cortical neuronal migration by glutamate and GABA”, *Frontiers in Cellular Neuroscience*, 9(JAN), p. 1–15. doi: 10.3389/fncel.2015.00004.

Lybrand, Z. R. *et al.* (2021) “A critical period of neuronal activity results in aberrant

neurogenesis rewiring hippocampal circuitry in a mouse model of epilepsy", *Nature Communications*, (2021), p. 1–14. Available at: http://dx.doi.org/10.1038/s41467-021-21649-8.

Magloire, V. *et al.* (2019) "GABAergic Interneurons in Seizures: Investigating Causality With Optogenetics", *Neuroscientist*, 25(4), p. 344–358. doi: 10.1177/1073858418805002.

Malkov, A. E. *et al.* (2021) "Rhythmic Activity in the Hippocampus and Entorhinal Cortex is Impaired in a Model of Kainate Neurotoxicity in Rats in Free Behavior", *Neuroscience and Behavioral Physiology*, 51(1), p. 73–84. doi: 10.1007/s11055-020-01041-7.

Manford, M. (2017) "Recent advances in epilepsy", *Journal of Neurology*, 264(8), p. 1811–1824. doi: 10.1007/s00415-017-8394-2.

Maslanski, J. A. *et al.* (1994) "Assessment of the muscarinic receptor subtypes involved in pilocarpine-induced seizures in mice", *Neuroscience Letters*, 168(1–2), p. 225–228. doi: 10.1016/0304-3940(94)90456-1.

Mathalon, D. H. e Sohal, V. S. (2015) "Neural oscillations and synchrony in brain dysfunction and neuropsychiatric disorders it's about time", *JAMA Psychiatry*, 72(8), p. 840–844. doi: 10.1001/jamapsychiatry.2015.0483.

Matsumoto, A. *et al.* (2013) "Pathological and physiological high-frequency oscillations in focal human epilepsy", *Journal of Neurophysiology*, 110(8), p. 1958–1964. doi: 10.1152/jn.00341.2013.

Mcintyre, D. C. e Gilby, K. L. (2010) "Atlas of Epilepsies", *Atlas of Epilepsies*. doi: 10.1007/978-1-84882-128-6.

Merino, P (2019) "The GABAergic System", in Merino, Pedro (org.) *Chemical Biology*

of Neurodegeneration: A Molecular Approach. 1º ed, p. 199–226. doi: 10.1002/9783527813421.ch6.

Miles, R. *et al.* (1996) “Differences between Somatic and Dendritic Inhibition in the Hippocampus”, *Neuron*, 16, p. 815–823.

Molony, C. e Parmelee, A. H. (1954) “Vitamin B6: Vitamin B6 deficiency”, p. 405–406. Available at: https://ods.od.nih.gov/factsheets/VitaminB6-HealthProfessional/.

Mula, M. (2011) “GABAergic drugs in the treatment of epilepsy: Modern or outmoded?”, *Future Medicinal Chemistry*, 3(2), p. 177–182. doi: 10.4155/fmc.10.296.

Nadler, J. V., Perry, B. W. . e Cotman, C. W. (1978) “Intraventricular kainic acid preferentially destroys hippocampal pyramidal cells.pdf”, p. 676–677. doi: 10.1038/271676a0.

Nagao, T., Massimo, A. e Gloor, P. (1994) “Interictal discharges in the hippocampus of rats with long-term pilocarpine seizures”, 174, p. 160–164.

Nakahara, S. *et al.* (2018) “Hippocampal Pathophysiology: Commonality Shared by Temporal Lobe Epilepsy and Psychiatric Disorders”, *Neuroscience Journal*, 2018, p. 1–9. doi: 10.1155/2018/4852359.

Navidhamidi, M., Ghasemi, M. e Mehranfard, N. (2017) “Epilepsy-associated alterations in hippocampal excitability”, *Reviews in the Neurosciences*, 28(3), p. 307–334. doi: 10.1515/revneuro-2016-0059.

Nelson, E. M. (1956) “Association of vitamin B6 deficiency with convulsions in infants.”, *Public health reports*, 71(5), p. 445–448. doi: 10.2307/4589435.

Ngugi, A. K. *et al.* (2010) “Estimation of the burden of active and life-time epilepsy: A meta-analytic approach”, *Epilepsia*, 51(5), p. 883–890. doi: 10.1111/j.1528-

1167.2009.02481.x.

Ngugi, A. K. *et al.* (2011) “Incidence of epilepsy: A systematic review and meta-analysis”, *Neurology*, 77(10), p. 1005–1012. doi: 10.1212/WNL.0b013e31822cfc90.

Nina, B. *et al.* (2014) “Slowing of EEG background activity in Parkinson’s and Alzheimer’s disease with early cognitive dysfunction”, *Frontiers in Aging Neuroscience*, 6(OCT), p. 1–6. doi: 10.3389/fnagi.2014.00314.

Nirwan, N., Vyas, P. e Vohora, D. (2018) “Animal models of status epilepticus and temporal lobe epilepsy: A narrative review”, *Reviews in the Neurosciences*, 29(7), p. 757–770. doi: 10.1515/revneuro-2017-0086.

Noebels, J. L. *et al.* (2012) *Jasper ’ s Basic Mechanisms of the Epilepsies Jasper ’ s Basic Mechanisms of the Epilepsies Jasper ’ s Basic Mechanisms of the Epilepsies Jasper ’ s Basic Mechanisms of the Epilepsies*. 4th ed. Organizado por J. L. Noebels et al.

O’Mara, S. (2005) “The subiculum: What it does, what it might do, and what neuroanatomy has yet to tell us”, *Journal of Anatomy*, 207(3), p. 271–282. doi: 10.1111/j.1469-7580.2005.00446.x.

Olejniczak, P. (2006) “Neurophysiologic Basis of EEG”, *J Clin Neurophysiol*, 23(3), p. 186–189.

Panuccio, G. *et al.* (2010) “In vitro ictogenesis and parahippocampal networks in a rodent model of temporal lobe epilepsy”, *Neurobiology of Disease*, 39(3), p. 372–380. doi: 10.1016/j.nbd.2010.05.003.

Paschen, E. *et al.* (2020) “Hippocampal low-frequency stimulation prevents seizure generation in a mouse model of mesial temporal lobe epilepsy”, *eLife*, 9, p. 1–57. doi: 10.7554/ELIFE.54518.

Pasquetti, M. V. *et al.* (2019) “Hippocampal CA1 and cortical interictal oscillations in the pilocarpine model of epilepsy”, *Brain Research*, 1722. doi: 10.1016/j.brainres.2019.146351.

Pearce, A. *et al.* (2013) “Temporal changes of neocortical high-frequency oscillations in epilepsy”, *Journal of Neurophysiology*, 110(5), p. 1167–1179. doi: 10.1152/jn.01009.2012.

Percie Du Sert, N. *et al.* (2020) “The ARRIVE guidelines 2.0: Updated guidelines for reporting animal research”, *BMC Veterinary Research*, 16(1), p. 1–7. doi: 10.1186/s12917-020-02451-y.

Perreault, P. e Avoli, M. (1991) “Physiology and pharmacology of epileptiform activity induced by 4-aminopyridine in rat hippocampal slices”, *Journal of Neurophysiology*, 65(4), p. 771–785. doi: 10.1152/jn.1991.65.4.771.

Pitkänen, A. *et al.* (2005) “Administration of diazepam during status epilepticus reduces development and severity of epilepsy in rat”, *Epilepsy Research*, 63(1), p. 27–42. doi: 10.1016/j.eplepsyres.2004.10.003.

Pitkänen, A. (2010) “Therapeutic approaches to epileptogenesis - Hope on the horizon”, *Epilepsia*, 51(SUPPL. 3), p. 2–17. doi: 10.1111/j.1528-1167.2010.02602.x.

Pitkänen, A. *et al.* (2016) “Advances in the development of biomarkers for epilepsy”, *The Lancet Neurology*, 15(8), p. 843–856. doi: 10.1016/S1474-4422(16)00112-5.

Pitkänen, A. e Sutula, T. P. (2002) “Is epilepsy a progressive disorder? Prospects for new therapeutic approaches in temporal-lobe epilepsy”, *Lancet Neurology*, 1(3), p. 173–181. doi: 10.1016/S1474-4422(02)00073-X.

Purves, D. *et al.* (2010) *Neurociências | 4ª Edição*. 4º ed.

Quilichini, P. P. *et al.* (2012) “Hub GABA neurons mediate gamma-frequency oscillations at ictal-like event onset in the immature hippocampus”, *Bone*, 74(1), p. 57–64. doi: 10.1016/j.neuron.2012.01.026.Hub.

Racine, R. J. (1972) “MODIFICATION OF SEIZURE ACTIVITY BY ELECTRICAL Modification of after-discharge”, *Electroencephalography and Clinical Neurophysiology*, 32, p. 281–294.

Racine, R. J., Gartner, J. G. e McIntyre Burnham, W. (1972) “Epileptiform activity and neural plasticity in limbic structures”, *Brain Research*, 47(1), p. 262–268. doi: 10.1016/0006-8993(72)90268-5.

Ren, H. *et al.* (2014) “The role of the entorhinal cortex in epileptiform activities of the hippocampus”, *Theoretical Biology and Medical Modelling*, 11(1), p. 1–22. doi: 10.1186/1742-4682-11-14.

Ren, L. *et al.* (2015) “Gamma oscillations precede interictal epileptiform spikes in the seizure onset zone”, *Neurology*, 84(6), p. 602–608. doi: 10.1212/WNL.0000000000001234.

Reschke, C. R. *et al.* (2018) “Systemic delivery of selective EP1 and EP3 receptor antagonists attenuates pentylenetetrazole-induced seizures in mice.”, *International journal of physiology, pathophysiology and pharmacology*, 10(1), p. 47–59. Available at: http://www.ncbi.nlm.nih.gov/pubmed/29593850%0Ahttp://www.pubmedcentral.nih.gov/articlerender.fcgi?artid=PMC5871629.

Reyes-Garcia, S. Z. *et al.* (2018) “Different patterns of epileptiform-like activity are generated in the sclerotic hippocampus from patients with drug-resistant temporal lobe epilepsy”, *Scientific Reports*, 8(1), p. 1–15. doi: 10.1038/s41598-018-25378-9.

Riban, V. *et al.* (2002) “Evolution of hippocampal epileptic activity during the development of hippocampal sclerosis in a mouse model of temporal lobe epilepsy”, *Neuroscience*, 112(1), p. 101–111. doi: 10.1016/S0306-4522(02)00064-7.

Richardson, R. M. *et al.* (2008) “Developing cell transplantation for temporal lobe epilepsy”, *Neurosurgical Focus*, 24(3–4), p. 1–8. doi: 10.3171/FOC/2008/24/3-4/E15.

Righes Marafiga, J., Vendramin Pasquetti, M. e Calcagnotto, M. E. (2020) “GABAergic interneurons in epilepsy: More than a simple change in inhibition”, *Epilepsy and Behavior*. doi: 10.1016/j.yebeh.2020.106935.

Roach, B. J. e Mathalon, D. H. (2008) “Event-related EEG time-frequency analysis: An overview of measures and an analysis of early gamma band phase locking in schizophrenia”, *Schizophrenia Bulletin*, 34(5), p. 907–926. doi: 10.1093/schbul/sbn093.

Rosati, A. *et al.* (2003) “Intractable temporal lobe epilepsy with rare spikes is less severe than with frequent spikes”, *Neurology*, 60(8), p. 1290–1295. doi: 10.1212/01.WNL.0000058761.12715.0E.

Royer, S. *et al.* (2012) “Control of timing, rate and bursts of hippocampal place cells by dendritic and somatic inhibition”, *Nature Neuroscience*, 15(5), p. 769–775. doi: 10.1038/nn.3077.

Rutecki, P. A., Lebeda, F. J. e Johnston, D. (1987) “4-Aminopyridine produces epileptiform activity in hippocampus and enhances synaptic excitation and inhibition”, *Journal of Neurophysiology*, 57(6), p. 1911–1924. doi: 10.1152/jn.1987.57.6.1911.

Salami, P., Lévesque, M., *et al.* (2014) “Dynamics of interictal spikes and high-frequency oscillations during epileptogenesis in temporal lobe epilepsy”, *Neurobiology of Disease*, 67, p. 97–106. doi: 10.1016/j.nbd.2014.03.012.

Salami, P., Levesque, M., *et al.* (2014) “Dynamics of interictal spikes and high-frequency oscillations during epileptogenesis in temporal lobe epilepsy”, *Epilepsia*, 54, p. 52. doi: 10.1016/j.nbd.2014.03.012.Dynamics.

Salami, P. *et al.* (2015) “Distinct EEG seizure patterns reflect different seizure generation mechanisms”, *Journal of Neurophysiology*, 113(7), p. 2840–2844. doi: 10.1152/jn.00031.2015.

Sato, Y. *et al.* (2017) “Spatiotemporal changes in regularity of gamma oscillations contribute to focal ictogenesis”, *Scientific Reports*, 7(1), p. 1–9. doi: 10.1038/s41598-017-09931-6.

Savanthrapadian, S. *et al.* (2014) “Synaptic properties of SOM-and CCK-expressing cells in dentate gyrus interneuron networks”, *Journal of Neuroscience*, 34(24), p. 8197–8209. doi: 10.1523/JNEUROSCI.5433-13.2014.

Scharfman, H. E. (2007) “The neurobiology of epilepsy”, *Current Neurology and Neuroscience Reports*, 7(4), p. 348–354. doi: 10.1007/s11910-007-0053-z.

Scharfman, H. E. (2019) “The Dentate Gyrus and Temporal Lobe Epilepsy: An ‘Exciting’ Era”, *Epilepsy Currents*, 19(4), p. 249–255. doi: 10.1177/1535759719855952.

Scheffer-Teixeira, R. e Tort, A. B. L. (2017) “Unveiling fast field oscillations through comodulation”, *eNeuro*, 4(4). doi: 10.1523/ENEURO.0079-17.2017.

Scheffer, I. E. *et al.* (2017) “ILAE classification of the epilepsies: Position paper of the ILAE Commission for Classification and Terminology”, *Epilepsia*, 58(4), p. 512–521. doi: 10.1111/epi.13709.

Scheffzük, C. *et al.* (2013) “Global slowing of network oscillations in mouse neocortex by diazepam”, *Neuropharmacology*, 65, p. 123–133. doi:

10.1016/j.neuropharm.2012.09.014.

Schevon, C. A. *et al.* (2009) “Spatial characterization of interictal high frequency oscillations in epileptic neocortex”, *Brain*, 132(11), p. 3047–3059. doi: 10.1093/brain/awp222.

Schmidt, R. *et al.* (2019) “Beta oscillations in working memory, executive control of movement and thought, and sensorimotor function”, *Journal of Neuroscience*, 39(42), p. 8231–8238. doi: 10.1523/JNEUROSCI.1163-19.2019.

Schultz, C. e Engelhardt, M. (2014) “Anatomy of the hippocampal formation”, *The Hippocampus in Clinical Neuroscience*, 34, p. 6–17. doi: 10.1159/000360925.

Schultz, H., Sommer, T. e Peters, J. (2015) “The role of the human entorhinal cortex in a representational account of memory”, *Frontiers in Human Neuroscience*, 9(NOVEMBER), p. 1–8. doi: 10.3389/fnhum.2015.00628.

Scorza, F. A. *et al.* (2009) “The pilocarpine model of epilepsy: What have we learned?”, *Anais da Academia Brasileira de Ciencias*, 81(3), p. 345–365. doi: 10.1590/S0001-37652009000300003.

Shah, P. *et al.* (2019) “High interictal connectivity within the resection zone is associated with favorable post-surgical outcomes in focal epilepsy patients”, *NeuroImage: Clinical*, 23(April), p. 101908. doi: 10.1016/j.nicl.2019.101908.

Sharma, A. K. *et al.* (2007) “Mesial temporal lobe epilepsy: Pathogenesis, induced rodent models and lesions”, *Toxicologic Pathology*, 35(7), p. 984–999. doi: 10.1080/01926230701748305.

Shorvon, S. D. (2011) “The etiologic classification of epilepsy”, *Epilepsia*, 52(6), p. 1052–1057. doi: 10.1111/j.1528-1167.2011.03041.x.

Singh, A. e Trevick, S. (2016) “The Epidemiology of Global Epilepsy”, *Neurologic Clinics*, 34(4), p. 837–847. doi: 10.1016/j.ncl.2016.06.015.

Sirven, J. I. (2015) “Epilepsy: A Spectrum Disorder”, *Cold Spring Harbor perspectives in medicine*, 5(9), p. a022848. doi: 10.1101/cshperspect.a022848.

Sloviter, R. S. (1987) “Decreased hippocampal inhibition and a selective loss of interneurons in experimental epilepsy”, *Science*, 235(4784), p. 73–76. doi: 10.1126/science.2879352.

Sloviter, R. S. (2008) “Hippocampal epileptogenesis in animal models of mesial temporal lobe epilepsy with hippocampal sclerosis: The importance of the ‘latent period’ and other concepts”, *Epilepsia*, 49(SUPPL. 9), p. 85–92. doi: 10.1111/j.1528-1167.2008.01931.x.

Smith, B. N. e Dudek, F. E. (2001) “Short- and long-term changes in CA1 network excitability after kainate treatment in rats”, *Journal of Neurophysiology*, 85(1), p. 1–9. doi: 10.1152/jn.2001.85.1.1.

Sorokin, J. M., Paz, J. T. e Huguenard, J. R. (2016) “Absence seizure susceptibility correlates with pre-ictal β oscillations”, 110, p. 372–381. doi: 10.1016/j.jphysparis.2017.05.004.Absence.

Sparks, F. T. *et al.* (2020) “Hippocampal adult-born granule cells drive network activity in a mouse model of chronic temporal lobe epilepsy”, *Nature communications*, 11(1), p. 6138. doi: 10.1038/s41467-020-19969-2.

Spatazza, J., Mancia Leon, W. e Alvarez-Buylla, A. (2017) “Transplantation of GABAergic interneurons for cell-based therapy”, *Physiology & behavior*, 176(1), p. 100–106. doi: 10.1016/bs.pbr.2016.11.005.Transplantation.

Staba, R. J. *et al.* (2002) “Quantitative analysis of high-frequency oscillations (80-500

Hz) recorded in human epileptic hippocampus and entorhinal cortex", *Journal of Neurophysiology*, 88(4), p. 1743–1752. doi: 10.1152/jn.2002.88.4.1743.

Staba, R. J. *et al.* (2017) *Oscillatory activity: Neuronal networks generating pathological high frequency oscillations*, *The Curated Reference Collection in Neuroscience and Biobehavioral Psychology*. Elsevier. doi: 10.1016/B978-0-12-809324-5.00171-1.

Staba, R. J., Stead, M. e Worrell, G. A. (2014) "Electrophysiological Biomarkers of Epilepsy", *Neurotherapeutics*, 11(2), p. 334–346. doi: 10.1007/s13311-014-0259-0.

Subramanian, D. *et al.* (2018) "Gamma oscillatory activity in vitro: A model system to assess pathophysiological mechanisms of comorbidity between autism and epilepsy", *Translational Psychiatry*, 8(1). doi: 10.1038/s41398-017-0065-7.

Sutula, T. *et al.* (1989) "Mossy fiber synaptic reorganization in the epileptic human temporal lobe", *Annals of Neurology*, 26(3), p. 321–330. doi: 10.1002/ana.410260303.

Takeuchi, Y. e Berényi, A. (2020) "Oscillotherapeutics – Time-targeted interventions in epilepsy and beyond", *Neuroscience Research*, 152, p. 87–107. doi: 10.1016/j.neures.2020.01.002.

Tang, X., Jaenisch, R. e Sur, M. (2021) "The role of GABAergic signalling in neurodevelopmental disorders", *Nature Reviews Neuroscience*, 22(5), p. 290–307. doi: 10.1038/s41583-021-00443-x.

Thijs, R. D. *et al.* (2019) "Epilepsy in adults", *The Lancet*, 393(10172), p. 689–701. doi: 10.1016/S0140-6736(18)32596-0.

Thom, M. (2014) "Review: Hippocampal sclerosis in epilepsy: A neuropathology review", *Neuropathology and Applied Neurobiology*, 40(5), p. 520–543. doi: 10.1111/nan.12150.

Thomschewski, A., Hincapié, A. S. e Frauscher, B. (2019) “Localization of the epileptogenic zone using high frequency oscillations”, *Frontiers in Neurology*, 10(FEB). doi: 10.3389/fneur.2019.00094.

Thurman, D. J. *et al.* (2011) “Standards for epidemiologic studies and surveillance of epilepsy”, *Epilepsia*, 52(SUPPL. 7), p. 2–26. doi: 10.1111/j.1528-1167.2011.03121.x.

Tolner, E. A. *et al.* (2007) “Synaptic responses in superficial layers of medial entorhinal cortex from rats with kainate-induced epilepsy”, *Neurobiology of Disease*, 26(2), p. 419–438. doi: 10.1016/j.nbd.2007.01.009.

Tomson, T., Nashef, L. e Ryvlin, P. (2008) “Sudden unexpected death in epilepsy: current knowledge and future directions”, *The Lancet Neurology*, 7(11), p. 1021–1031. doi: 10.1016/S1474-4422(08)70202-3.

Tort, A. B. L. *et al.* (2013) “Theta-associated high-frequency oscillations (110-160Hz) in the hippocampus and neocortex”, *Progress in Neurobiology*, 100(1), p. 1–14. doi: 10.1016/j.pneurobio.2012.09.002.

Toyoda, I. *et al.* (2013) “Early activation of ventral hippocampus and subiculum during spontaneous seizures in a rat model of temporal lobe epilepsy”, *Journal of Neuroscience*, 33(27), p. 11100–11115. doi: 10.1523/JNEUROSCI.0472-13.2013.

Traub, R. D. *et al.* (1996) “Analysis of gamma rhythms in the rat hippocampus in vitro and in vivo”, *Journal of Physiology*, 493(2), p. 471–484. doi: 10.1113/jphysiol.1996.sp021397.

Traub, R. D. *et al.* (2004) “Cellular mechanisms of neuronal population oscillations in the hippocampus in vitro”, *Annual Review of Neuroscience*, 27, p. 247–278. doi: 10.1146/annurev.neuro.27.070203.144303.

Traub, R. D. ., Colling, S. B. . e Jefferys, J. G. (1995) “Cellular mechanisms of 4-

aminopyridine-induced synchronized after-discharges in the rat hippocampal slice.”, *The Journal of Physiology*, 489(1), p. 127–140. doi: 10.1113/jphysiol.1995.sp021036.

Treiman, D. M. (2001) “GABAergic mechanisms in epilepsy”, *Epilepsia*, 42(SUPPL. 3), p. 8–12. doi: 10.1046/j.1528-1157.2001.042Suppl.3008.x.

Trevelyan, A. J. e Schevon, C. A. (2013) “How inhibition influences seizure propagation”, *Neuropharmacology*, 69, p. 45–54. doi: 10.1016/j.neuropharm.2012.06.015.

Turski, W. A. *et al.* (1983) “Limbic seizures produced by pilocarpine in rats: Behavioural, electroencephalographic and neuropathological study”, *Behavioural Brain Research*, 9(3), p. 315–335. doi: 10.1016/0166-4328(83)90136-5.

Uhlhaas, P. J. *et al.* (2010) “Neural synchrony and the development of cortical networks”, *Trends in Cognitive Sciences*, 14(2), p. 72–80. doi: 10.1016/j.tics.2009.12.002.

Uhlhaas, P. J. e Singer, W. (2006) “Neural Synchrony in Brain Disorders: Relevance for Cognitive Dysfunctions and Pathophysiology”, *Neuron*, 52(1), p. 155–168. doi: 10.1016/j.neuron.2006.09.020.

Uhlhaas, P. J. e Singer, W. (2010) “Abnormal neural oscillations and synchrony in schizophrenia”, *Nature Reviews Neuroscience*, 11(2), p. 100–113. doi: 10.1038/nrn2774.

Uva, L. *et al.* (2005) “Propagation dynamics of epileptiform activity acutely induced by bicuculline in the hippocampal-parahippocampal region of the isolated guinea pig brain”, *Epilepsia*, 46(12), p. 1914–1925. doi: 10.1111/j.1528-1167.2005.00342.x.

Uva, L. *et al.* (2017) “High-frequency oscillations and seizure-like discharges in the entorhinal cortex of the in vitro isolated guinea pig brain”, *Epilepsy Research*, 130, p.

21–26. doi: 10.1016/j.eplepsyres.2017.01.001.

Vendramin Pasquetti, M. *et al.* (2017) “Impairment of GABAergic system contributes to epileptogenesis in glutaric acidemia type I”, *Epilepsia*, 58(10), p. 1771–1781. doi: 10.1111/epi.13862.

Voskuyl, R. A. e Albus, H. (1985) “Spontaneous epileptiform discharges in hippocampal slices induced by 4-aminopyridine”, *Brain Research*, 342(1), p. 54–66. doi: 10.1016/0006-8993(85)91352-6.

Walker, M. C. (2015) “Hippocampal sclerosis: Causes and prevention”, *Seminars in Neurology*, 35(3), p. 193–200. doi: 10.1055/s-0035-1552618.

Walther, H. *et al.* (1986) “Epileptiform activity in combined slices of the hippocampus, subiculum and entorhinal cortex during perfusion with low magnesium medium”, *Neuroscience Letters*, 69(2), p. 156–161. doi: 10.1016/0304-3940(86)90595-1.

Wang, J. *et al.* (2013) “Resting state EEG abnormalities in autism spectrum disorders”, *Journal of Neurodevelopmental Disorders*, 5(1), p. 1–14. doi: 10.1186/1866-1955-5-24.

Ward, L. M. (2003) “Synchronous neural oscillations and cognitive processes”, *Trends in Cognitive Sciences*, 7(12), p. 553–559. doi: 10.1016/j.tics.2003.10.012.

Warren, C. P. *et al.* (2010) “Synchrony in normal and focal epileptic brain: The seizure onset zone is functionally disconnected”, *Journal of Neurophysiology*, 104(6), p. 3530–3539. doi: 10.1152/jn.00368.2010.

Weiss, S. A. *et al.* (2016) “Ictal onset patterns of local field potentials, high frequency oscillations, and unit activity in human mesial temporal lobe epilepsy”, *Epilepsia*, 57(1), p. 111–121. doi: 10.1111/epi.13251.

Wendling, F. *et al.* (2002) “Epileptic fast activity can be explained by a model of impaired GABAergic dendritic inhibition”, *European Journal of Neuroscience*, 15(9), p. 1499–1508. doi: 10.1046/j.1460-9568.2002.01985.x.

Whittington, M. A. *et al.* (1997) “Recurrent excitatory postsynaptic potentials induced by synchronized fast cortical oscillations”, *Proceedings of the National Academy of Sciences of the United States of America*, 94(22), p. 12198–12203. doi: 10.1073/pnas.94.22.12198.

Witter, M. P. *et al.* (2000) “Anatomical organization of the parahippocampal-hippocampal network”, *Annals of the New York Academy of Sciences*, 911, p. 1–24. doi: 10.1111/j.1749-6632.2000.tb06716.x.

Witter, M. P. e Amaral, D. G. (2004) *Hippocampal Formation*. Second Edi, *The Rat Nervous System*. Second Edi. Elsevier Inc. doi: 10.1016/B978-012547638-6/50022-5.

Worrell, G. A. *et al.* (2008) “High-frequency oscillations in human temporal lobe: Simultaneous microwire and clinical macroelectrode recordings”, *Brain*, 131(4), p. 928–937. doi: 10.1093/brain/awn006.

Wu, C. e Sun, D. (2015) “GABA receptors in brain development, function, and injury”, *Metabolic Brain Disease*, 30(2), p. 367–379. doi: 10.1007/s11011-014-9560-1.

Wu, Z. Z. *et al.* (2009) “Aminopyridines potentiate synaptic and neuromuscular transmission by targeting the voltage-activated calcium channel β subunit”, *Journal of Biological Chemistry*, 284(52), p. 36453–36461. doi: 10.1074/jbc.M109.075523.

Yaari, Y. e Beck, H. (2002) “‘Epileptic neurons’ in temporal lobe epilepsy”, *Brain Pathology*, 12(2), p. 234–239. doi: 10.1111/j.1750-3639.2002.tb00438.x.

Yamamoto, C. (1972) “Intracellular study of seizure-like afterdischarges elicited in thin hippocampal sections in vitro”, *Experimental Neurology*, 35(1), p. 154–164. doi:

10.1016/0014-4886(72)90066-0.

Yener, G. G. e Basar, E. (2013) “Brain oscillations as biomarkers in neuropsychiatric disorders: Following an interactive panel discussion and synopsis”, *Supplements to Clinical Neurophysiology*, 62, p. 343–363. doi: 10.1016/B978-0-7020-5307-8.00016-8.

Zaitsev, A. V. (2017) “The Role of GABAergic Interneurons in the Cortex and Hippocampus in the Development of Epilepsy”, *Neuroscience and Behavioral Physiology*, 47(8), p. 913–922. doi: 10.1007/s11055-017-0491-2.

Zandt, M. A. Van e Naegele, J. R. (2017) “GABAergic Synapse Dysfunction and Repair in Temporal Lobe Epilepsy”, *Synaptic Plasticity*. doi: 10.5772/67218.

Zhang, L., Fan, D. e Wang, Q. (2017) “Transition dynamics of a dentate gyrus-CA3 neuronal network during temporal lobe epilepsy”, *Frontiers in Computational Neuroscience*, 11(July), p. 1–14. doi: 10.3389/fncom.2017.00061.

Zhang, W. *et al.* (2009) “Surviving hilar somatostatin interneurons enlarge, sprout axons, and form new synapses with granule cells in a mouse model of temporal lobe epilepsy”, *Journal of Neuroscience*, 29(45), p. 14247–14256. doi: 10.1523/JNEUROSCI.3842-09.2009.

Zhang, W. *et al.* (2021) “The Role of the GABAergic System in Diseases of the Central Nervous System”, *Neuroscience*, 470, p. 88–99. doi: 10.1016/j.neuroscience.2021.06.037.

Zhang, Y. F. *et al.* (2014) “Pilocarpine-induced epilepsy is associated with actin cytoskeleton reorganization in the mossy fiber-CA3 synapses”, *Epilepsy Research*, 108(3), p. 379–389. doi: 10.1016/j.eplepsyres.2014.01.016.

Zijlmans, M. *et al.* (2011) “Ictal and interictal high frequency oscillations in patients with

focal epilepsy", *Clinical Neurophysiology*, 122(4), p. 664–671. doi: 10.1016/j.clinph.2010.09.021.

Zijlmans, M. *et al.* (2012) "High-frequency oscillations as a new biomarker in epilepsy", *Annals of Neurology*, 71(2), p. 169–178. doi: 10.1002/ana.22548.

ANEXO 1 Carta de Aprovação do Comitê de Ética no Uso de Animais

U F R G S
UNIVERSIDADE FEDERAL
DO RIO GRANDE DO SUL

PRÓ-REITORIA DE PESQUISA

Comissão De Ética No Uso De Animais

CEUA UFRGS

CARTA DE APROVAÇÃO

Comissão De Ética No Uso De Animais analisou o projeto:

Número: 33274
Título: ESTUDO IN VITRO DO ACOPLAMENTO DE FREQUÊNCIAS HIPOCAMPAIS E O ENVOLVIMENTO DO SISTEMA GABAÉRGICO EM MODELO EXPERIMENTAL DE EPILEPSIA

Vigência: 01/10/2017 à 30/09/2021

Pesquisadores:

Equipe UFRGS:

MARIA ELISA CALCAGNOTTO - coordenador desde 01/10/2017
LIANA MARENGO DE MEDEIROS - Aluno de Doutorado desde 01/10/2017
MAYARA VENDRAMIN PASQUETTI - Aluno de Doutorado desde 01/10/2017
Francine de Souza Dalpian - Aluno de Doutorado desde 01/10/2017
Joseane Righes Marafiga - Aluno de Doutorado desde 01/10/2017

Comissão De Ética No Uso De Animais aprovou o mesmo , em reunião realizada em 19/06/2017 - SALA 330 DO ANEXO I DO PRÉDIO DA REITORIA - CAMPUS CENTRO - UFRGS-PAULO DA GAMA,110 BAIRRO FARROUPILHA - em seus aspectos éticos e metodológicos, para a utilização de 382 ratos Wistar machos de 1 a 3 meses de idade, pesando em torno de 150 - 300 gramas, provenientes do Biotério do Departamento de Bioquímica da UFRGS; de acordo com os preceitos das Diretrizes e Normas Nacionais e Internacionais, especialmente a Lei 11.794 de 08 de novembro de 2008, o Decreto 6899 de 15 de julho de 2009, e as normas editadas pelo Conselho Nacional de Controle da Experimentação Animal (CONCEA), que disciplinam a produção, manutenção e/ou utilização de animais do filo Chordata, subfilo Vertebrata (exceto o homem) em atividade de ensino ou pesquisa.

Porto Alegre, Quinta-Feira, 29 de Junho de 2017

MARCELO MELLER ALIEVI
Coordenador da comissão de ética

ANEXO 2 Resumo da metodologia empregada no Capítulo I (Parte II)

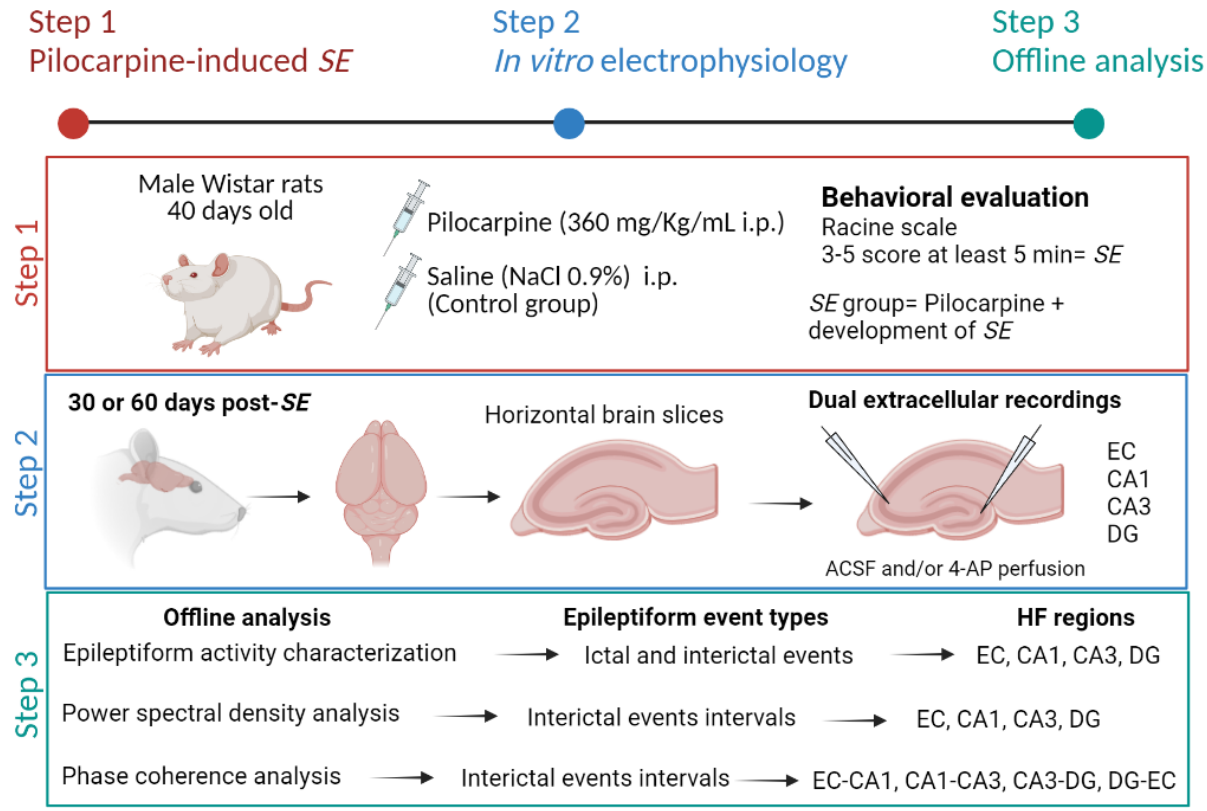

Step 1: Aged-matched rats were randomly divided in two groups: (1) injected with pilocarpine, and (2) injected with saline instead of pilocarpine. Each animal was observed for 90 minutes, while their seizure behavior was scored according to the Racine scale (Racine, Gartner e McIntyre Burnham, 1972). Status epilepticus (*SE*) was defined as continuous seizures with Racine score III to V, with no return to lower scores for at least 5 min. The *SE* was ended after 90 min using diazepam (10 mg/Kg, i.p.). In our experimental protocol, *SE* induced by pilocarpine caused approximately 10% of mortality. The heterogeneity of data as susceptibility and latency of seizures during the *SE* induction (data not shown), may to certify that the SRS observed at 30 and 60 days after *SE* induction are in fact, a characteristic chronic epileptic condition, established due an ensemble of cellular and molecular alterations in the brain network. Only rats who developed *SE* were used in this group (*SE* group). **Step 2:** Rats were euthanized by decapitation. Horizontal hippocampal-EC slices were prepared from epileptic rats at 30 and 60 days after *SE* induction, and age-matched controls. Dual extracellular recordings were performed simultaneously in EC-CA1, CA1-CA3, CA3-DG and/or DG-EC. The spontaneous local field potentials (LFP) of hippocampus and EC were recorded during 5 min of nACSF slice perfusion. Thereafter, field potential profiles were recorded during nACSF slice perfusion with 4-AP (50-100µM) for at least 2 hours, to the development of epileptiform activity. **Step 3**: We used between 1-2 slices per animal to performed the offline analysis in EC, CA1, CA3 and DG, as follow: the latency for the first interictal and ictal event, rate of occurrence of events (number of events/30s for interictal events, number of events/30min for ictal events), duration of ictal events, and percentage of slices generating ictal events. Thereafter, to analyze the power spectral densities (PSD) during 4-AP-induced hyperexcitability or spontaneous network activity, we chose 5s-epochs of interictal intervals events (IIE) or 5-epochs of basal activity, respectively; from EC, CA1, CA3 and DG extracellular recordings. To analyze the phase coherence, we chose paired recordings of EC-CA1, CA1-CA3, CA3-DG, DG-EC at the same conditions previously described. The PSD and phase coherence analysis were performed using the mean of all epochs per group. At least 5 epochs per slice were used, in order to have a better sampling of the interictal period. HF: hippocampal formation; EC: entorhinal cortex; DG: dentate gyrus; 4-AP: 4-aminopyridine. Created with BioRender.com.

ANEXO 3 Participação em outros trabalhos

ANEXO 3.1 Hippocampal gamma and sharp-wave ripple oscillations are altered in a Cntnap2 mouse model of autism spectrum disorder

Autores: Rosalia Paterno; Joseane Righes Marafiga; Harrison Ramsay; Tina Li; Kathryn A. Salvati; Scott C. Baraban.

Status: Publicado na revista científica ***Cell Reports***, 37, 2021.

DOI: https://doi.org/10.1016/j.celrep.2021.109970

Parte deste trabalho foi desenvolvido durante o meu doutorado sanduíche, no laboratório de Epilepsia do Prof. Dr. Scott C. Baraban, da Universidade da Califórnia, São Francisco, EUA; no período de 2019 a 2020. O objetivo era investigar o papel do gene Cntnap2 no hipocampo, realizando uma série de estudos anatômicos, comportamentais, eletrofisiológicos *in vitro* e *in vivo* usando camundongos nocaute Cntnap2 adultos.

A minha partipação nesse estudo foi através da realização da eletrofisiologia *in vitro*, onde pude caracterizar a transmissão sináptica inibitória de células piramidais de CA1, em animais nocaute para Cntnap2 e animais controle. Além disso, avaliamos as propriedades intrínsecas de interneurônios PV^+ dos animais mencionados anteriormente. Logo após a realização dos experimentos, foi também realizada a análise estatística, discussão dos dados e escrita do artigo científico.

ANEXO 3.2 Hippocampal CA1 and cortical interictal oscillations in the pilocarpine model of epilepsy

Autores: Mayara Vendramin Pasquetti, Letícia Meier, Joseane Righes Marafiga, Letícia Barbieri Caus , Adriano Bretanha Lopes Tort, Maria Elisa Calcagnotto.

Status: Publicado na revista científica Brain Research, 1722, November 1, 2019.

DOI: https://doi.org/10.1016/j.brainres.2019.146351

Este trabalho focou na investigação das alterações nos padrões oscilatórios interictais *in vivo* no modelo de epilepsia induzido por pilocarpina; do qual participei da realização da metodologia, principalmente na indução de *SE* nos animais; assim como na interpretação e discussão dos dados. A partir da identificação de alterações nos padrões oscilatórios e de sincronia no hipocampo e no córtex *in vivo* durante os períodos interictais sem atividade epileptiforme, tivemos o interesse pela investigação dos padrões oscilatórios hipocampais *in vitro* no modelo de epilepsia induzido por pilocarpina.

ANEXO 3.3 Neuroprotective effect of resveratrol against valproic acid-induced impairment in interneuronal network in the primary somatosensory area, seizure activity and disrupted cortical oscillation pattern

Autores: Mellanie Fontes-Dutra*; Joseane Righes Marafiga*; Júlio Santos-Terra; Iohanna Deckmann; Gustavo Brum Schwingel; Bruna Rabelo; Rafael Kazmierzak de Moraes; Marília Rockenbach; Mayara Vendramin Pasquetti; Carmem Gottfried, Maria Elisa Calcagnotto. *MFD and JRM contributed equally to this work.

Status: Submetido para publicação.

O desenvolvimento desse trabalho foi uma parceria entre o laboratório de Neurofisiologia e Neuroquímica da Excitabilidade Neuronal e Plasticidade Sináptica (NNNESP), coordenado pela Profa. Dra. Maria Elisa Calcagnotto, e o laboratório Grupo de Pesquisa Translacional de Desordens do Espectro do Autismo (GETTEA), coordenado pela Profa. Dra. Carmem Gottfried. O objetivo foi investigar se a exposição pré-natal ao ácido valpróico (VPA) afeta diferentes subpopulações interneuronais, a expressão de fatores de transcrição como LHX6, a transmissão sináptica inibitória em diferentes camadas corticais da área primária somatossensorial *in vitro,* e as oscilações corticais *in vivo*. Além disso, investigamos se o resveratrol (RSV) poderia prevenir os efeitos da exposição pré-natal ao VPA.

Em vista disso, minha contribuição para o estudo foi a realização dos experimentos de eletrofisiologia *in vitro* (correntes inibitórias pós-sinápticas espontâneas e em miniatura, CIPSs e CIPSm, respectivamente), seguida da análise estatística, discussão dos resultados da eletrofisiologia *in vitro* e também de todo conjunto de dados, e por fim, a escrita do artigo científico.